NASA TECHNICAL MEMORANDUM

NASA TM X-52154

NASA TM X-52154

CENTAUR AC-4 NOSE FAIRING JETTISON TESTS

by Jack C. Humphrey
Lewis Research Center
Cleveland, Ohio

NATIONAL AERONAUTICS AND SPACE ADMINISTRATION · WASHINGTON, D.C. · 1966

CENTAUR AC-4 NOSE FAIRING JETTISON TESTS

by Jack C. Humphrey

Lewis Research Center

CENTAUR AC-4 NOSE FAIRING JETTISON TESTS

Abstract

N66-22941

A series of tests performed to determine the effectiveness of the Centaur nose fairing jettison system used in the AC-3 flight, the design changes needed, and the flight readiness of the nose fairing used on the AC-4 flight are described. These tests were made at pressure conditions similar to those experienced by the nose fairing during flight jettison but without the vehicle accelerations experienced during flight. Data presented give pressures, accelerations, forces, and angular velocities experienced by the fairing during the described tests. It was concluded that:

1. Jettison tests of nose fairings with internal jet expansion separation devices must be conducted in a vacuum environment.

2. Use of internal jet expansion separation devices as the means of providing force for jettison is possible without causing damage to the payload contained by the fairing.

Author

Introduction

During the AC-3 flight of Centaur on June 30, 1964, an interruption was experienced by the guidance computer during nose fairing jettison. Since the guidance system was on open loop, this interruption did not affect the flight. Although successful nose fairing jettison tests had previously been performed at sea level conditions of temperature and pressure, it was decided that the pressure environment could make a difference and that these tests should be conducted under vacuum pressure conditions similar to those experienced by the vehicle during flights.

Objectives

The purpose of these tests was to determine (1) which components of the AC-3 type fairing were underdesigned and (2) to flight qualify the redesigned components for AC-4. In flight qualifying the fairing, it was necessary that the following tasks be accomplished: elimination of interference of any of the fairing components with the rest of the vehicle, functional check of complete fairing and all newly designed systems, structural verification of the redesigned deflector bulkhead to 1.50 times operational pressure, check of ability to separate and of adequacy of the trajectory using only one thrustor bottle, and determination of the nose fairing hinge loads.

An additional objective was to determine the ability of the Surveyor mast and attached panels to survive the shock pressure loads generated during separation.

Test Article

A standard flight type Centaur nose fairing was used for all tests and consisted of four major pieces: two barrel section halves and two cone section halves. The separation plane of the fairing halves was considered the x-x axis and the y-y axis was perpendicular to the separation plane. The barrel sections rest on a right angle ring, called the 219 ring, which is welded to the Centaur fuel tank. During flight a tension strap is wrapped around the tank and fairing and is bolted to both. A shaped charge cuts this strap 24.5 seconds before jettison. Figure 1(a) shows the 219 ring assembly. Four explosive type bolts along each of the fairing split lines hold the two halves of the fairing together and are fired one half second before jettison. Separation of the fairings is then accomplished by exploding a pyrotechnic latch pin puller allowing the nozzle plug in each of the two high pressure thrustor bottles to be blown out by bottle pressure. Figure 1(b) shows the thrustor bottle assembly. The exhaust jets from these bottles force the fairing halves apart. Rotation about two hinges, located one on each fairing half at the y-y axis, is begun and continues for approximately 35° at which time the hinge halves separate and the fairing halves take off on a trajectory away from the vehicle. Figure 1(c) shows details of the flight hinge. Two bulkheads are installed in the fairing to protect the payload. The deflector bulkhead is located directly under the thrustor bottles and over the payload and a thermal bulkhead is located below the payload. The deflector bulkhead keeps most of the gas from the bottles from impinging on the payload. The AC-3 type deflector bulkhead used in tests 1 and 2 was made of fiberglass and bolted to a right angle piece which in turn was bolted to the nose cone, by "JO" bolts. The bulkhead was made in two pieces which butted together on the x-x axis and were installed perpendicular to the z axis. Figure 1(d) shows the AC-3 type bulkhead. A bulkhead designed by NASA was used in tests 3 and 4 and is shown in figure 1(e). The AC-4 type bulkhead used in tests 6 through 13 was also made of fiberglass but each half was supported by an aluminum channel at the x-x axis and by angle supports on both top and bottom of the bulkhead. The top angle support was fastened by bolting to inserts potted in fairing structure. The bottom angle support was bolted to the fairing structure by the use of "JO" bolts. The bulkhead was made of two overlapping pieces and a hinged flap on the end of the I-IV part of the bulkhead so that thrustor bottle gas flow to the payload area would be impeded. This type bulkhead was installed at 17° to a plane perpendicular to the z axi. Figure 1(f) shows the AC-4 type bulkhead. The thermal bulkhead was annular in shape, bolted to the joint between cone and barrel section and supported on its inner edges by five struts for each half of the bulkhead. A rubberized cloth seal was attached to the inner edge of the bulkhead and to the adapter used to support the payload. Figure 1(g) shows the thermal bulkhead and struts.

The payload was supported by the above mentioned adaptor which was attached to the top of the Centaur fuel tank. The payload used on the AC-4 was a mass simulation of the Surveyor.

A shelf attached to the top of the Centaur fuel tank and called an equipment shelf supported various pieces of electronic equipment. Clearance between these pieces and the thermal bulkhead was a critical item to be evaluated. A flight type telemetry transmitter was located on this shelf and was used to transmit signals from flight transducers mounted on the nose fairing to determine the effect of separation on the instrumentation, and to give data for exact comparison with flight data.

Since tests 1 through 4 were made to determine the cause of problems experienced on the AC-3 flight and to investigate methods of correcting these problems, the configuration for these tests was not an AC-4 flight duplicate. All tests after the fourth were made with flight configuration as it was known at the time of the test. Since changes were made after each test due to results of the previous test, only the final test was a duplicate of the AC-4 flight nose fairing. Table I and figure 2 gives the configuration for each test.

Inasmuch as tests 1 through 4 were not flight configuration no effort was made to mount the fairing on a Centaur tank. For tests 6 through 13, however, a geometric simulation of the Centaur tank forward bulkhead was used. It contained a station 219 ring, equipment shelf, a flange for the Surveyor payload adaptor, and an attachment for mounting the tank half of the flight hinges. Complete 219 ring flight hardware except for the shaped charge was used for all tests from test 6 to completion of the test program. Inasmuch as no shaped charge was used, the tension strap was cut before the separation tests with a hacksaw.

Test Facility

These tests were conducted in a vacuum chamber which was a long cylindrical structure with the major axis parallel to the ground. The length of the chamber was approximately 90 feet and its maximum diameter was 30 feet. Evacuation of the chamber is accomplished in three stages. Two mechanical pumps in parallel are used for the roughing stage, the intermediate stage consists of a rotary positive displacement pump, and the final high vacuum stage consists of 10 oil diffusion pumps. By use of this three stage system it is possible to evacuate the chamber to 5×10^{-5} torr in approximately 24 hours. The chamber can also be evacuated to about 30 millimeters of Hg through the use of the Lewis Research Center central exhausting system in approximately 2 hours.

In tests 1 through 4 no effort was made to simulate actual mounting of the nose fairing on the Centaur station 219 ring nor to determine the trajectory after the flight hinge became disconnected from the Centaur vehicle. Figure 3(a) shows the facility arrangement for this type of test. Flight type hinges and facility hinges having the same centerline were used to mount the fairing halves on a flat bed plate. Although the facility hinges did not disengage (at any angle of rotation) and kept the fairings tied to the bed

plate at all times, they did not prevent the flight hinges from disengaging. After 20° of rotation both fairings were stopped by large pads covered with aluminum honeycomb and attached to a horizontal shaft at the level of the fairing center of percussion. Movement of the shaft crushed more aluminum honeycomb contained in a large box thereby absorbing the nose fairing kinetic energy.

By proper selection of the crushing strength of the honeycombs it was possible to absorb the energy of the moving fairing without excessively damaging it. After the first vacuum separation (in which the tips of the fairings were broken) it was found that it was necessary to make the catching pad larger and 2 feet higher (same shaft centerline). The honeycomb on the face of the pads was increased in thickness from 2 inches to 3 inches and the crushing strength was decreased from 40 to 20 pounds per square inch. The crushing strength of the honeycomb in the piston boxes was also decreased from 60 to 40 pounds per square inch. After test number 4, the catching mechanism on one side was moved closer to the end of the test area so as to obtain greater clearance between the nose fairing assembly and the adjacent Centaur environmental test facility which was located in the same test area. The other catcher pad was removed and a nylon net was installed so that one half of the fairing could freely follow its natural trajectory. Figure 3(b) shows this arrangement.

A further modification to the facility consisted of a tether rope attached to the fly away half of the nose fairing on one end and to a rack and ratchet on the other end. This rack was caused to pull on the tether rope by an elastic cord and by the action of gravity. The tension in the elastic cord was set so that the tether rope takeup was very nearly the same speed as the horizontal velocity of the nose fairing and thus caused no deviation in the fairing trajectory. An explosive pin pulling device was fired at the instant of thrustor bottle firing to initiate the takeup of the tether rope. Figure 3(b) also shows this tether line takeup.

Facility Electrical System

A program timer was used to give power to the various electrical devices in the test system at the proper times. This electrical system remained unchanged through test 6 and a schematic diagram of the system is shown in figure 4. Due to the addition of the new pyrotechnic electrical system on the nose cone, the system was changed as indicated by the note on figure 4 for use on tests 7, 8 and 9. Further revision to the electrical system as indicated was made for tests 10 through 13.

Facility Instrumentation and Cameras

A block diagram of the instrumentation system is shown in figure 5. Due to the transient nature of the data, minimum response of 1000 cycles per second for all types of transducer and recording combinations was required.

Some of the signals (up to 16 channels) were recorded on oscillographs using light beam type galvometers and located in the local control room (at the Space Power Chamber). The remainder of the signals (up to 22 channels) were recorded on frequency modulated tape after being transmitted on a quarter mile of landline to the LeRC Central Data Facility. A telemetry transmitter was also used to broadcast (up to 16 channels) to a telemetry ground station where it was received and recorded on another direct record magnetic tape recorder. Figure 6 shows locations of transducers for all tests, and table II gives description and accuracies of all types of transducer-amplifier combinations used in the complete series of tests. The test numbers in which the transducer was used, and location of transducer for each test are also included.

Two types of movie cameras were used for photographing various parts of the test hardware during separation tests. These cameras were enclosed in heavy stainless steel containers capable of sealing atmospheric air for the time required to evacuate the test chamber. Both types of cameras used 35 millimeter film. One was capable of running at 600 frames per second with speed controlled within ±1 percent. The other camera had a maximum speed of 3000 frames per second but speed varied from start to finish. A plan view of camera locations for all tests is shown in figure 7 and the camera positions for each test are given in table II.

Test Description

General

Table I lists the test hardware, its arrangement, and the facility configuration for each test.

Test I

The first test was conducted mainly to obtain experience in handling the test hardware, facility setup, and instrumentation. Figure 9 is a photo of the test setup. A fairing similar to the AC-3 flight hardware was used, mounted on a flat bed plate. Cameras were used in positions 1, 2, 3 and 4. Pipe masts were mounted on the bed plate in such a position that a T21 Surveyor mast, a guidance platform model, and a computor model could occupy positions such as they occupied in the AC-3 flight. The surveyor mast assembly was a prototype test model. The mast was slightly heavier than the actual flight model. The solar panel and antenna were not installed on the mast. The jettison was accomplished at atmospheric pressure with thruster bottle pressure of 3000 psi. There was no damage to the test hardware or to the facility. The flight trajectory is shown in figure 8.

Test 2

The test configuration used in the second test was the same as that used in the first test in all details. In this test the chamber was sealed and a vacuum equivalent to an altitude of 70 miles was drawn. The pressure in the thruster bottles was set at 2800 psi. Extensive damage to the test hardware resulted from the jettisoning. Both nose cone tips were broken directly above the top of the catcher pads; the deflector bulkhead in each half was torn from its fastening to the cones by the discharge from the thruster bottles. A photo of the damage is shown in figure 10(a). Movies taken during the separation clearly show that the deflector bulkheads were torn from their position before the fairings contacted the catchers. An enlargement of a frame of this movie at the time of failure is shown in figure 10(b). Figure 11 shows plots of the pressure data taken during this test and figure 12 shows the angular position of the fairing against time for this test, for previous sea level pressure test conducted by GD/C, and for theoretical data calculated by GD/C.

Test 3

New cone sections were obtained for the next test. A NASA redesigned deflector bulkhead and attachment hardware was installed in the cone halves. This bulkhead (shown in fig. 1(e) was made of aluminum plates and was attached to the cone by an angle around its circumference held by bolts completely through the honeycomb of the nose cone and backed up by an exterior metal circumferential strip. Four inch aluminum channels were attached to the cone at each end and were placed beneath the bulkhead to support it at the split line of the cone halves. Radial 12 inch angles were attached to the channels and to the cones to further support the bulkhead. A two piece hinged flapper plate held down by coil springs was installed on the I-IV half of the deflector bulkhead so as to protect the payload from the thruster bottle blast as long as possible during separation. The smaller piece of the flapper was attached to the larger by hinges and leaf springs deflected it downward. This flapper was designed so that opening of the deflector bulkhead gap did not occur until the included angle between the cone halves reached a value of 3.5°. A 1/2 inch diameter steel tie rod was installed in each cone half at the split line and as far above the deflector bulkhead as possible to prevent spreading of the cone half. Figure 13 shows the bulkhead and tie rod on the I-IV cone half, and figure 14 shows the flapper plate. Prior to this test it was thought that in order to reduce the peak pressure in the thruster bottle cavity to a tolerable level, it might be necessary to remove the rounded cap on top of the cones before firing the thruster bottles. In order to evaluate this situation the rounded cap located on the 1-4 half and the honeycomb plate covering the top of the 2-3 cone half were removed for this test. It was also decided to reduce the thruster bottle throat orifice to 0.882 inch diameter and the bottle pressure to 2500 psi.

As in test number 2, this test was run in a vacuum. The separation was accomplished with no visible damage except for the breaking of the small

springs on the small extension to the flapper. Figure 15 shows the raw data for this test and figure 16 shows the trajectory plot. Due to faulty setup, pressure and acceleration records in the payload and equipment shelf area were not recorded. High speed movies showed that the flapper door did not remain in contact with the bulkhead at all times during the trajectory.

Test 4

Further consideration of the removable cap design indicated that the bulkhead should be designed for higher pressures so that in the event of a failure of the cap removal mechanism the flight would not abort. It was thus decided to repeat test number 3 but with the cap in place. For this reason the cap was replaced on the 1-4 cone half and an aluminum plate was installed on the top of 2-3 half. The leaf springs on the small flap of the complete flapper assembly were not used on this test but were replaced by coil springs. In addition, in order to evaluate the effect of pressure impingement, flight type Surveyor solar panel and antenna were installed on the mast for this test. The solar panel was a flight model having about one-fourth of the total number of the required solar cells installed. The planar array antenna was a geometrically similar model made of plywood and having pressure taps installed. The solar panel is shown in figure 17, the planar array antenna is shown in figure 19.

For this test separation was accomplished without any visible damage to the nose fairing or the Surveyor mast assembly. Close examination of before and after photographs of the solar panel verified that none of the solar cells sustained any damage.

Figure 20(a) through 20(f) are the raw data. Figure 16(a), (b) and (c) show the angular position and angular velocity.

Test 5

Alteration to the facility occurred after test 4 as described in the section on facility hardware. Test 5 was aborted before separation so that a further modification to the facility could be made.

Test 6

The NASA type deflector bulkhead was removed and a deflector bulkhead similar to the design to be used on the AC-4 flight vehicle was installed. The basic differences between the two bulkheads are that the AC-4 bulkhead has more overlap and it is fiberglass construction. The included angle between fairing halves when separation of the bulkhead occurs with the AC-4 type bulkhead is 8° as compared to only 3.5° with the NASA bulkhead. A payload thermal bulkhead was also installed at this time. This bulkhead was

a nonflight type article. Figure 21 shows the deflector and thermal bulkheads of the II-III fairing half and figure 22 shows the same bulkheads for the I-IV fairing half. Sixteen hooks were installed on the II-III nose fairing half in such a manner that they would catch in the net and keep the fairing from rebounding off of the net. Eyes were installed in the II-III barrel section to allow tie lines to be fastened to the fairing and floor to limit the travel of the fairing. Figure 23 shows the arrangement of the hooks. Due to the lengthened path of the nose fairing travel on the fly-away side and the interest in the trajectory of the hinge points new cameras were added. A camera was also added inside the fairings approximately in the position shown in figure 22.

Although nose cone separation was accomplished without damage to the fairings and the newly added deflector and thermal bulkheads, damage was done to the fairing halves by the facility. The trajectory of the II-III half was such that the top of the fairing contacted the tether rope take up mechanism and the barrel section of the same half rebounded after hitting the net and hit the Centaur forward bulkhead model. Figure 24 shows the damage to the II-III half forward bulkhead and the barrel section. It can be seen that the interior of the barrel section was crushed in the 219 ring area. Damage was also done to the I-IV cone in the area of attachment of the ratches rods used to prevent rebounding after contact is made with the catcher pad. It was noticed after the test that one of the ratchet rods was badly bent probably as a result of the rod striking some fixed part of the deaccelerating box. Figure 25(a) through (e) shows the raw data and figure 26(a) through (c) shows trajectory plots.

Test 7

For this test new fairings were received from General Dyanmics. These fairings were to be given a flight qualification test and had the newly designed AC-4 type deflector bulkheads, thermal bulkheads, explosive bolt fixtures, bolts, and fairings, pyrotechnic electric system including batteries, relays, harness, and squibs, new thrustor bottle pin puller, a simulated equipment shelf, a flight type telemetry system, flight type transducers and a mass model of Surveyor similar to that to be flown on AC-4. A mass model with center of gravity at the proper location was substituted for the flight type hydrogen vent fin. A geometric model of the guidance platform was placed on the equipment shelf.

During the checkout of the pyrotechnic electrical system it was found that one of the circuits of the eight circuit relay assembly (55-60162-803) was faulty. A thermal overload relay (incorporated in each circuit) had been actuated thereby causing an open circuit. This malfunction was traced to the use of a 28 volt test lamp which had a high current surge. The checkout procedure was changed and no more difficulty was encountered. Inasmuch as another one of the three relay boxes used only four of the eight available circuits it was possible to swap the relay boxes and still use the same electrical harness. The electrical checkout was accomplished after this change was made.

The firing of the explosive bolts was accomplished before the test chamber was evacuated by manually closing the firing circuit. In preparing for this part of the test all explosive bolts were installed and torqued to required setting, squibs were installed, retainers installed on bolt housings, and fairings installed. During installation of the squibs, one squib or matching bolt was found to have defective threads so that the squib and bolt became galled. The threads between the two parts of the bolt were also found to be galled and the bolt was removed by over torquing and breaking it into two parts. After the defective bolt was replaced the actual firing of the bolts was accomplished. All bolts separated but various fragments were found upon removing the fairings. Shrapnel from the bolts up to pieces with maximum dimension of 1/16 inch were found. The charge retainer and diaphragm of of the squibs were also found inside the bolt fairings and inside the nose fairing. Figure 27 shows some of the parts recovered.

After testing the explosive bolts the test chamber was closed and evacuated. The separation of the nose fairing was successfully accomplished except for some damage to the barrel section of the I-IV fairing, some bending of one of the struts supporting the thermal bulkhead, and minor damage to the tip of the cone section. It was later found that the damage to the strut was caused by the dynamics of the fairing motion and not collision with the catcher pad. The damage to the barrel section was probably caused by weakening of the 219 ring area when a tension tie was pulled away by a facility hose that was improperly installed. This weak spot allowed the barrel section honeycomb to be cracked when rebound from the net caused it to collide with the Centaur forward bulkhead. Damage to the nose tip was caused by impact of the tip with the heavy nylon rope used to support the net.

The raw data is shown on figure 28(a) through (i) and figure 29(a) through (c) gives trajectory information.

Test 8

Damage to the II-III barrel section incurred in test number 7 was repaired by bolting two 43 inch by 37 inch by 3/16 inch aluminum plates one over the outside and one over the inside of the cracked area and reinstalling the tension tie to the 219 ring channel. Damage to the tip of the cone was repaired by filling the damaged area with epoxy cement and the damage fairing strut was replaced by a new strut of the same design. Because of the additional weight added by the repair to the II-III fairing half and because it was feared that it may have been weakened by the damage, the entire nose fairing assembly and Centaur forward bulkhead was rotated 180° about the Z axis so that the I-IV nose fairing half now became the one that could fly free and be caught in the net. For test number 8 a new set of pyrotechnic system flight type batteries and two new flight type relay assemblies were installed. As in test 7 the relay assemblies were checked (using the 28 volt bulb and mating harness plug) before installation, but after installation, checkout revealed two circuits were open. Investiagation of the checkout bulbs revealed

that although the steady state current was less than that required to trip the relay thermal overload the transient current during start up was sufficient to open it. The test lamp was, therefore, changed to a 120 volt lamp, the harness was rerouted through the relays to use the undamaged circuits and electric checkout was accomplished without further mishaps.

Calibration of LeRc installed strain gauges for measuring vertical nose cone hinge loads and determination of the vertical and horizontal spring constant of the Centaur simulated forward bulkhead on which the vehicle half of the hinge is mounted was made with the use of fixtures and a hydraulic loading device. Figure 1(c) shows the hinge to which the strain gauges were attached. Figure 30(a) and (b) gives the strain gauge calibration and figure 30(c) and (d) gives the spring constants of the bulkhead.

In conducting test number 8 explosive bolts were again fired before evacuating the test chamber. All bolts fired and separated successfully. Again upon removing the bolt fairings the squib charge retainer rings and diaphragms were found. High speed movies of the bolt at the knee joint of the fairing were taken during the bolt firing by means of leaving this one explosive bolt fairing off. The electrical cable to one of the squibs on this bolt was torn loose during the firing, but the threads on the connector were not damaged.

After evacuation of the chamber an attempt was made to separate the fairing. A facility electrical failure prevented the firing of the thrustor bottle mechanism and the operation of the cameras and lights. The chamber was brought up to atmospheric pressure and an examination of the electrical system and instrumentation showed that a facility enabling relay had not actuated thereby absolving the flight pyrotechnic electrical system of blame. The chamber was again evacuated and a successful separation took place.

Examination of the fairing after the test revealed that two thermal bulkhead struts suffered compressive type failures and one of the aforementioned strut brackets was damaged. These failures were caused by the dynamic forces during jettison and not by collision with deaccelerating devices. Figure 31 shows one of the damaged struts located at the YY axis in the II-III half of the fairing. Also in this test the air conditioning duct which is attached to the thermal bulkhead by an adhesive was torn loose. Figure 32 shows this damage. Motion pictures again revealed that the I-IV fairing half rebounded off the net and hit the Centaur forward bulkhead but in this case no damage occurred on the fairing. Figures 33(a) through (i) show the raw data obtained from this test and figures 34(a) through (c) show the trajectory.

Test 9

Repair of the air conditioning duct damaged in test 8 was made by use of bolts which passed completely through the thermal bulkhead and the duct flange; the damaged struts were replaced by new ones.

Inasmuch as test number 9 involved an over pressure test of the deflector bulkhead and fairing and a flight sequence test of the explosive bolts it was

necessary to make changes to the thrustor bottle nozzle and the firing circuit for the bolts. The 0.828 inch diameter washer used on all tests from number 3 through 8 was removed from the nozzle and the full throat diameter of 1.063 inches became effective. Figure 1(b) shows this nozzle and washer. The electrical circuit for the explosive bolts was changed from manual actuation to program timer actuation and the timer was set to fire the bolts 0.52 seconds before thrustor bottle firing. The Surveyor model was removed so that a camera could be installed to view the deflector bulkhead. The flight hinge was modified by enlarging the pin socket on the Centaur tank half of the hinge by 0.020 inch on the diameter. The pin socket is shown in figure 1(c). This allowed a maximum clearance between pin and socket of about 0.050 inches, which was the value set for this test.

The setting of the maximum clearance was accomplished by first removing the bolts holding the fairing half of the hinge, moving the hinge upward until the pins contacted the top of the hinge socket (mounted on the simulated Centaur tank) and then reinstalling and tightening the hinge bolts to keep the fairing half of the hinge in contact with the top of the socket.

Separation was accomplished with no damage to the deflector bulkhead, however, four struts were damaged: strut on YY axis of II-III half, strut on YY axis of I-IV half, strut 45° off YY axis on II quad, and strut 45° off YY axis in III quad were damaged. Again, damage occurred during jettison and not on collision with the catcher pad. Separation of the air conditioning duct on the II-III fairing half near the YY axis also occurred in this test.

Raw data for this test is shown in figure 35(a) through (j) and figure 36(a) through (c) gives the trajectory data.

Test 10

As a result of test 9 damage, the air conditioning duct was again repaired by the use of through bolts, and the damaged struts were replaced with new struts. For test 10, strain gauges were placed on the two struts located on the YY axis, one being on the II-III fairing half and the other being on the I-IV half. A modified flight type hinge (provided by General Dynamics) having a 0.127 inch maximum possible clearance between pin and socket and incorporating vertical load strain gauges was installed (fig. 37).

A clearance of 0.097 inches between pin and the bottom of the socket was set. All hinges in future tests had this same clearance.

In addition strain gauges numbered 135 and 136 were installed on the fly-away part of the hinge as shown in figure 6(c) so as to measure radial load. Calibration of the radial load strain gauges was made with the fixture previously used. Figure 38 gives this calibration.

New flight type relays and batteries were used on this test. The 0.828 diameter orifice insert was installed in the thruster bottle nozzle. Explosive bolts and bolt fairing were again installed except that no bolt or fairing was installed at the bolt housing located at the joint between the cone and barrel section of the quad III-IV split line due to the fact that only seven bolt assemblies were available. The electrical signal for actuating the explosive bolts was again made by the program timer 0.52 seconds before jettison. Measurements were made of the clearance between the bottom of the barrel section channel and the top of the 219 ring. These clearances are shown on figure 39. Nose fairing jettison was accomplished with no evidence of contact between the fairing and the Centaur forward bulkhead model. Two struts on the II-III fairing half were damaged again and the electrical disconnect on the I-IV fairing half showed evidence of arcing. Damage to the struts was caused by separation inertia forces and not collision with catcher pads. Noise was recorded on all channels of the F/M tape recorder at approximately the time that the disconnects were separated and four of these channels were rendered unuseable. Figure 40 shows physical evidence of the arcing on one half of the disconnect fitting.

Raw data for this run is shown in figures 41(a) through (k). Trajectory data is shown in figure 42.

Test 11

Inasmuch as much of the hinge strain gauge data was lost during test 10 due to arcing of the pyrotechnic electrical system on disconnect, it was decided that for test 11 a facility type electrical system with batteries, relay assemblies and power supplied by the facility for igniting the thrustor bottle pin puller would be used. The explosive bolts were not installed for this test. Two strain gauges were installed on each of three struts, and a testing machine calibration of four of the strain gauges is shown figure 43. This calibration agreed closely with strains calculated from the manufacturer's strain gage factor.

For this test a successful jettison was obtained with the only damage on the fairing being limited to one strut on the II-III fairing half at the YY axis. Figure 44 shows this damage. Movies taken during the separation clearly show that this failure was caused by vibration of the thermal bulkhead during separation and not upon collision of the fairing with the catcher pad.

Figures 45(a) through (h) show raw data taken during this test. Figure 46(a) through (c) shows trajectory data.

Test 12

This test was conducted to demonstrate the ability of the fairing to separate with only one thrustor bottle active. The bottle on the II-III

fairing half was pressurized to 2500 psi and the 0.828 inch diameter orifice was used in the nozzle. A camera was installed inside the fairing to photograph the thermal bulkhead and strain gauges were installed on the strut on the YY axis of the I-IV fairing half. The tie line was removed because it was felt that it could possibly affect the trajectory.

An additional test of the flight system transducers was desired and, therefore, all transducers that had previously been removed with the Surveyor mass model were reinstalled on the equipment platform. A strip of modeling clay was installed on top of the guidance platform mount to provide a measure of the minimum clearance between the guidance platform and the thermal bulkhead encountered during jettison. There was an average clearance of 1/8 inch between the top of the clay and the bottom of bulkhead as measured before jettison.

For this test separation was accomplished successfully and there was no evidence of collision between the Centaur simulated forward bulkhead and the I-IV fairing half. A strut on the II-III half at the YY axis was damaged and the modeling clay on top of the guidance platform mount showed evidence of having been contacted by the thermal bulkhead. Figure 47 shows the modeling clay installed on top of the mount. The clay was centered on top of the mount and held there by strips of tape. The picture shows that it has been given an outboard displacement after separation. Movies showed that the fairing dropped immediately after leaving the hinge but cleared the forward bulkhead at all times. Figures 48(a) through (e) show the raw data taken during the run and the trajectory data is shown in figures 49(a) through (c).

Test 13

For this test newly designed struts having double shear connectors were installed in all positions on both halves of the thermal bulkhead. Figure 50 shows the clevis parts installed on each end of the new struts. These struts were strain gauged as before. The air conditioning duct was redesigned to give greater clearance between it and both the guidance platform mount and the A/P programmer. Figure 51 shows the duct as used in test 13. Figures 52 and 53 show the redesign of the duct on both the top and bottom of the bulkhead to provide clearance with the A/P programmer.

Figures 54 and 55 show the redesign of the air conditioning duct to provide clearance with the guidance platform mount. The guidance platform mount and the A/P programmer were accurately located on the equipment platform as shown in figure 56 and 57. Rows of toothpicks were installed on both the programmer and guidance platform mount as shown in figures 58 and 59. Position indicators were mounted as a reference for reading the distance between the equipment shelf and the thermal bulkhead and between the payload adapter and the thermal bulkhead at both the position of the A/P programmer and the Guidance Platform mount. The facility camera looking in the barrel section door on the II-III side was relocated so as to better view the guidance platform.

Separation was successfully accomplished. One strut was bent as shown in figure 60. Examination of data revealed this damage occurred after fairing contacted the catcher plate. Toothpicks on both the Guidance Platform mount and the A/P programmer were broken but the remaining shorter toothpicks showed that sufficient clearance existed between the bulkhead and the packages. Minimum clearance as shown by toothpicks was 0.3. Figure 61 and 62 show the toothpicks, that were undamaged. Figure 63(a) through (f) shows the raw data and figure 64(a) through (c) show the trajectory.

Discussion of Test Results and Design Changes

Deflector Bulkhead and Payload Cavity Pressures

The purpose of the deflector bulkhead is to minimize pressure impingement on the payload during nose fairing jettison. The bulkhead was originally designed (fig. 1(d)) as two butting semicircular halves with the capability of withstanding a differential pressure varying from 4.5 psi at the free edge to 9.0 psi at the intersection of the bulkhead, fairing, and Y axis (ref. 1). Tests 1 and 2 were conducted with this type of bulkhead and with jettison bottle pressure and configuration the same as used in the AC-3 flight. Test 1 was conducted at sea level test chamber pressure and no damage to the bulkhead was observed. Test 2 was conducted with a chamber pressure equivalent to that at an altitude of 70 miles. In this test both halves of the bulkhead were torn from the fairing. High speed motion pictures of the II-III half of the bulkhead show this action occurring at approximately 0.015 seconds after the first motion of the fairing. Figure 10(b) is one frame of the test 2 motion picture showing the bulkhead being torn from the fairing. Jettison bottle pressures used this test were 2800 psi (fig. 12), and measured pressures on the deflector bulkhead (fig. 11) varied from 20 to 10 psia. Pressures in the payload cavity are also shown in figure 11 and varied from 6 psia at station -8.0 to 1 psia at station 24.5.

A new overlapping bulkhead fabricated by NASA was installed and the nose-cap was removed for test 3 as shown in figure 1(e). This bulkhead was designed to withstand the pressures measured in test 2 and to reduce the impingement pressures in the payload cavity. The thruster bottle pressure was reduced to 2500 psi and the nozzle orifice diameter was decreased from 1.063 to 0.828 inch. The effect of these changes was to lower the peak pressure and to prolong the duration of thrust. The resultant bottle pressure decay curve and other pertinent pressures is shown in figure 15. The pressure measured inside the payload compartment at station 24.0 was reduced to a maximum of 0.3 psia. The cap on top of the fairing was reinstalled for test 4 and the same nozzle diameter, bottle pressure and deflector bulkhead was used. Reinstalling the cap increased the pressure on top of the bulkhead to 9 psia but only increased the pressure inside the payload compartment to 0.35 psia (fig. 20).

The AC-4 flight type bulkhead as shown in figure 1(f) was used in all tests from test 6 through 13 without any failures. This bulkhead had an even

greater overlap than the NASA design and was designed to withstand differential pressures shown in figure 65. The additional angle supports around the circumference of the bulkhead, stronger bolting, and the extruded section supporting the XX axis diameters contributed to the ability to withstand this greater pressure differential. At flight bottle pressures of 2500 psi and with the 0.825 inch orifice the pressure on top of the bulkhead varied between 14 to 15 psia for transducer number 42 facing forward and 7 to 8 psia for transducer number 29 reading pressure parallel to the XX axis. Transducer number 56 measuring pressure inside the payload cavity at station 48.0 read a maximum pressure of only 0.1 psia. Figures 25, 28, 33, 41, 45 and 63 show these pressures.

An overpressure test was run with thruster bottle pressures at 2700 psi and with the nozzle orifice having a 1.063 inch diameter. The pressure read on transducer number 42 for this test was 18 psia, on transducer number 29 was 11 psia, and on transducer number 56 was 0.19 psia, (fig. 35).

To demonstrate the redundance of the two thrustor bottles, test number 12 was run with only the bottle in the II-III quad charged to operating conditions.

In this test the transducer facing forward, number 42, read the same as in the two bottle tests, 14 psia. The other transducer on top the bulkhead read only 4 psia. Figure 48 shows these pressures.

Fairing Separation Effects on the Payload

Test number 4 with the NASA designed overlapping deflector bulkhead was conducted to determine if the primary function of the nose fairing, protection of the Surveyor payload, was being performed. Pressure gages were mounted on the antenna flush with its surfaces and at the top of the payload mast. The antenna transducer number 31 indicated a maximum pressure of 0.1 psia and the transducer on top of the payload mast, number 30, a maximum pressure of 0.3 psia (fig. 20). The AC-4 flight type bulkhead with the greater overlap was even more effective in shielding the payload as shown by comparing transducer number 30 for test number 4 (fig. 20) with transducer number 56 used in tests with the AC-4 type deflector bulkhead (located in the same position) which read 0.1 psia (fig. 28 or 33).

Strains on the mast during fairing jettison were measured by strain gages in location shown in figure 6(c). Gages number 38 and 39 measuring bending on the solar panel arms showed a maximum stress on 3500 psi (10 percent of maximum allowable stress). Gages 32, 33, 35 and 36 measuring bending on the lower mast showed a maximum stress of 8500 psi (14 percent of maximum allowable stress). Gage number 34 measuring torsion on the lower mast indicated a maximum stress of 3500 psi (10 percent maximum allowable stress) and gage number 37 measuring torsion on the antenna support arm showed a maximum stress of 4000 psi (20 percent of maximum allowable stress). Figure 20 shows the strain gage values.

The solar panel used in this test had 192 solar cells attached as shown in figure number 17. A map was made detailing damaged cells before the test and inspection of each solar cell after the test revealed that none of the cells were damaged during the test by flying particles.

Nose Fairing Trajectory

Plots of angular position, angular velocity, and vertical and horizontal position against time are given for all tests. These plots are shown in figurer 8, 16, 26, 29, 34, 36, 42, 46, 49, and 64. These results indicate that for all conditions tested the nose fairing has a satisfactory trajectory.

The data for these plots were obtained from enlarged frames of the high speed motion pictures of the nose fairing separation. Angle measurements of the nose fairing tips in tests 1 through 4 were made for successive frames of the motion picture and plotted against time. Since the field of view of the cameras used for these measurements was limited, only about 16° of motion of the fairings could be plotted for these tests. In tests 6 through 13 the pictures used for measurements were of the flight hinge on the fairing that flew into the net. Angular measurements and displacements were measured at this point and were made for complete travel of the fairing half until it struck the net. Discrepancies between the two measurement positions were caused by bending of the fairings. Cameras photographing the top and bottom of the nose fairings show that the tip of the fairing can have up to 2° motion before the barrel section even starts to move. The starting time of the trajectories varies from run to run because the time reference for trajectories was a photo flash bulb which was ignited by different sources for different runs.

Test 1 (AC-3 type configuration) was fired at sea level pressure and achieved a maximum angular velocity of 135° per second (fig. 8) while test 2 (also AC-3 type) was fired at an altitude of 70 miles reached a maximum angular velocity of 225° per second (fig. 16). As will be recalled, tests 3 and 4 were run with reduced pressure bottle conditions (table I) and using an overlapping bulkhead designed by NASA. The maximum angular velocity for these tests varied between 122° to 160° per second (fig. 16). The I-IV fairing half in each test being about 30° per second faster than the II-III half.

Tests 6, 7, 8, 10, 11 and 13 were made with essentially the AC-4 flight configuration. (The difference from the flight configuration for any one test was not enough to change the trajectory). Figure 67 is a compilation of the trajectories of tests 6, 7, 8, 10, 11, 13 and it can be observed that the spread in angular position for any given time is not greater than 10° at any time. In tests 6 and 7 the II-III fairing half flew into the net and in tests 8, 10, 11, and 13 the I-IV fairing half flew into the net. The maximum angular velocities measured for these tests ranged from 165° to 195° per second. The increase in the maximum angular velocity of this group of tests over tests 3 and 4 which were run with the same thruster bottle conditions

but with different deflector bulkheads can be attributed to the increased overlap of the bulkhead plus the increased volume (and resulting increased wall area) of the cavity above the deflector bulkhead. Figure 66 is a two dimensional drawing showing the position of the fairing during testing with respect to the Centaur forward bulkhead at various times until the fairing half struck the net. Measurements for this drawing were made from the separation motion pictures. It can be observed that the typical motion of the nose fairing is outward and upward.

Test 9 which was the over pressure test (thruster bottle pressure of 2700 pounds per square inch and a thruster bottle nozzle diameter of 1.063 inches) achieved a maximum angular fairing velocity of 232° per second (fig. 36). Test 12 was run with only one active thruster bottle on the II-III fairing (pressurized to 2500 pounds per square inch and having a nozzle diameter of 0.828 inches) to demonstrate that a satisfactory separation could be accomplished if one bottle failed to operate in flight. The resultant fairing trajectory was such that after hinge separation instead of the hinge pin on the nose fairing rising above its mated position, it dropped below. Maximum I-IV fairing angular velocity in test 12 was 107° per second. The II-III fairing half velocity was greater than the I-IV fairing half velocity and reached a maximum velocity of 117° per second at the time it contacted the catcher (fig. 4(b)). Although the vertical motion was in a direction opposite to that obtained with two bottles, the worst trajectory measured (I-IV fairing) was still considered to be satisfactory.

In all of the tests at LeRC there was no duplication of the additional acceleration imposed on the fairing during jettison caused by the engine forces. Since in test 12 only one bottle was used and the I-IV trajectory gave the least clearance between the fairing and flight vehicle after jettison, a calculation was made to determine the effect of the additional acceleration imposed by flight conditions using the following equation:

$$Y_F = Y_L + \frac{1}{2} A (t - to)$$

A flight acceleration (g's) minus 1.0 g.
Y_F vertical displacement under flight conditions.
Y_L vertical displacement seen on LeRC test trajectories.
t any time for which calculation is made.
to time fairing hinge half separated from tank hinge half.

The results of this calculation for test 12 are shown in figure 49(d). It is apparent that at all times the fairing is moving outward from the vehicle. If this ratio of displacement to movement along the axis (ratio of 0.45) is maintained, by the time the fairing is passing the Atlas pads it will be 450 inches radially outward from its original position with respect to the longitudinal center line of the vehicle. Since the condition with one bottle not operating provides the worst combination of the fairing trajectory with the effect of flight acceleration, it is felt that although flight acceleration was not simulated in these tests, it will not cause a harmful trajectory.

The AC-4 flight was conducted after these tests and tape type transducers were installed on the nose fairing to measure its trajectory. Similar transducers were also installed on LeRC tests and information from these transducers agreed with the trajectories calculated from the motion pictures. The AC-4 flight fairing trajectory is compared with test 11 fairing trajectory in figure 68. Since a tape transducer was located in each quadrant two angular velocities are given for each fairing half. The averaged maximum values of the angular velocity of the II-III fairing for the AC-4 flight was 178° per second as compared with a maximum angular velocity at the hinge point of 193° per second computed from motion pictures from test 11. The tape transducers show that rotation about the Z axis in a counter-clockwise direction (viewed from aft) must have occurred for the AC-4 flight; whereas in test 11(a) clockwise rotation (viewed from aft) was obtained. The I-IV fairing half did not show this discrepancy. In both the AC-4 flight and in test 11 the rotation about the Z axis was clockwise (viewed from aft).

Hinge Loads

The dynamic vertical and radial loads developed by the nose fairing during separation are partially transmitted to the Centaur vehicle through the flight hinges. The remainder of the load is transferred through the 219 ring. (The hinges were strain gauged in the positions shown in fig. 6(c)). Table III gives the maximum loads experienced during each test and the angle of fairing rotation at which these loads occurred. The highest maximum vertical load measured (6670 lb) occurred during test 9 in which the thruster bottle conditions were considerably more severe than those specified for flight. The next highest load (5080 lb) occurred on test 7 when the initial clearance between the hinge pin and socket was considerably less than the AC-4 flight value. In all of the following tsets where the AC-4 flight clearance (0.127 in.) was used the loads varied from 2070 pounds to 3545 pounds. These loads were all compression loads and occurred by 1.8° rotation of the fairing. The maximum tension load measured usually occurred at least 9° after start of fairing rotation. The highest valve measured was 2730 pounds which occurred during test 8 with an initial hinge pin clearance of 0.027 inch. Reference 2 indicates that the maximum compressive vertical design load is 6000 pounds and the maximum vertical tension design load is 3500 pounds. Data obtained from the AC-4 flight on the hinge show that the maximum vertical compression load was 2650 pounds and the maximum vertical tension load was 1100 pounds.

Strain gages were also installed on the fairing half of the hinge immediately behind the hinge pins for tests 10 through 13 to measure radial compression loads. A static calibration of these strain gages made by applying a radial load to the hinge is shown in figure 38. The effect of vertical loads on these strain gages was not determined. The inboard radial loads measured during these tests ranged from 850 pounds in test 12 to 1500 pounds in test 10. The design inboard radial hinge load (ref. 2) was 2125 pounds.

The loads obtained from the LeRC separation tests are probably different from those experienced in flight due to the fact that the spring constant of

the simulated forward bulkhead used in the LeRC tests was higher than that for an actual flight tank. The spring constants of the forward bulkhead used in these tests and the strain gauge calibration of the gauges on the hinge are shown in figure 30. The spring constants of the hinge attached to the actual flight tank are as follows: vertical is 36,700 pounds per inch and horizontal is 9000 pounds per inch.

Since the hinge loads depend upon the flexible body dynamics of the fairing an effort was made to define the dynamics by installing accelerometers at the top of the nose fairing measuring acceleration in the Y-Z plane perpendicular to the X-Z plane. The record obtained was filtered to eliminate the higher unwanted frequencies. Figures 28, 41, 45, 48 show the filtered and unfiltered records of this accelerometer. The filtered record indicates that the fairing acts as an approximately 50 percent critically damped second order system. This does not agree with later experimental data showing the critical damping factor to be approximately 8 percent. This factor was obtained at LeRC by applying varying frequency loads with a maximum 5 "g" amplitude to a free-free Centaur nose fairing half.

Visual integration of the curves does not check with angular velocity attained by photographic studies. The differences between this data and other data may be because of malfunction of the instrumentation, nonlinearity of the nose fairing structure, or because some of the higher frequency eliminated by filters is necessary to give an accurate indication.

Thermal Bulkhead Clearance

Clearance between the thermal bulkhead and the autopilot programmer and the bulkhead and the guidance platform mount (both located on the equipment shelf) is critical. It was learned during these tests that when nose fairing separation starts, the dynamics of motion are such that the thermal bulkhead tends to deflect aft with respect to the equipment shelf and decrease the clearance between the bulkhead and the packages on the equipment shelf. The air conditioning duct on the thermal bulkhead is directly above the two critical packages. The original design of this duct had a reduction in cross sectional area above the packages but even with this reduction the minimum clearance was 0.7 inch in the static position.

Tests with modeling clay on the guidance platform mount during test 12 showed that the thermal bulkhead contacted the top of platform mount. The location of the clay after the test is shown in figure 47. Modification of the bulkhead was made before test 13 to the final AC-4 configuration as shown in figures 51, 52, 53, 54, and 55. The guidance platform mount and autopilot programmer were located on the equipment shelf as shown in figures 56 and 57. Toothpicks were installed on both the guidance platform mount and the autopilot programmer as shown in figures 57, 58, 61 and 62. From the length of the unbroken toothpicks after the tests it was apparent that a clearance of 1.0 inch on the guidance platform mount and 0.3 inch on the autopilot programmer existed during jettison.

Thermal Bulkhead Struts

Struts supporting the thermal bulkhead failed in tests 7 through 13. Table IV gives the struts damaged during each test. Table V shows the maximum stress and the angle of fairing rotation at which the stress occurred. For all cases of complete breakage of the strut the damage occurred at the connection between strut and the bracket attached to the fairing. Most frequent broken strut location was on the YY axis. The maximum stress measured in the strut tubing at this location was approximately 23,000 pounds per square inch and occurred at about 0.5° of fairing rotation. This load was essentially pure tension as shown by the three strain gauge readings on the number 3 strut in test 13. A bending load was experienced by the number 9 strut which had a bend incorporated in its design so that it would not interfere with the air conditioning duct located beneath it. The maximum stress developed on this strut was 36,800 pounds per square inch.

As a result of the failures the struts were redesigned and the new design was used in test 13. The strut before and after redesign is shown in figure 50. One failure of the redesigned struts (the number 3 strut) did occur by bending in test 13 as shown in figure 60. This failure occurred however after contact with the facility catcher and would not occur on a flight separation of the fairing. No damage occurred at the previous failure point, the attachment of the strut to the fairing bracket, in test 13.

PYROTECHNIC DEVICES

Explosive type bolts (GD/C part number 55-71286) were used to hold the fairing halves together in tests 7 through 10. In tests 7, 8, and 10 the bolts were exploded at ambient pressure before the test chamber was evacuated. In test 9 the bolts were blown at altitude pressure and with the same time lead before initiation of the jettison bottles as the flight time lead (0.52 sec). In all cases the bolts separated properly; however shrapnel was observed after separation and defective threads were discovered during assembly.

Conax pin pullers (part number 1808010-02) as shown in figure 1(b) were used to pull pins which initiated the discharge of the jettison bottles in all tests. These pin pulling devices successfully operated in every test.

FLIGHT ELECTRICAL SYSTEM

The voltage and total current from the two AC4 flight type batteries are shown for tests 7 and 8 in figures 28 and 33. These batteries have a 35 volt no load level and will supply 0.5 amp hours of current. The voltage from each battery dropped from 5 to 7 volts for approximately 0.1 second and then returned to its starting voltage (35 volts). Current drain varied from 10 to 19 amps per battery. In no case did the batteries go below the minimum voltage level of 25 volts specified for a 20 amp load. Checkout of the pyrotechnic electrical circuits should be carefully done with devices having enough internal resistance so that the thermal overload relay in the circuit is not actuated.

CONCLUSIONS

Vacuum chamber jettison tests of the Centaur Surveyor nose fairing provided an excellent means of evaluating jettision system performance and flight qualifying all parts of the nose fairing.

The following items were evaluated and required modifications indicated:

A. Structural Components
    1. Deflector bulkhead
    2. Explosive bolt assemblies
    3. Thermal bulkhead
    4. Thermal bulkhead struts
    5. Surveyor payload
B. Trajectory of nose fairing halves
C. Impingement pressures from thruster bottles
D. Electrical Components
E. Pyrotechnic Components

These tests prove that:

1. Jettison tests of nose fairings with internal jet expansion separation device must be conducted in a vacuum environment.

2. Use of internal jet expansion device as the means of providing force for jettison is possible without causing damage to the payload contained by the fairing.

REFERENCES

1. Final Stress Analysis, AC-3 Vehicle, Volume II, Book I Surveyor Nose Fairing and Related Components, GD/C 63-1364, June 12, 1964.

2. External Design Loads, Centaur AC-4 Vehicle GD/C 63-1362-1, November 15, 1964 Revision A.

TABLE I. - CONFIGURATION OF FACILITY AND NOSE FAIRING AND DAMAGE SUSTAINED BY FAIRING

Test no.	Test date	Figure[a] for facility config.	Figure[a] for test article	Test chamb. alt., miles	Thruster bottle press., psi	Barrel section	Cone section	Nose cone cap	Flyaway half	Thrustor assembly config.	Deflector bulkhead	Thermal bulkhead	Explosive bolts
1	7-31-64	3(a)	2(a)	Sea level	3000	Pt. Loma furnished	EID 55-72006-1 303-0002 Pt. Loma Furnished	Used	None	2 bottles used 1.063 orifice	AC-3 Type fig. 1d	None used	None used
2	8-5-64	3(a)	2(a)	70.0	2800								
3	8-25-64	3(a)	2(b)	70.0	2500		EID 55-72007 55-0613-6 Plum Brook furnished	Not used		2 bottles used 0.828 orifice	NASA Design fig. 1(e)		
4	8-31-64	3(a)	2(c)	70.0	2500			Used					
5	------	----	----	----	----			----		----------	----------	---------	---------
6	10-1-64	3(b)	2(d)	62.0	2500			Used	II-III	2 bottles used 0.828 orifice	AC-4 Type 55-71258 fig. 1(f)	Test type fig. 21	None used
7	10-10-64	3(b)	2(e)	66.7	2500	EID 55-72086-1 402-0001	EID 55-72008-7 55-72008-9 55-0513-4		II-III	2 bottles used 0.826 orifice		GD/A Design near flight configuration	AC-4 Flight configuration bolts blown at atmos. press.
8	10-18-64	3(b)	2(e)	52.9	2500				I-IV	2 bottles used 1.063 orifice 2 bottles used 0.825 orifice			AC-4 Flight configuration bolts blown at altitude and 0.52 sec. before separation. Only 7 bolts used on run 10
9	10-23-64	3(b)	2(f)	66.7	2700								
10	10-30-64	3(b)	2(b)	65.5	2500								None used
11	11-5-64	3(b)	2(f)	70.4	2500					1 bottle fired (I-IV) 0.828 orifice 2 bottles fired 0.0828 orifice			
12	11-13-64	3(b)	2(f)	67	2500								
13	11-25-64	3(b)	2(f)	67	2500							AC-4 Flight configuration	

[a]Refers to report figure number showing drawing of facility or test article configuration.

Test no.	Equipment shelf simulation	Payload simulation	Pyrotechnic system power	Fairing hinges	Camera positions as per figure 7	Film MPD number	Repairs before test	Test damage
1	Computer and guidance package mounted on posts	Surveyor flight type mast on pipe platform - no panels	Facility	Facility	1,2,3,4	617	None	None
2						618	None	Both fairings broken off directly above catcher pads. Deflector bulkhead torn from fairing before contacting catcher.
3		Pipe mast in place of Surveyor.				623	Replaced both cone sections, installed NASA design deflector bulkhead, enlarged catcher pads. Decreased compressive strength of honeycomb. Cap off	Leaf Spring on deflector bulkhead flapper broken.
4		Surveyor mast on pipe platform with panels installed				624	Installed coil spring in place of leaf spring on deflected bulkhead hinge. Cap on.	None
5	----------	----------	-------	-------	------	---	----------	----------
6	Computer, Guidance platform mounted on posts	Pipe mast	Facility	Facility one half flight hinge other half	1,5,6,7,8,9,13	629	None	Barrel and cone of 1-4 fairing half. Cone of 2-3 fairing half.
7	Computer, Guidance package Telemetry on equipment shelf	AC-4 Surveyor mass model	Flight batteries and relays		1,5,6,8,9,10, 20	635	Complete new fairing assembly installed.	One explosive bolt galled. Shrapnel from explosive bolt squibs. Tension tie on 2-3 fairing barrel torn off. Barrel section of 2-3 fairing damaged. Thermal bulkhead struts.
8					1,5,6,9,10,11, 16,21	637	Repaired 2-3 barrel section by bolting aluminum plates to fairing. Reinstalled tension tie. Replaced struts. Rotated whole fairing 180°	Squib Shrapnel. Cable to explosive bolt squib torn off. Struts damaged. Air conditioning duct partially torn loose.
9		Pipe platform		Same as runs 7 and 8 except flight hinge socket enlarged 0.020"	1,6,9,11,12, 15,13	638	Bolted air conditioning duct to thermal bulkhead. Replaced struts	Struts damaged. Further separation of air conditioning duct.
10				AC-4 Flight type hinge	1,6,9,11,17, 15,14	640	Further bolting of air conditioning duct. Replaced struts.	Struts damaged - Arcing of electrical disconnect on 1-4 fairing.
11			Facility		1,6,9,11,18, 15,12	642	Strut replaced, change wiring so that facility power replaced. Pyrotechnic electric system power.	Strut damaged.
12					1,6,9,11,10 19,12	644	Replaced strut.	Strut damaged.
13	Computer guidance platform telemetry and auto pilot programmer mounted on equipment shelf.				1,6,11,18,15, 14	650	Replaced strut.	Strut damaged due to collision with catcher pad.

TABLE II. - TRANSDUCER INFORMATION

(a) Pressure, positions, and acceleration

Position number	Figure number showing position	Transducer number (on data)	Vendor	Vendor model number	Type measurement	Vendor's range	Test full scale range	Direct. of measurement	Freq. range	Overall accuracy % of test range	Tests numbers in which transducer was used (X) denotes use — Test no. 2	3	4	6	7	8	9	10	11	12	13	Record device
1	6a	1	Alinco	151	Press.	0-4000	0-3200	--	0-600	±2.5	X											Rec. Oscill.
2		2	Kissler	701		0-50	0-3	Z	0-1800	±18	X											F.M. Tape
3		3	Kissler	701		0-50	0-5	Z	0-1800	±10	X											
4		4	Kissler	701		0-50	0-5	Z	0-1800	±10	X	X										
5		5	Kissler	701		0-50	0-3	Z	0-1800	±18	X	X										
6	6a	28	Alinco	151	Press.	0-4000	0-3000	--	0-600	±2.5			X									Rec. Oscill.
7		31	Statham	PA208		0-5	0-3	X	0-600	±5.0			X									F.M. Tape
8		8	Kissler	701		0-50	0-40	Z	0-1800	±1.5	X											
9		9	Kissler	701		0-50	0-40	Z	0-1800	±1.5	X											
10		10	Kissler	701		0-50	0-4	Z	0-1800	±15	X											
11	6a	11	Endevco	2235	Accel.	±2g	±2g	Z	2-1800	±2	X											F. M. Tape
12		12		2235	Accel.	±2g	±2g	Z		±2	X											
13		13		2503	Press.	0-10	0-0.9	Y to		±25	X	X										
14		14		2503	Press.	0-10	0-0.9	Y away		±25	X	X										
15		15		2503	Press.	0-10	0-0.9	X		±25	X	X										
16	6a	16	Endevco	2503	Press.	0-10	0-0.9	X	2-1800	±25	X	X										F.M. Tape
17		17	Endevco	2503	Press.	0-10	0-0.9	Z	2-1800	±25	X	X	X									
18		18	Endevco	2235	Accel.	±2g	±2g	X	2-1800	±2	X	X										
19		19	Kissler	701	Press.	0-50	0-5	Z	0-1800	±2		X										
20		20	Endevco	2235	Accel.	±2g	±2g	Z	2-1800	±2	X	X										
21	6a	21	Endevco	2503	Press.	0-10	0-0.9	Y	2-1800	±25	X	X										F.M. Tape
22		22	Endevco	2503	Press.	0-10	0-0.9	X	2-1800	±25	X											
23		23	Endevco	2503	Press.	0-10	0-0.9	Z	2-1800	±25	X	X	X									
24		24	Endevco	2235	Accel.	±2g	±2g	Z	2-1800	±2	X	X										
25		6	Kissler	701	Press.	0-50	0-30	Z	0-1800	±2		X	X									
26	6a	7	Kissler	701	Press.	0-50	0-30	Z	0-1800	±2		X	X									F.M. Tape
27		7					0-30			±2		X	X									
28		3					0-1			±50		X										
29		22					0-0.3			±180		X										
30		9					0-1.0			±50		X	X									
31	6a	27	Alinco	151	Press.	0-4000	0-3200	--	0-600	±2.5	X	X	X									Rec. Oscill.
32		28	Data Sensor	151	Press.	0-4000	0-3200	--	0-600	----		X										Rec. Oscill.
33		12	Endevco	2235	Accel.	±2g	±2g	Z	2-1800	±2		X										F.M. Tape
34		11	Endevco	2235	Accel.	±2g	±2g	Z	2-1800	±2		X										F.M. Tape
35		31	Statham	PA208	Press.	0-5	0-1	Z	0-600	±5		X										Rec. Oscill.
36	6a	29	Alinco	151	Press.	0-50	0-25	X	0-600	±4.0		X	X									Rec. Oscill.
37		30	Statham	PA208		0-5	0-1	Z	0-600	±5.0		X	X									Rec. Oscill.
38		2	Kissler	701		0-50	0-5	Z	0-1800	±10			X									F.M. Tape
39		13	Kissler	701		0-50	0-0.5	X	0-1800	±100			X									F.M. Tape
40		14	Kissler	701		0-50	0-0.5	X	0-1800	±100			X									F.M. Tape
A	6b	CY740	Endevco	28208-15	Accel.	±15g	-----	--	0-81	±5					X	X						Telem. Tape
B		CY750	Endevco	28208-15	Accel.	±15g	-----	--	0-160						X	X						
C		CA44SP	Colvin	401A-3.5-75	Press.	0-35	-----	--	0-35						X	X	X	X	X	X	X	
D		Cy8P	T.S. 1	2461	Press.	0-15	-----	--	0-8						X	X						
E		CA39S	BLH	----	Strain	----	-----	--	0-39						X							
F	6b	CA38S	BLH	----	Strain	----	-----	--	0-45	±5						X	X	X	X	X	X	Telem. Tape
G		CY710	Endevco	28208-15	Accel.	±15g	-----	--	0-330						X	X						Telem. Tape
H		CY720	Endevco	28208-15	Accel.	±15g	-----	--	0-220						X	X						Telem. Tape
I		CA89D	Endevco	28202	Accel.	±15g	-----	--	0-450						X	X	X	X	X	X	X	Telem. Tape
J		CM201D	Space Craft	RSP200	Motion	0-80"	0-80"	Y	0-45						X	X	X	X	X	X	X	Telem. Tape and Rec. Oscill.
K	6b	CM202D	Space Craft	RSP200	Motion	0-80"	0-80"	Y	0-60	±5					X	X	X	X	X	X	X	Telem. Tape
L		CM203D	Space Craft	RSP200	Motion	0-80"	0-80"	Y	0-60						X	X	X	X	X	X	X	and Rec. Oscill.
M		CM204D	Space Craft	RSP200	Motion	0-80"	0-80"	Y	0-60						X	X	X	X	X	X	X	
N		CY101P	Endevco	28277-162.3	Press.	0-10	0-1	Z	0-600						X	X						Telem. Tape
O		CY102P	Endevco	28277-162.3	Press.	0-10	0-1	Z	0-790						X	X						Telem. Tape
P	6b	CM205Y	Gulton	ICN1806-H	Noise	------	------	Z	0-1000	±5					X	X	X	X	X	X	X	Telem. Tape
1		27	Alinco	151	Press.	0-3000	0-3000	--	0-600	±2					X	X	X	X	X	X	X	Rec. Oscill.
2		28	Alinco	151	Press.	0-3000	0-3000	--	0-600	±2					X	X	X	X	X	X	X	Rec. Oscill.
3		74	CEC	4-202	Accel.	±100g	±100g	Y	0-800	±1				X	X							F.M. Tape
4		76	CEC	4-202	Accel.	±100g	±100g	Y	0-800	±1				X	X							F.M. Tape
5	6b	42	CEC	4-202	Press.	0-50	0-50	Z	0-1800	±2				X	X	X	X	X	X	X		Rec. Oscill.
6		29	Alinco	151	Press.	0-50	0-25	X	0-600	±4				X	X	X	X	X	X	X		
7		W3	Claostt	53-C-1	Rotation	0-330°	+72 to -72°	--	0-600	±1				X	X	X	X	X	X			
8		57	Statham	PA208	Press.	0-15	0-15	Z	0-600	±1				X	X							
9		31	Scientific advances	M7	Press.	0-15	0-10	Z	0-600	±1				X	X	X						
10	6b	30	Scientific advances	M6	Press.	0-5	0-5	Z	0-600	±1				X	X	X		X				Rec. Oscill.
11		56	Dynisco	--		0-3	0-3	Z	0-600	--				X	X	X	X	X				
12		59	Dynisco	--		0-1	0-1	Z	0-600	--					X	X	X	X				
13		60	Dynisco	--		01	0-1	Z	0-600	--					X	X	X	X				
14		75	CEC	4-280	Accel.	±100g	±100g	X	2-1800	±2.0				X		X						F.M. Tape
15		W1 & W2	---	-----	Contact	-----	-----	--	0-250	±1				X	X	X	X	X				Rec. Oscill.
16	6b	57	Dynisco	-----	Press.	0-5	0-5	Z	0-600	--							X	X				Rec. Oscill.
17		75	CEC	4-202	Accel.	±100g	±100g	Y	0-800	±1						X						F.M. Tape
18		74	CEC	4-202	Accel.	±100g	±100g	Y	0-800	±1						X		X	X	X	X	F.M. Tape
19		75	CEC	4-202	Accel.	±100g	±100g	X	0-800	±1				X								F.M. Tape
20		76	CEC	4-202	Accel.	±100g	±100g	Y	0-800	±1								X	X	X		F.M. Tape
21	6b	57	Statham	PA208	Press.	0-5	0-5	Z	0-800	±1									X	X	X	Rec. Oscill.
22		56	Dynisco	-----	Press.	0-1	0-1	Z	0-600	--									X	X		Rec. Oscill.
23		59	Statham	PA208	Press.	0-5	0-1	Z	0-600	--									X	X		Rec. Oscill.
24		60	Statham	PA208	Press.	0-5	0-1	Z	0-600	--									X	X	X	Rec. Oscill.
25		75	Statham	A-69	Accel.	±100g	±100g	Y	0-1100	±1							X					F.M. Tape
26	6b	77	CEC	4-280	Press.	0-1	0-1	Z	2-1800	±2											X	F.M. Tape
27		42	Statham	PA208	Press.	0-50	0-5	Z	2-1800	±10											X	Rec. Oscill.
28		TD1	Markite	-----	Motion	1-10"	1-10"	Z	0-600	±1											X	Rec. Oscill.
29		TD2	Markite	-----	Motion	1-4"	1-4"	Y	0-600	±1											X	Rec. Oscill.
30		TD3	Markite	-----	Motion	1-10"	1-10"	Z	0-600	±1											X	Rec. Oscill.
31	6b	TD4	Markite	-----	Motion	1-4"	1-4"	Y	0-600	±1											X	Rec. Oscill.
32		13	Endevco	2503	Press.	0-10	0-1	Z		±20				X								Rec. Oscill.
33		14	Endevco	2503		0-10	0-1	Z		±20				X								F.M. Tape
34		43	CEC	----		0-50	0-50	Z		---				X								Rec. Oscill.
35		72	Statham	PM22D		±5	±5	Z		---				X								Rec. Oscill.
36		73	Statham	PM22D		±5	±5	Z		---				X								Rec. Oscill.

TABLE II. - TRANSDUCER INFORMATION

(b) Strain gages

Position	Figure showing position	Test no.									Transducer number (on data)	Vendor	Model	Strain sensitive	Test range	Record. method
		4	6	7	8	9	10	11	12	13						
1	6(d)	X									32	BLH	FAB 25-35	Bending	60,000 psi	Rec. Oscill.
2	6(d)	X									33		FAB 25-35	Bending	60,000 psi	Oscill.
3	6(d)	X									34		FAB 25-35	Torsion	35,000 psi	Oscill.
4	6(d)	X									35		FAB 25-35	Bending	60,000 psi	Oscill.
5	6(d)	X									36		FAB 25-35	Bending	60,000 psi	Oscill.
6	6(d)	X									37	BLH	FAB 25-35	Torsion	20,000 psi	Oscill.
7	6(d)	X									38	BLH	FAB 25-35	Bending	35,000 psi	Oscill.
8	6(d)	X									39	BLH	FAB 25-35	Bending	35,000 psi	Oscill.
9	6(d)		X								81	BUD	C12	Tension	700 μin./in.	F.M. Tape
10	6(d)		X								82	BUD	C12	Tension	700 μin./in.	F.M. Tape
11	6(d)		X								83	BUD	C12	Tension	2000 μin./in.	F.M. Tape
12	6(d)		X								84		C12		2000 μin./in.	
13	6(c)		X	X	X						61		C12-111		700 μin./in.	
14	6(c)		X	X							62		C12-111		700 μin./in.	
15	6(c)		X	X	X	X					63		C12-111		700 μin./in.	
16	6(c)		X	X	X						64	BUD	C12-121	Tension	2500 μin./in.	F.M. Tape
17	6(c)		X	X	X						65		C12-121		2500 μin./in.	
18	6(c)		X	X	X						66		C12-111		700 μin./in.	
19	6(c)		X	X	X						67		C12-111		700 μin./in.	
20	6(c)		X	X							68		C12-111		700 μin./in.	
21	6(c)		X	X	X	X					69	BUD	C12-121	Tension	700 μin./in.	F.M. Tape
22	6(c)		X	X	X	X					70		C12-121		700 μin./in.	
23	6(d)			X	X	X					91		C12		700 μin./in.	
24	6(d)			X	X	X					92		C12		1500 μin./in.	
25	6(d)			X	X	X					93		C12		600 μin./in.	
26	6(d)			X	X	X					94	BUD	C12	Tension	600 μin./in.	F.M. Tape
27	6(c)				X	X					81				1800 μin./in.	
28	6(c)				X	X					82				1800 μin./in.	
29	6(e)					X	X				121				4000 μin./in.	
30	6(e)					X	X				122				4000 μin./in.	
31	6(e)					X					123	BUD	C12	Tension	3000 μin./in.	F.M. Tape
32	6(e)					X					124				3000 μin./in.	
33	6(e)					X					125				3000 μin./in.	
34	6(e)					X					126				3000 μin./in.	
35	6(e)					X	X	X	X		93				600 μin./in.	
36	6(e)					X	X	X	X		84	BUD	C12	Tension	600 μin./in.	F.M. Tape
37	6(c)					X					81				2700 μin./in.	
38	6(c)					X					82				270 μin./in.	
39	6(e)						X				123				1000 μin./in.	
40	6(e)						X				124				1000 μin./in.	
41	6(e)						X				125	BUD	C12	Tension	1000 μin./in.	F.M. Tape
42	6(e)						X				126				1000 μin./in.	
43	6(c)						X	X	X	X	131				600 μin./in.	
44	6(c)						X	X	X	X	132				600 μin./in.	
45	6(c)						X	X	X	X	133				1800 μin./in.	
46	6(c)						X	X	X	X	134	BUD	C12	Tension	1800 μin./in.	F.M. Tape
47	6(c)						X		X	X	135				1000 μin./in.	F.M. Tape
48	6(c)						X		X	X	136				1000 μin./in.	F.M. Tape
49	6(c)							X			135				2000 μin./in.	F.M. Tape
50	6(c)							X			136				2000 μin./in.	Rec. Oscill. F.M. Tape Rec. Oscill.
51	6(e)							X			141	BUD	C12	Tension	4000 μin./in.	F.M. Tape Rec. Oscill.
52	6(e)							X			142					F.M. Tape
53	6(e)							X	X		143					F.M. Tape
54	6(e)							X	X		144					F.M. Tape
55	6(e)							X			145					F.M. Tape
56	6(e)							X			146	BUD	C12	Tension	4000 μin./in.	F.M. Tape
57	6(e)									X	152					
58	6(e)									X	154					
59	6(e)									X	155					
60	6(e)									X	156					
61	6(e)									X	160	BUD	C12	Tension	4000 μin./in.	F.M. Tape
62	6(e)									X	161					
63	6(e)									X	162					
64	6(e)									X	166					
65	6(e)									X	167					
66	6(e)									X	168	BUD	C12	Tension	1000 μin./in.	F.M. Tape
67	6(e)									X	169	BUD	C12	Tension	1000 μin./in.	F.M. Tape

Table III

Maximum Hinge Dynamic Loads

Test Number	Maximum Vertical Hinge Load Compression		Maximum Vertical Hinge Load Tension		Maximum Radial Hinge Load Compression		Hinge Pin Clearance
	Load	Fairing Rotation	Load	Fairing Rotation	Load	Fairing Rotation	
	Lbs.	Degrees	Lbs.	Degrees	Lbs.	Degrees	Inches
7	5080	1.0	987	9.6	no data	---	.030
8	2850	1.0	2730	16.0	no data	---	.027
9*	6670	0.7	1181	9.0	no data	---	.047
10	2601	1.1	no data	---	1500	0.2	.127
11	3365	1.8	none	---	1200	2.4	.127
12	2070	0.7	none	---	850	2.4	.127
13	2698	0.8	no data	---	1350	0.7	.127

* Thrustor compartment overpressure proof test

E-3265

Table IV

Thermal Bulkhead Struts Damaged During Nose Fairing Separation Tests

Test Number	Damaged Struts Position as per Sketch	Type of Failure
7	8	Compression bending of strut at connection to fairing
8	3, 5	Damage to both same as test 7
9	2, 3, 4 and 8	Struts 3, 4, and 8 broken at fairing bracket connection Strut 2 bent in center
10	2, 3	Struts bent at center
11	3	Strut broke at fairing bracket connection
12	3	Strut bent at fairing bracket connection
13	3	Strut bent in center

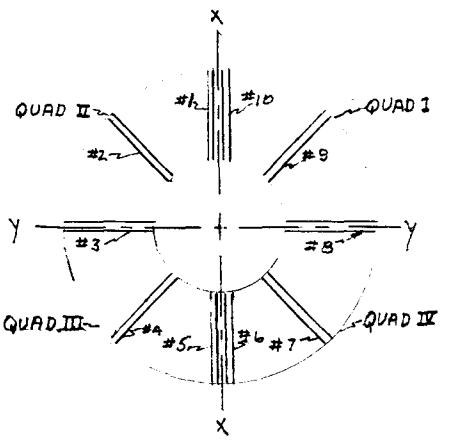

Table V

Maximum Stresses on Thermal Bulkhead Struts

Strut No.	Test No.	Stress* PSI	Rotation of Fairing at Occurrence Degrees	Strain Gage No. (as per fig. 6C)	Gage Locations on Strut
8	9	18,700	0.5	122	top
8	10	21,700	0.8	122	top
3	10	21,700	0.8	121	top
6	11	4,400	1.0	141	top
6	11	5,200	0.9	142	bottom
8	11	16,450	0.8	143	top
8	11	17,000	0.8	144	bottom
3	11	15,100	0.8	145	top
3	11	16,450	0.8	146	bottom
8	12	9,400	0.6	143	top
8	12	10,200	0.6	144	bottom
2	13	7,900	0.5	152	top
3	13	24,400	0.5	154	left side
3	13	23,000	0.5	155	top
3	13	20,300	0.5	156	right side
8	13	18,900	0.5	160	left side
8	13	17,000	0.4	161	top
8	13	17,500	0.4	162	right side
9	13	36,800	0.4	166	top
9	13	-34,400	0.4	167	bottom

* Tension is positive

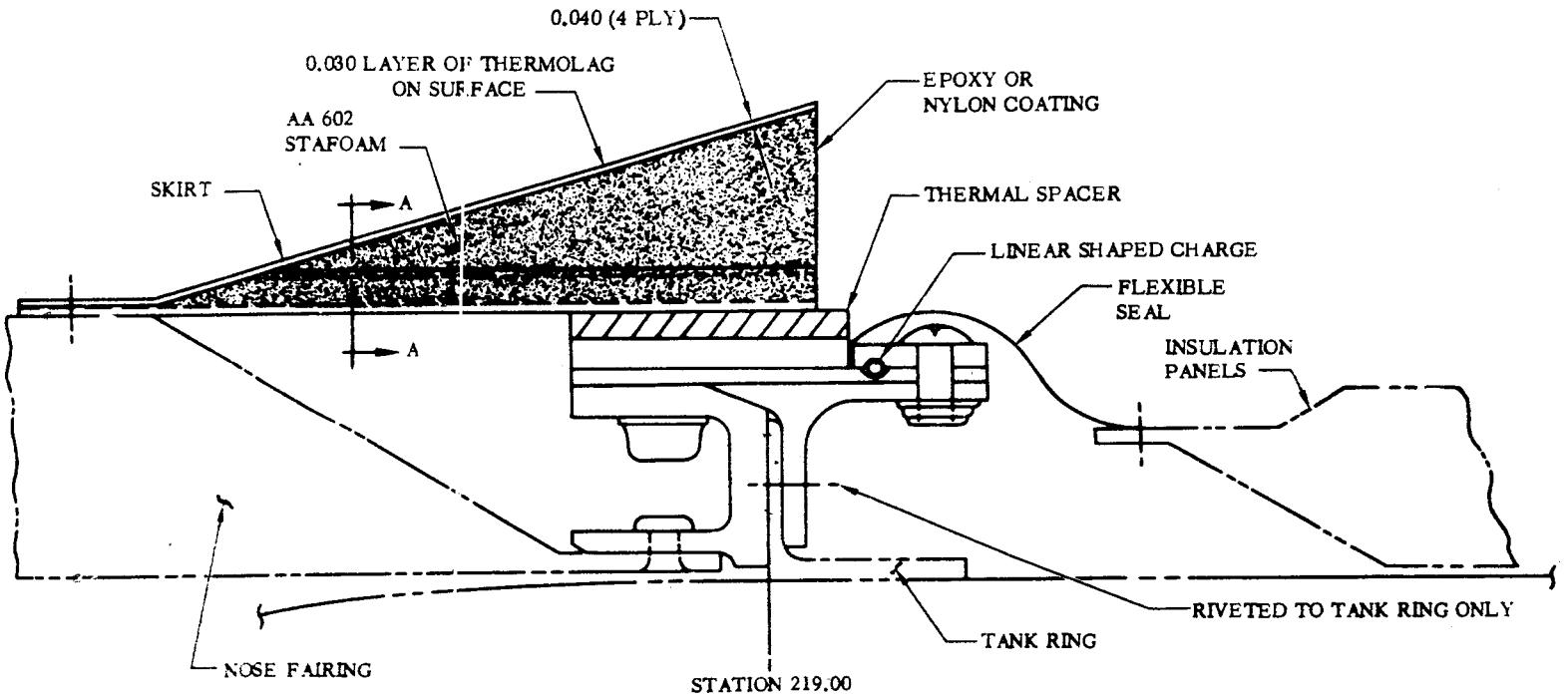

(a) Nose fairing skirt and station 219 ring assembly.

Figure 1. - Details of test article.

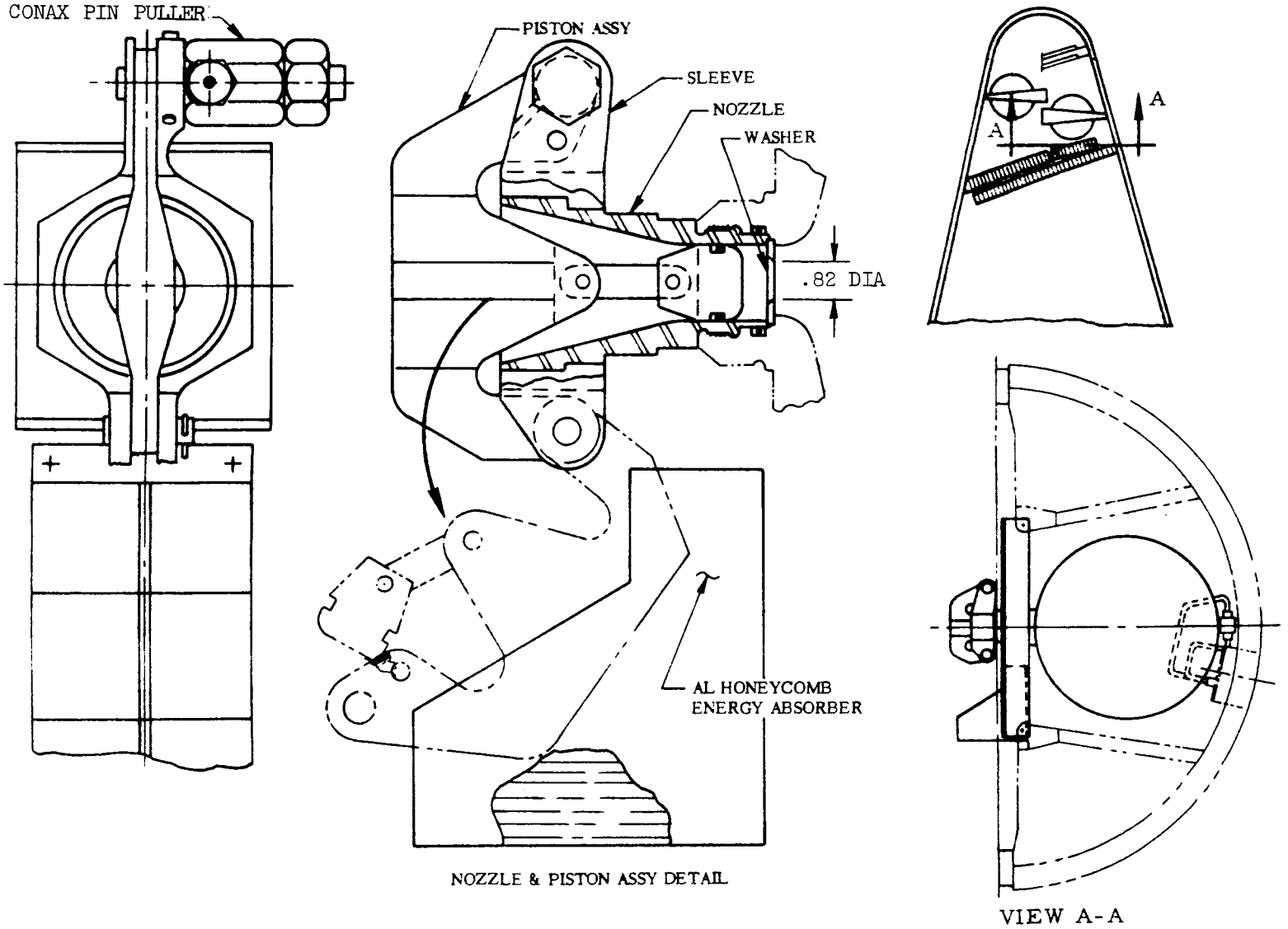

(b) Thruster bottle assembly.

Figure 1. - Continued.

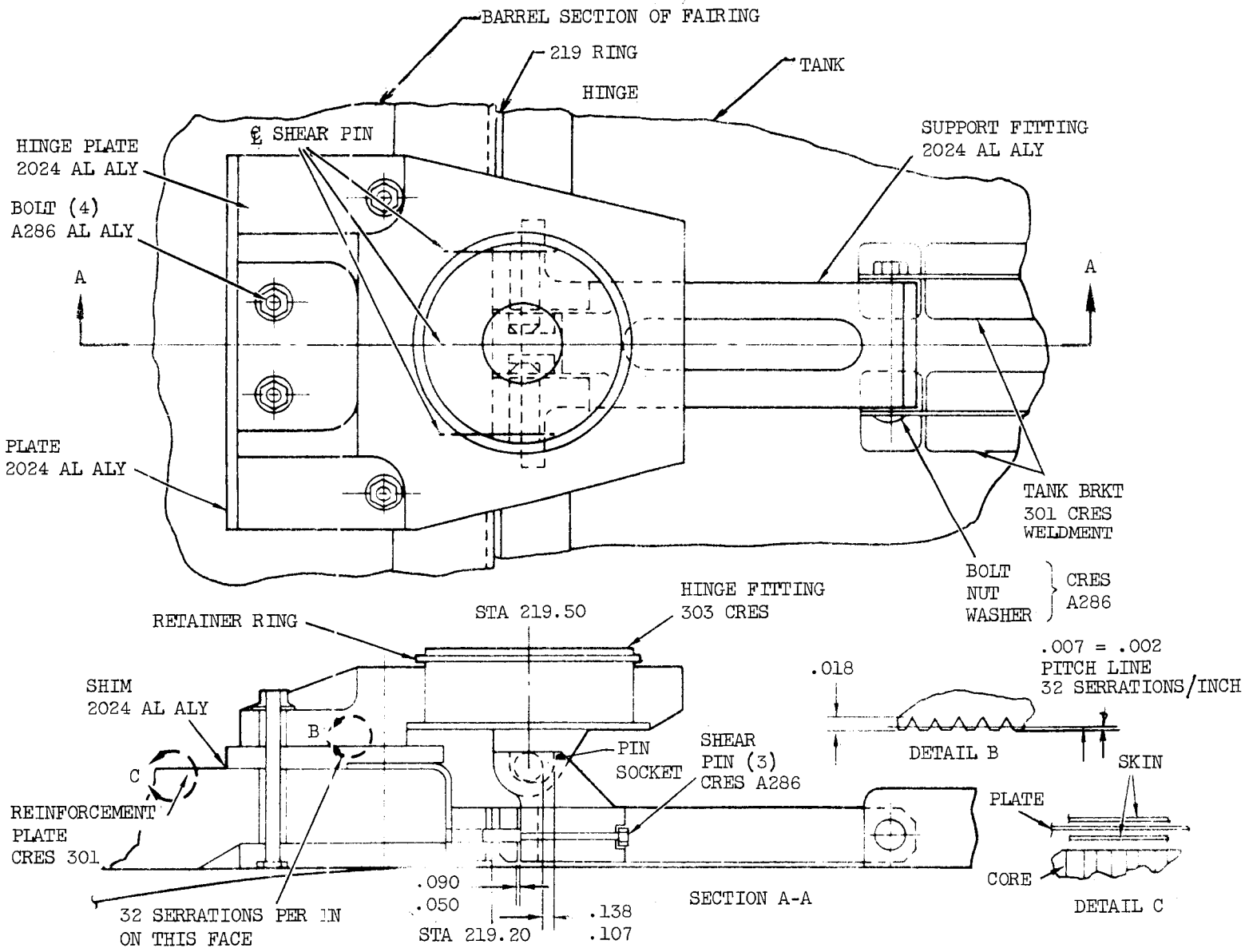

(c) Flight hinge.

Figure 1. - Continued.

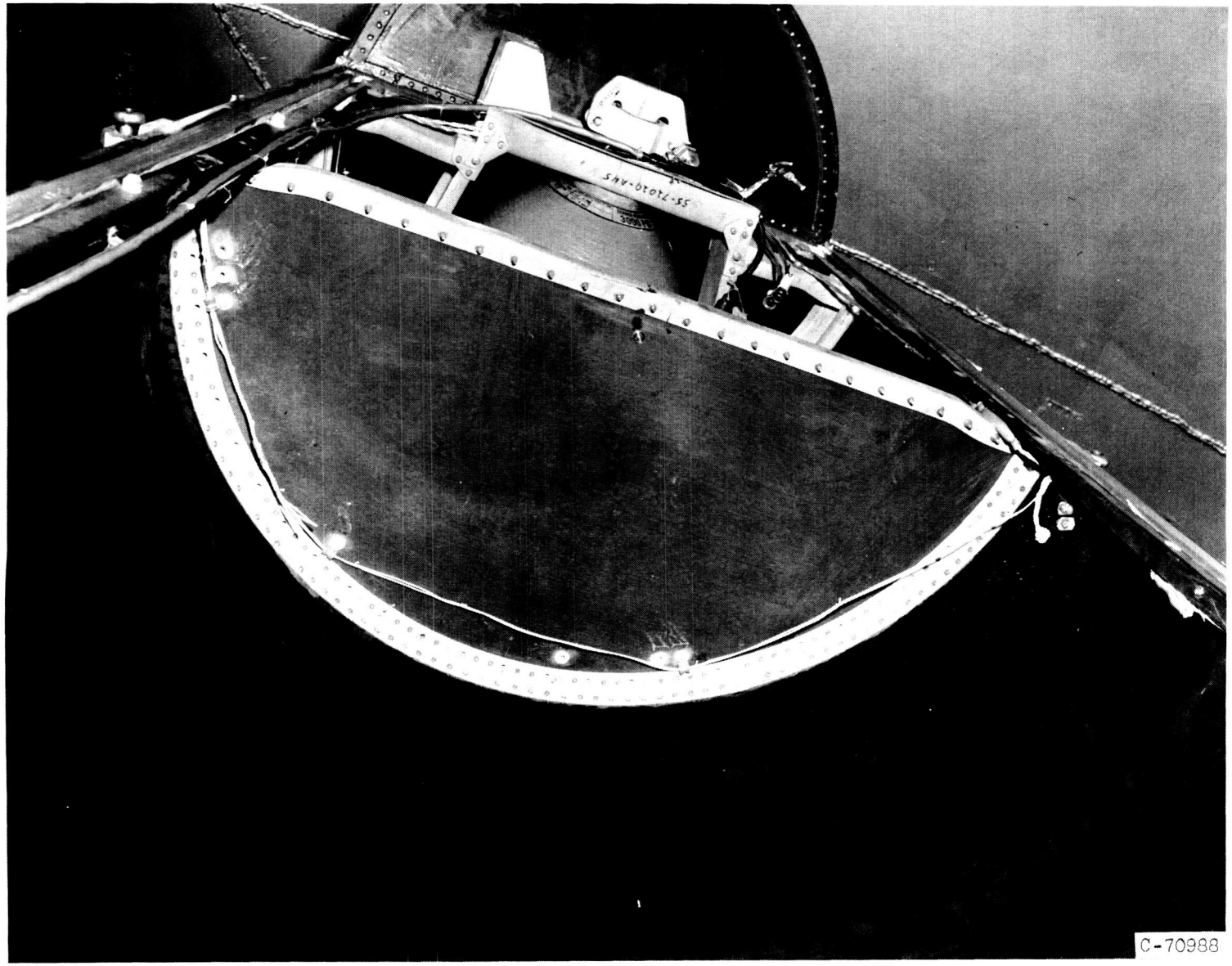

(d) Deflector bulkhead-AC3 type.

Figure 1. - Continued.

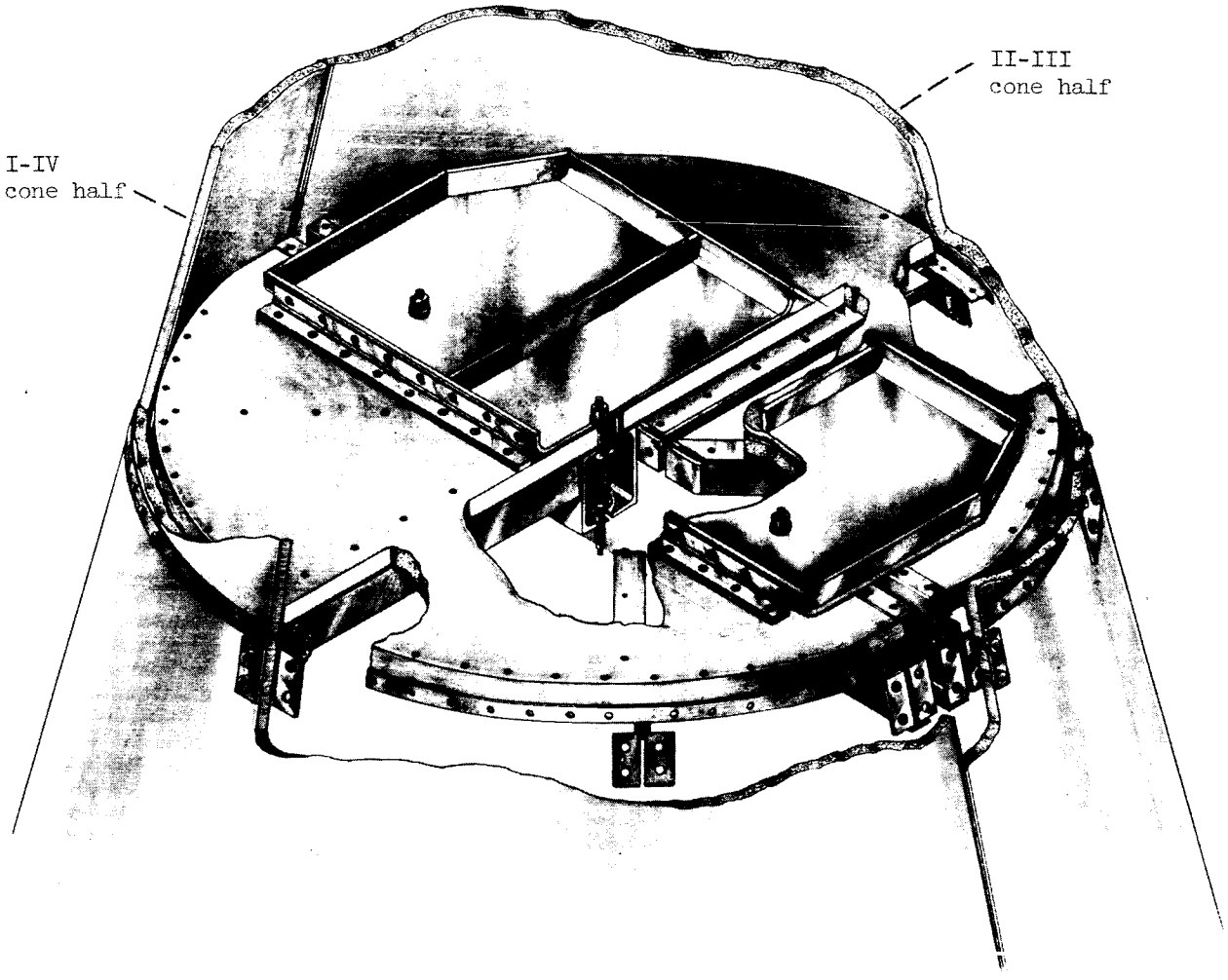

(e) Deflector bulkhead, NASA design.

Figure 1. - Continued.

DEFLECTOR BULKHEAD INSTALLATION
55-71258

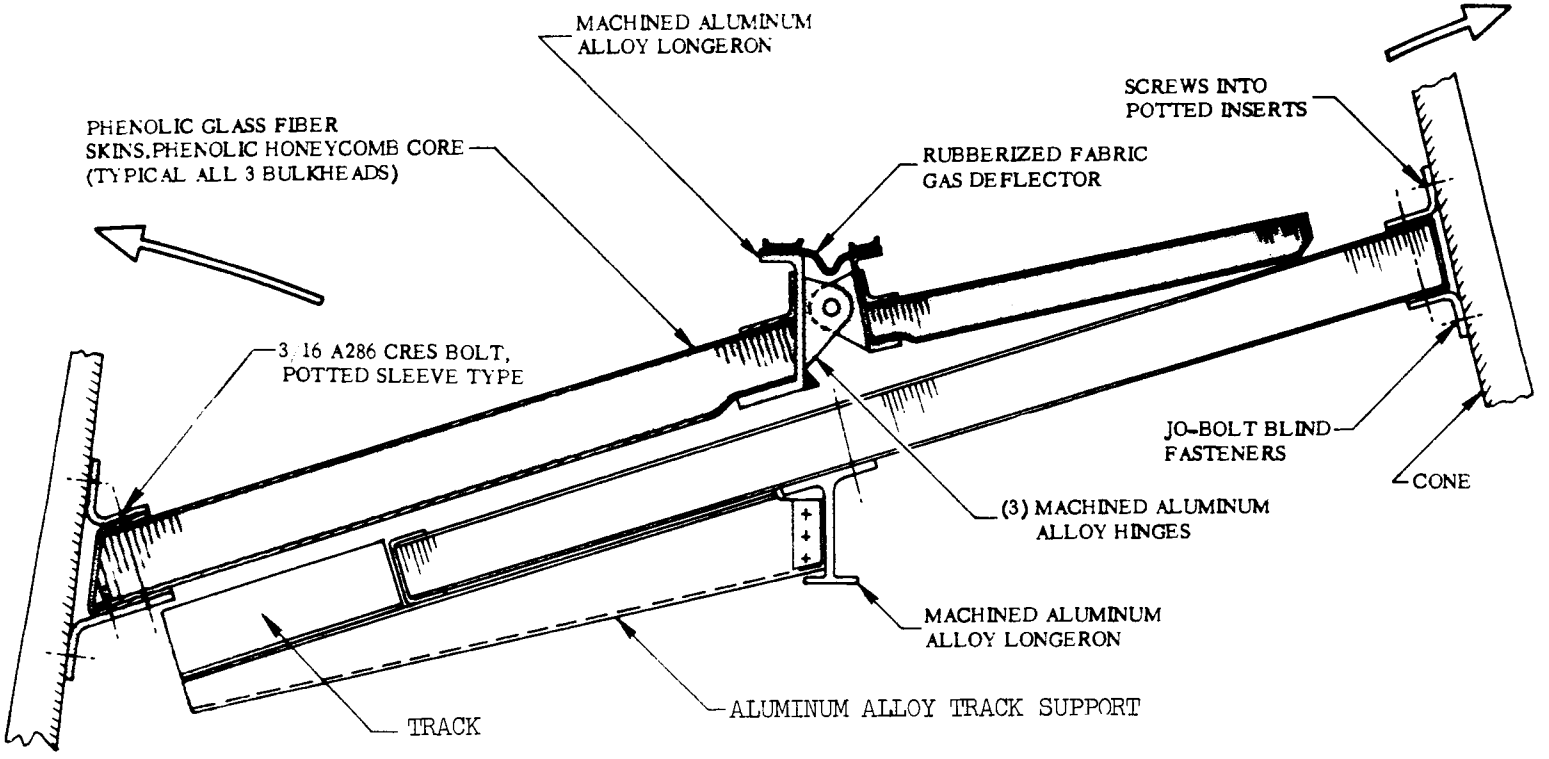

(f) Deflector bulkhead-AC4 type.

Figure 1. - Continued.

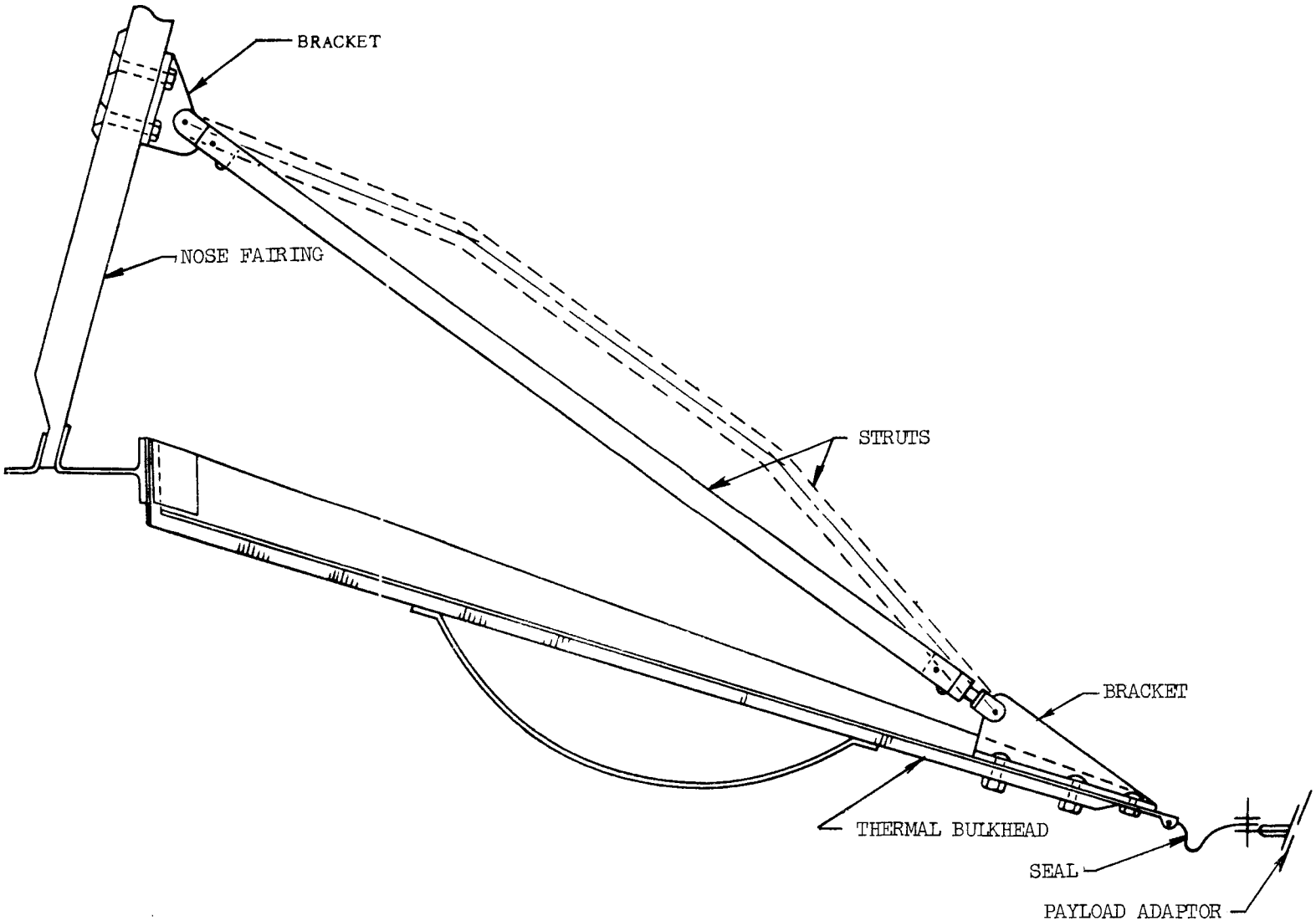

(g) Thermal bulkhead and struts.

Figure 1. - Concluded.

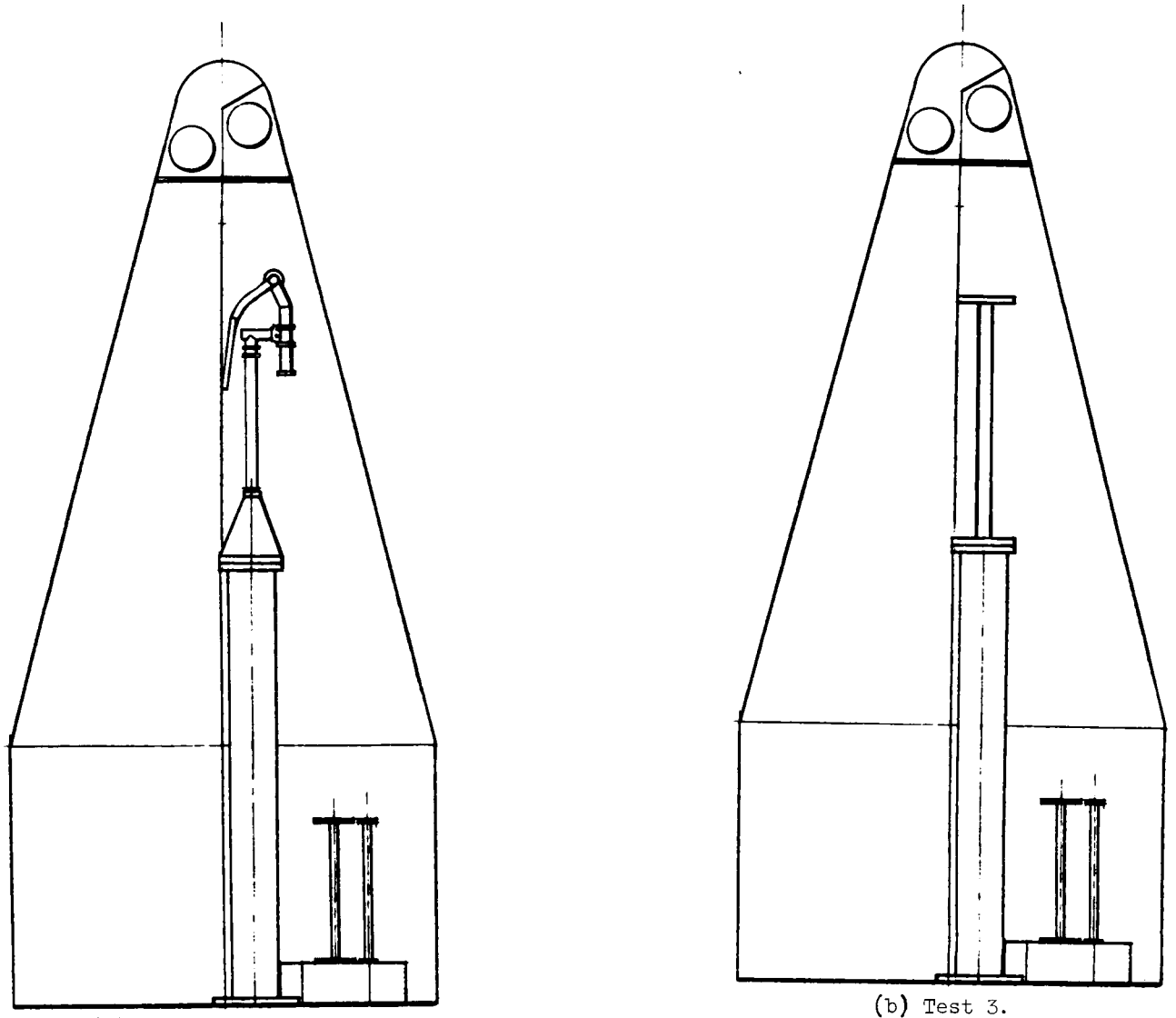

(a) Test 1 and Test 2.

(b) Test 3.

Figure 2. - Test article configuration.

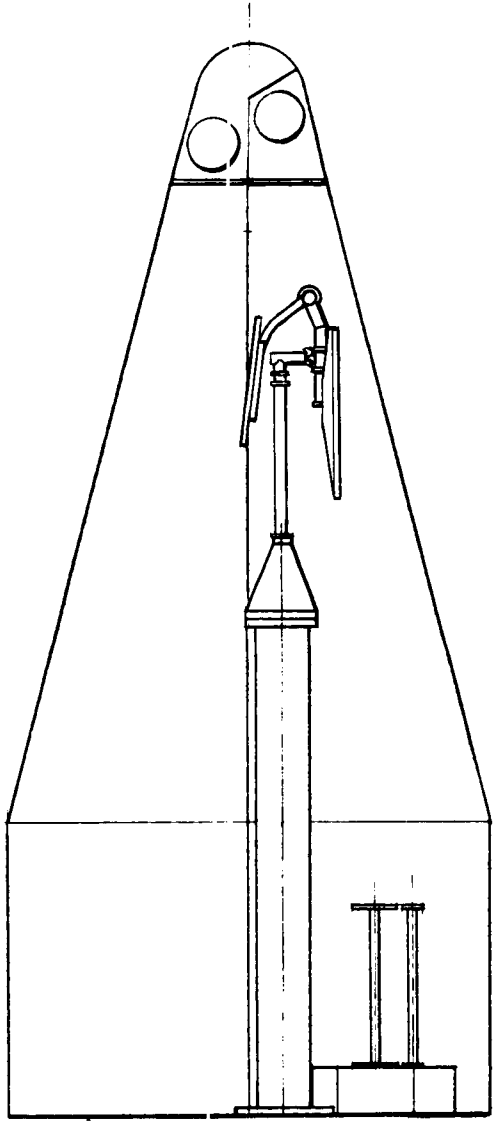

(c) Test 4.

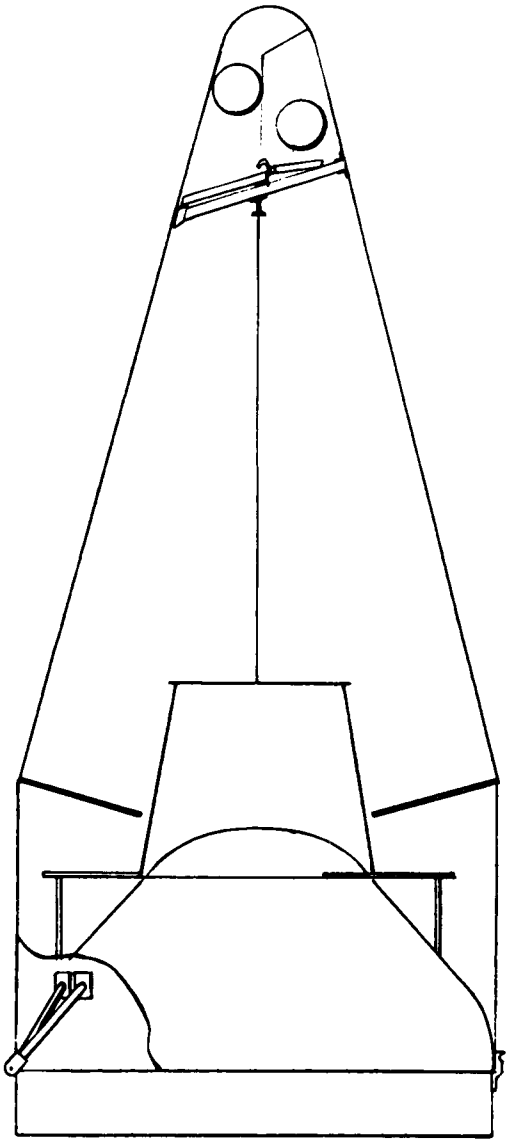

(d) Test 6.

Figure 2. - Continued.

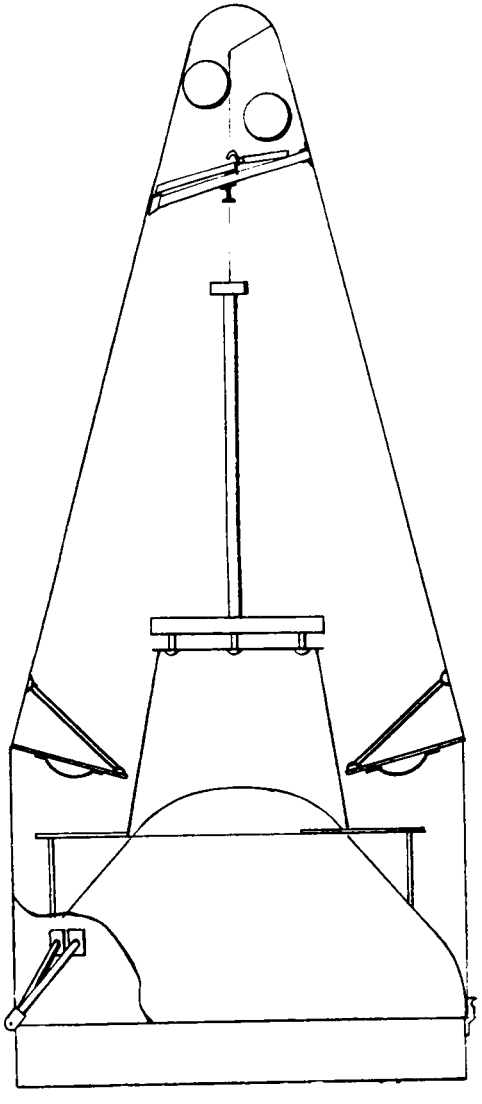

(e) Test 7 and Test 8.

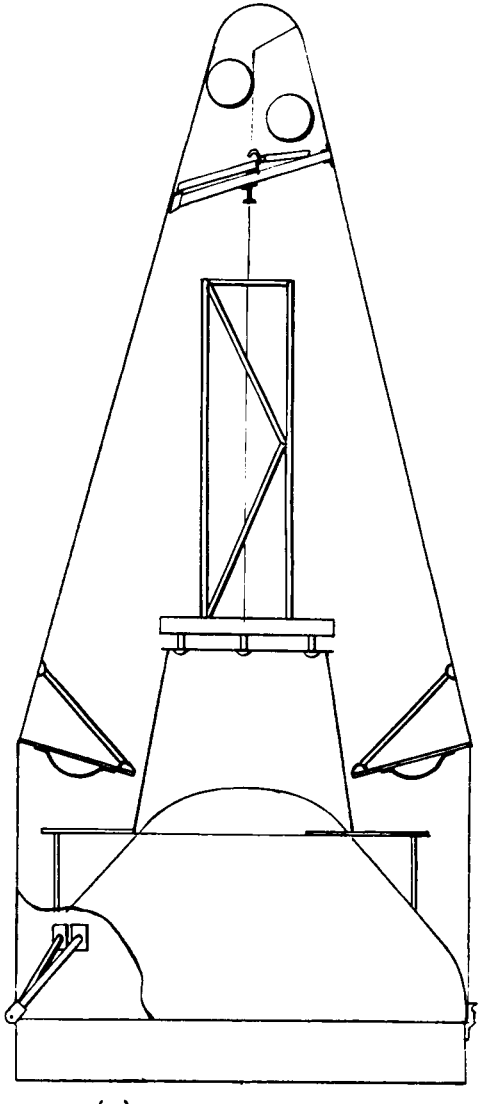

(f) Test 9 through 13.

Figure 2. - Concluded.

CD-8032

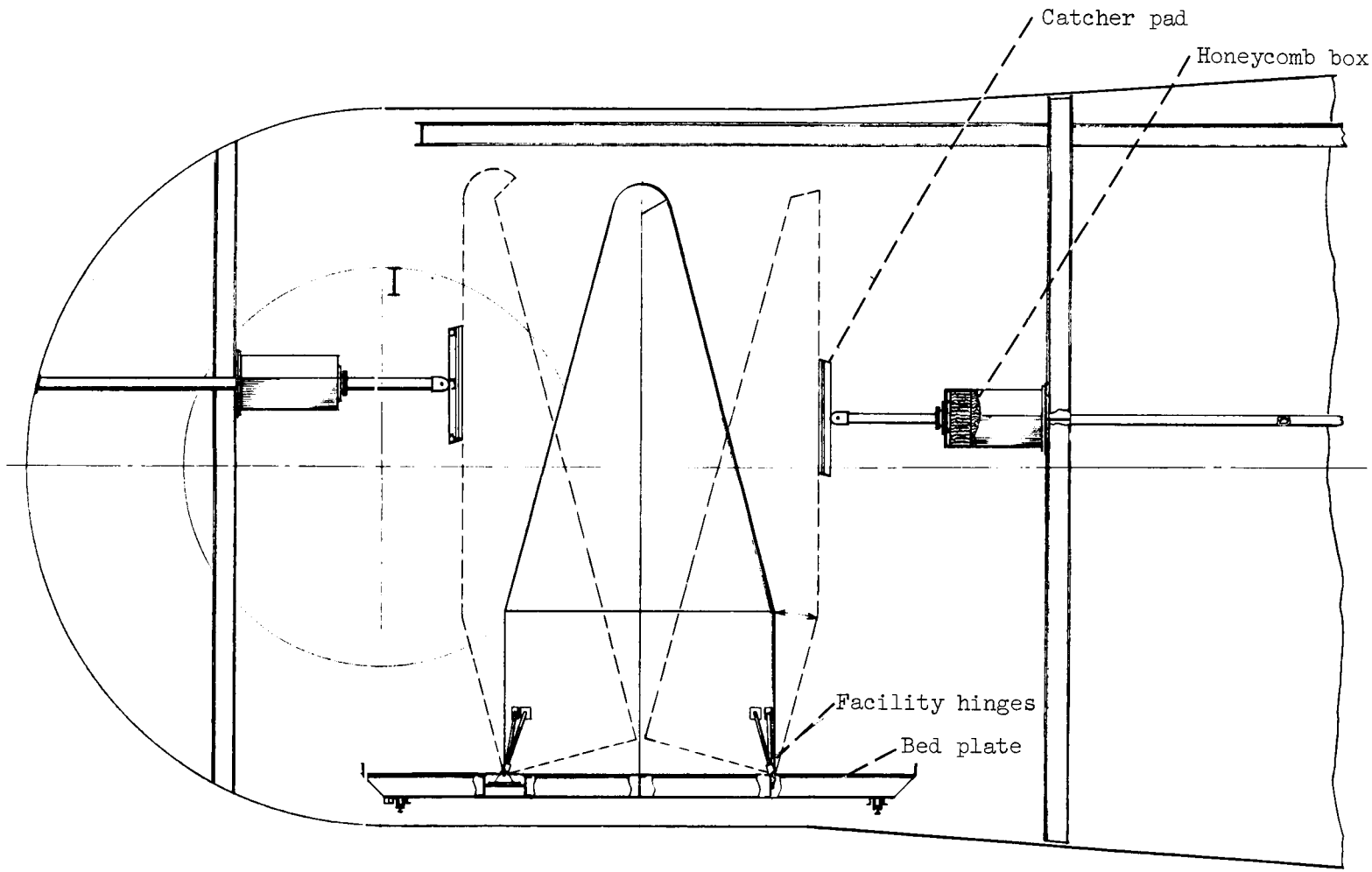

(a) Tests 1 through 4.

CD-8005

Figure 3. - Facility configuration.

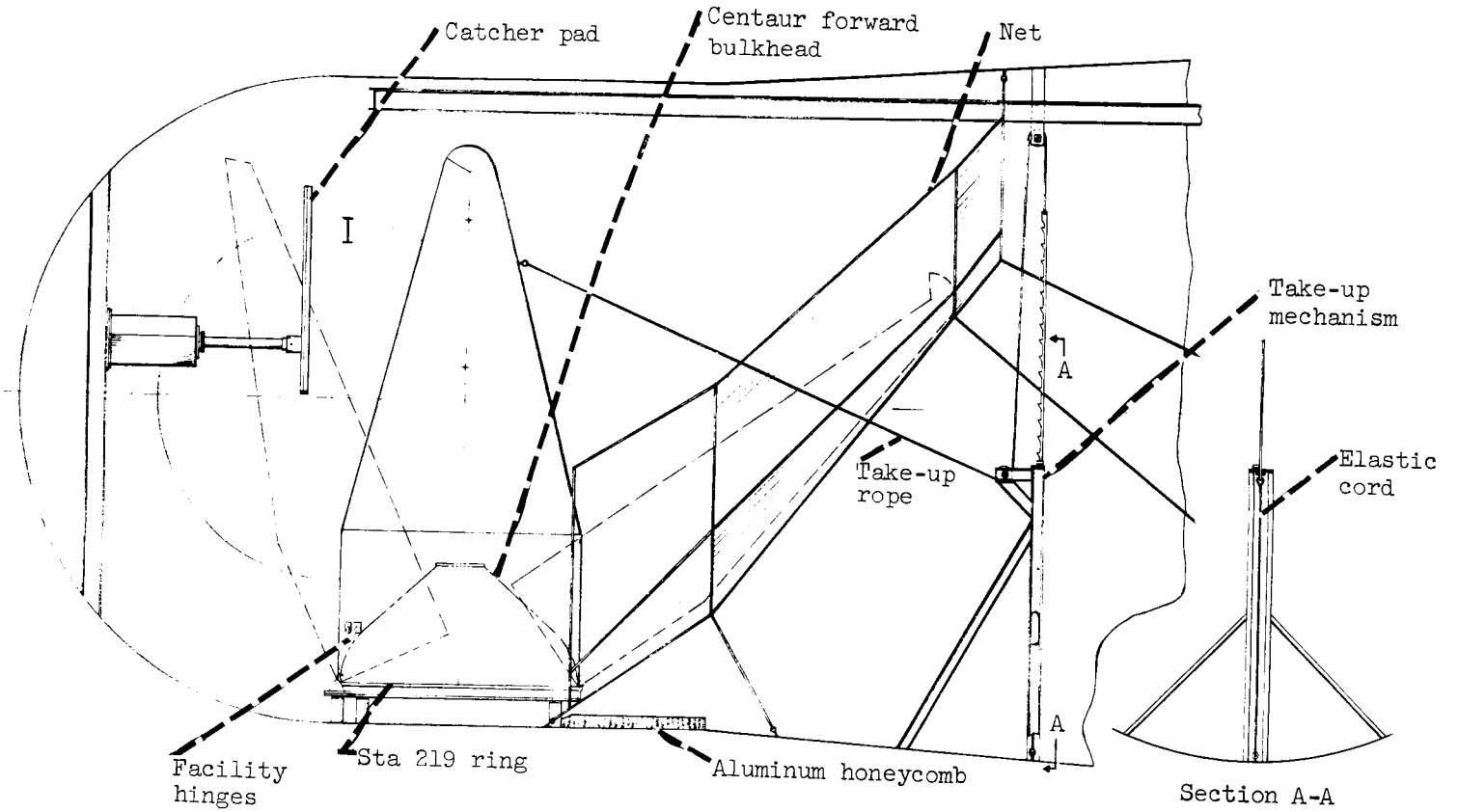

(b) Tests 6 through 13.

CD-8003

Figure 3. - Concluded.

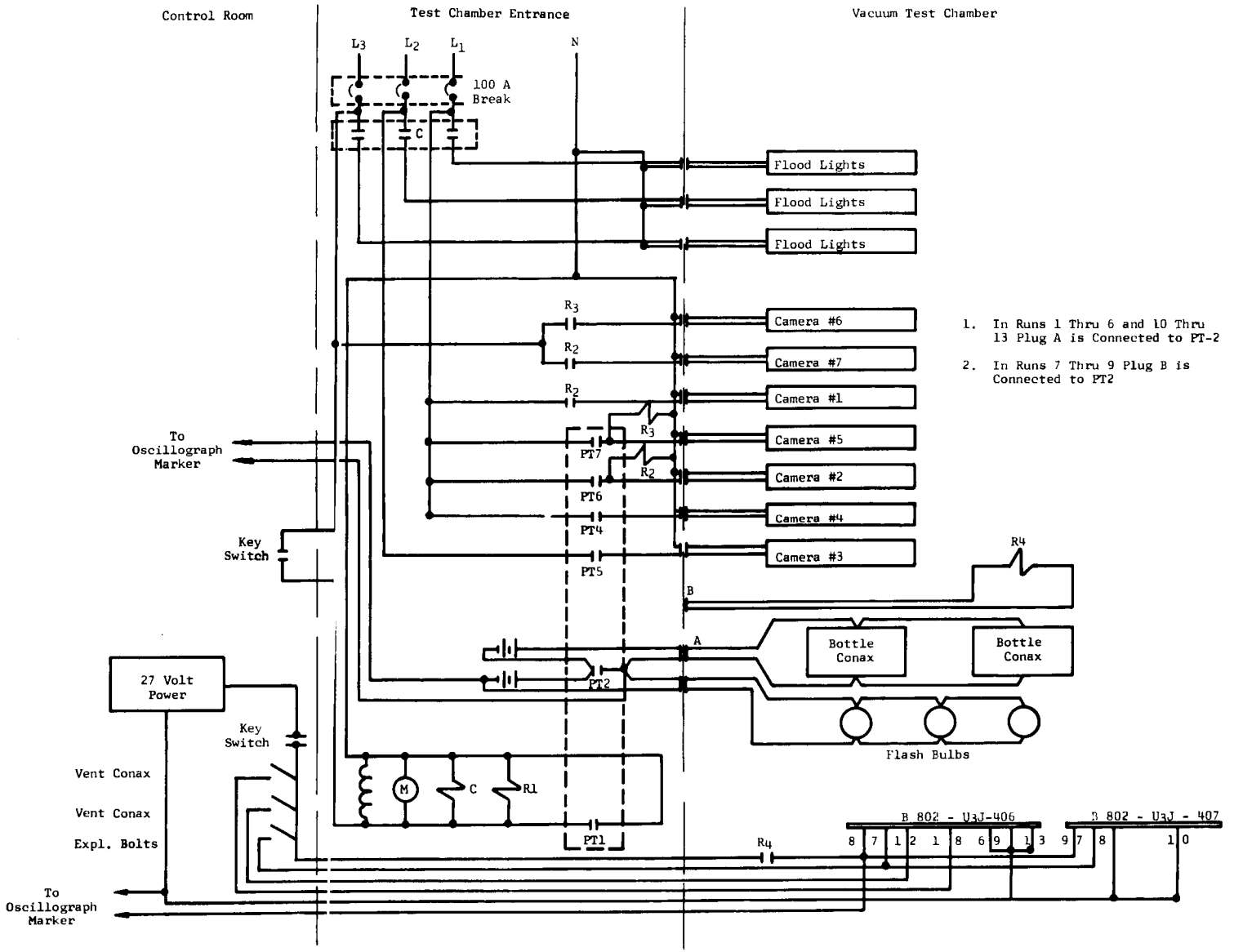

Figure 4. - Facility electrical system.

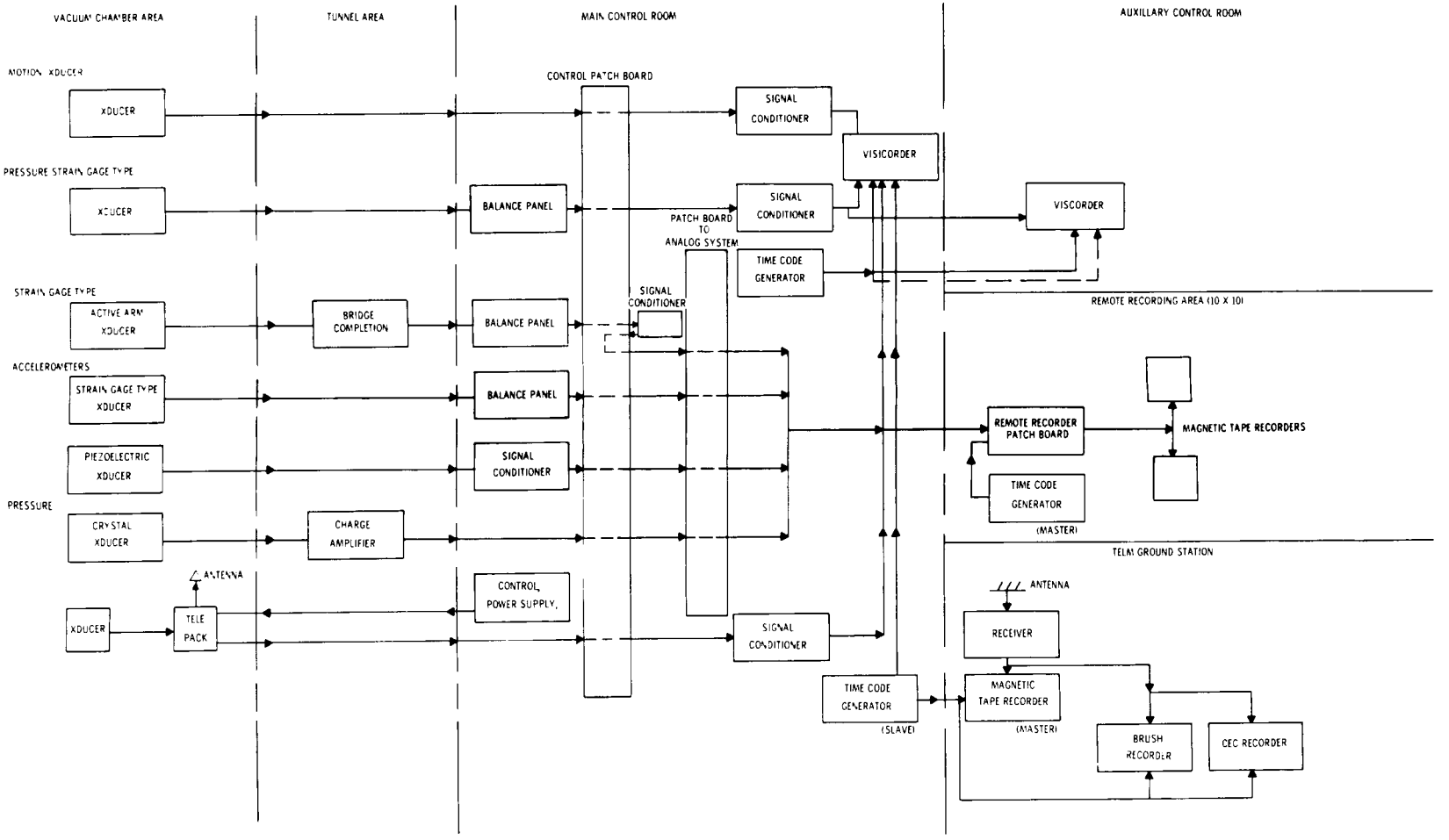

Figure 5. - Instrumentation block diagram.

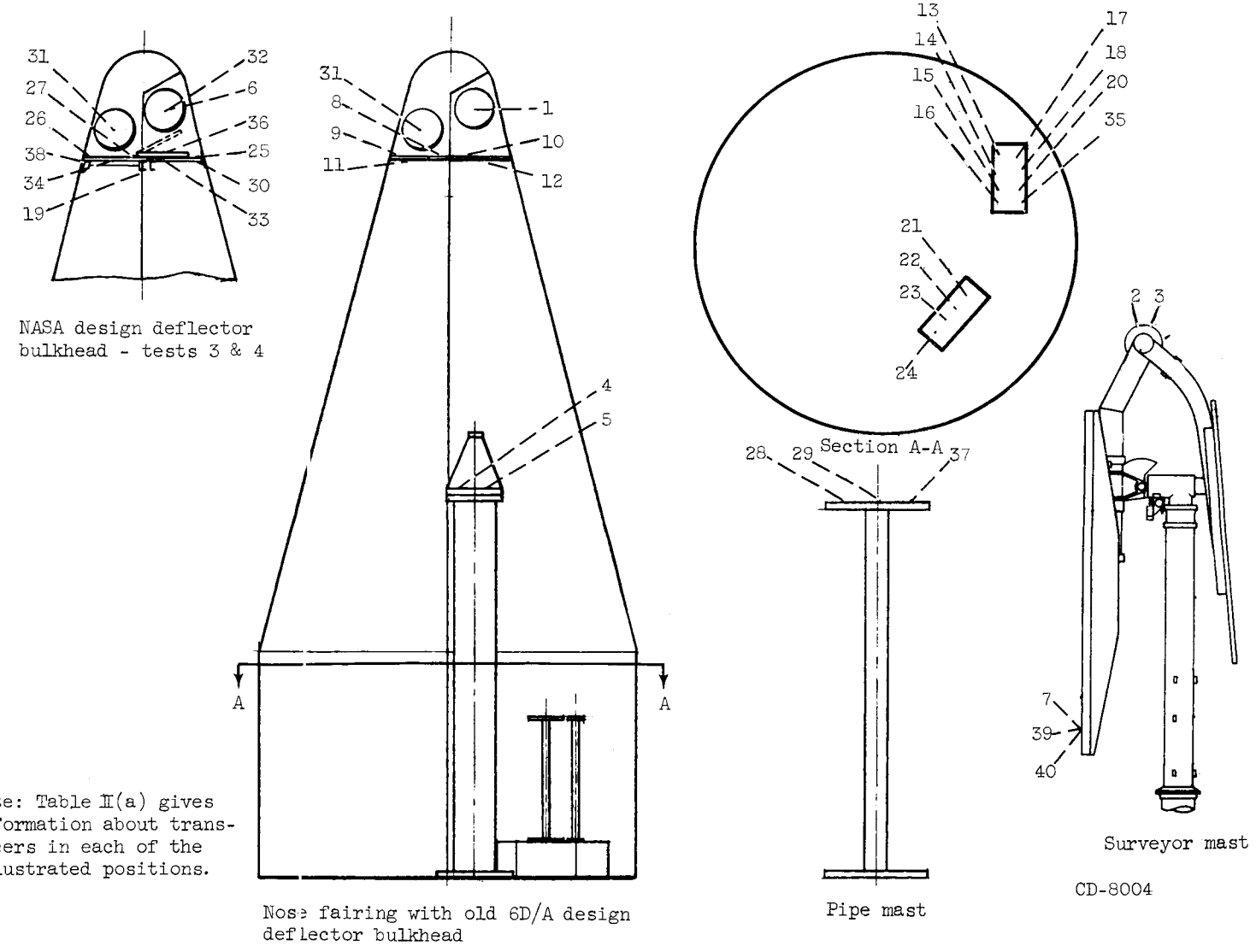

Note: Table II(a) gives information about transducers in each of the illustrated positions.

(a) Table I(a) transducers for tests 1 through 4.

Figure 6. - Diagram of transducer locations.

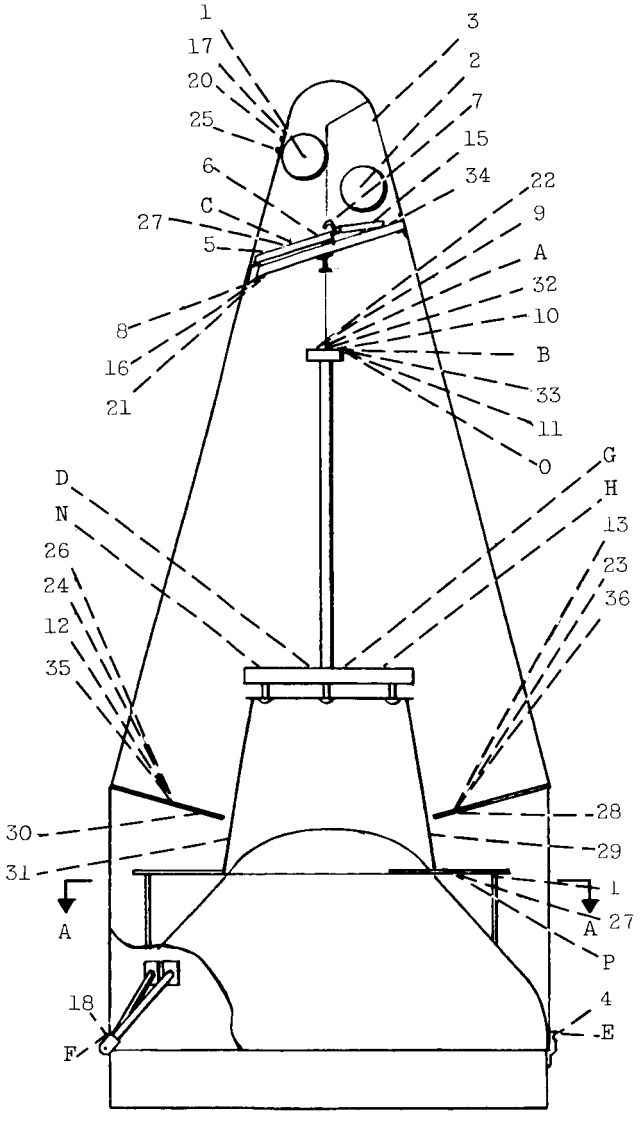

Note: Table II(a) gives information about transducers in each of the illustrated positions.

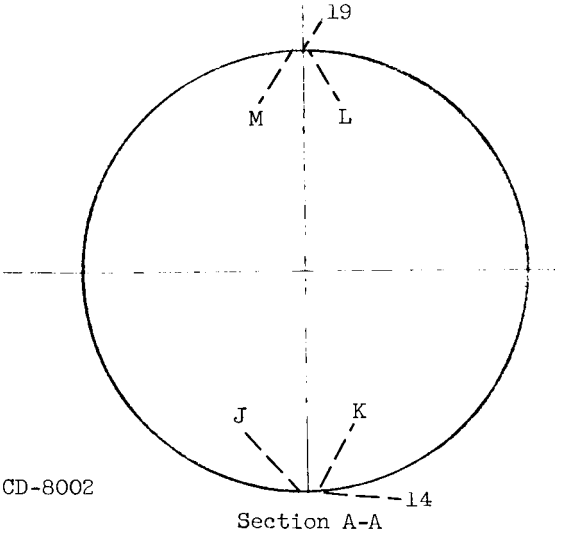

(b) Table II(a) transducers for tests 6 through 13.

Figure 6. - Continued.

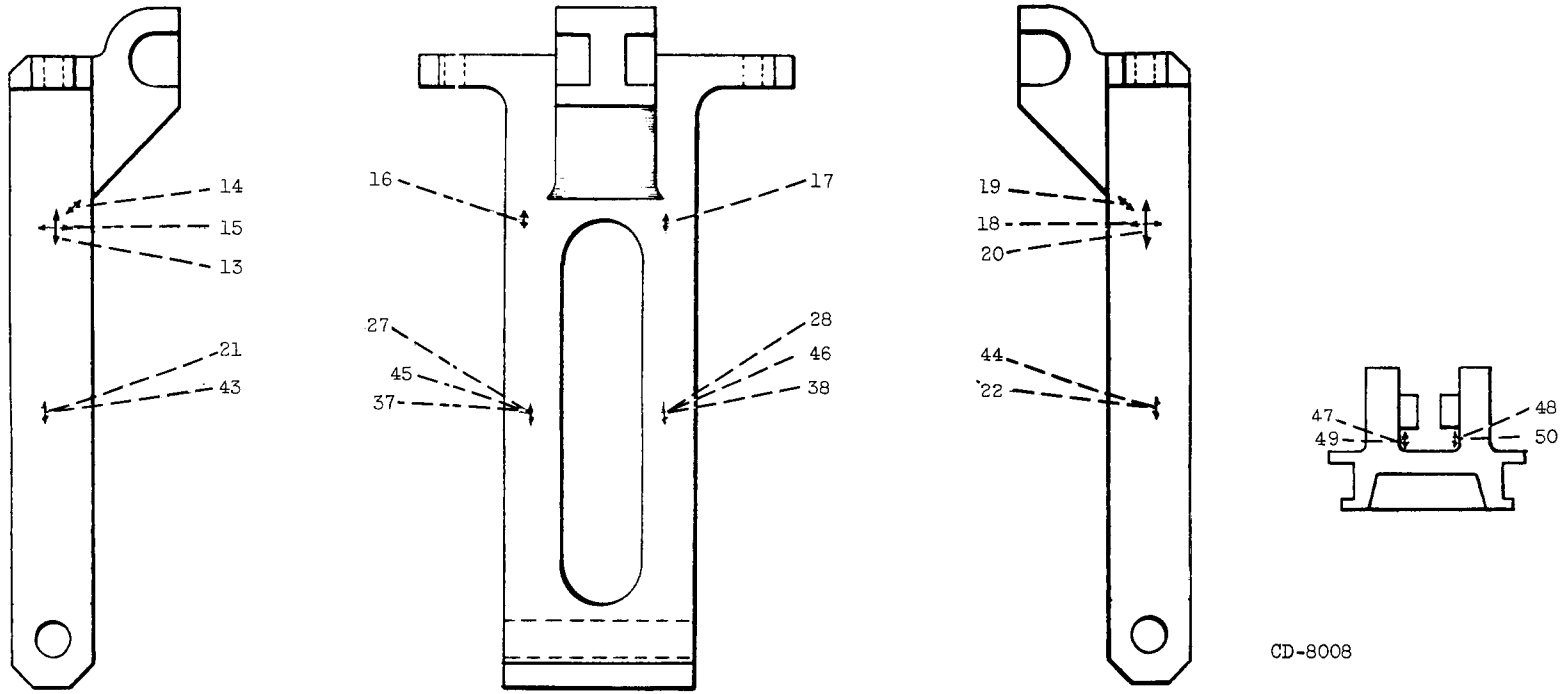

Flight hinge - tank half

Flight hinge - fairing half

Note: Table II(b) gives information about strain gages in each of the illustrated positions.

(c) Strain gage locations for all tests as per Table I(b)

Figure 6. - Continued.

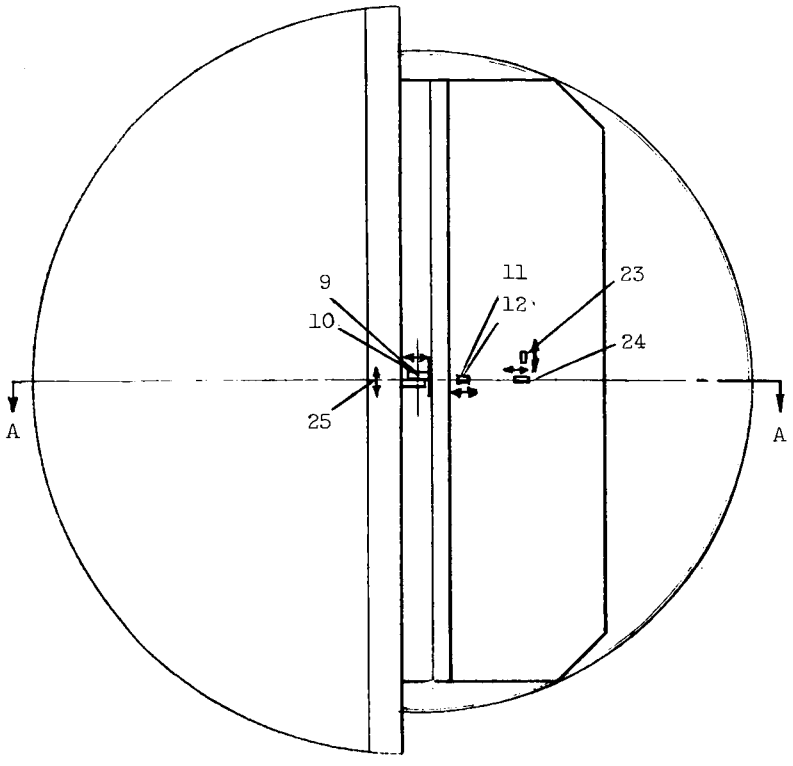

CD-8007

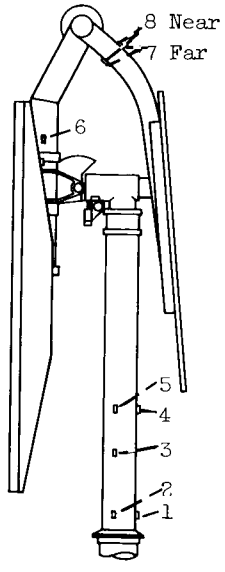

Surveyor mast

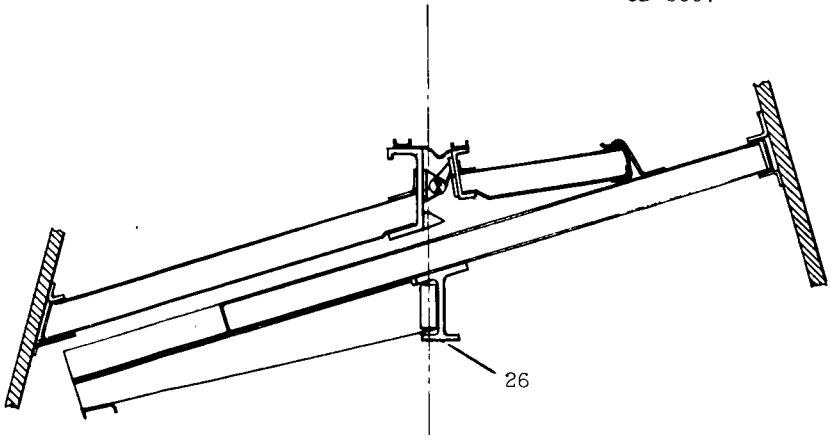

Section A-A

Deflector bulkhead

(d) Strain locations for all tests as per Table II(b).

Figure 6. - Continued.

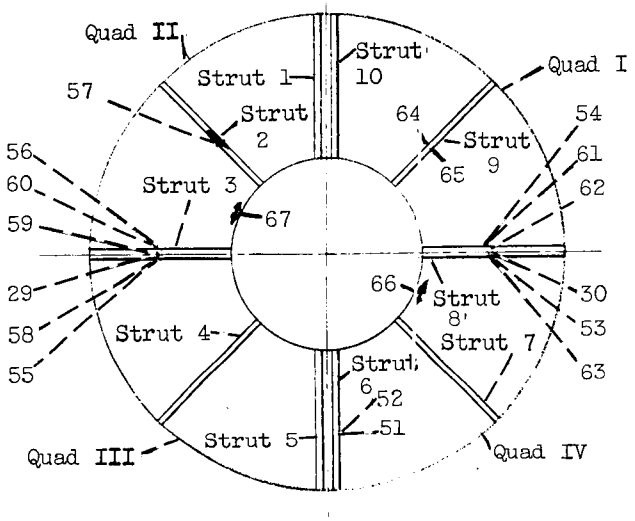

Strain gages on thermal bulkhead and struts

(All gages on struts in tension along axis of struts)

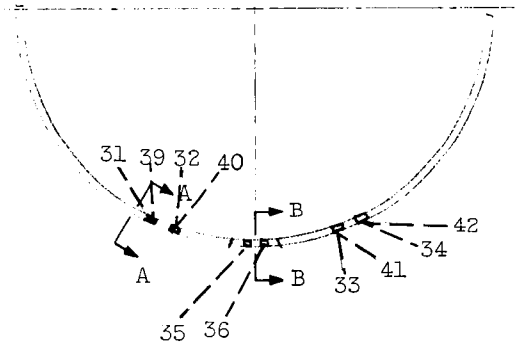

CD-8006

219 Ring

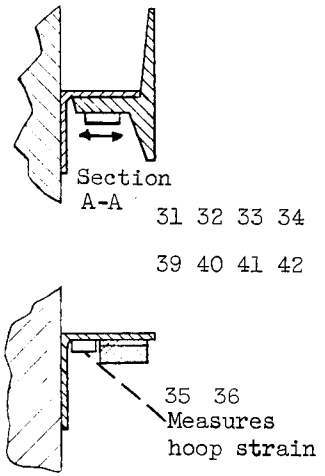

Section B-B

(e) Table II (b) strain gages for all tests.

Figure 6. - Concluded.

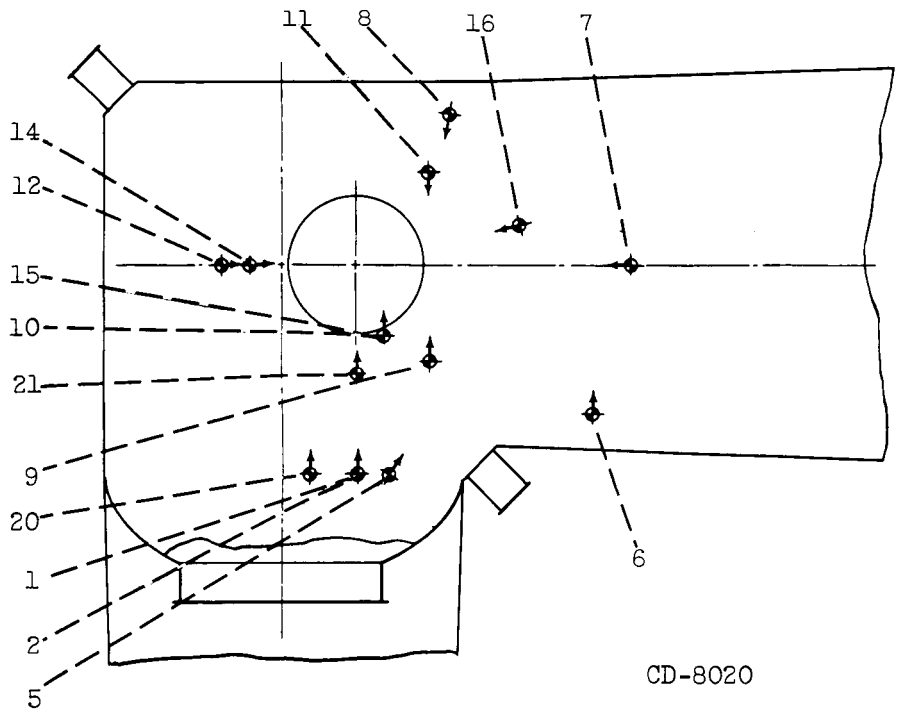

Camera position	Camera height above 219 ring	Camera angle with horizon
1	4'6"	+35°
2	2'6"	0
3	8'	60°
4	6'	70°
5	4'6"	30°
6	11'	0
7	21'	-10°
8	0	0
9	3'	-10°
10	21'	-90°
11	0	0
12	3'	15°
13	7'6"	90°
14	4'	10°
15	21'	-75°
16	0	15°
17	11'	-75°
18	17'	-75°
19	17'	-75°
20	4'6"	30°
21	6'	0

(a) Outside of nose fairing.

Figure 7. - Camera locations for all nose fairing tests.

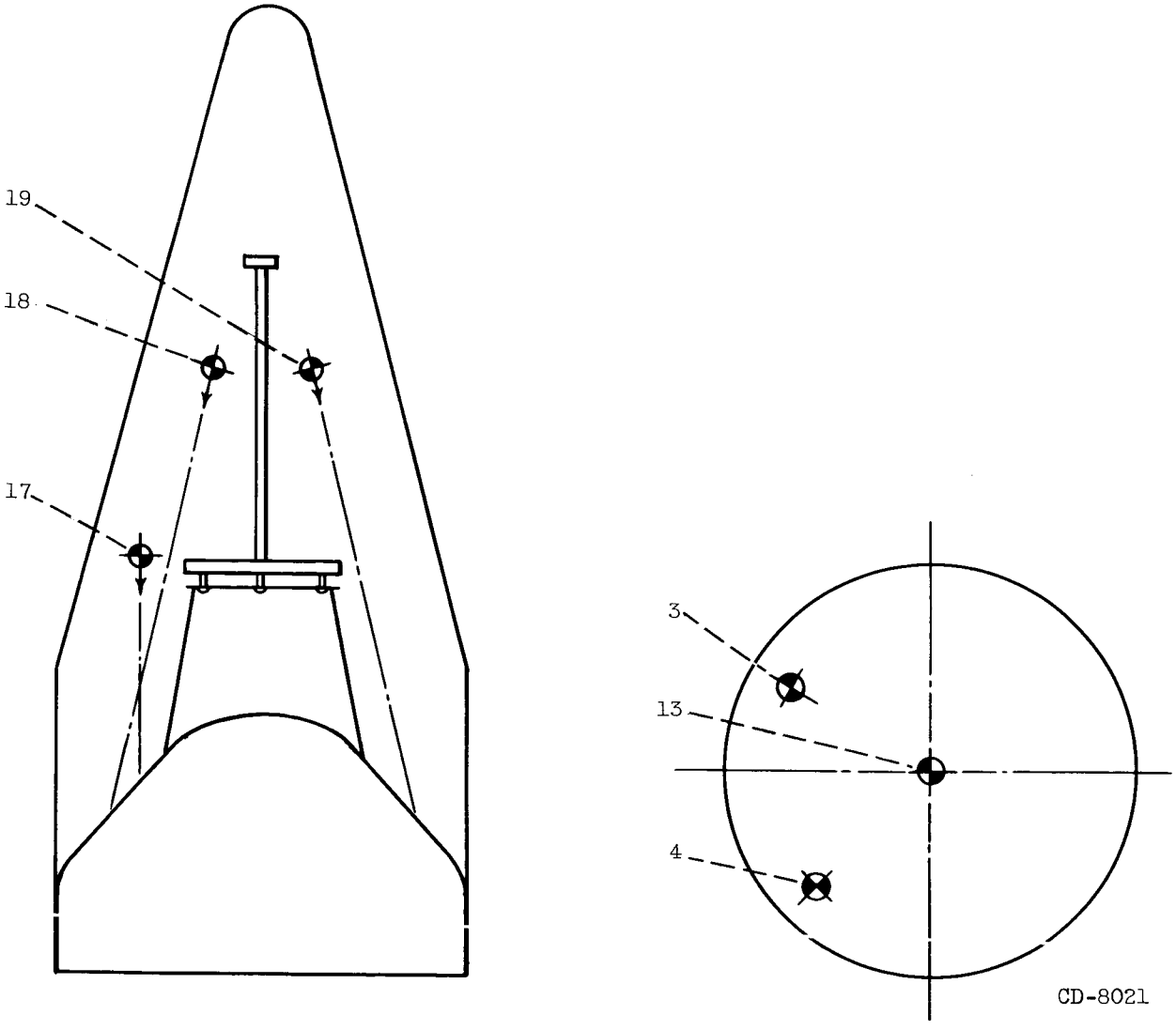

(b) Inside nose fairing.

Figure 7. - Concluded.

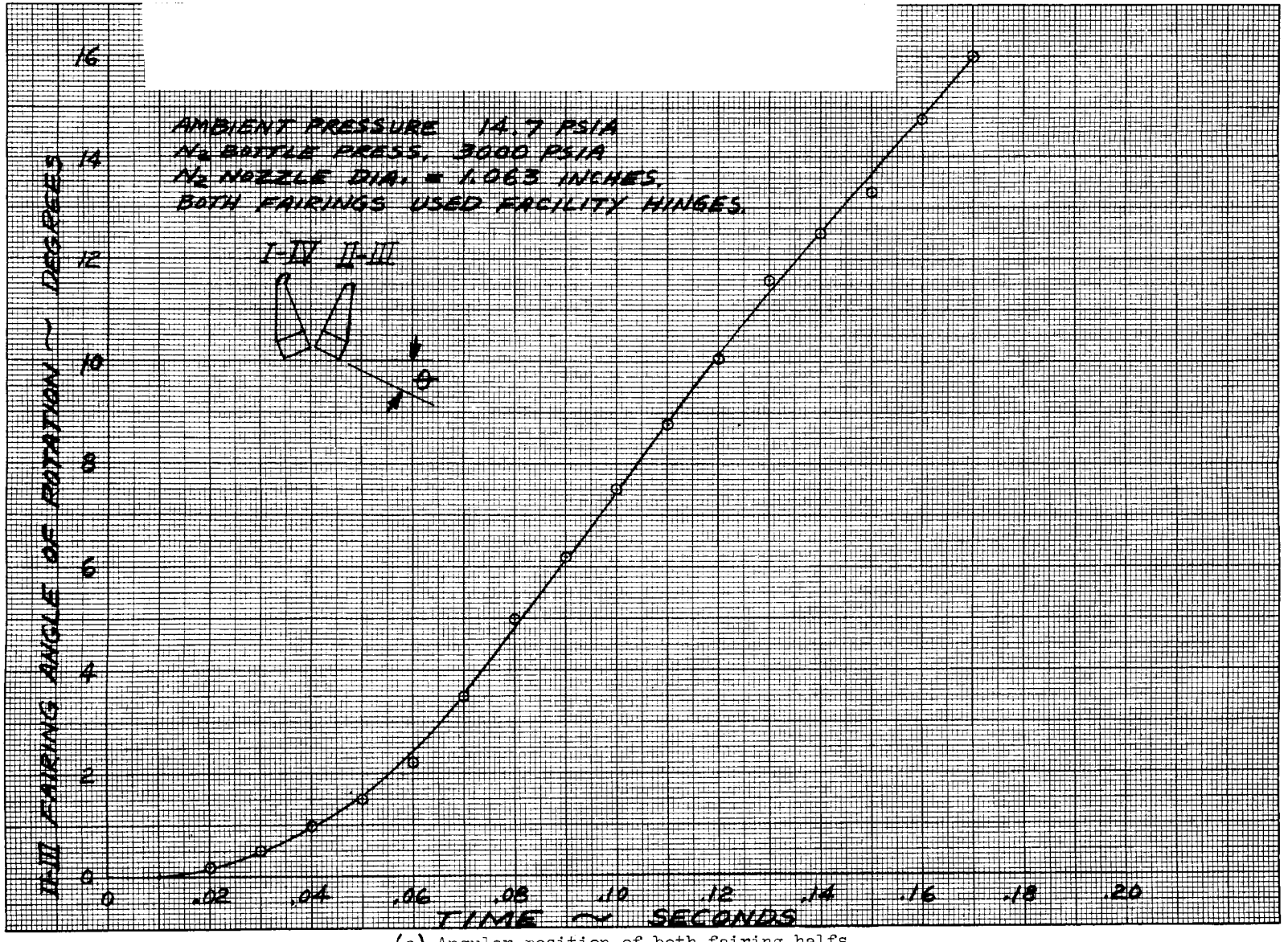

(a) Angular position of both fairing halfs.

Figure 8. - Centaur nose fairing trajectory. Test 1.

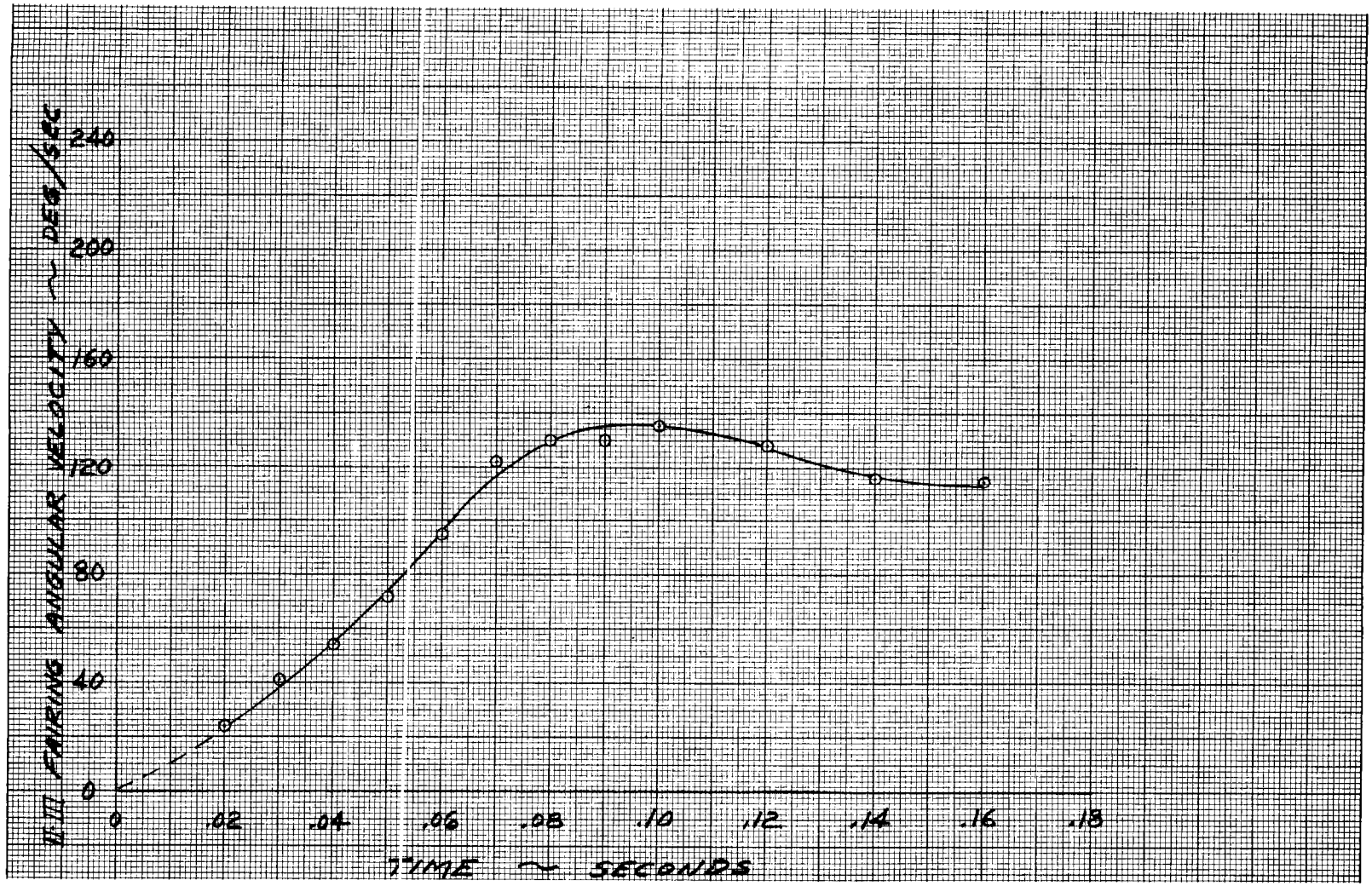

(b) Angular velocity of both fairing halfs.

Figure 8. - Concluded.

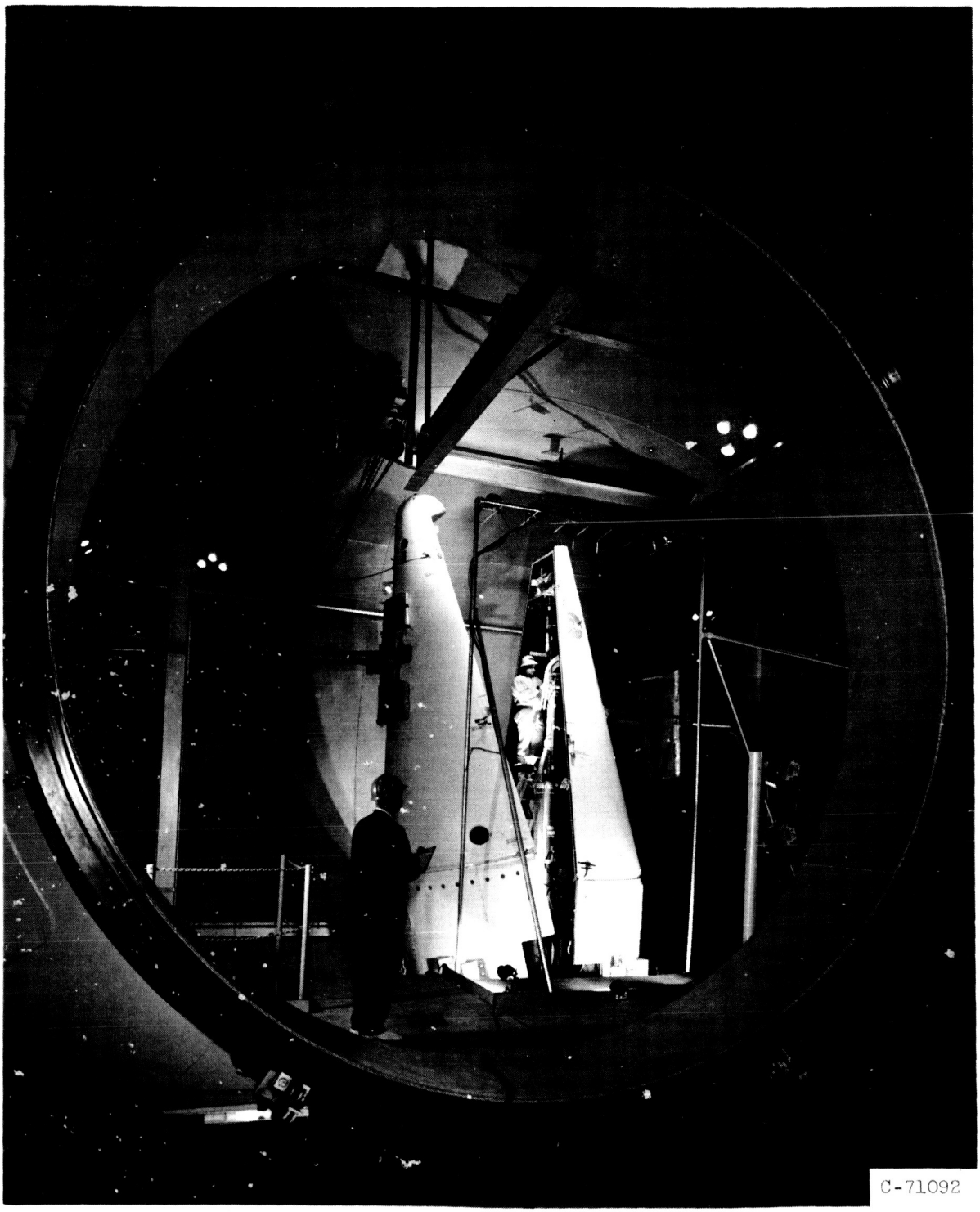

Figure 9. - Overall test setup, test 1.

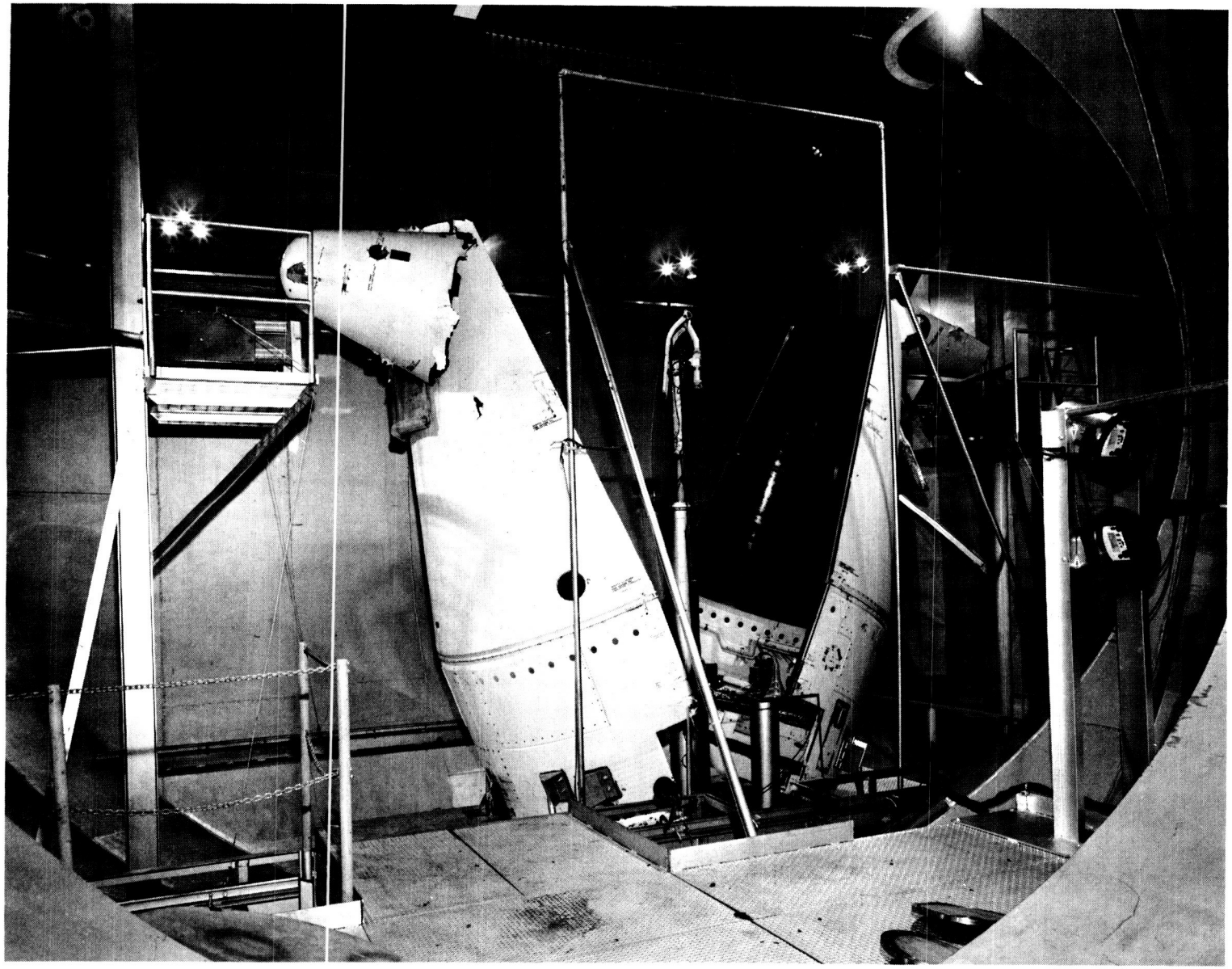

(a) Overall view.

Figure 10. - Damage caused by test 2.

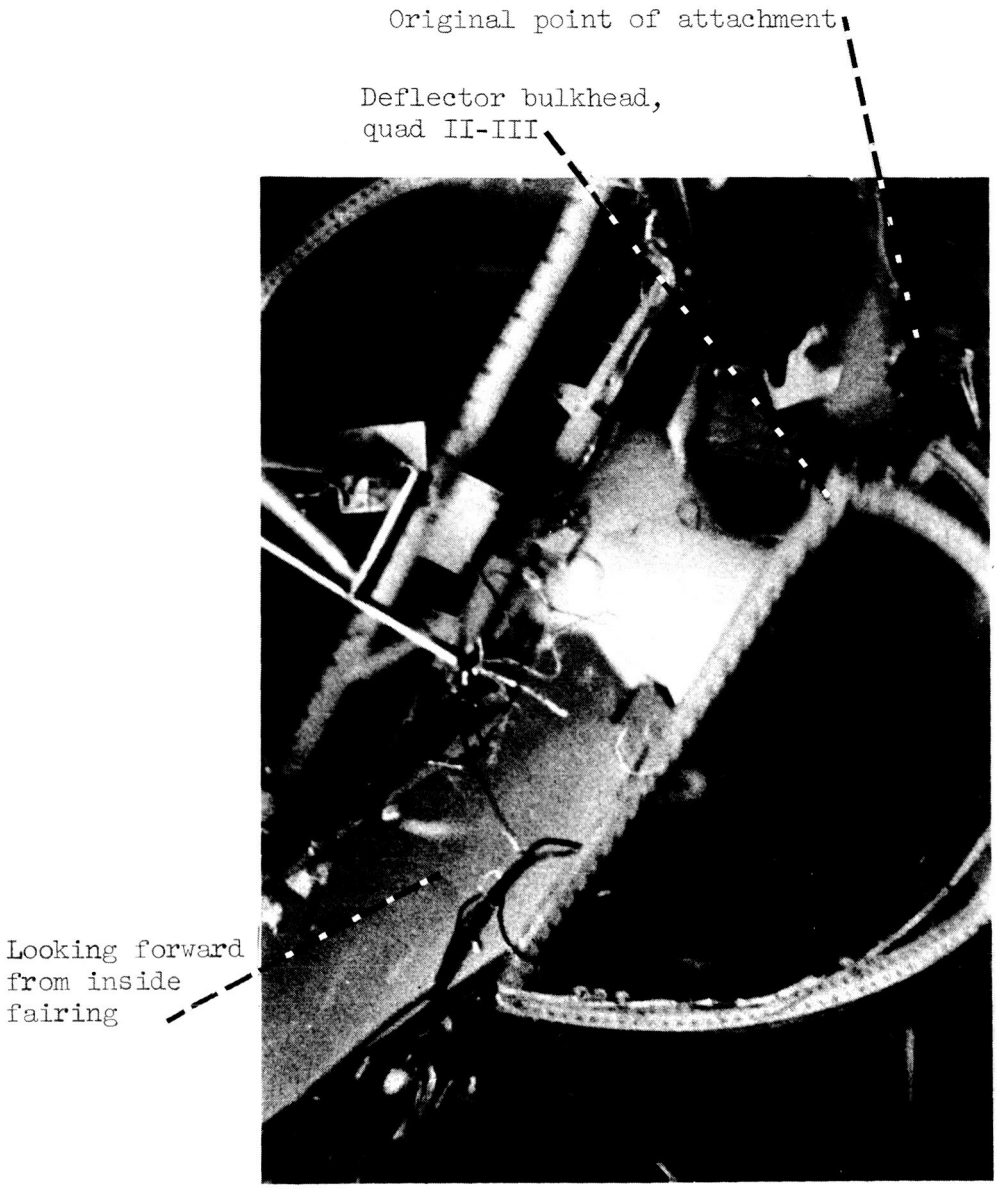

(b) Deflector bulkhead being torn from nose cone.

Figure 10. - Concluded.

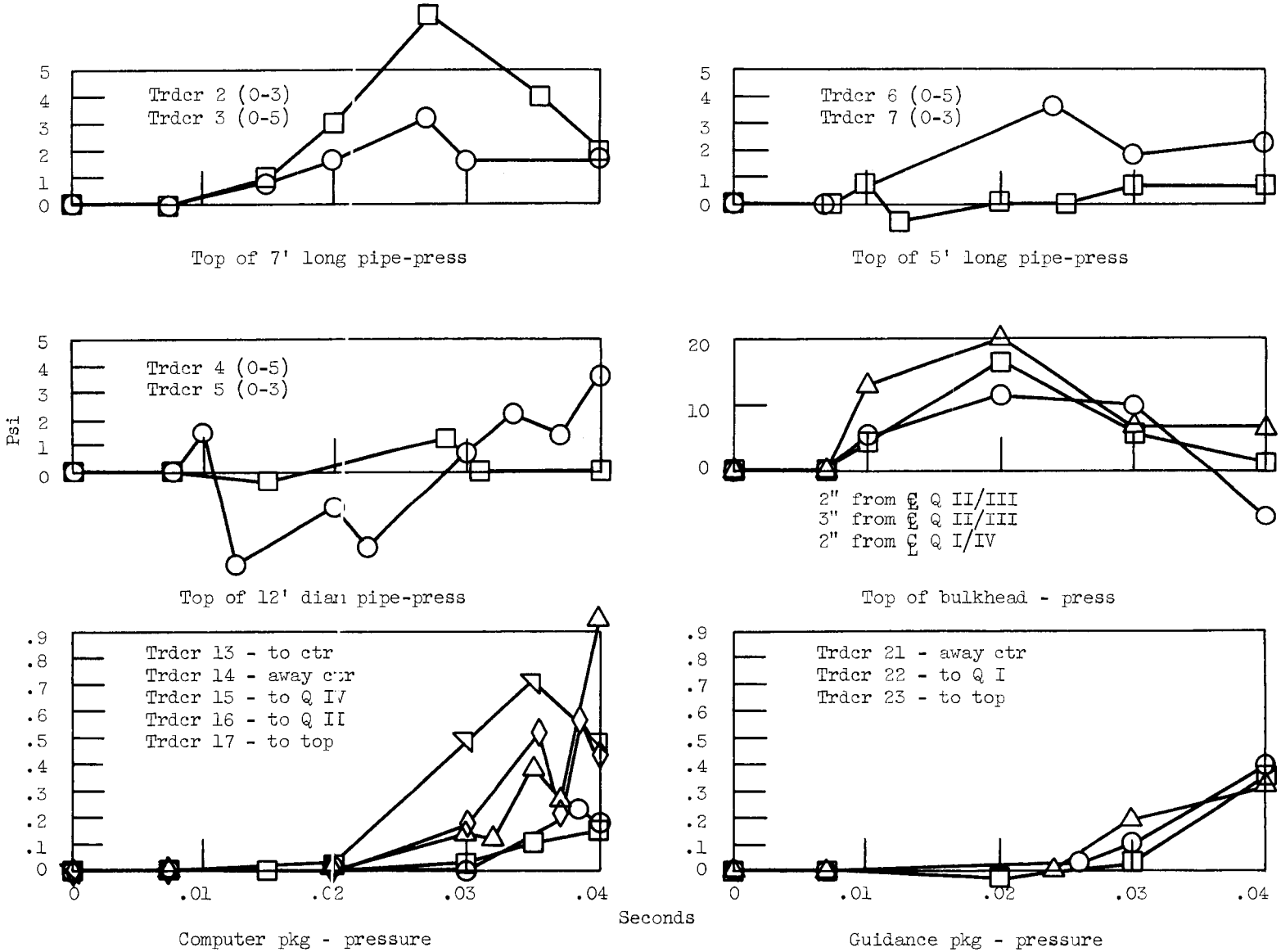

Figure 11. - Nose fairing separation data, Test 2.

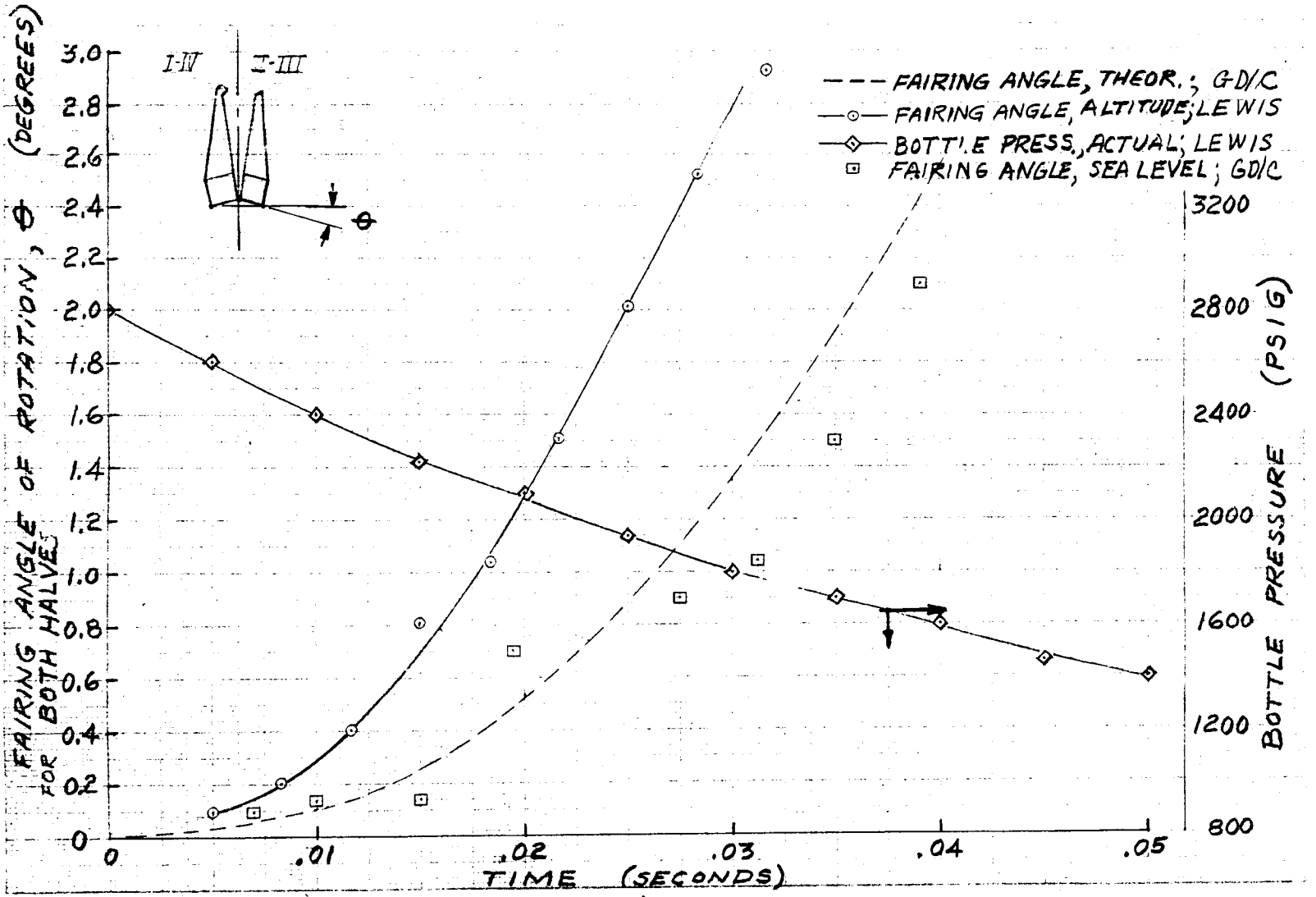

Figure 12. - Comparison of Lewis test 2 and GD/C atmospheric pressure nose fairing trajectories.

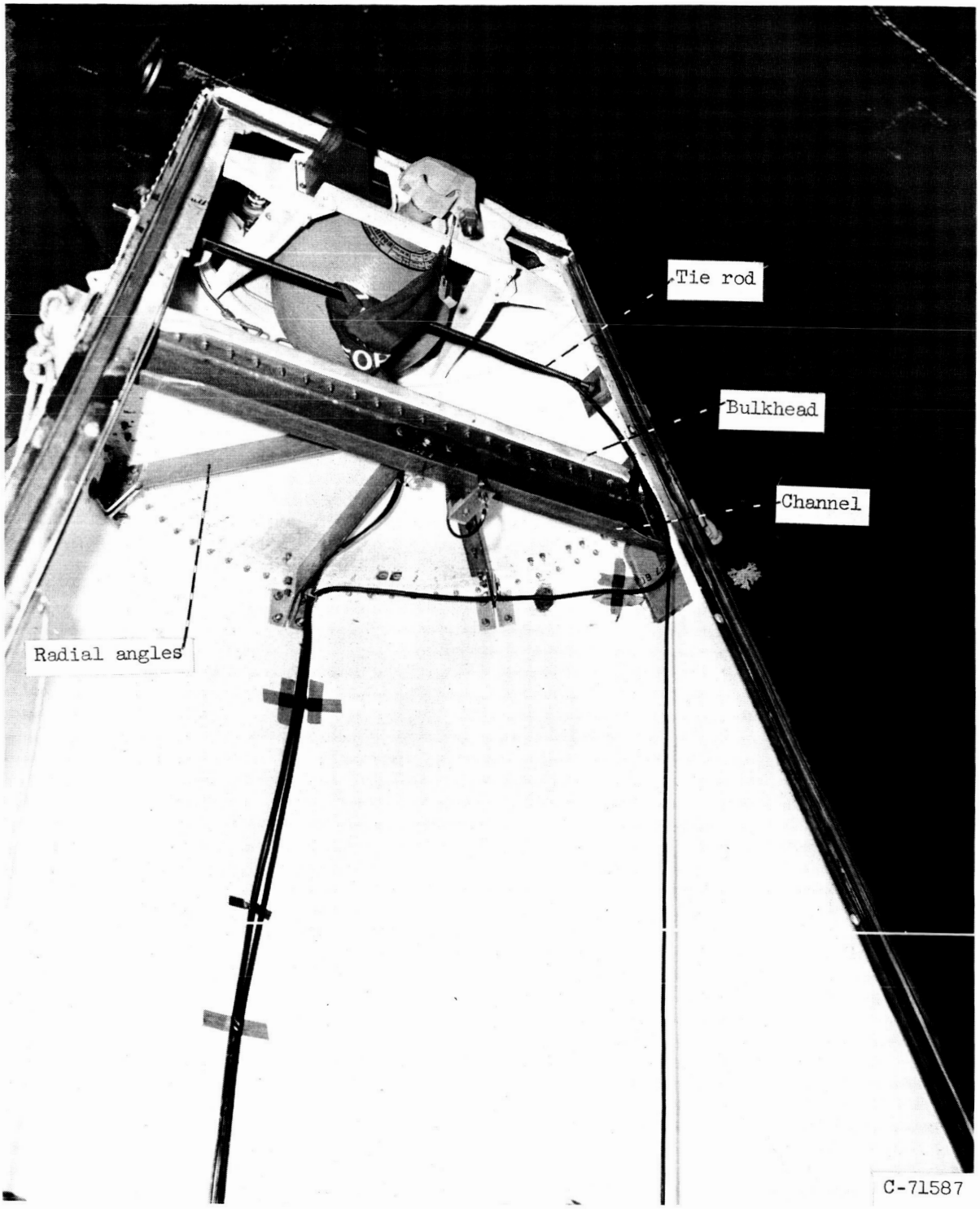

Figure 13. - NASA design separation bulkhead and tie rods.

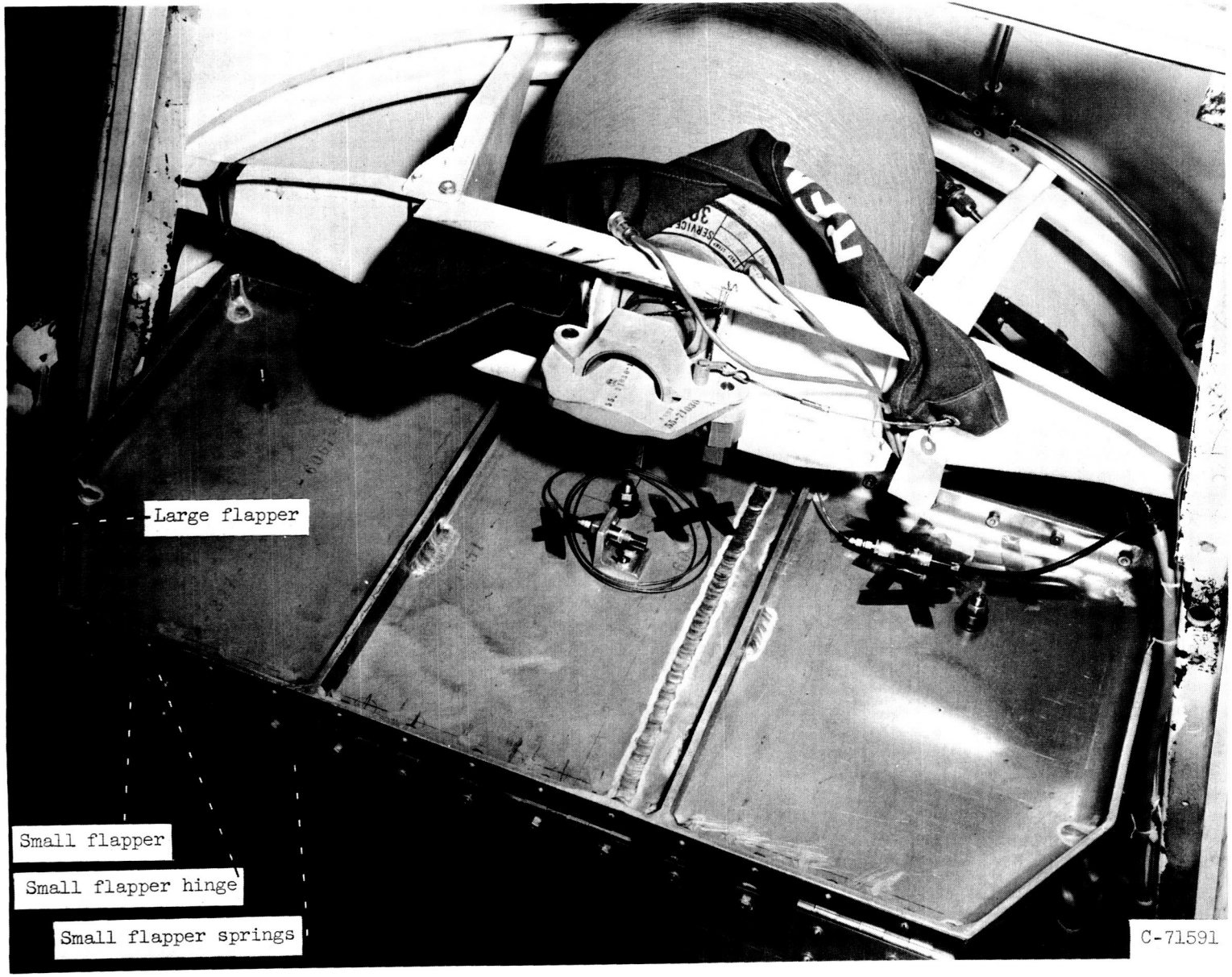

Figure 14. - Separation bulkhead flapper plate.

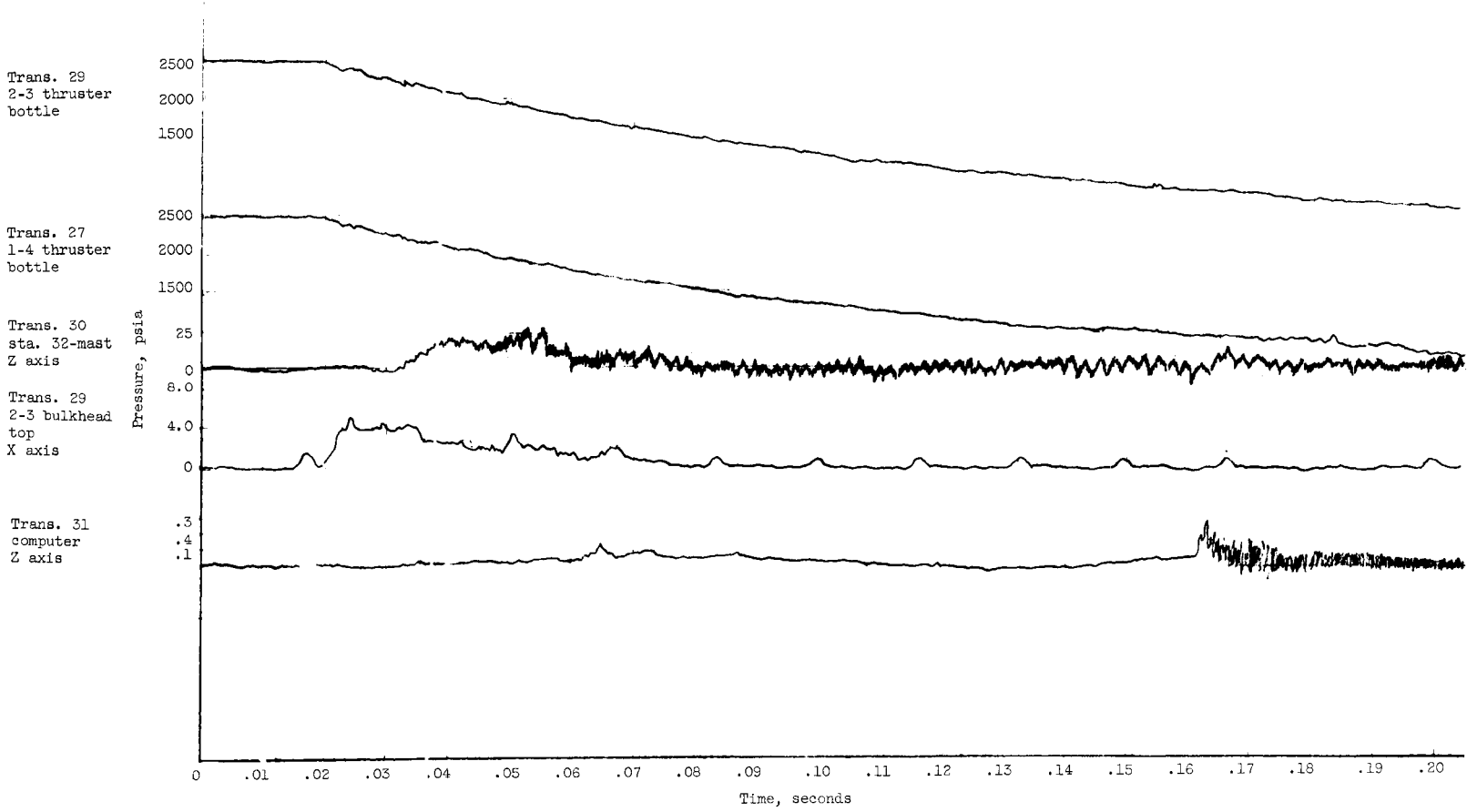

Figure 15. - Nose fairing separation data, test 3.

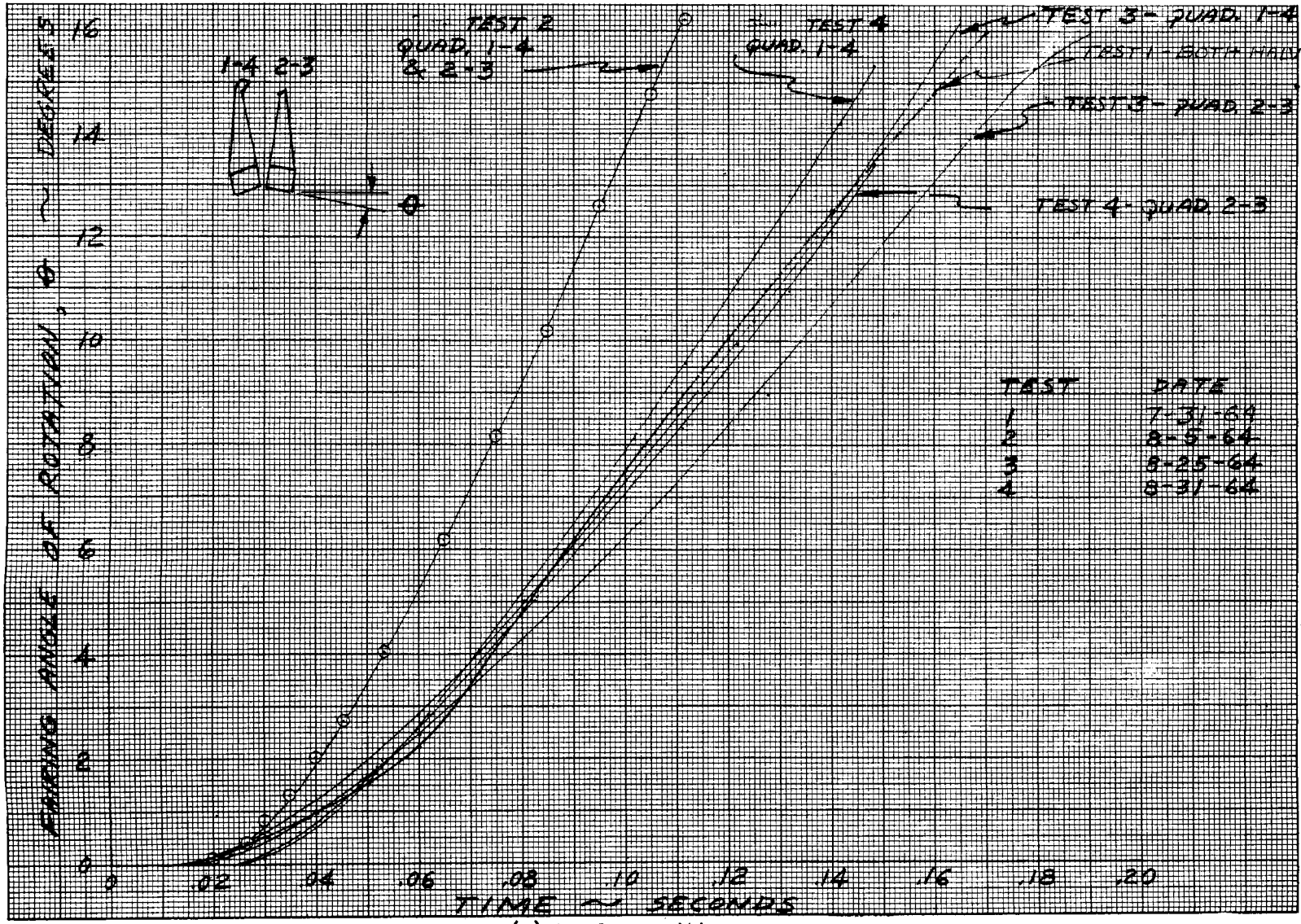

(a) Angular position.

Figure 16. - Centaur nose fairing trajectory for tests 1,2,3,4.

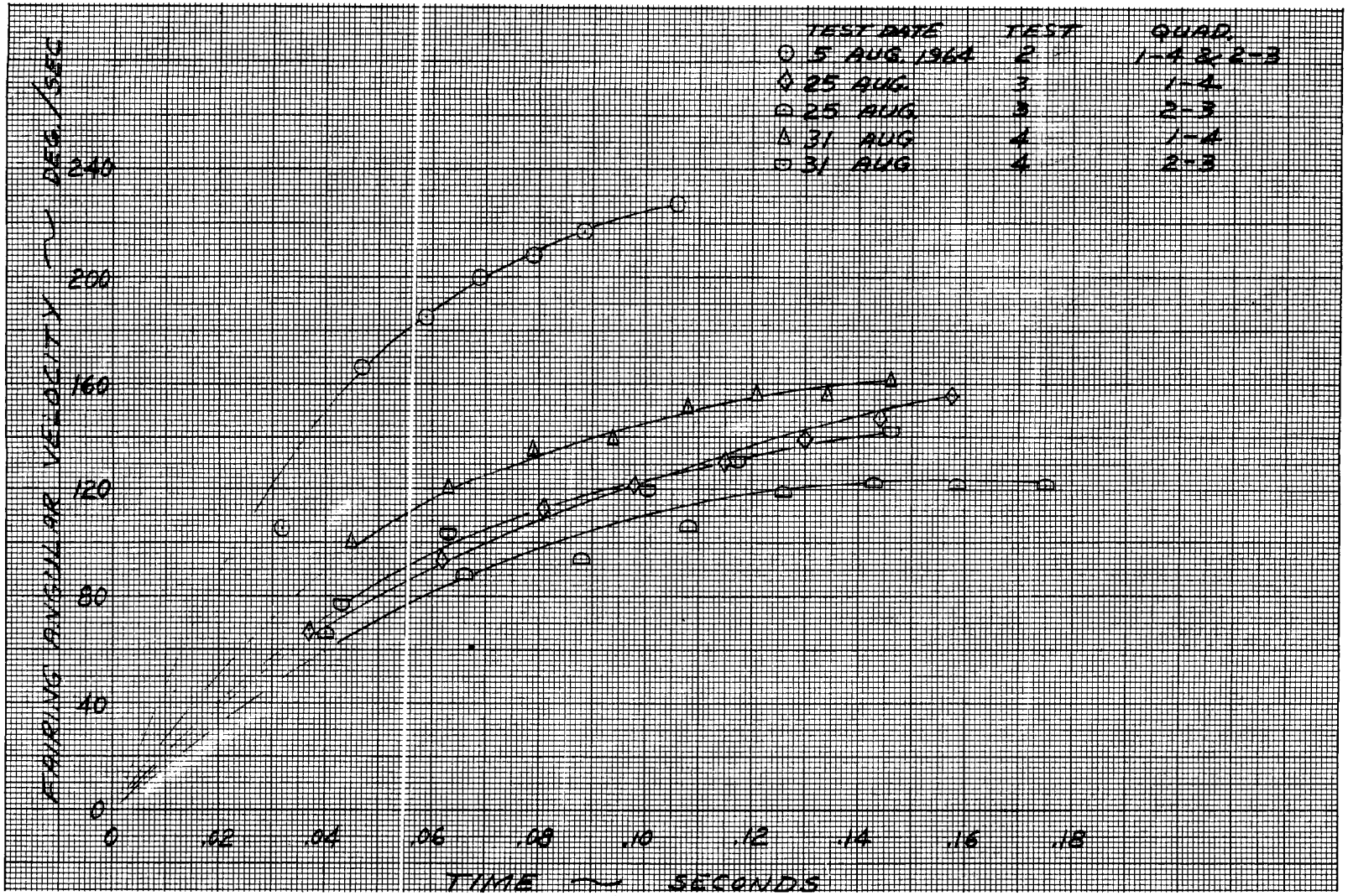

(b) Angular velocity.

Figure 16. - Continued.

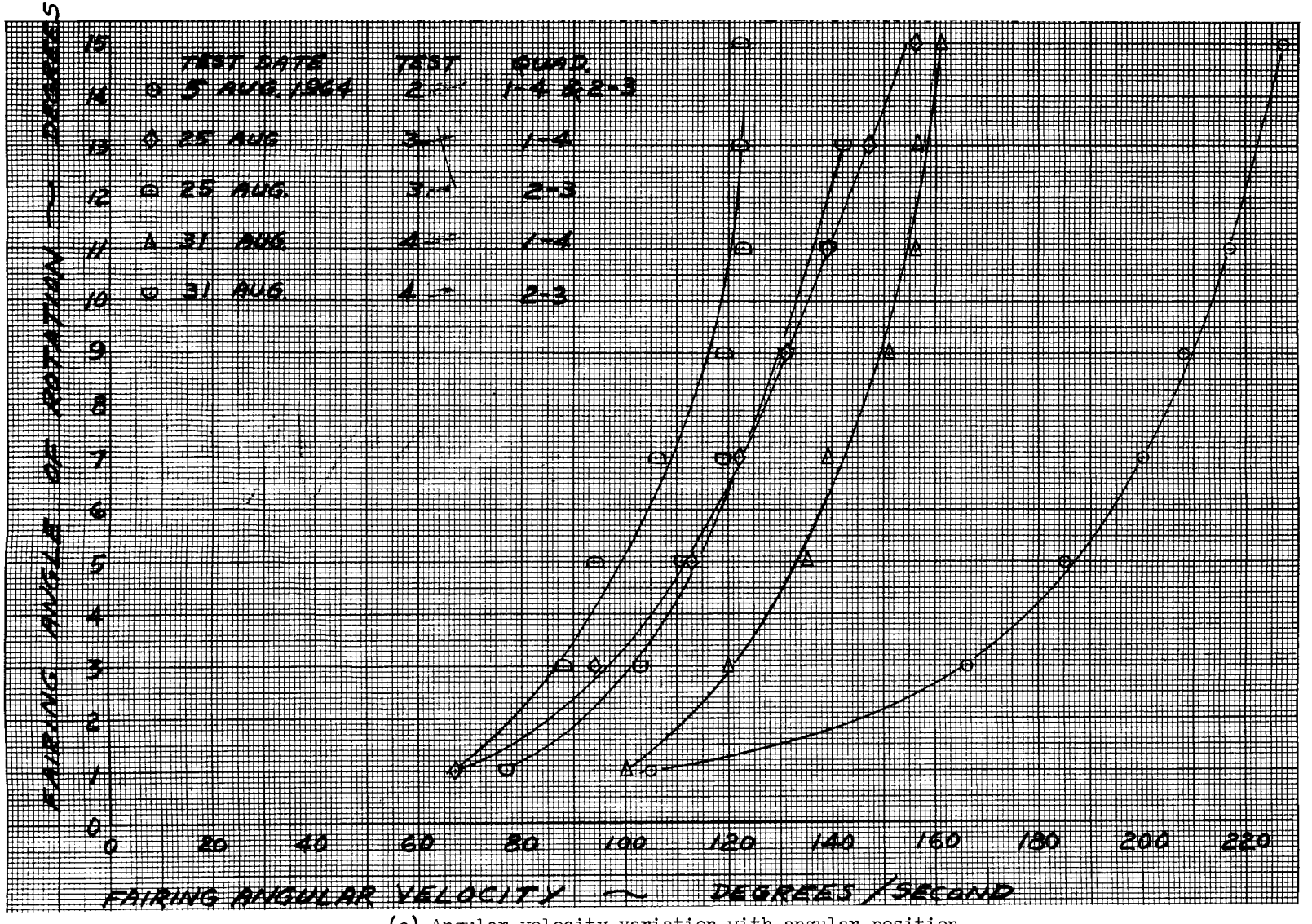

(c) Angular velocity variation with angular position.

Figure 16. - Concluded.

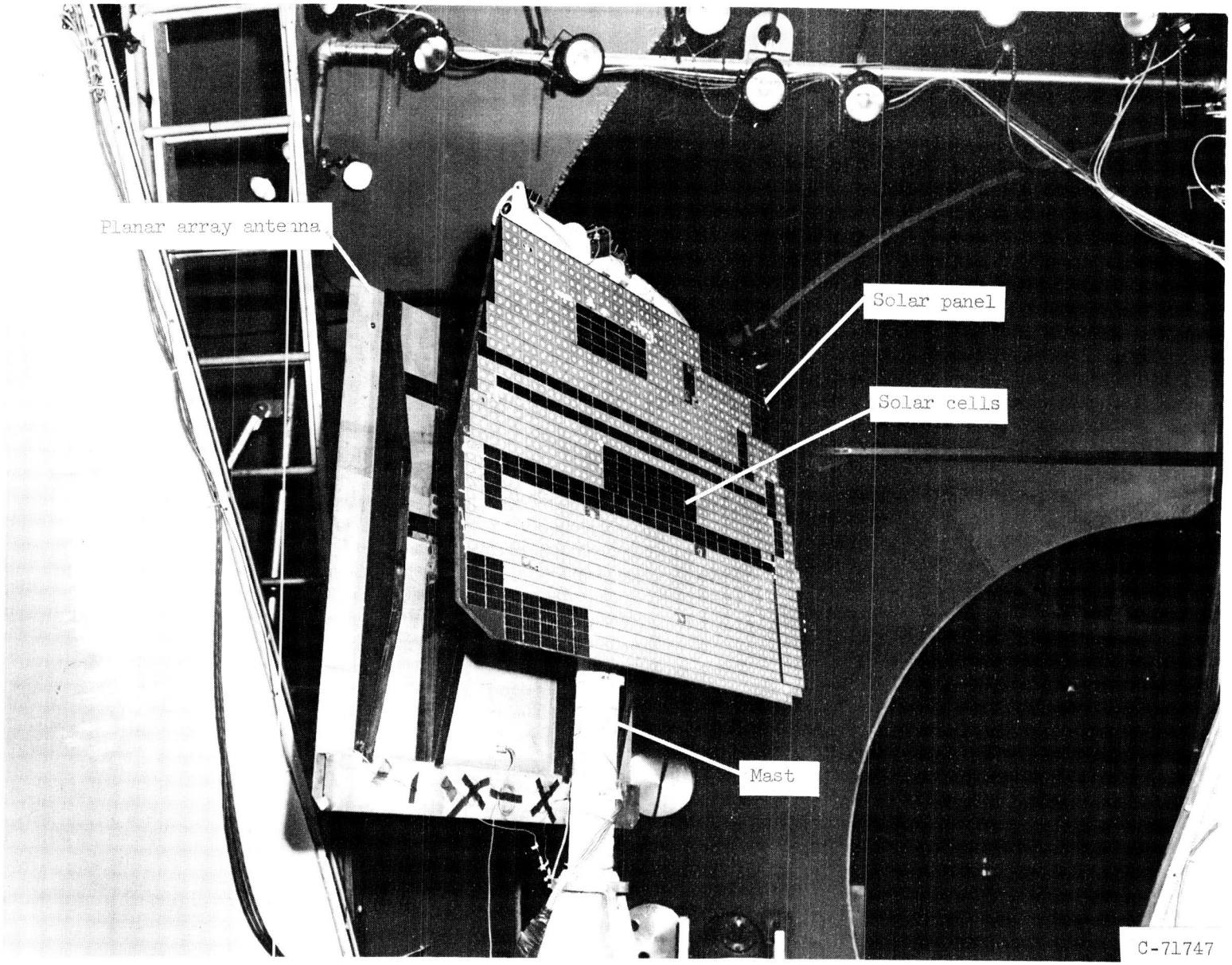

Figure 17. - Surveyor solar panel, Test 4.

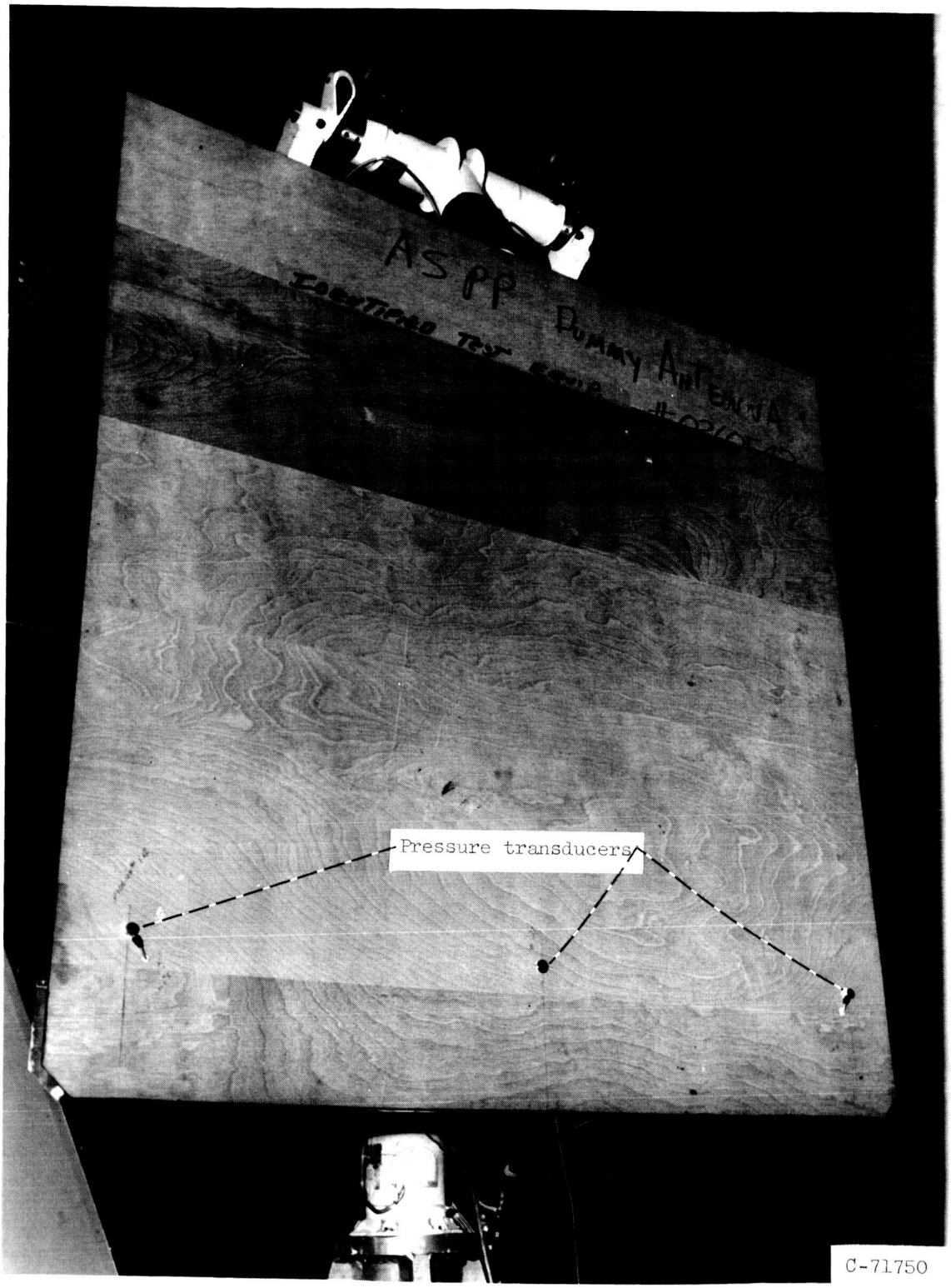

Figure 18. - Surveyor planar array antenna simulation, Test 4.

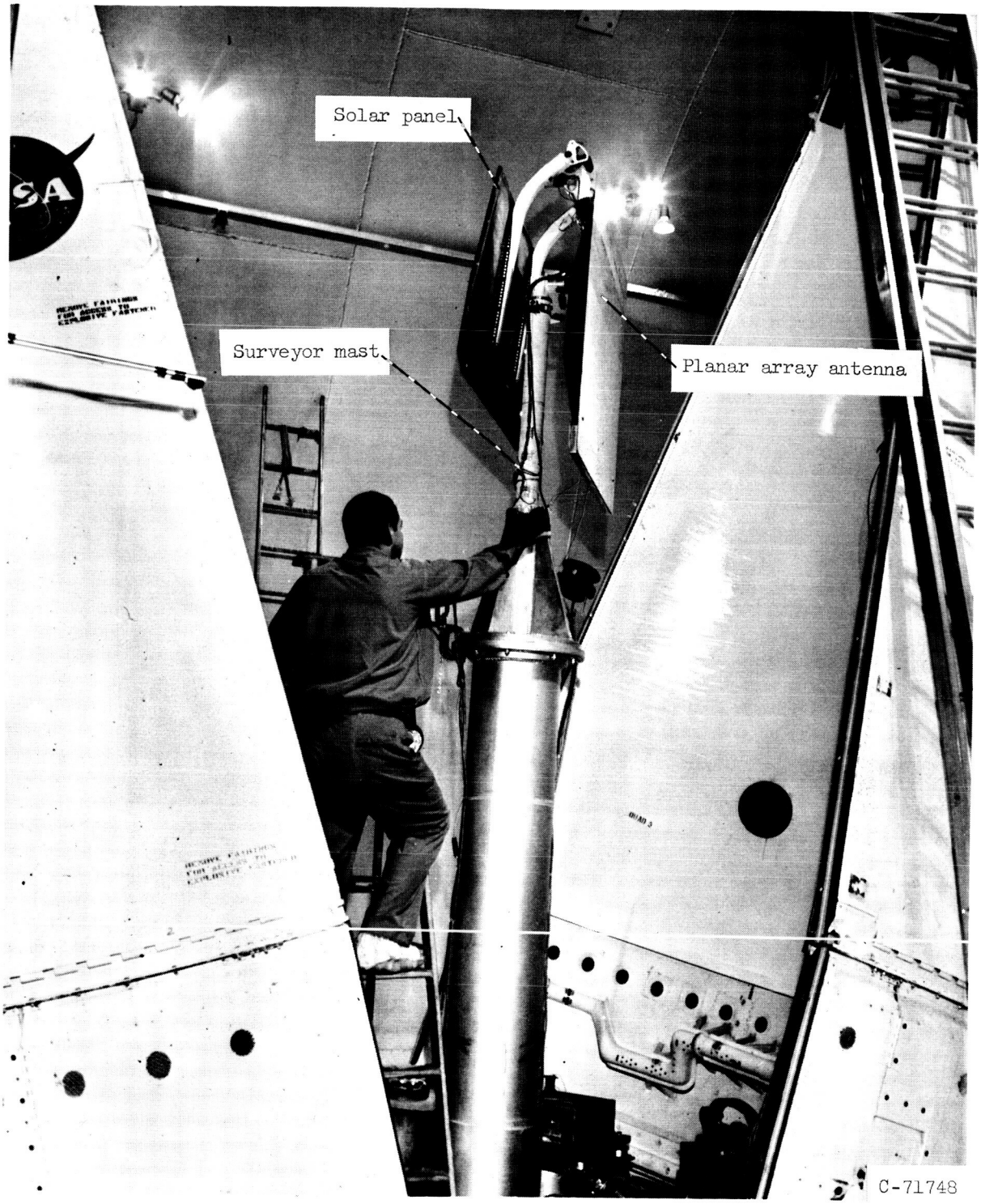

Figure 19. - Surveyor mast set-up, Test 4.

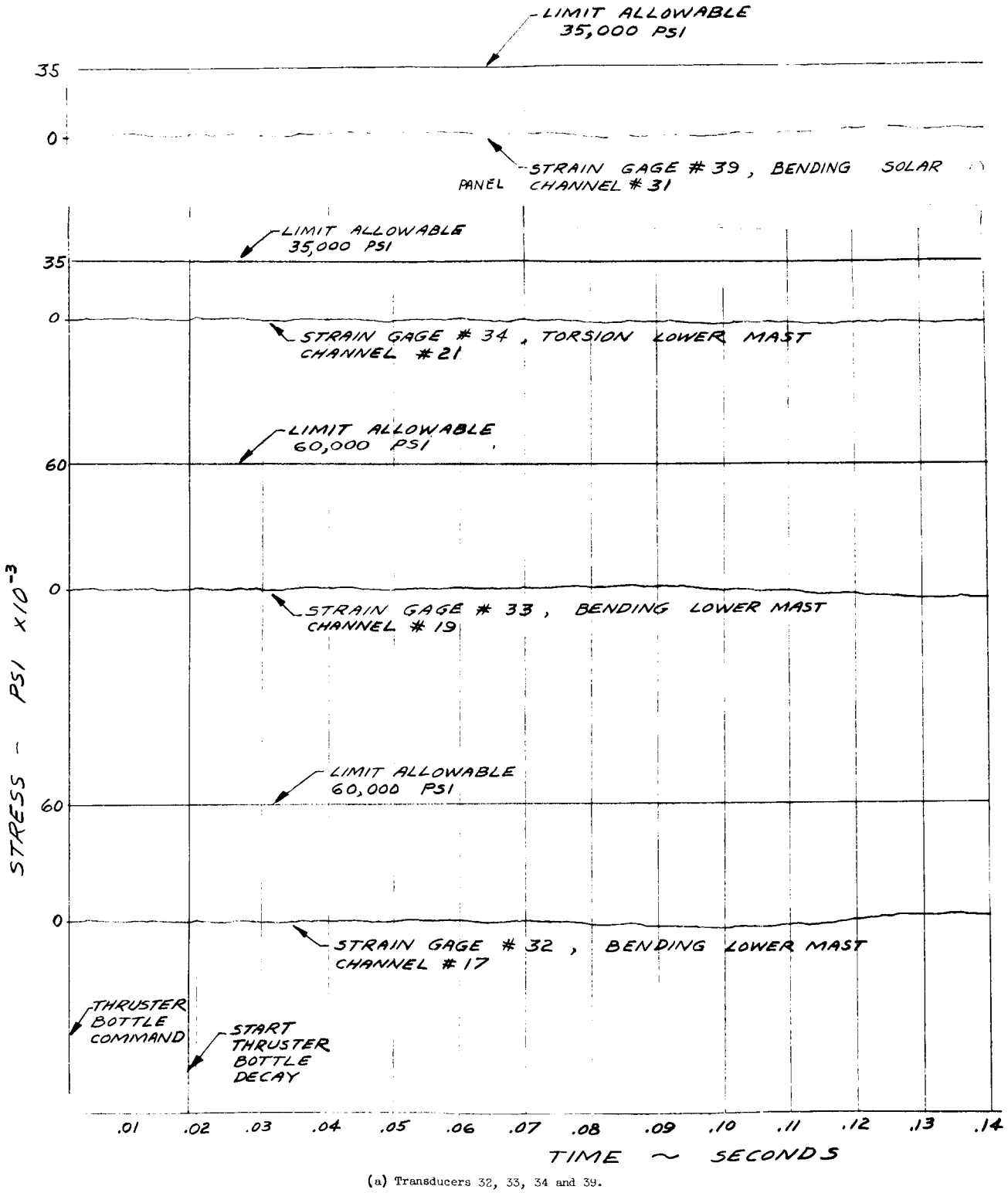

(a) Transducers 32, 33, 34 and 39.

Figure 20. - Nose fairing separation data. Test 4.

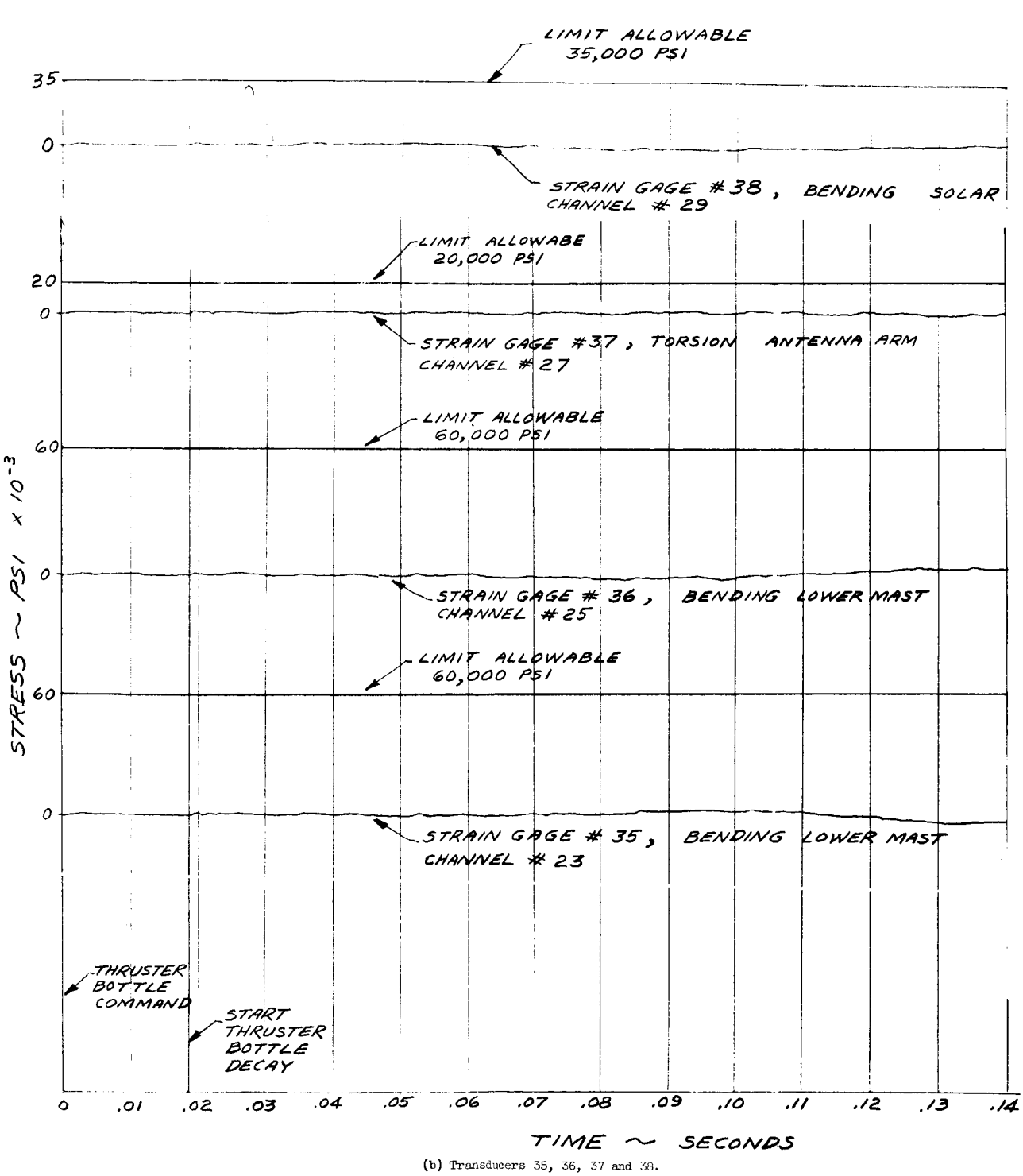

(b) Transducers 35, 36, 37 and 38.

Figure 20. - Continued.

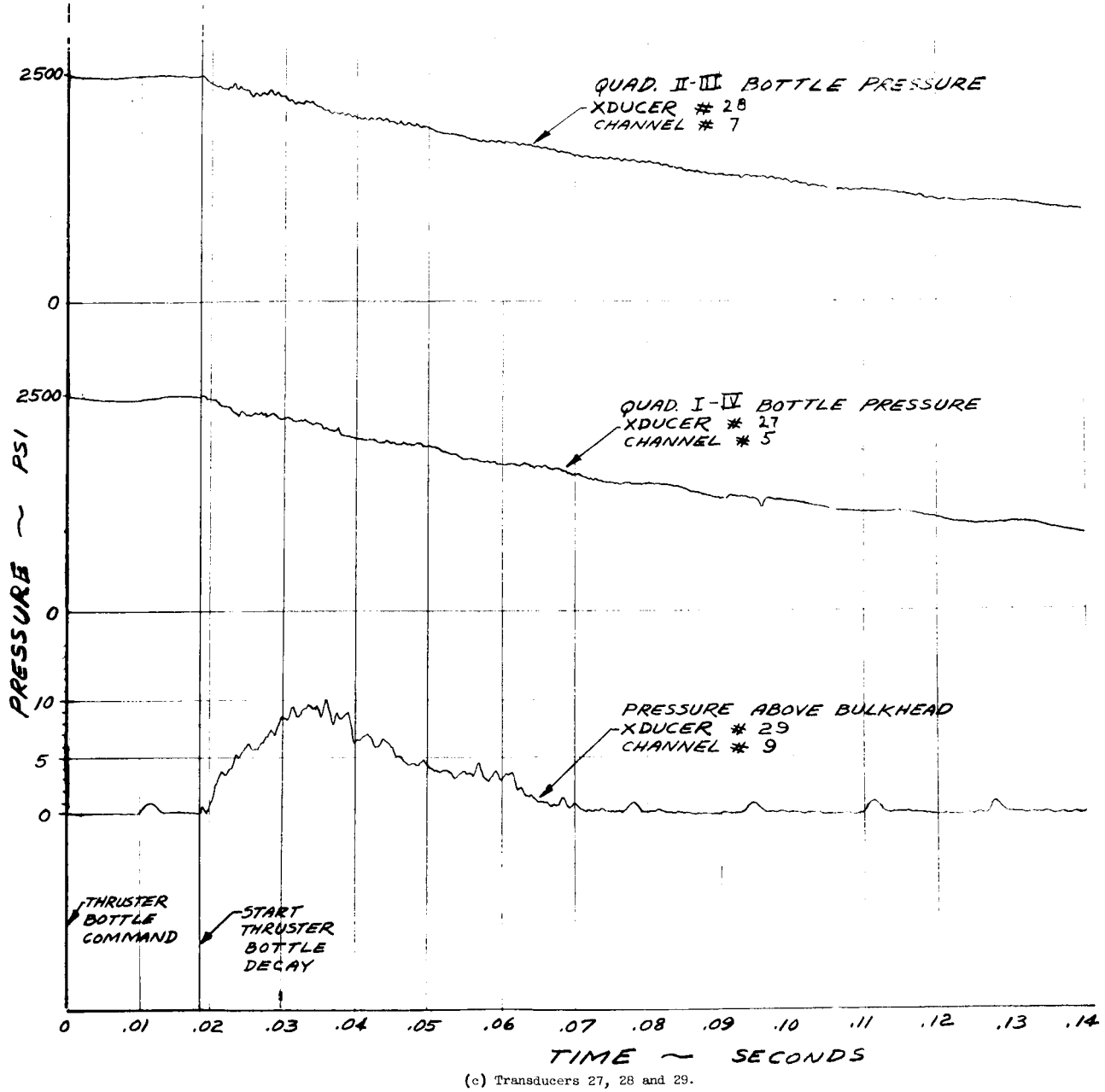

(c) Transducers 27, 28 and 29.

Figure 20. - Continued.

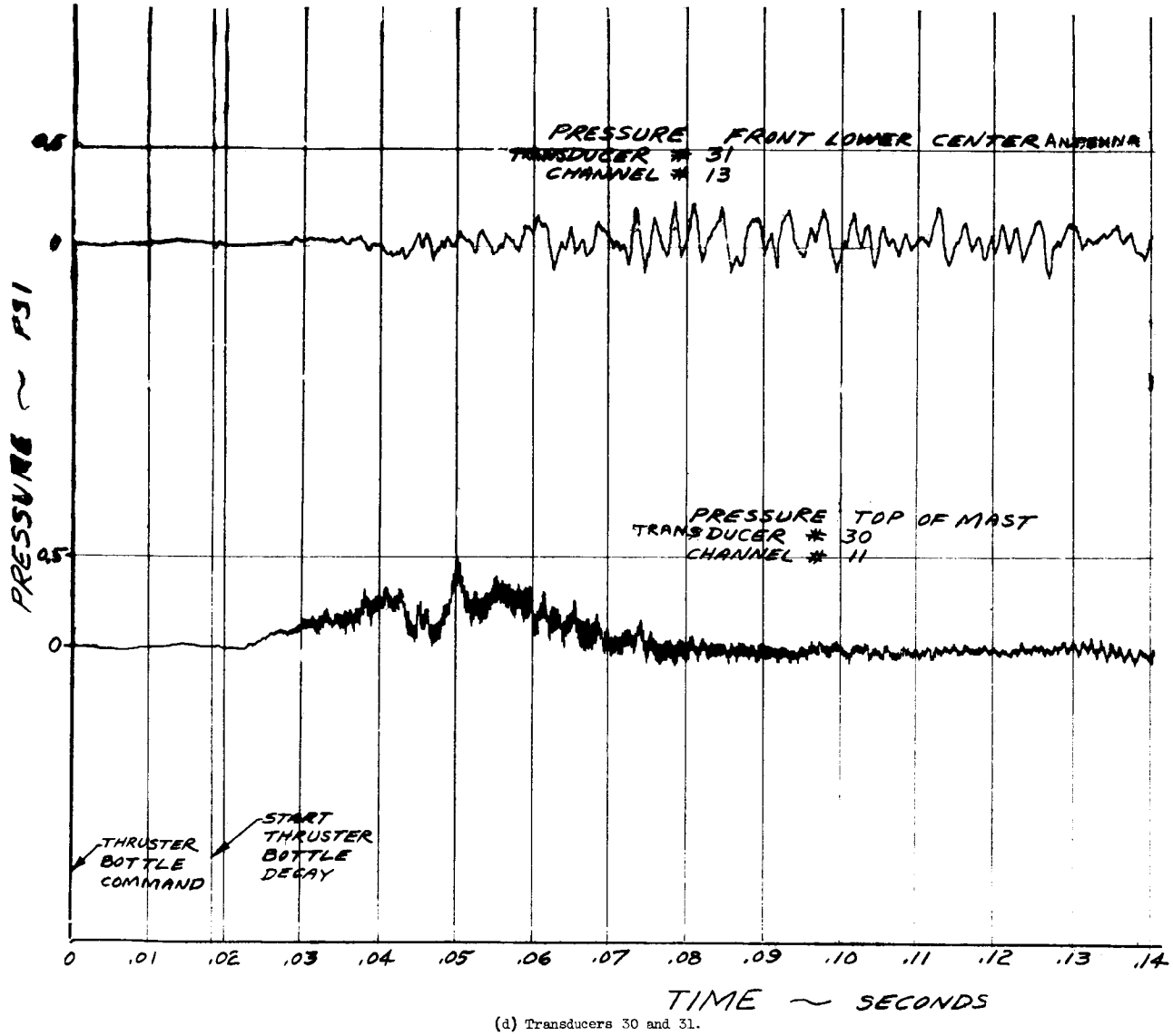

(d) Transducers 30 and 31.

Figure 20. - Continued.

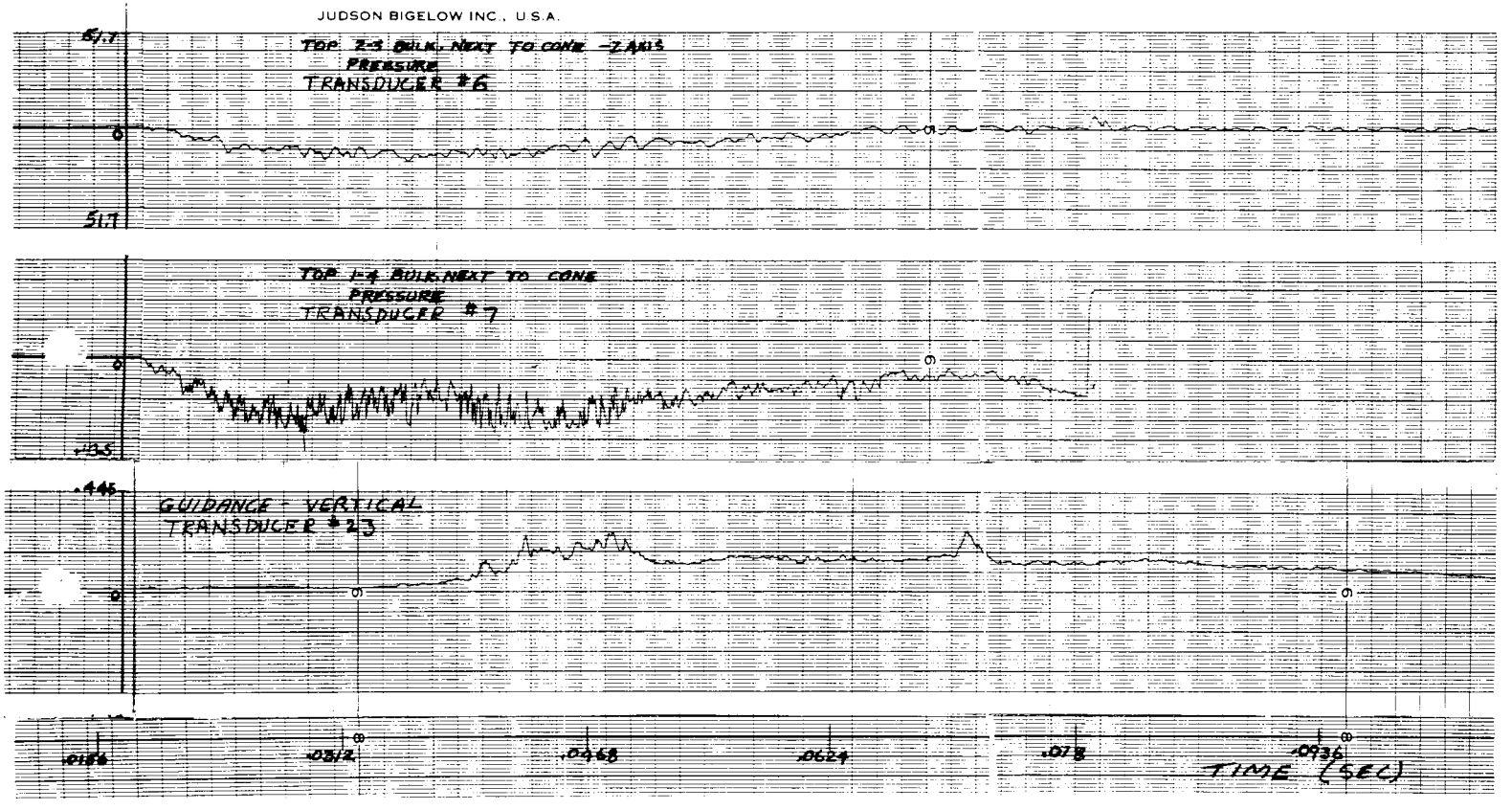

(e) Transducers 6, 7 and 23.

Figure 20. - Concluded.

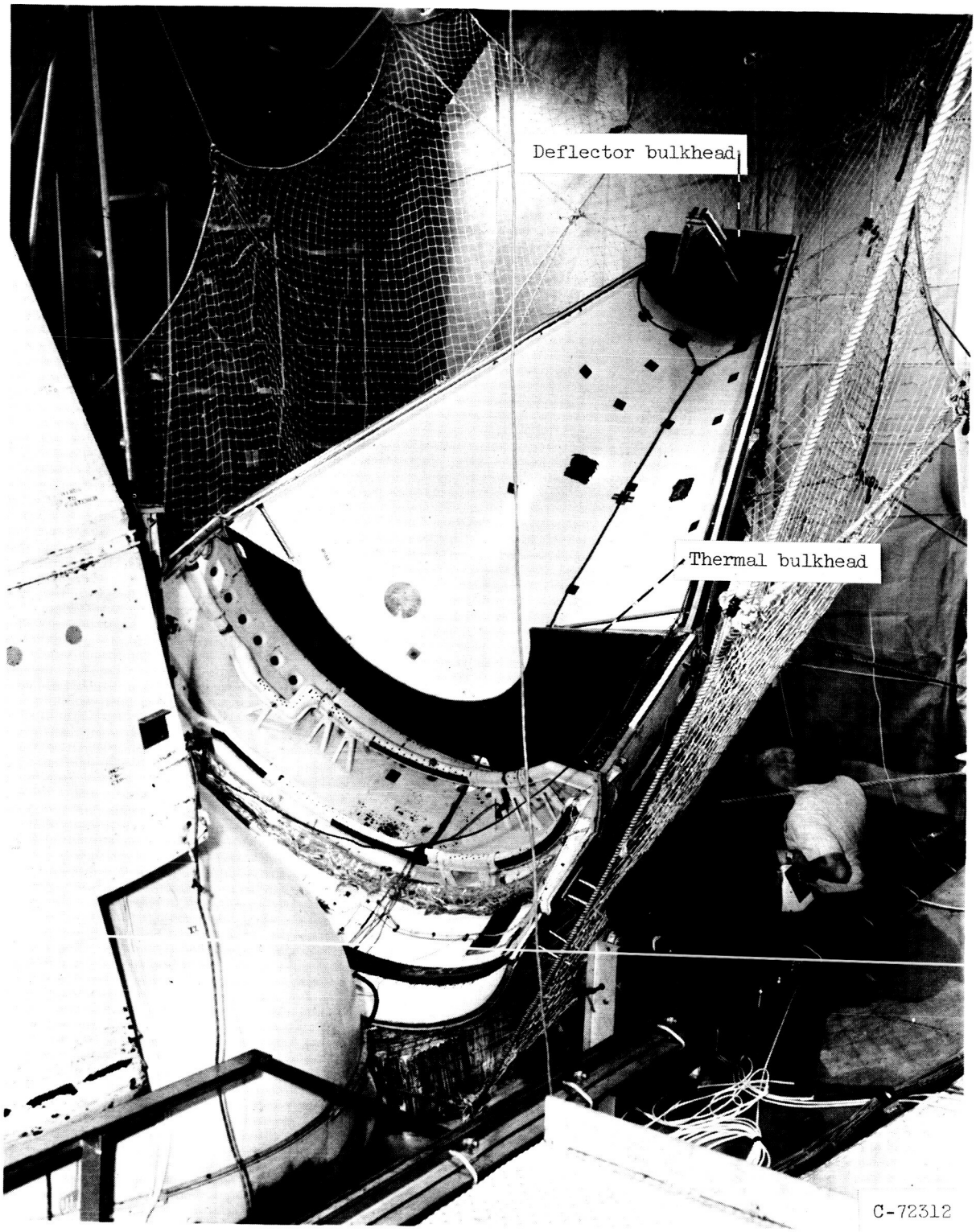

Figure 21. - Deflector and thermal bulkheads of II-III fairing.

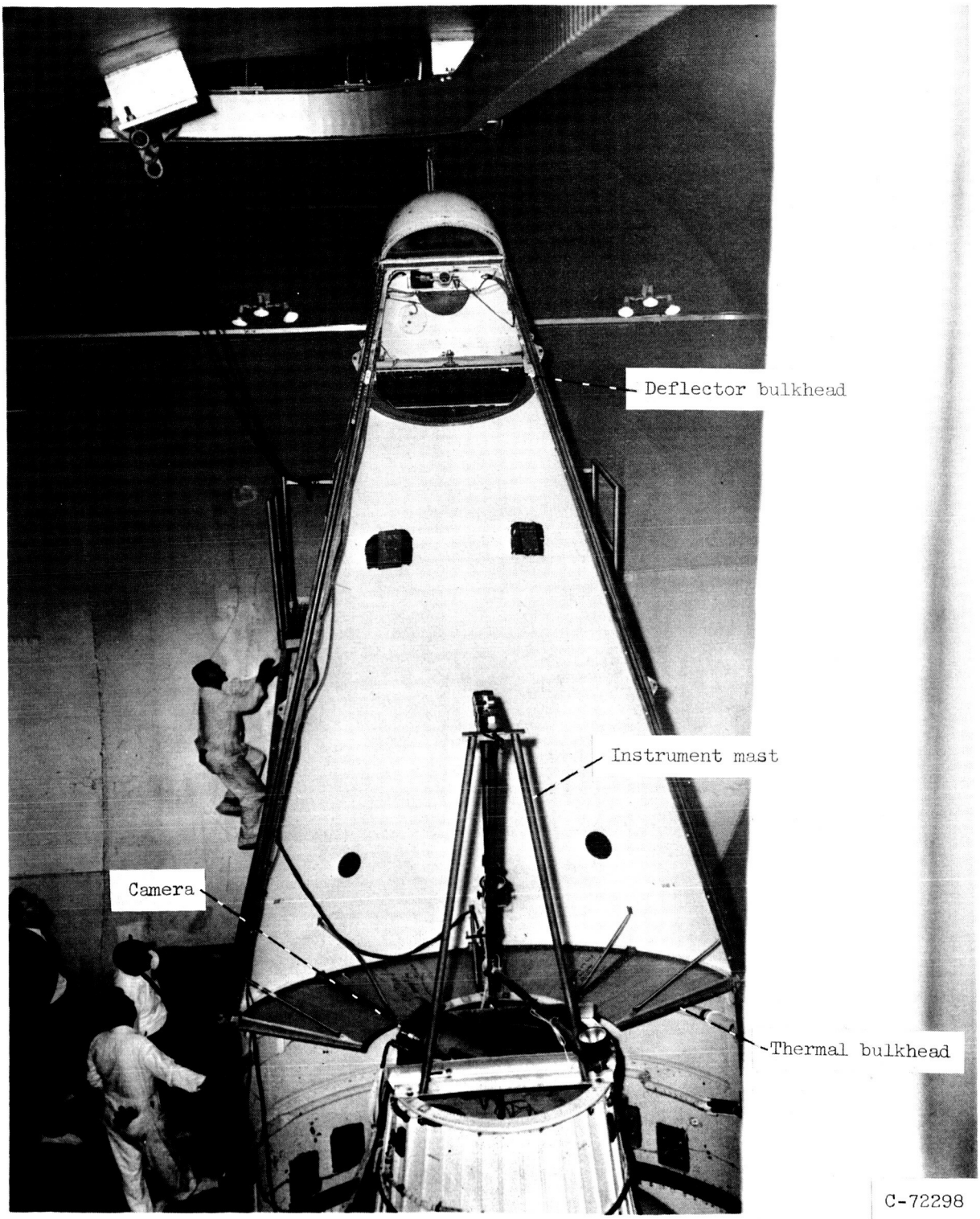

Figure 22. - Nose fairing with deflector and thermal bulkheads, Test 6.

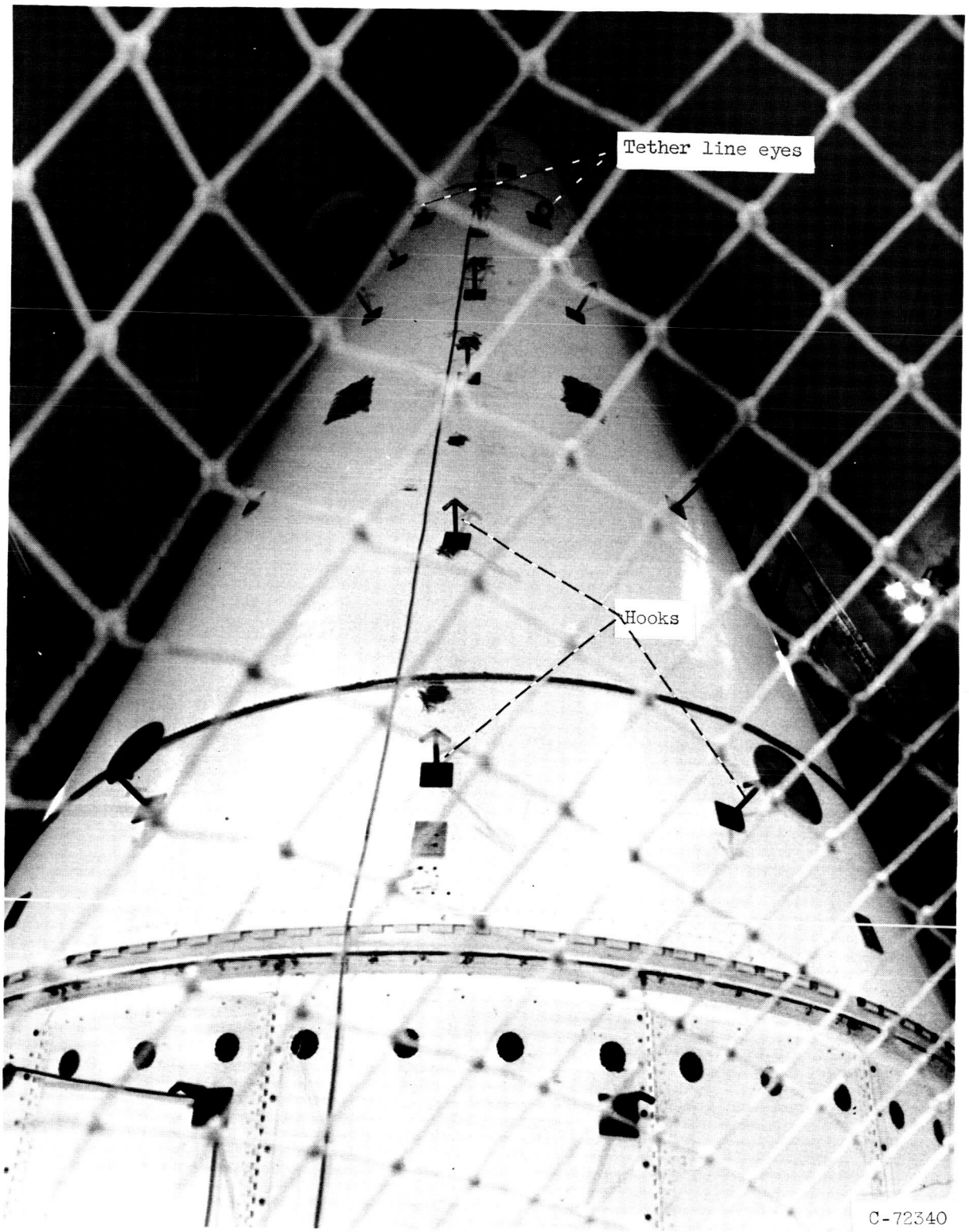

Figure 23. - Hooks installed on nose fairing to hold fairing in net.

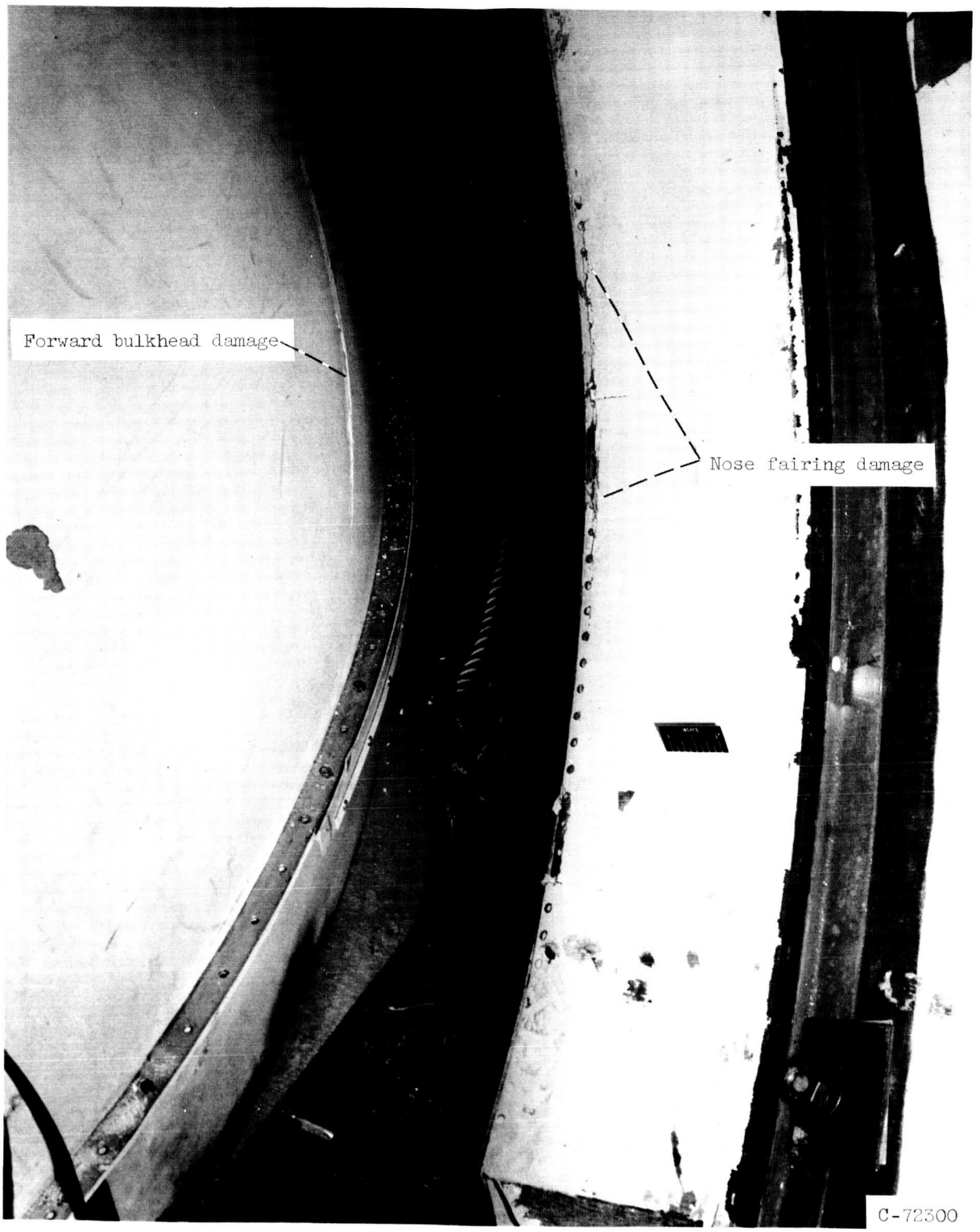

Figure 24. - Damage to forward bulkhead and to barrel section. Test 6.

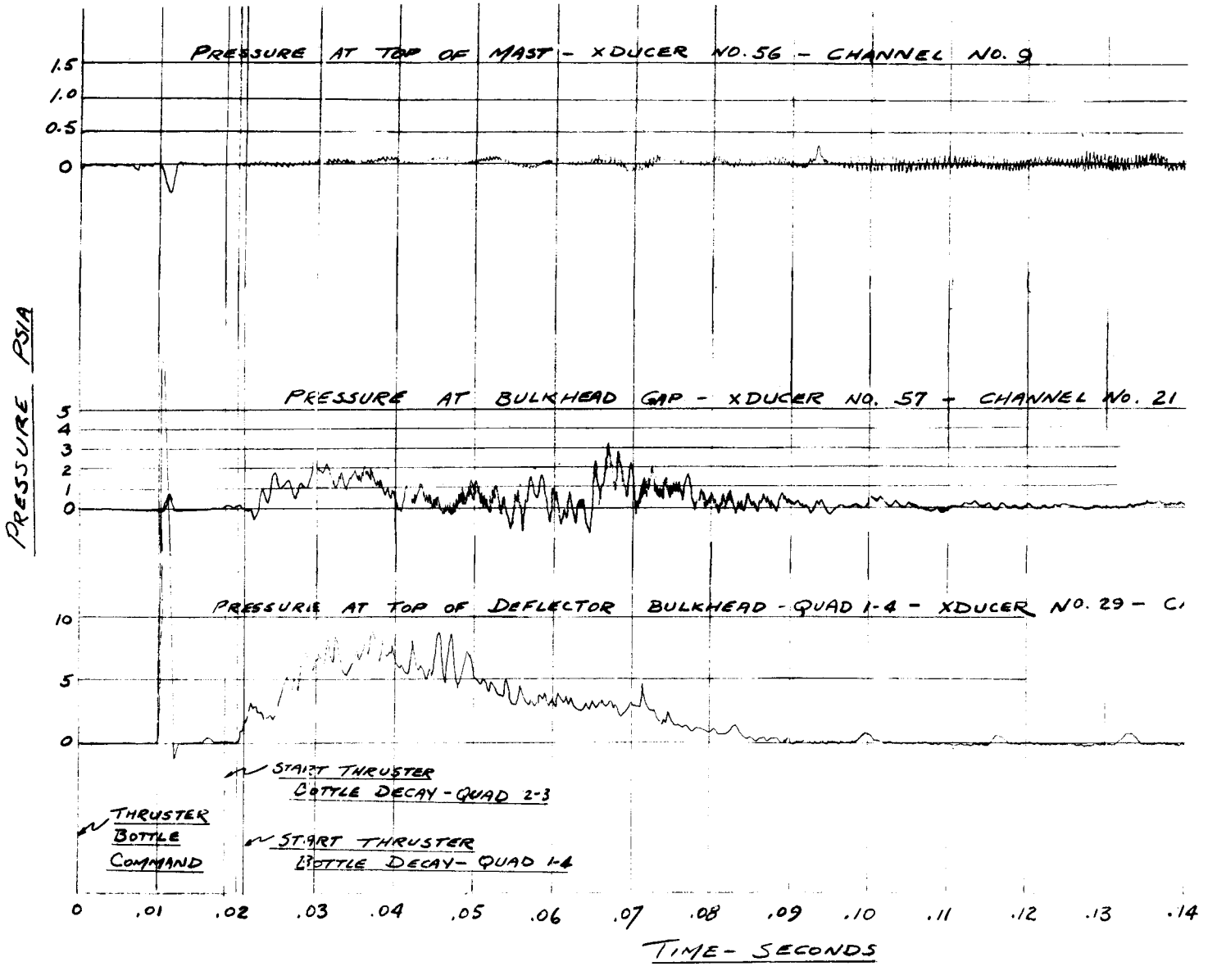

(a) Transducers 29, 56, 57.

Figure 25. - Nose fairing separation data. Test 6.

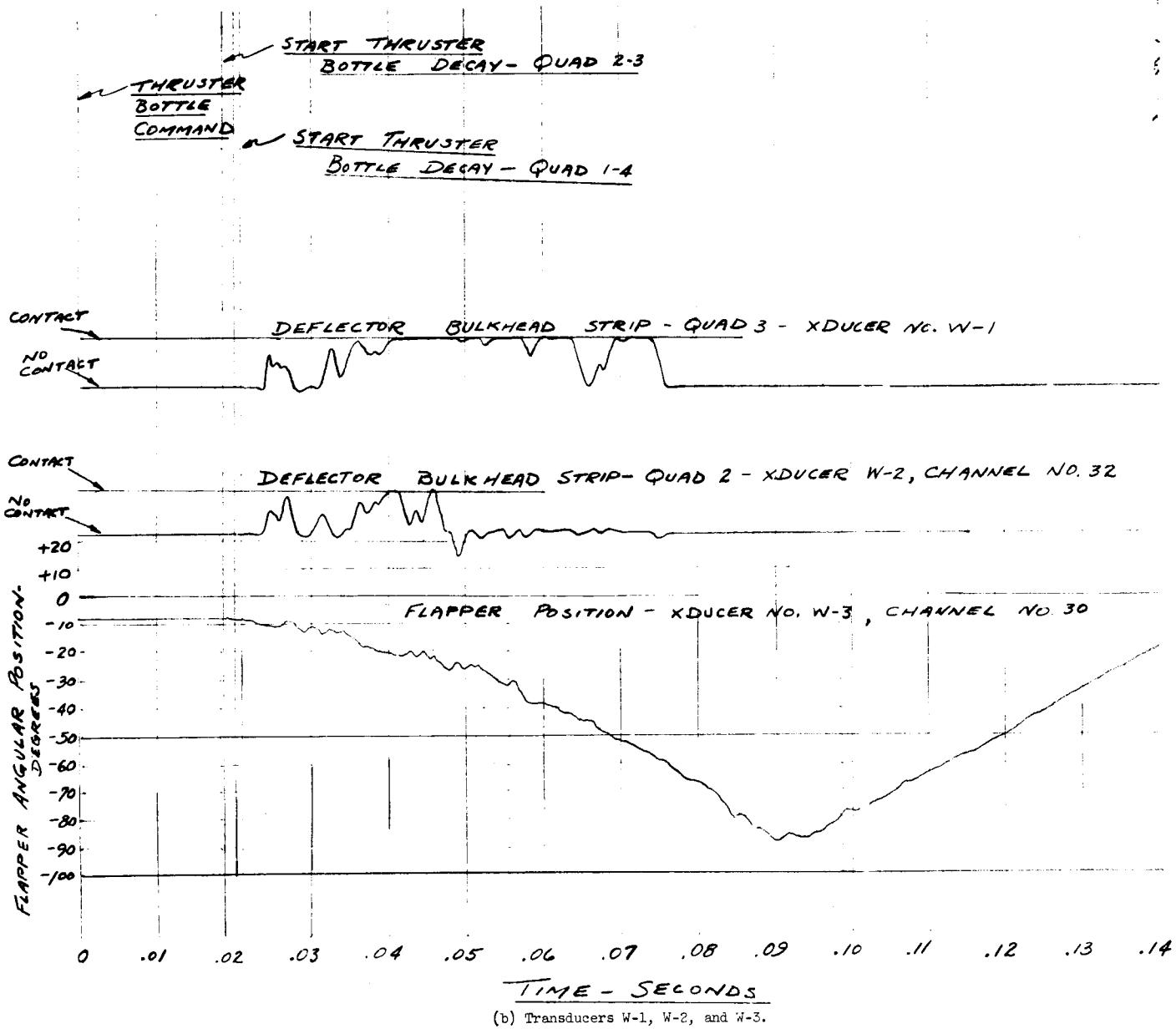

(b) Transducers W-1, W-2, and W-3.

Figure 25. - Continued.

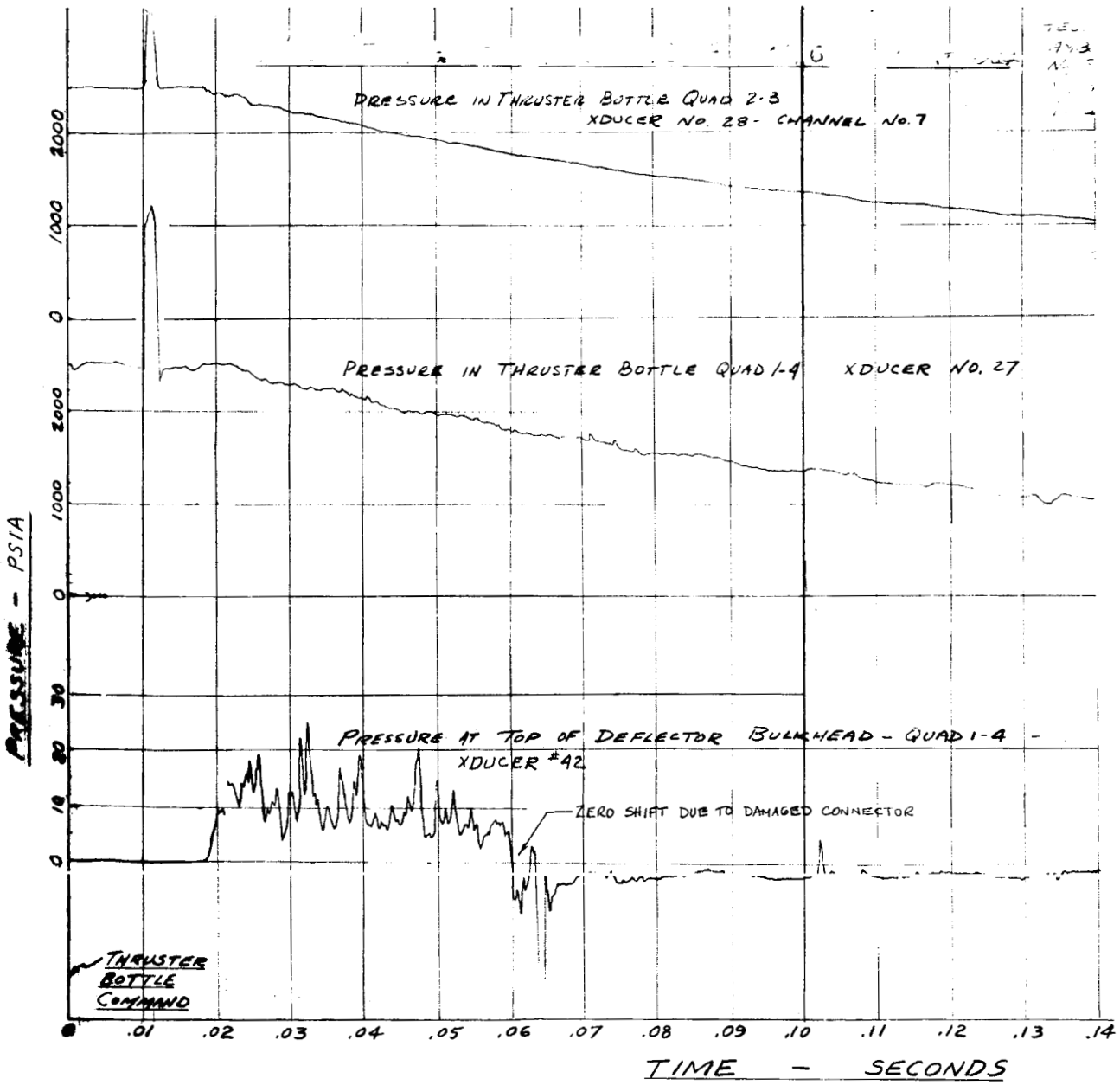

(c) Transducers 28, 27, and 42.

Figure 25. - Continued.

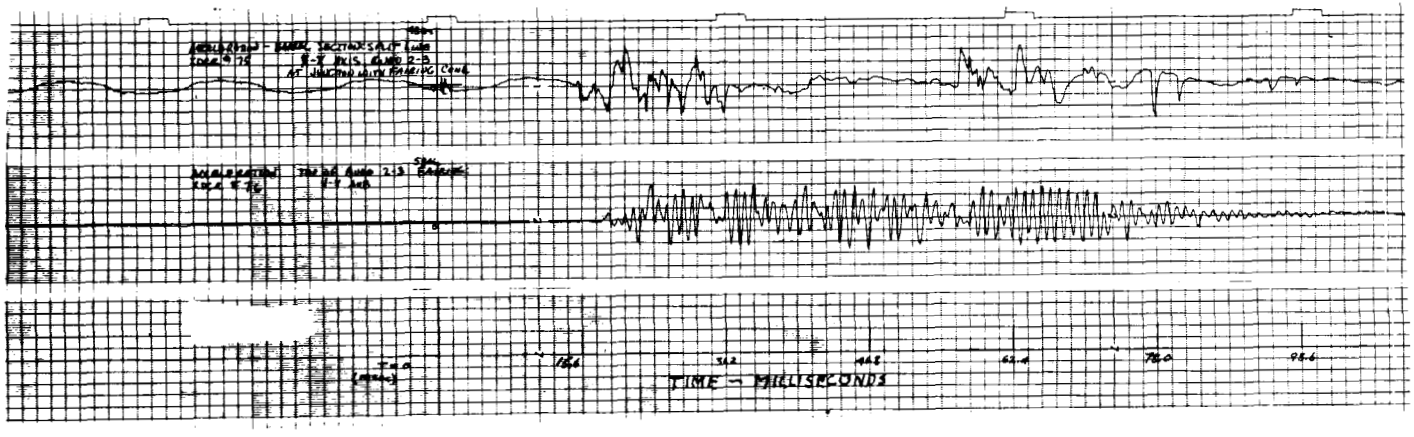

(d) Transducers 75 and 76.

Figure 25. - Continued.

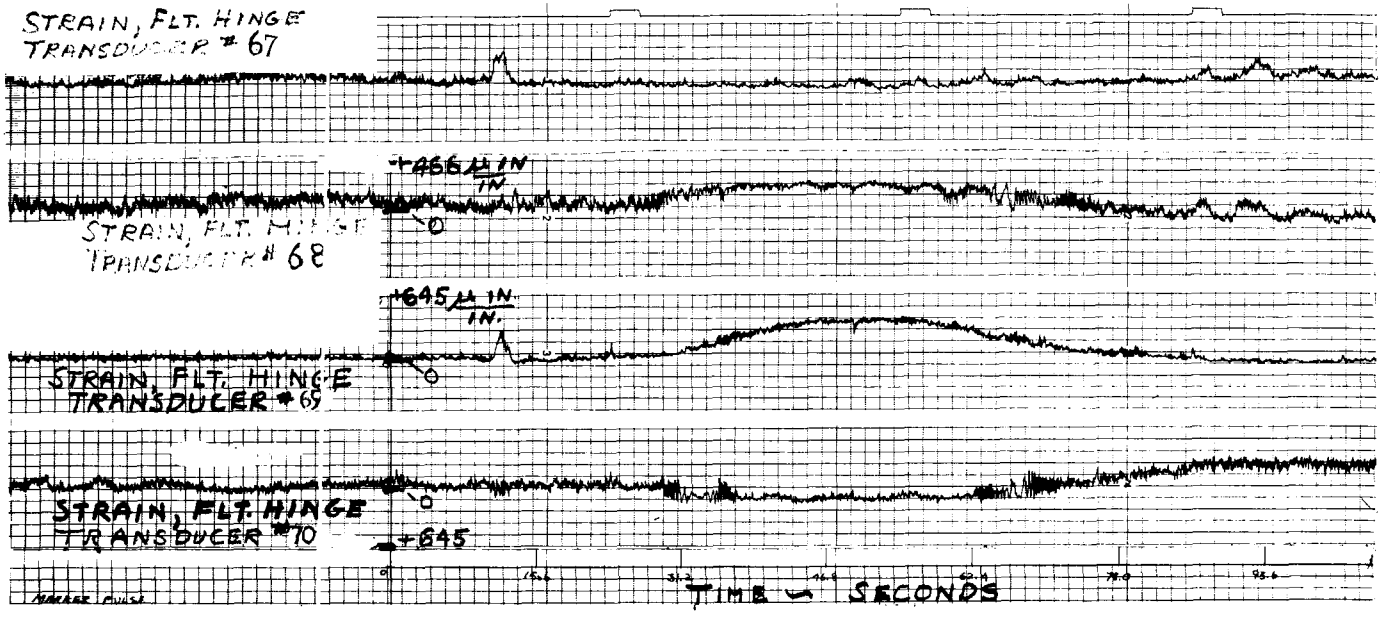

(e) Transducers 7, 8, 9, 10.

Figure 25. - Concluded.

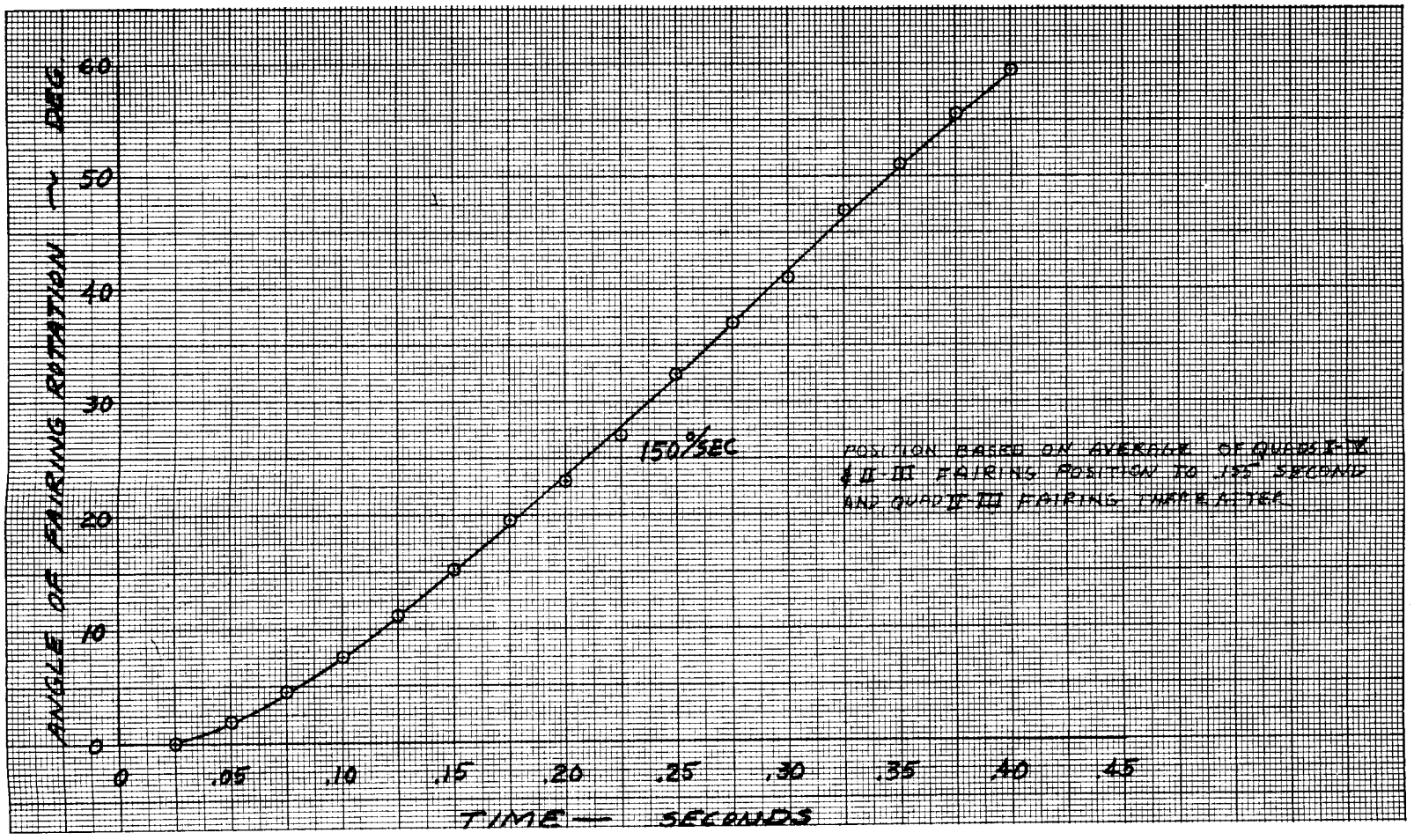

(a) Angular position.

Figure 26. - Centaur nose fairing trajectory, Test 6.

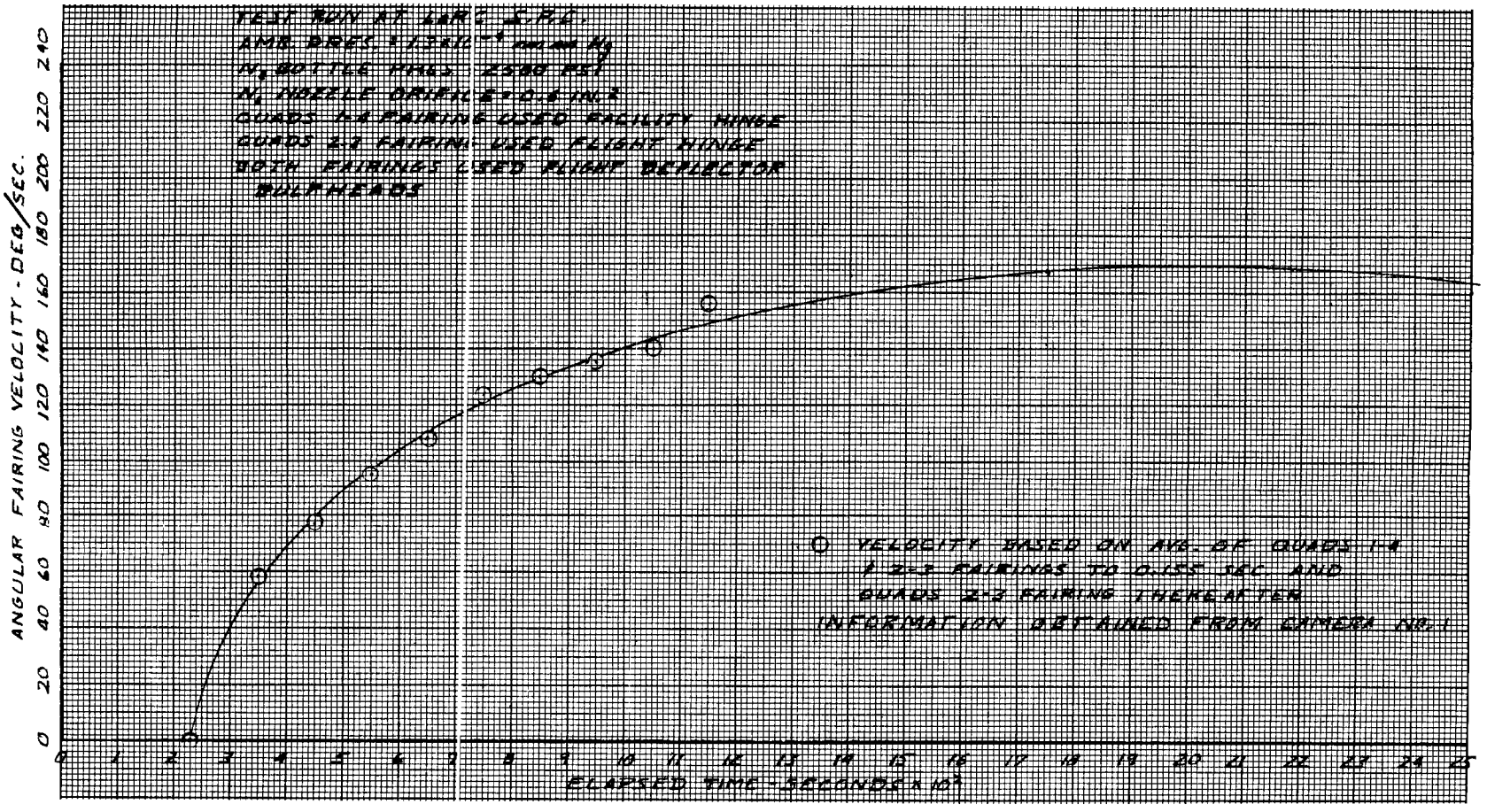

(b) Angular velocity.

Figure 26. - Continued.

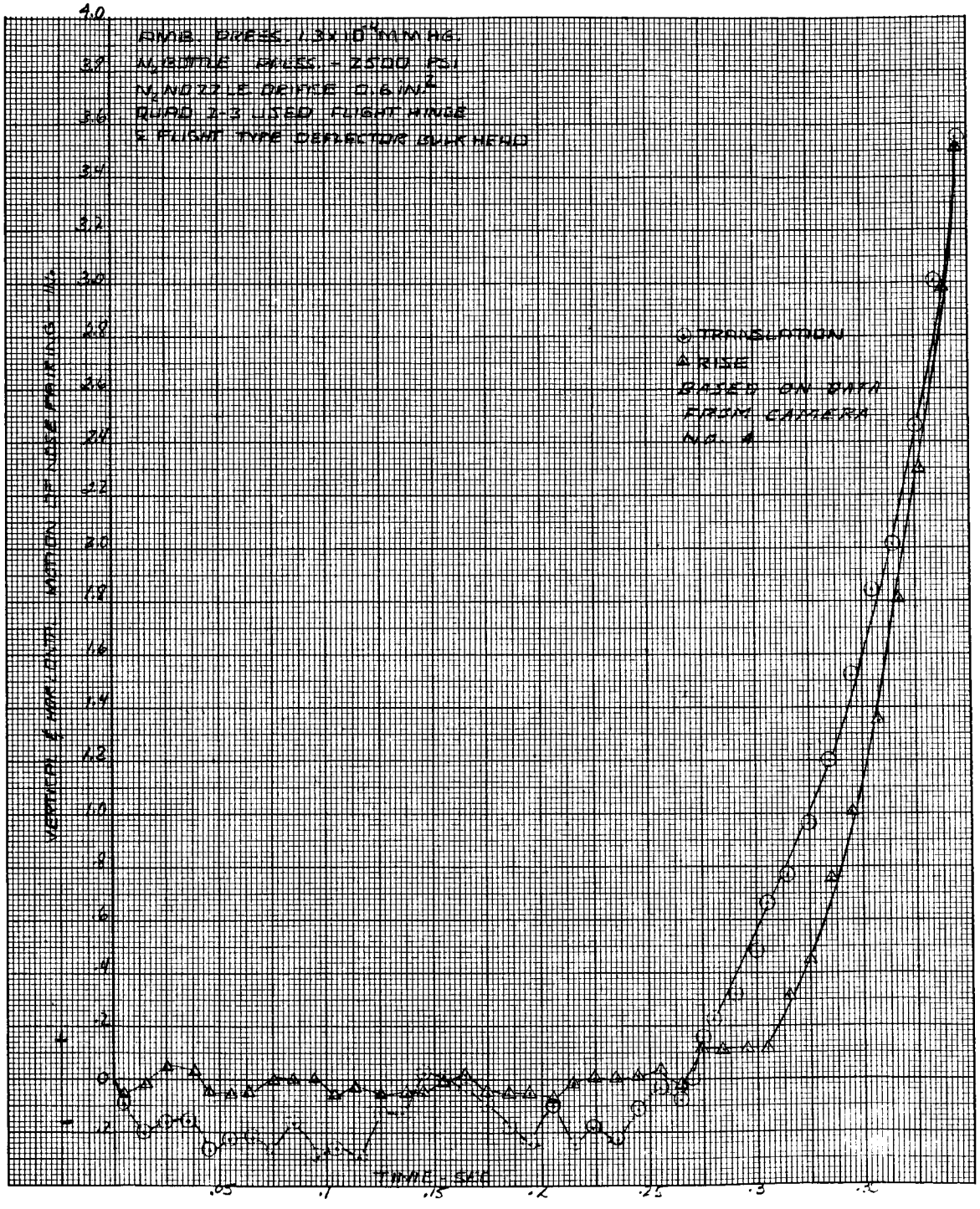

(c) XY motion of II-III fairing hinge.

Figure 26. - Concluded.

C-65-1385

Figure 27. - Shrapnel from explosive bolt squibs.

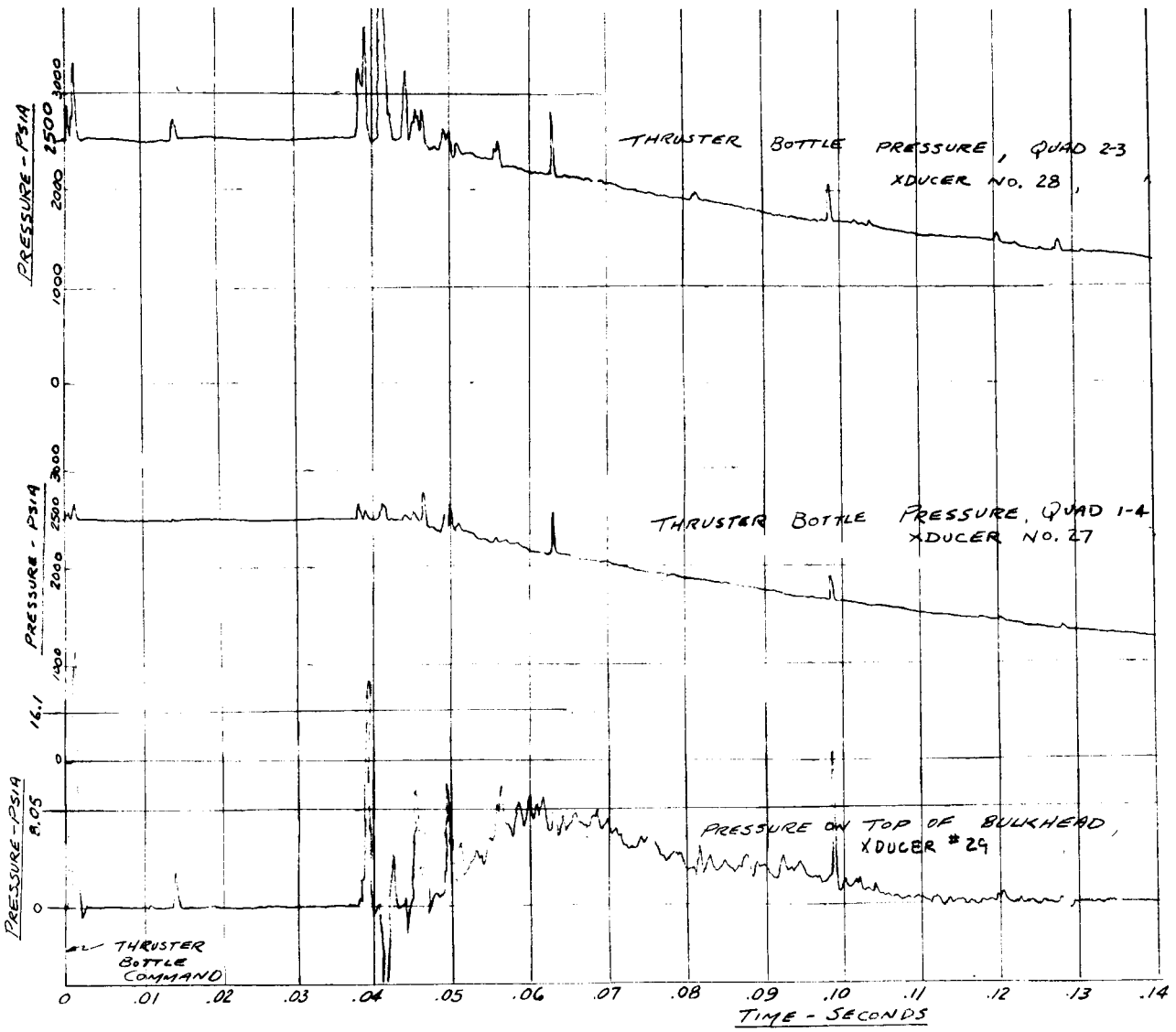

(a) Transducers 27, 28 and 29.

Figure 28. - Nose fairing separation data. Test 7.

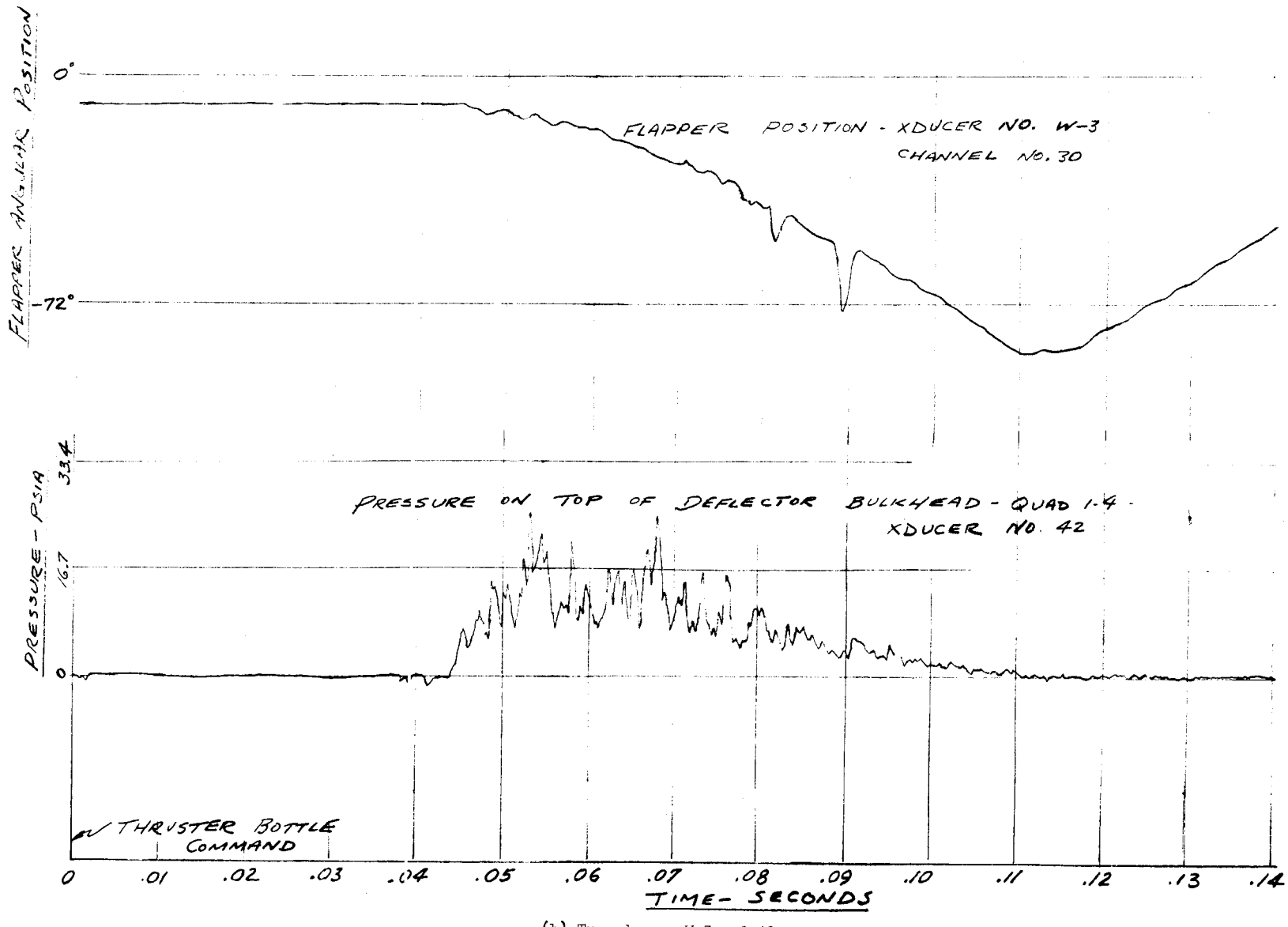

(b) Transducers W-3 and 42.

Figure 28. - Continued.

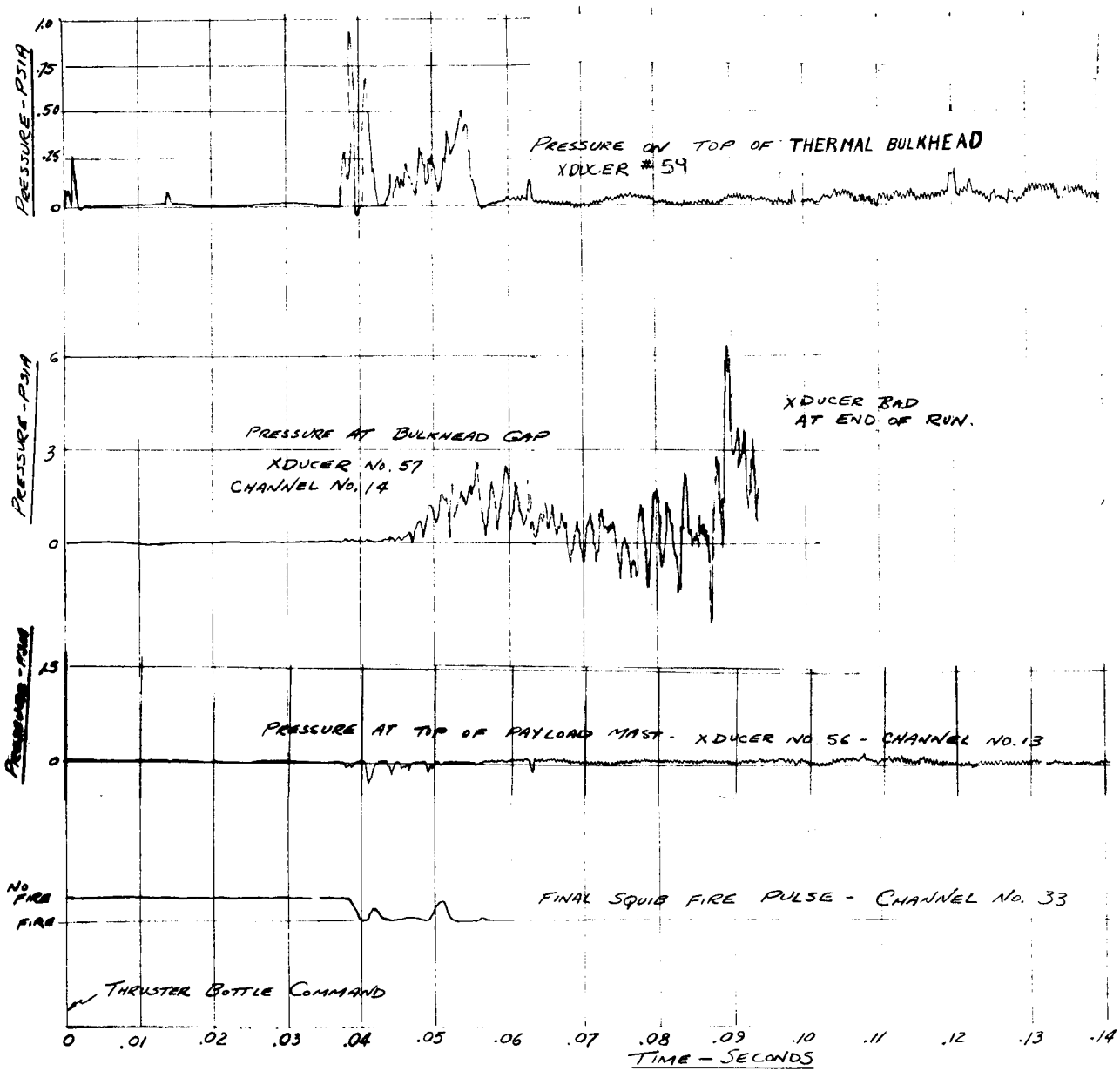

(c) Transducers 57, 56 and 110.

Figure 28. - Continued.

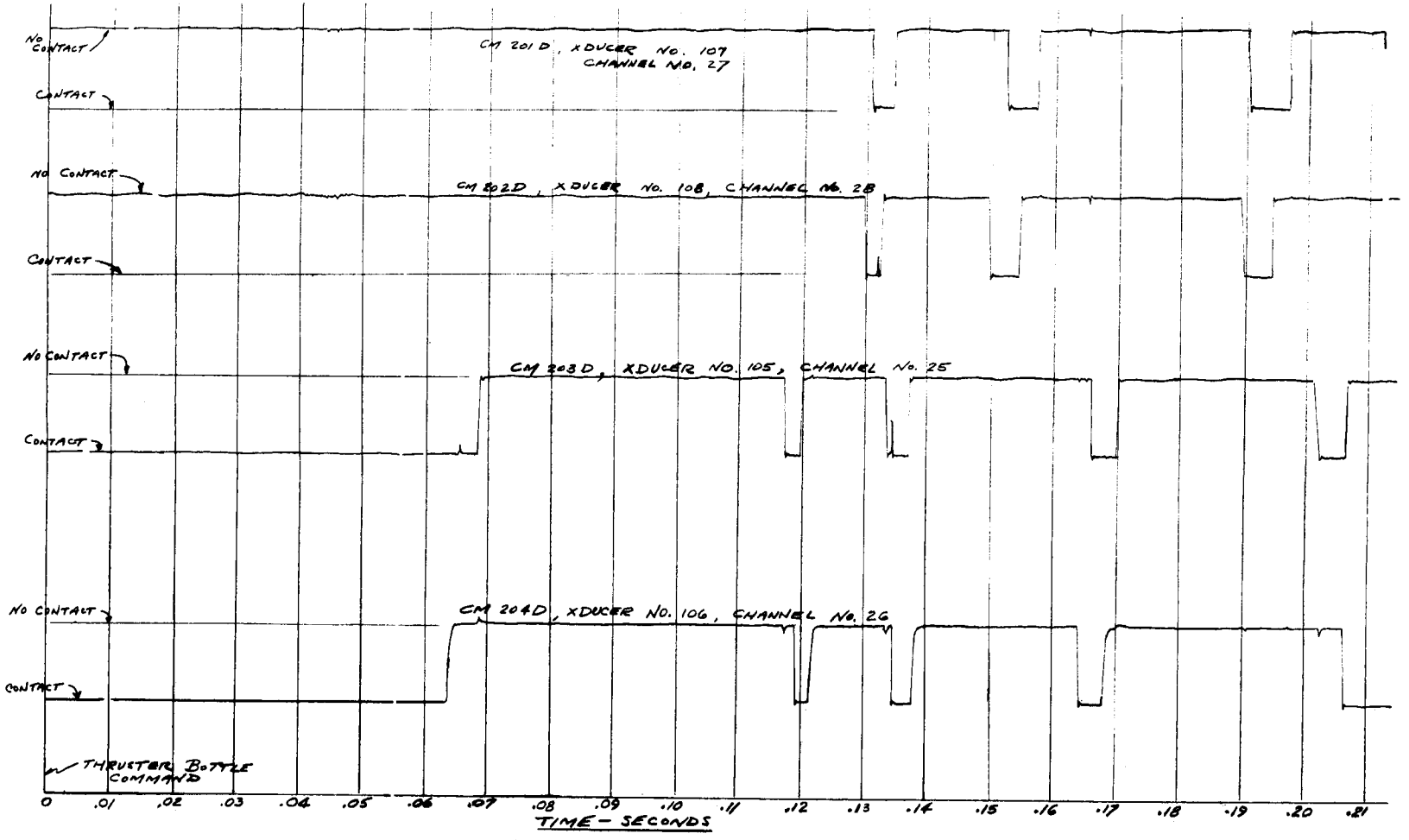

(d) Transducers 105, 106, 107 and 108.

Figure 28. - Continued.

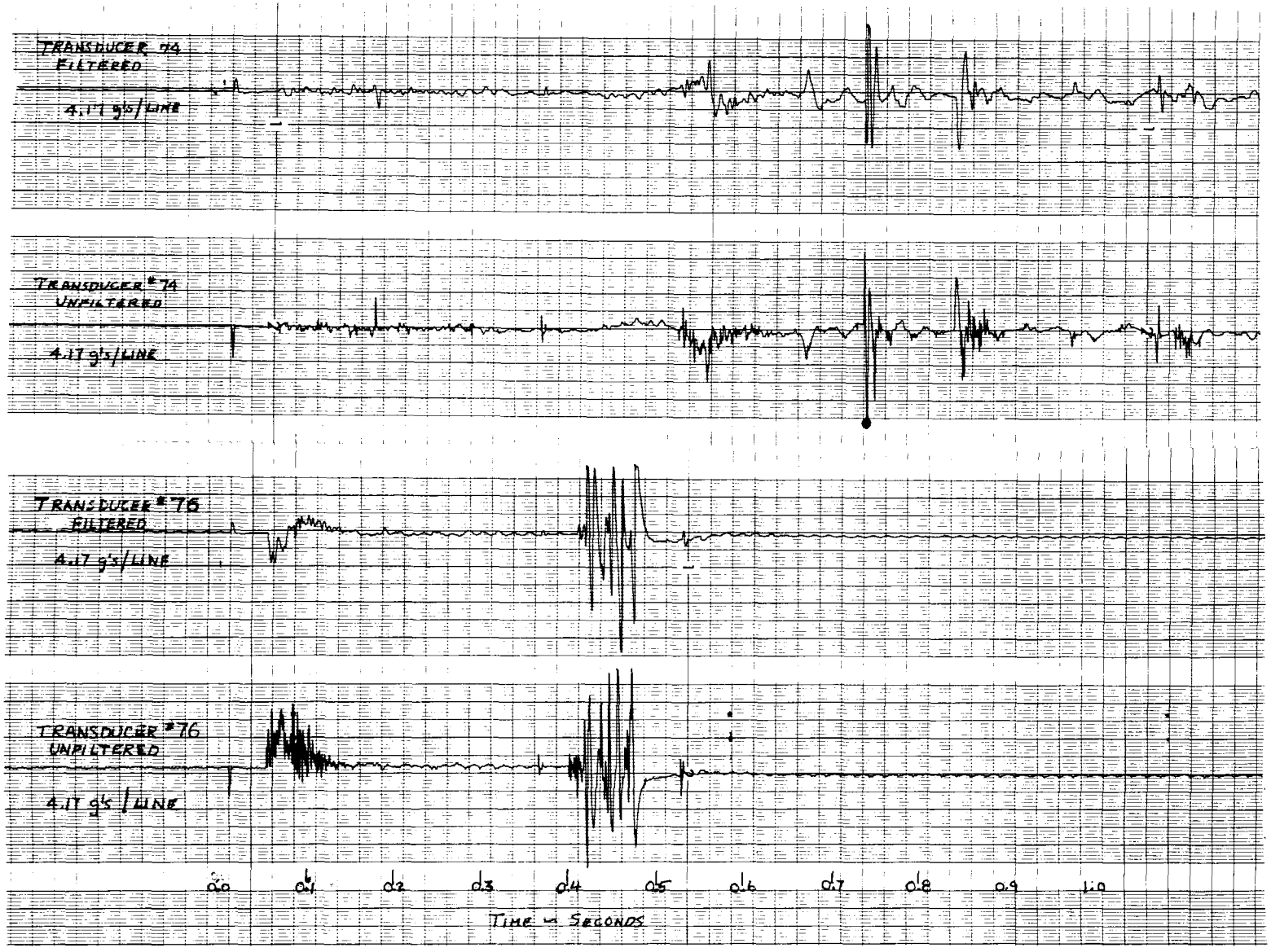

(e) Transducers 74 and 76 filtered and unfiltered by 50 cps lo pass filter.

Figure 28. - Continued.

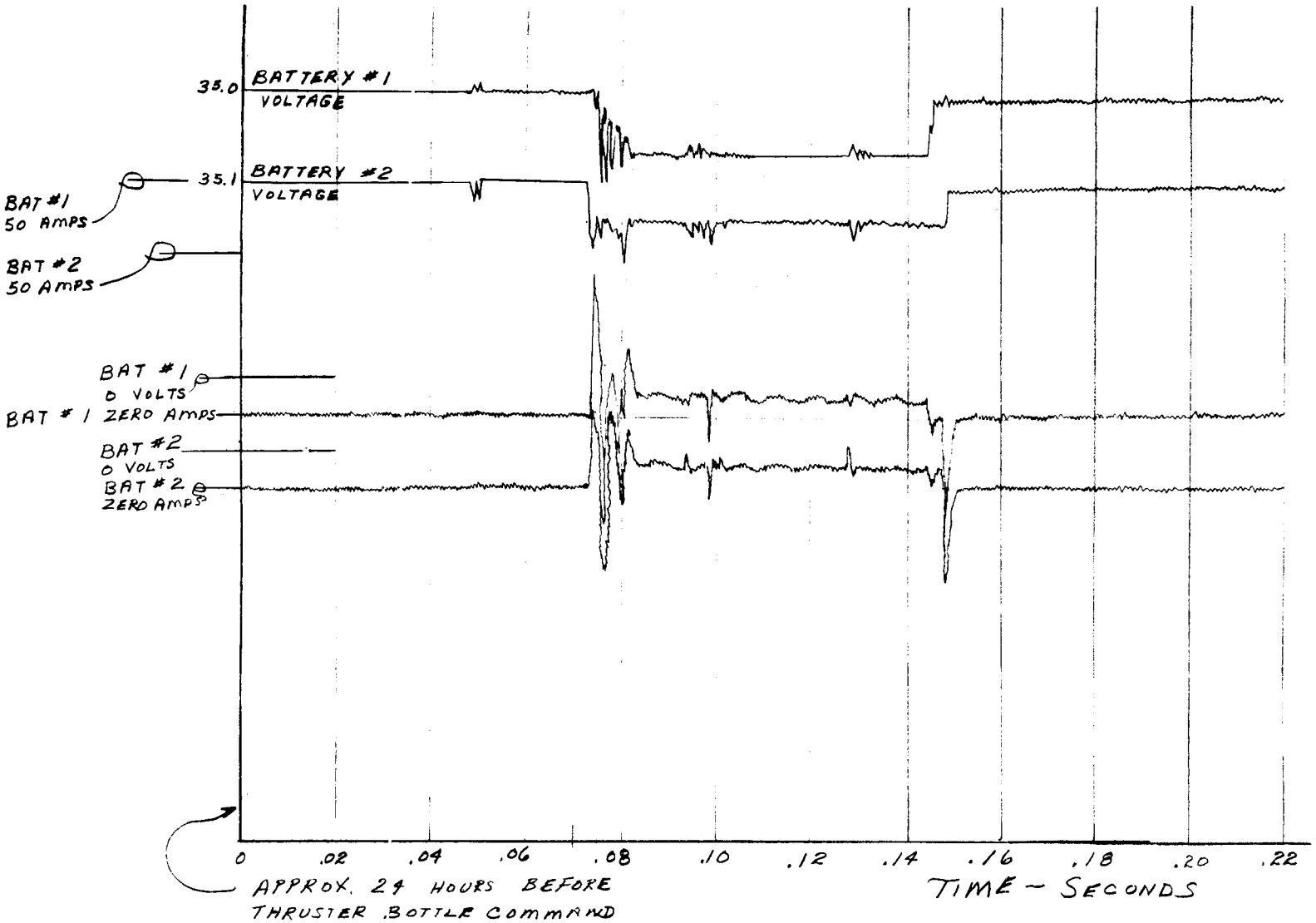

(f) Battery 1 and 2 voltages and current.

Figure 28. - Continued.

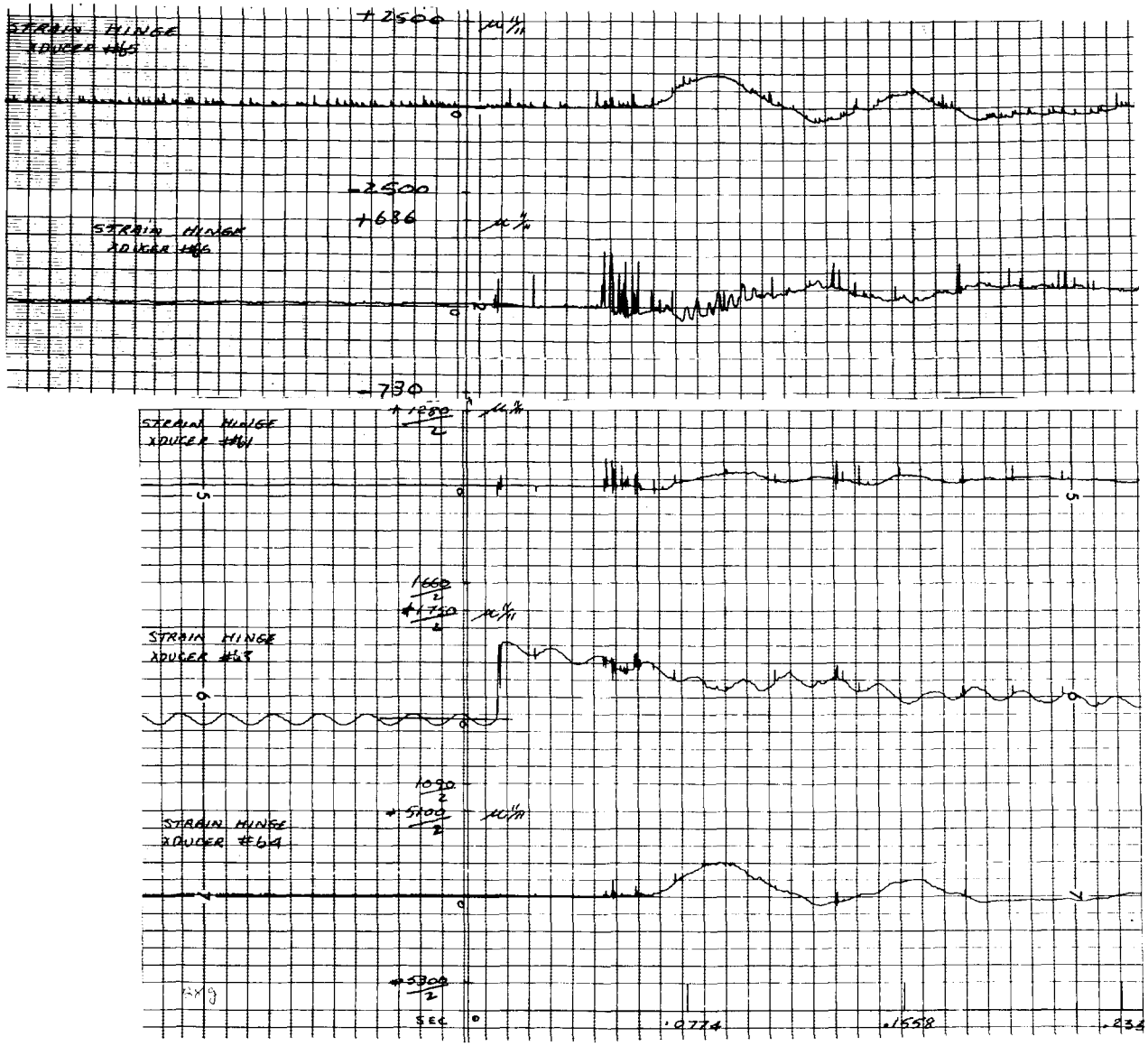

(g) Strain gages 61, 63, 64, 65 and 66.

Figure 28. - Continued.

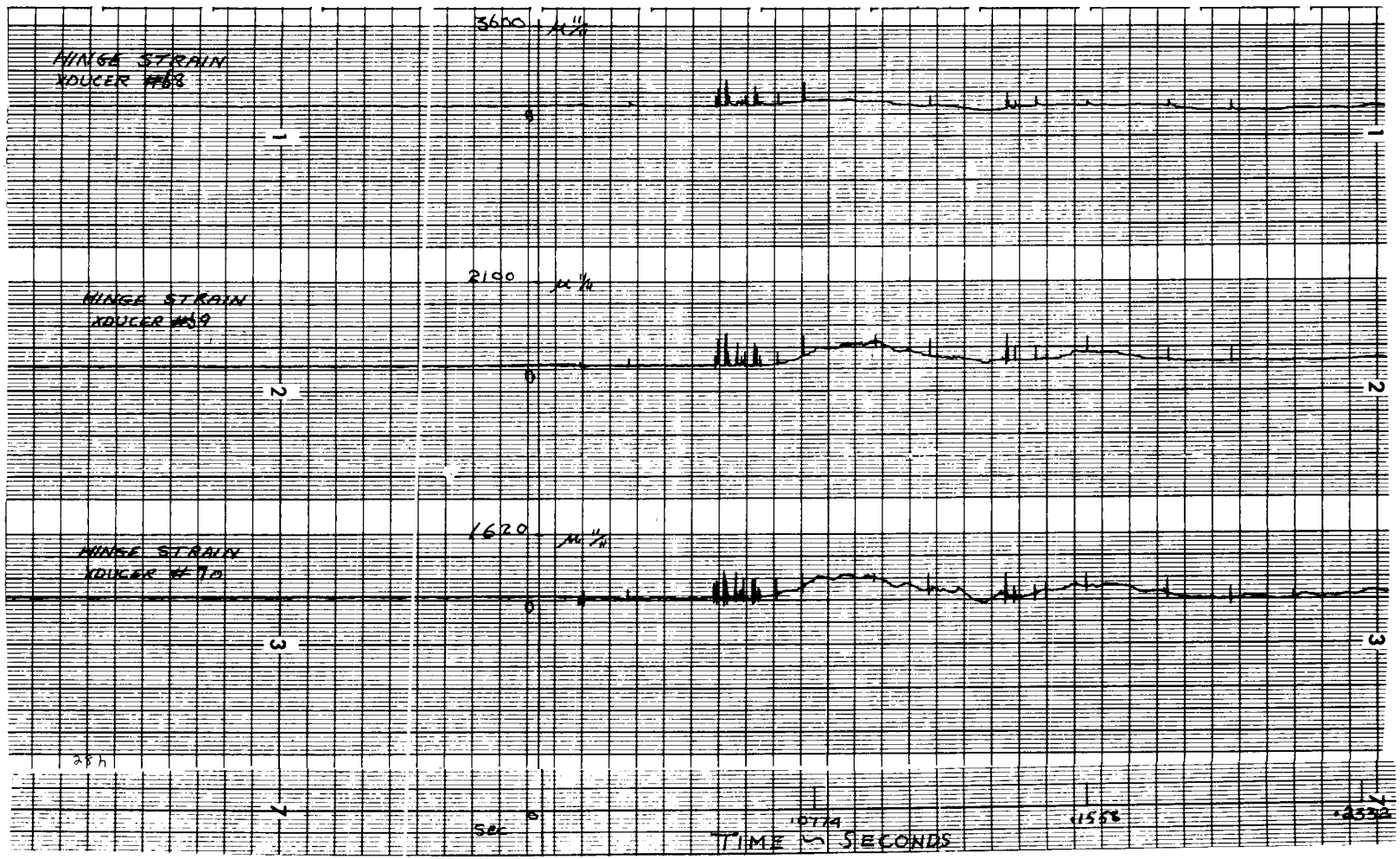

(h) Strain gages 68, 69, and 70.

Figure 28. - Continued.

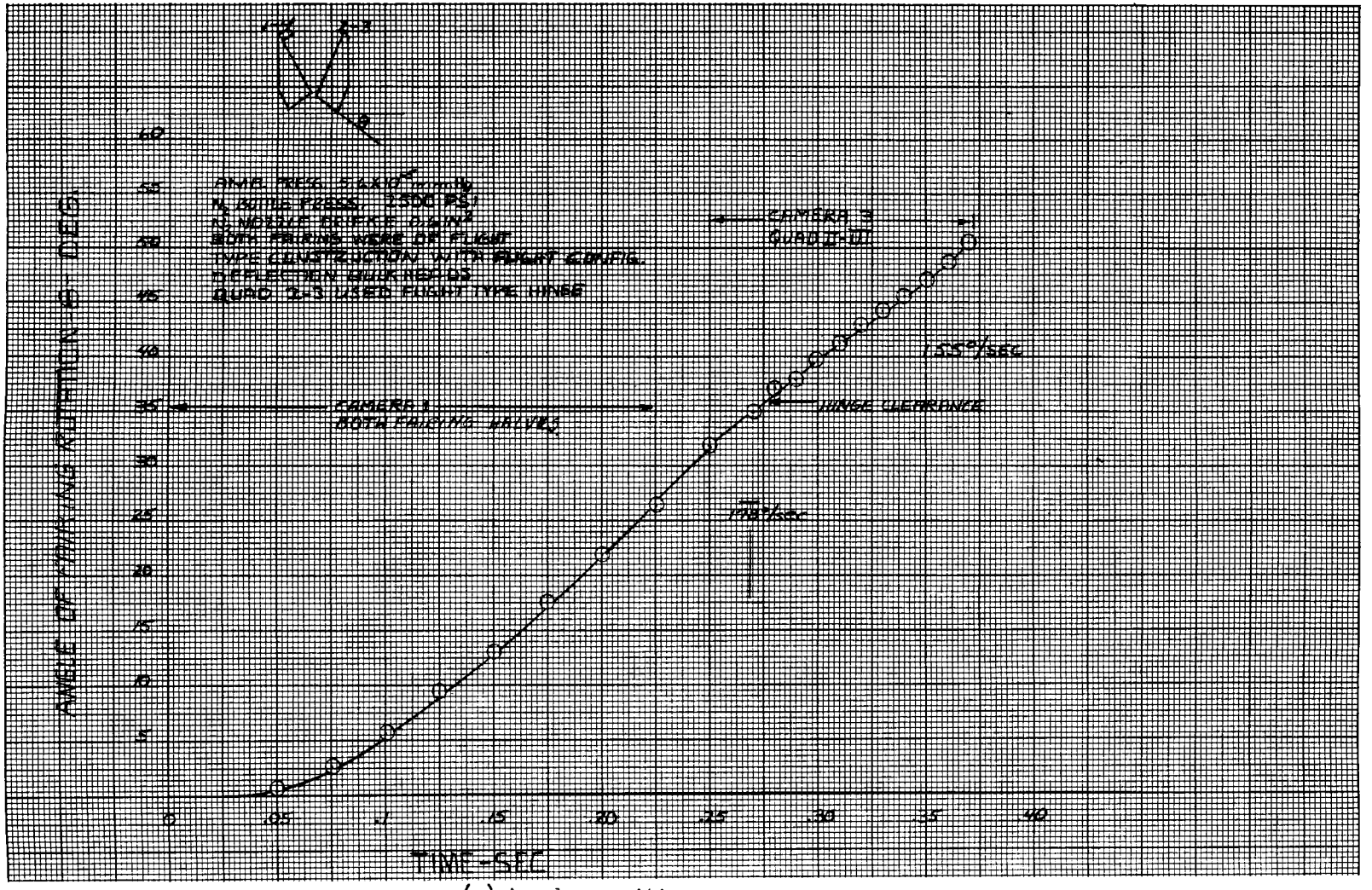

(a) Angular position.

Figure 29. - Centaur nose fairing trajectory, Test 7.

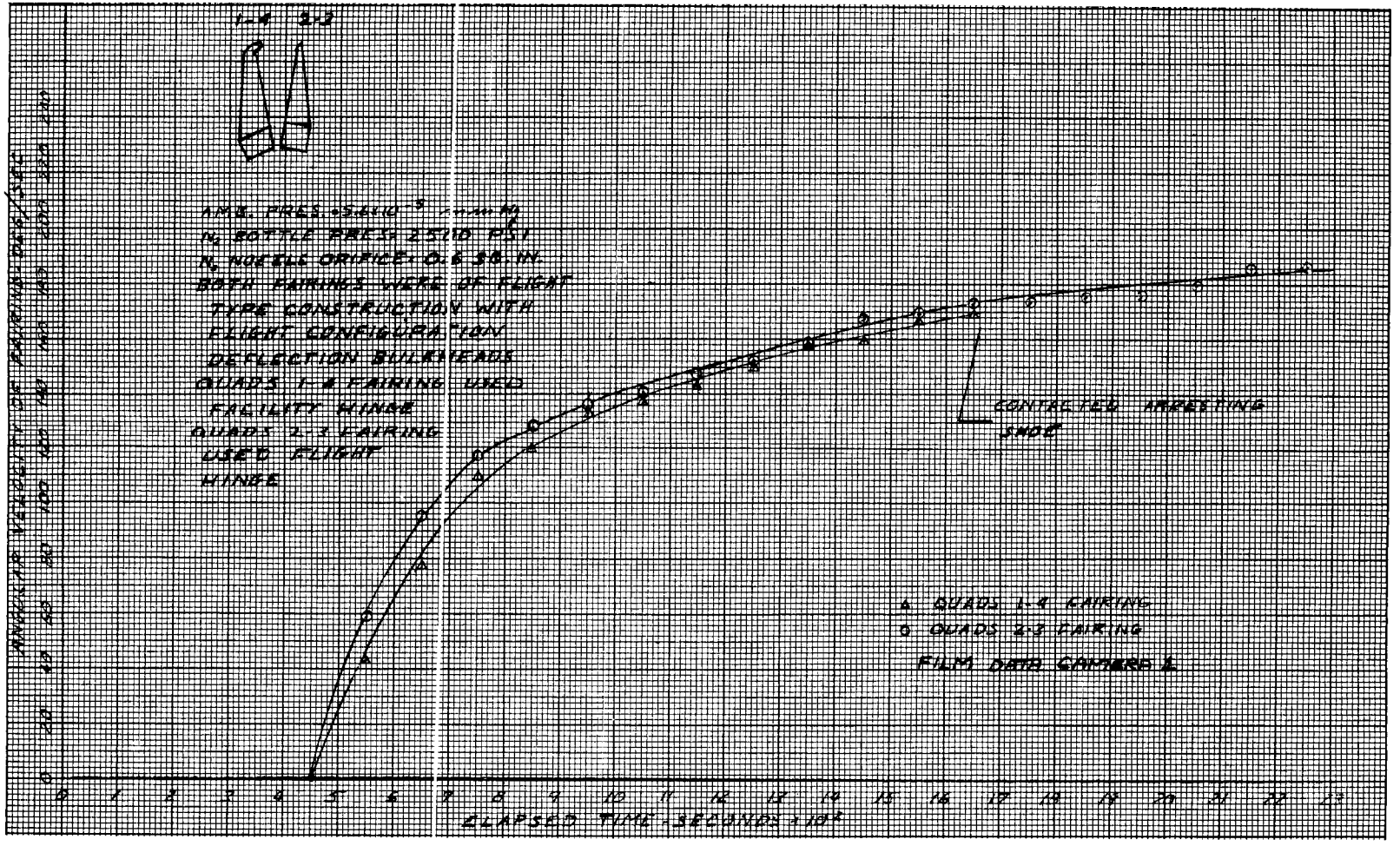

(b) Angular velocity.

Figure 29. - Continued.

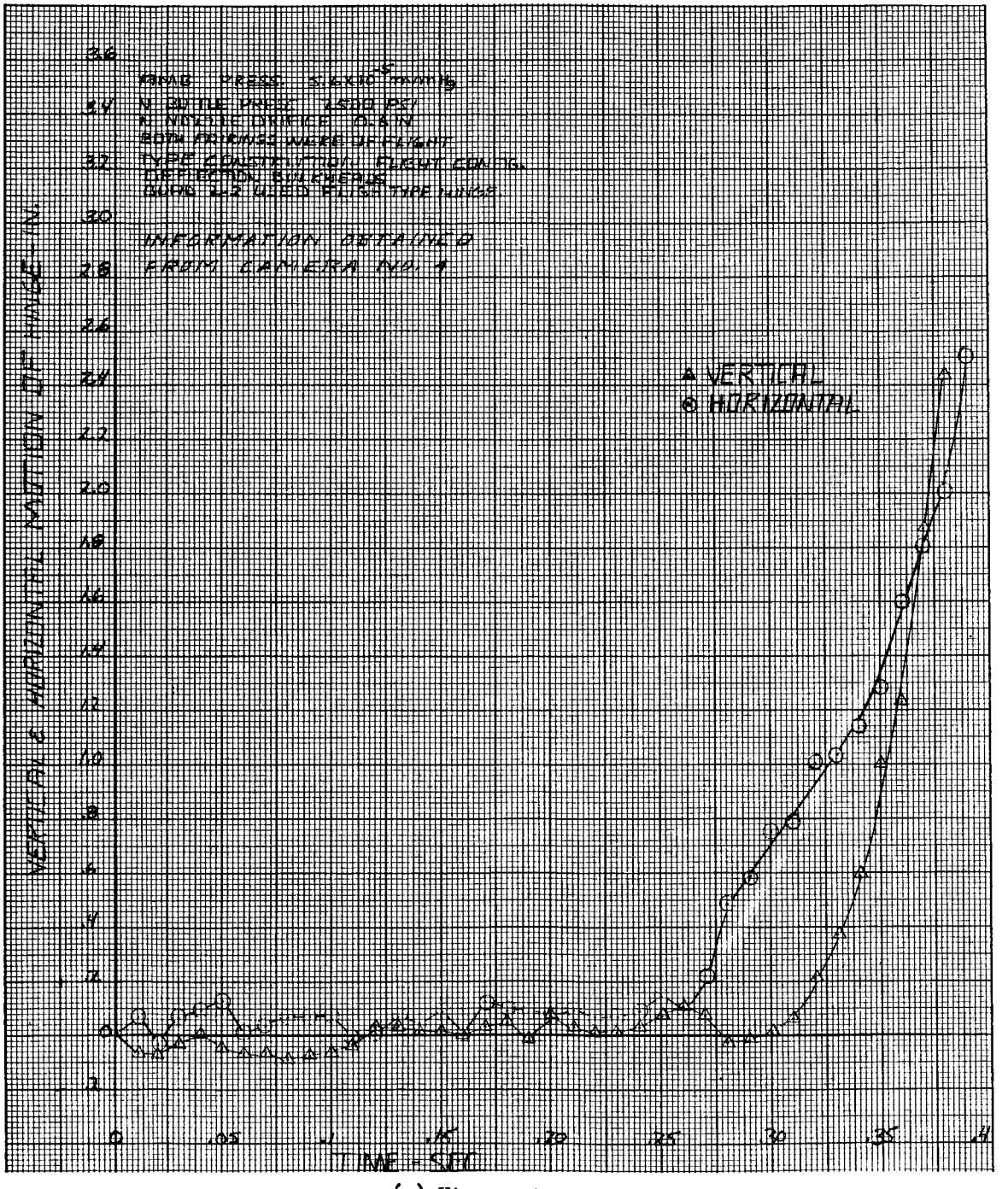

(c) Hinge motion.

Figure 29. - Concluded.

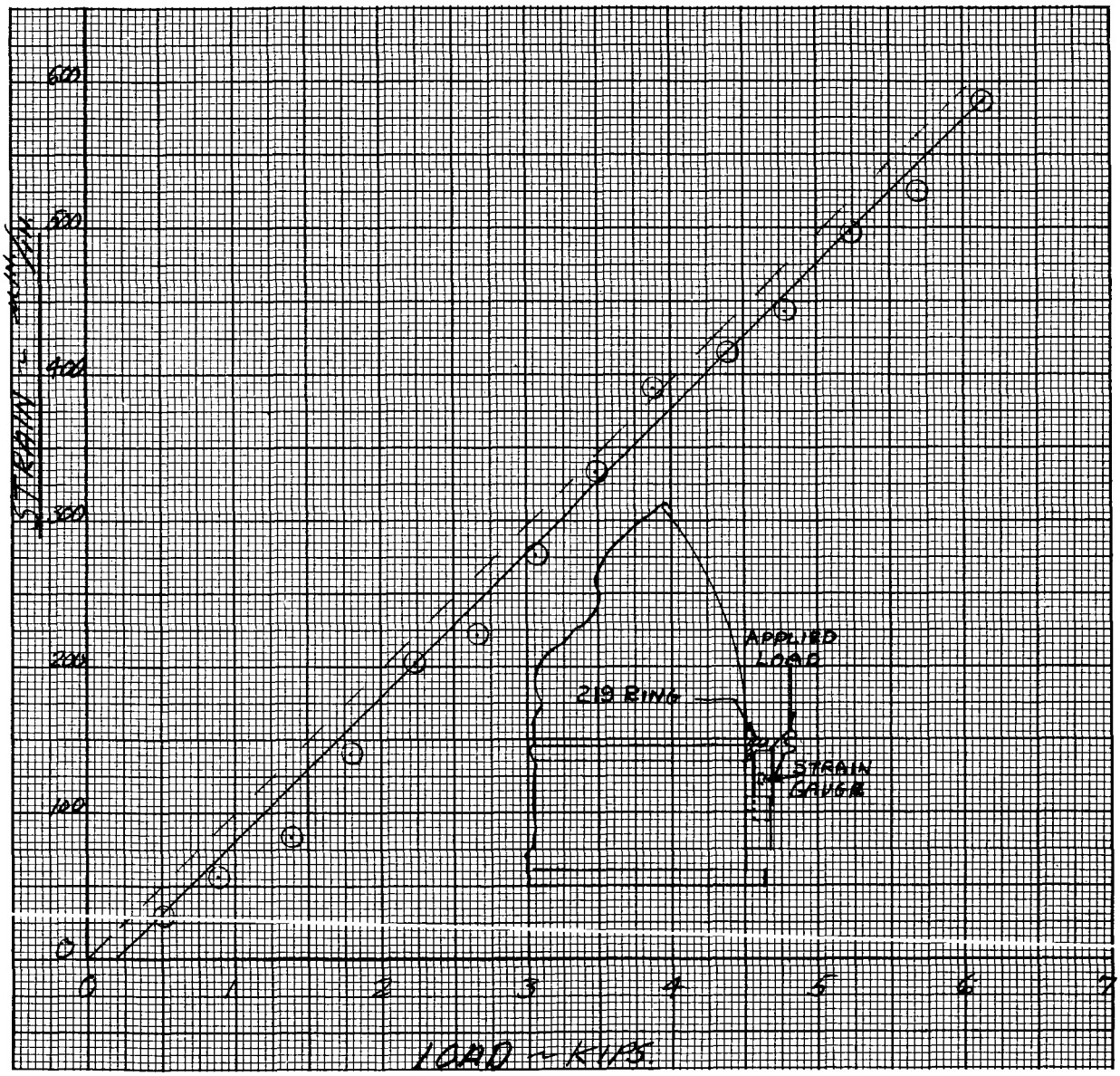

(a) Calibration of strain gage 70.

Figure 30. - Calibration of tank half finge strain gages and spring rate determination.

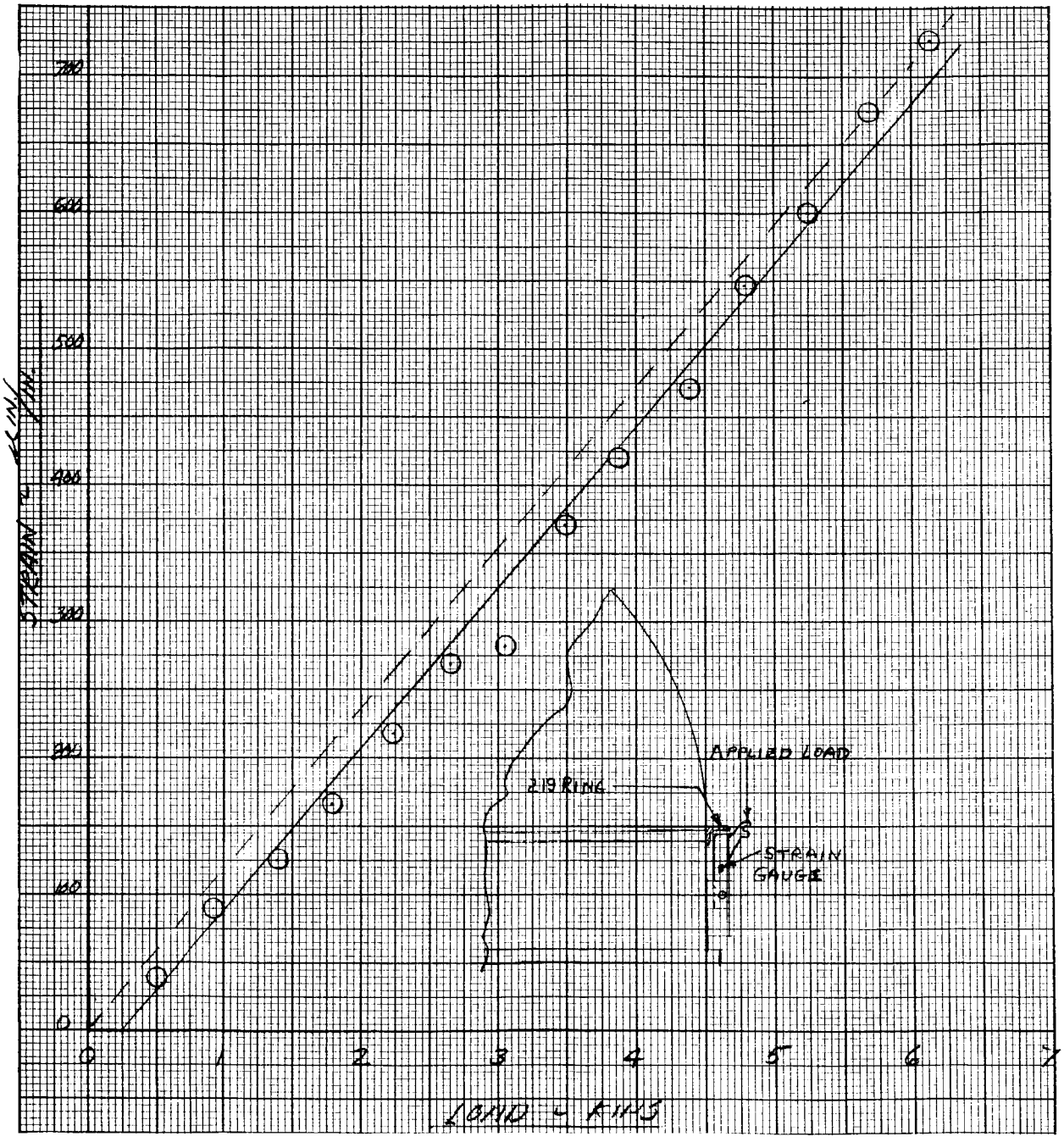

(b) Calibration of strain gage 69.

Figure 30. - Continued.

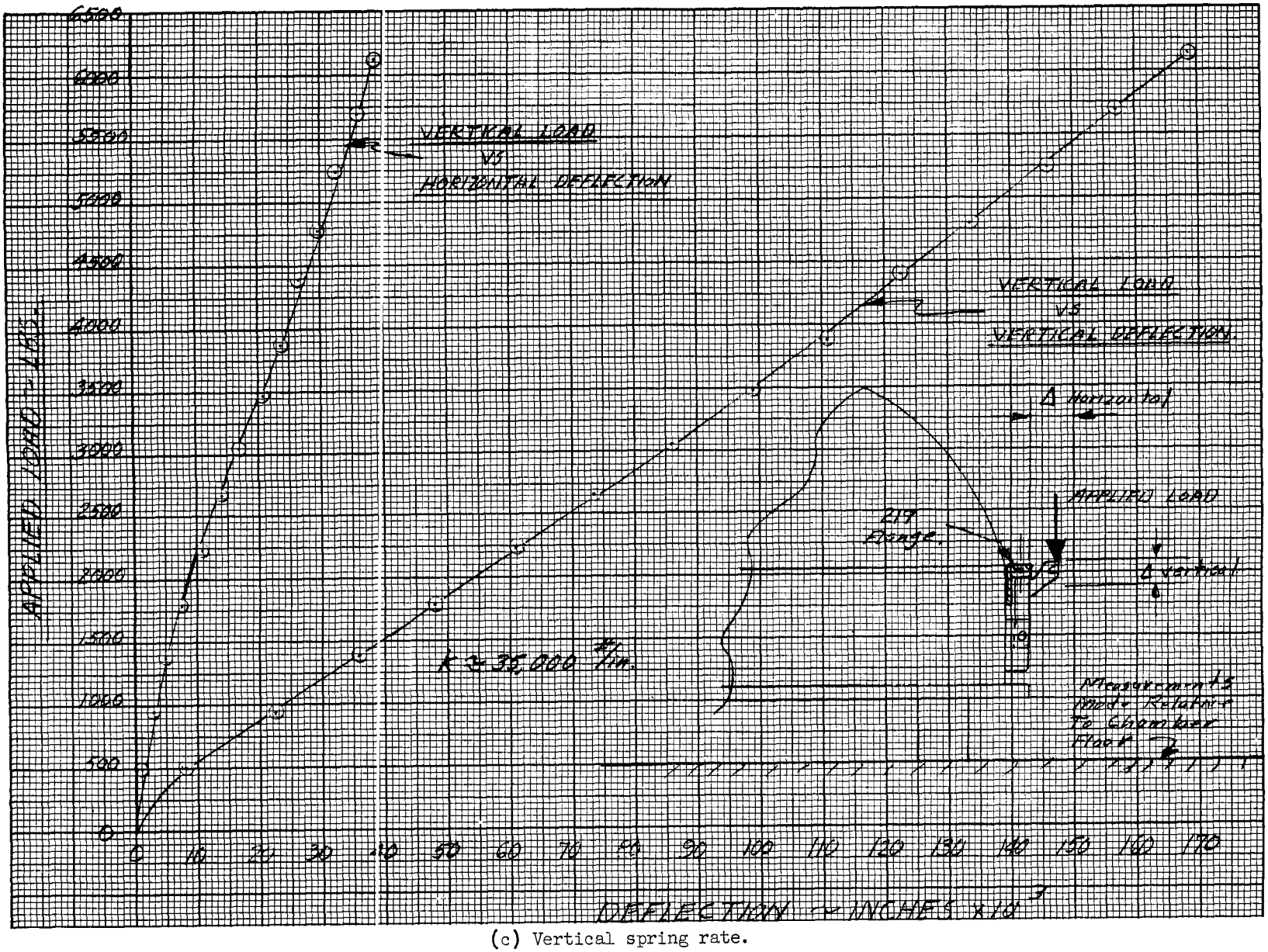

(c) Vertical spring rate.

Figure 30. - Continued.

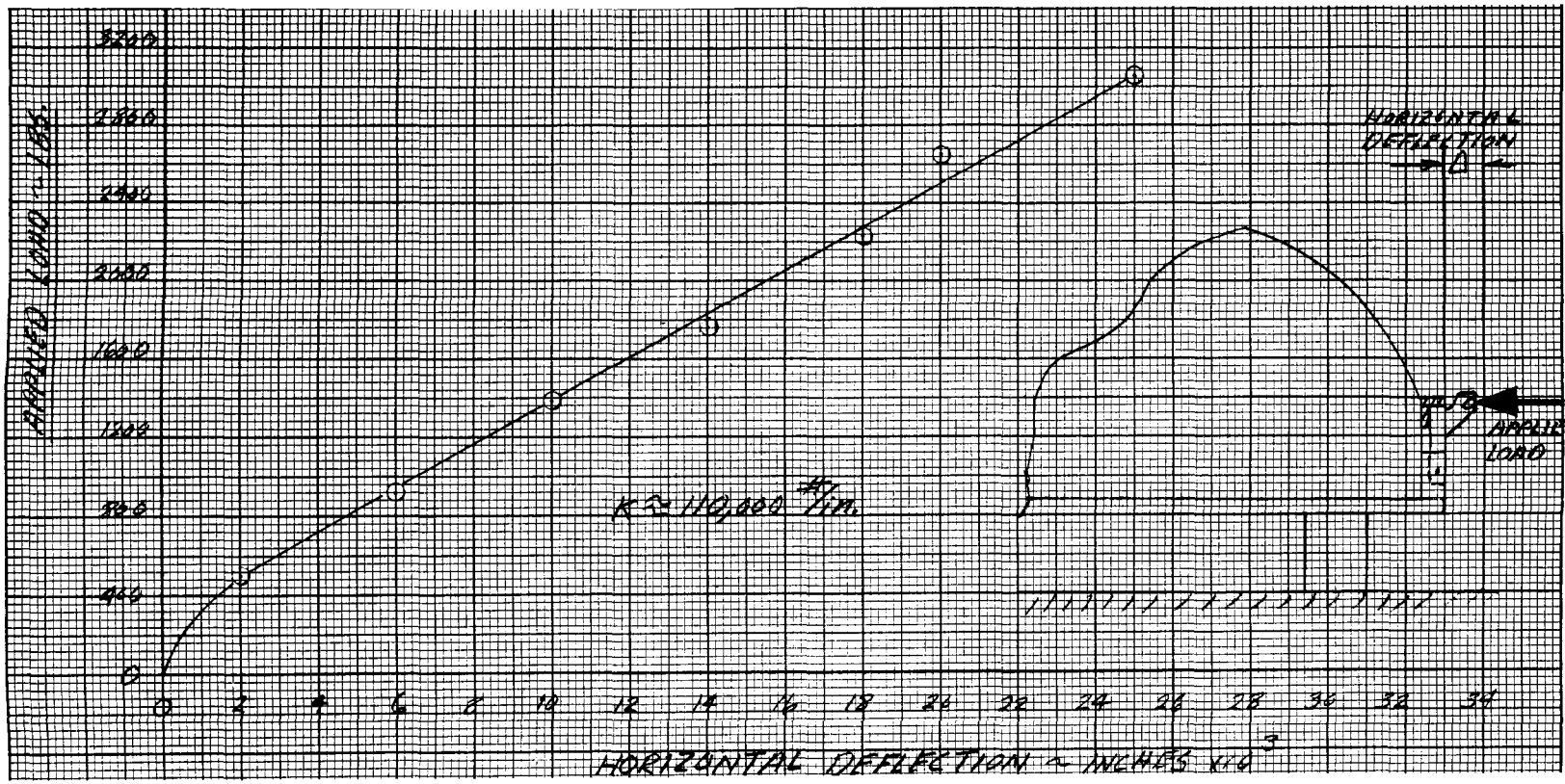

(d) Horizontal spring rate.

Figure 30. - Concluded.

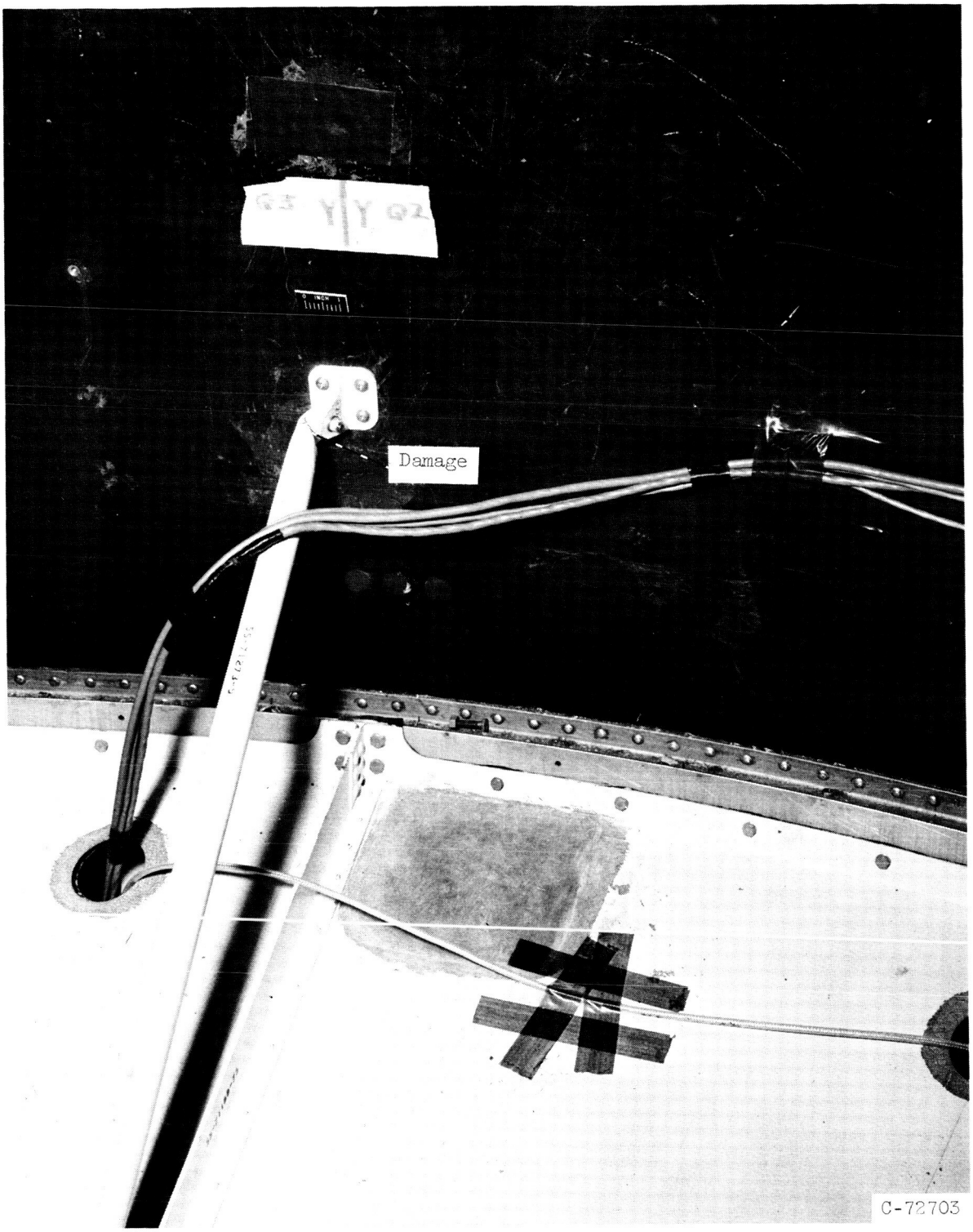

Figure 31. - Strut located on YY axis of II-III half of fairing during Test 8.

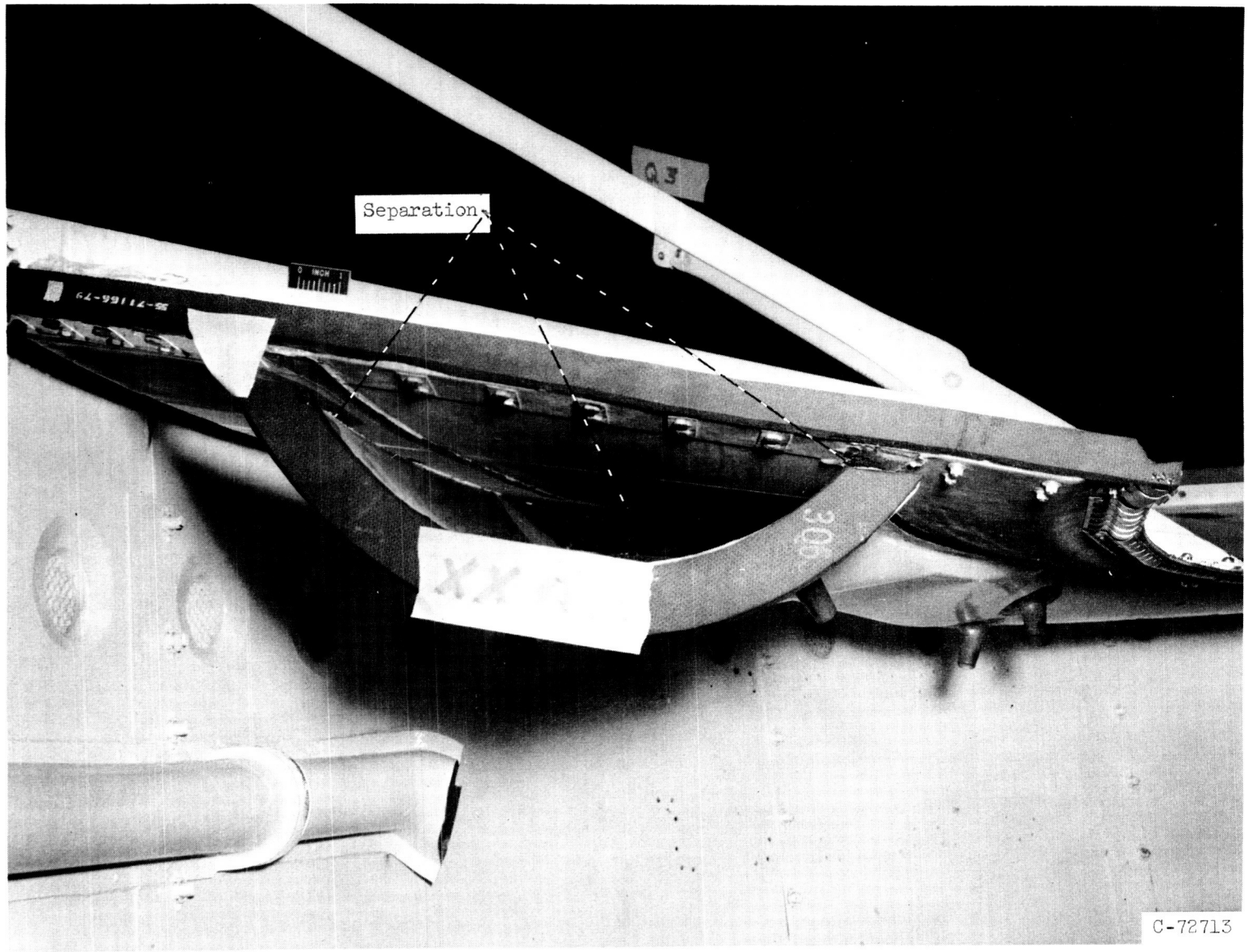

Figure 32. - Failure of air-conditioning duct, Test 8.

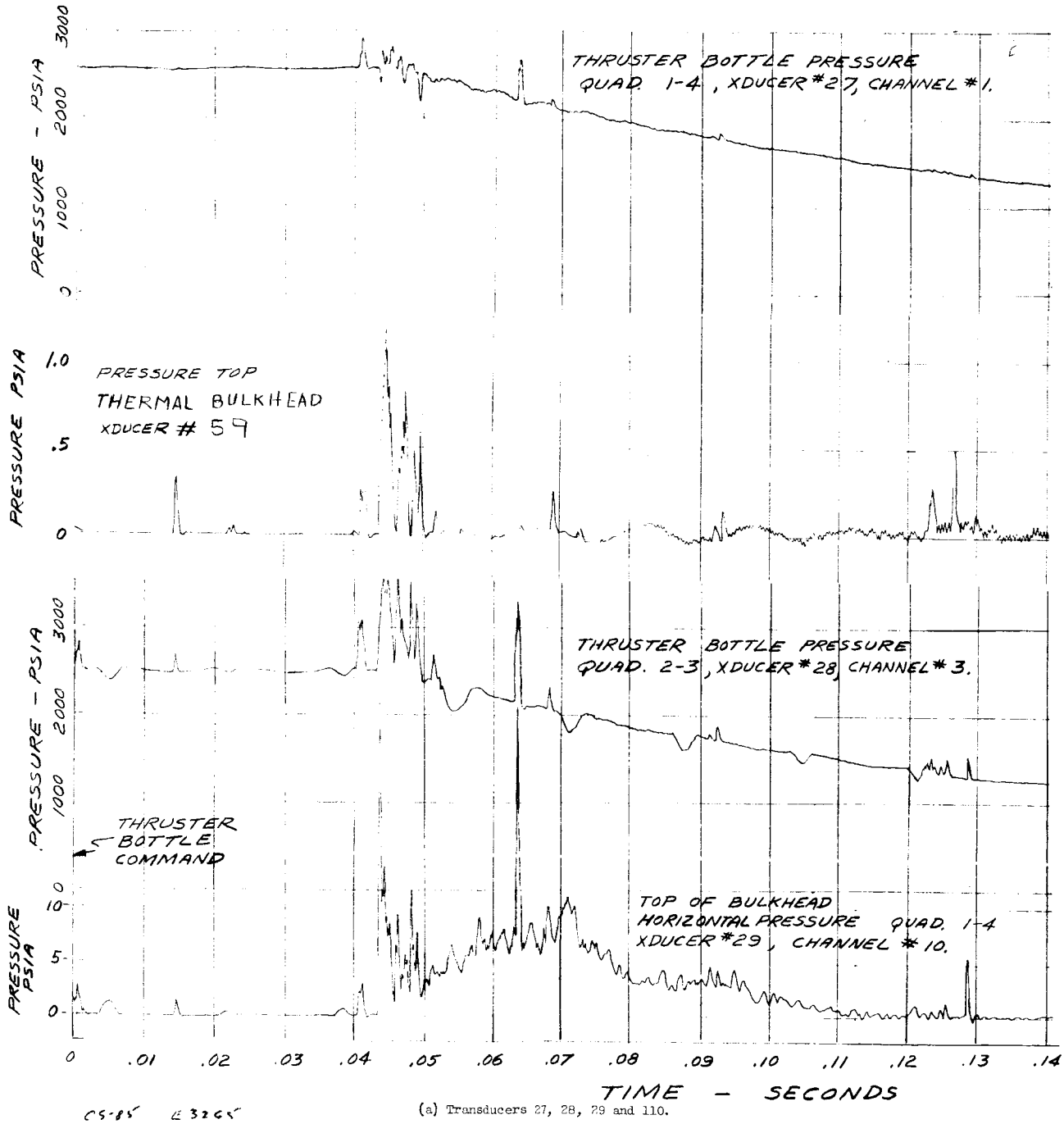

(a) Transducers 27, 28, 29 and 110.

Figure 33. - Nose fairing separation data. Test 8.

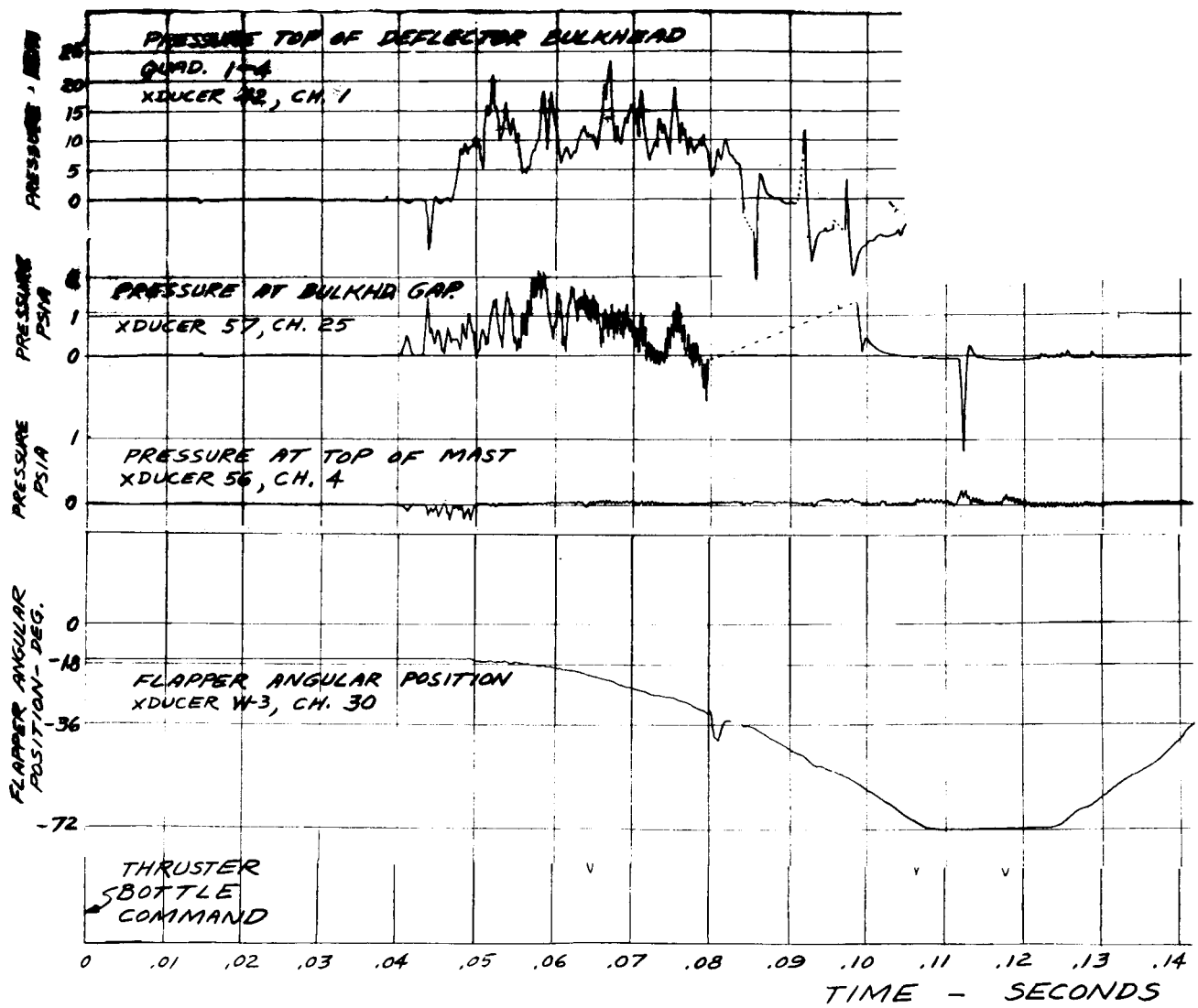

(b) Transducers 42, 56, 57 and W3.

Figure 33. - Continued.

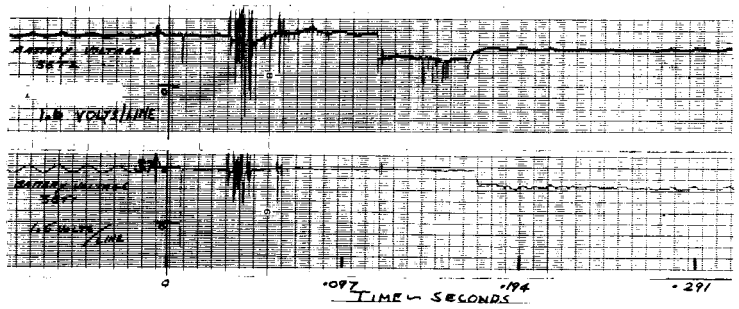

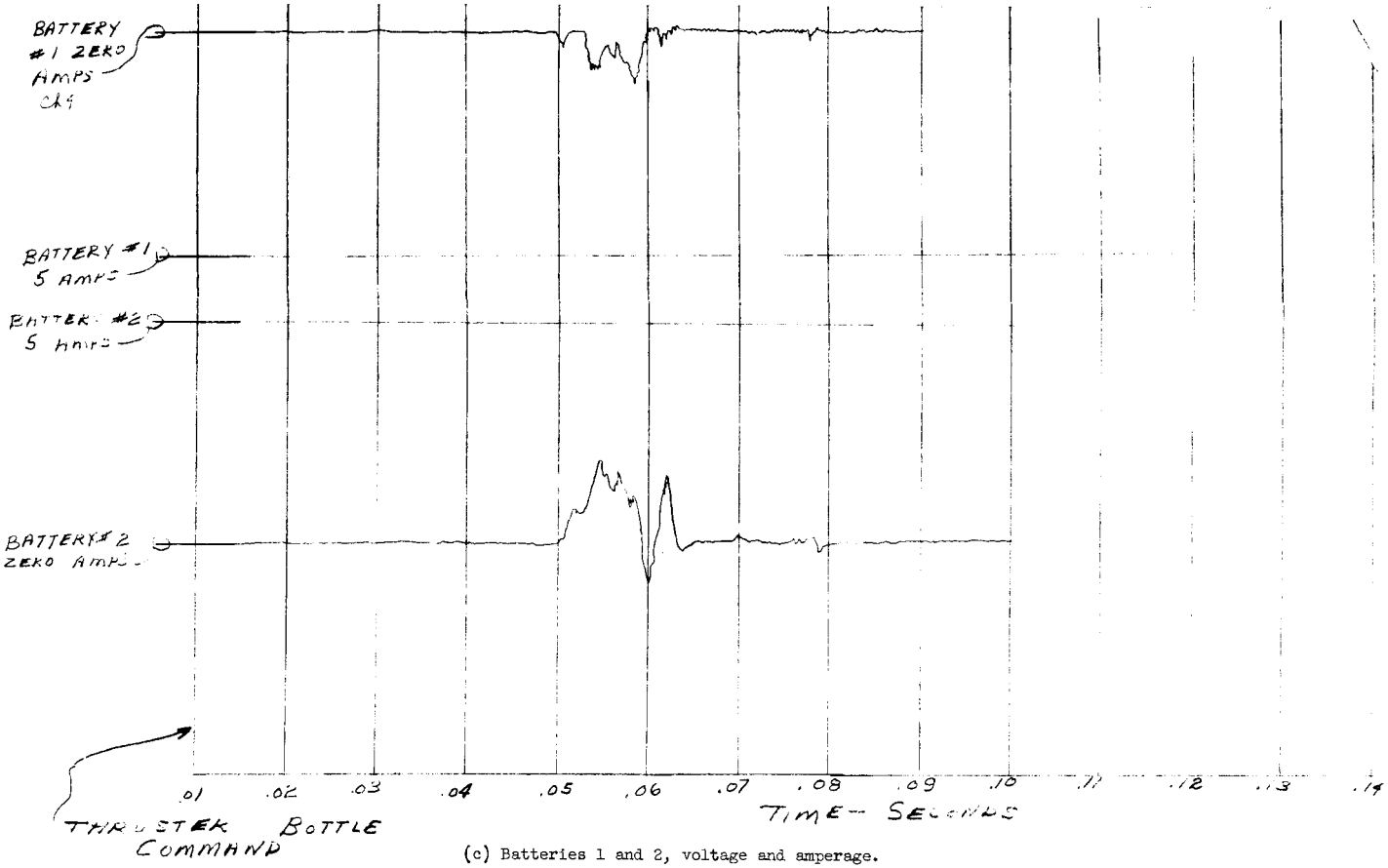

(c) Batteries 1 and 2, voltage and amperage.

Figure 33. - Continued.

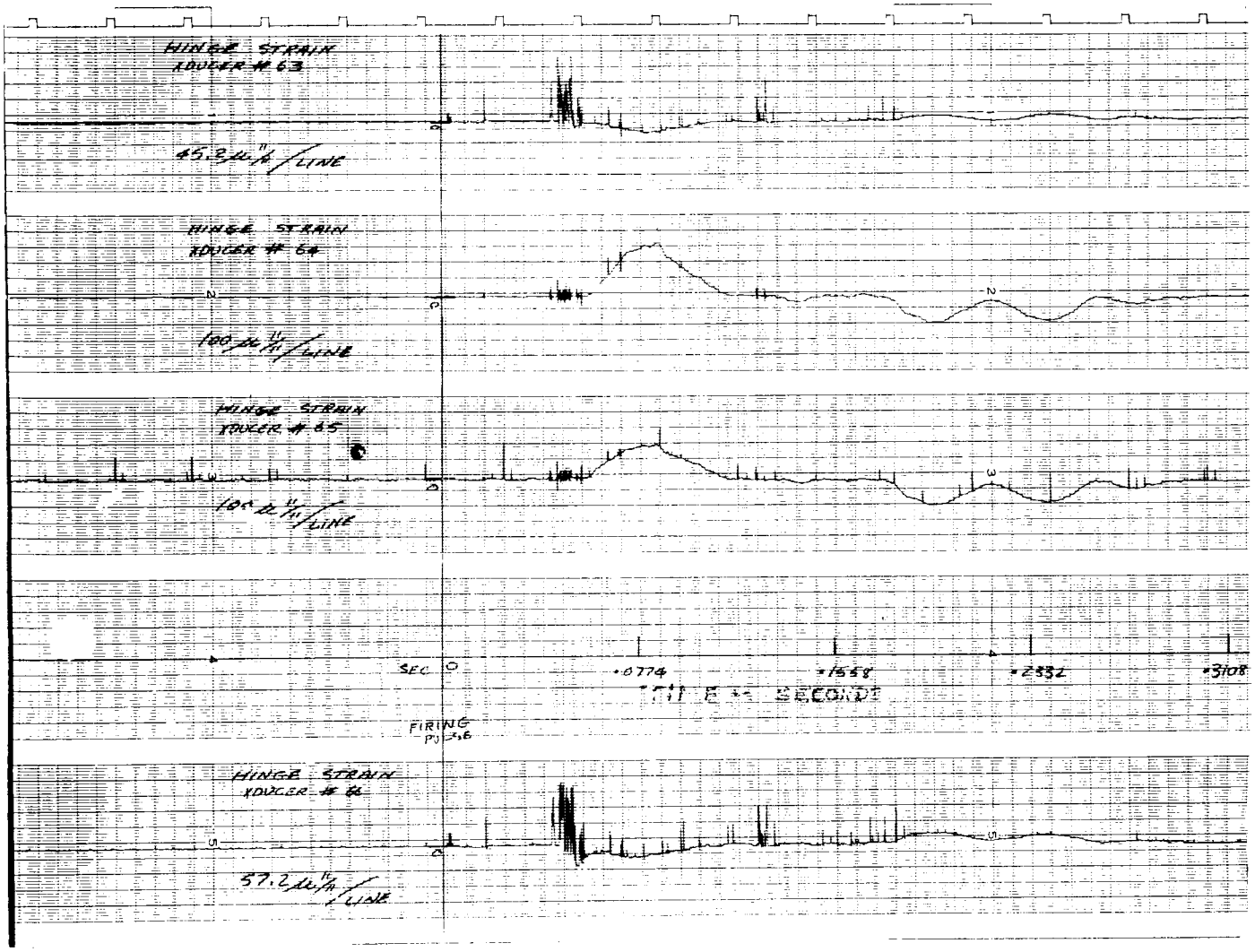

(d) Strain gages 63, 64, 65 and 66.

Figure 32. - Continued.

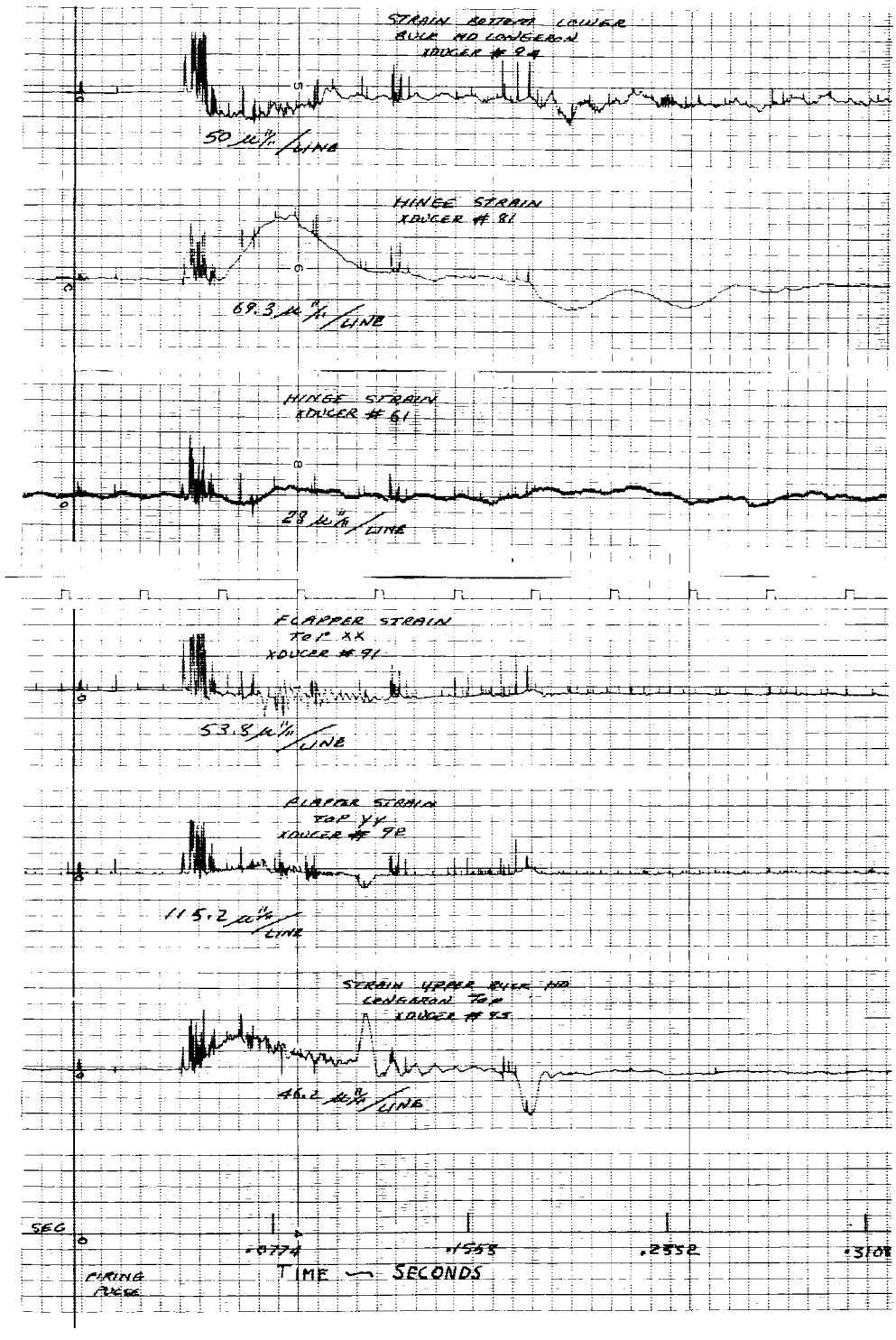

(e) Strain gages 61, 81, 91, 92, 93 and 94.

Figure 33. - Continued.

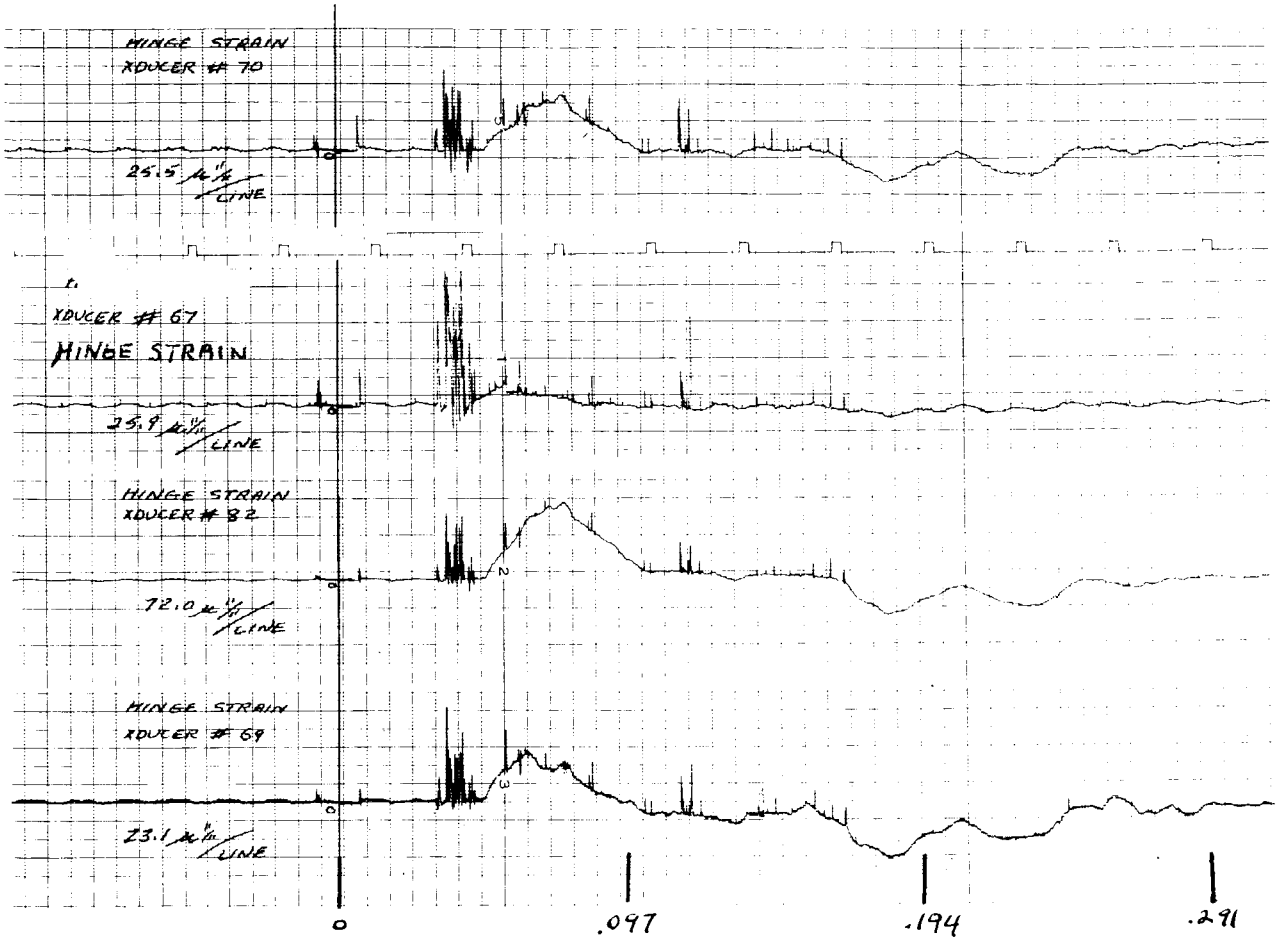

(f) Strain gages 67, 69, 70 and 82.

Figure 33. - Concluded.

E-3265

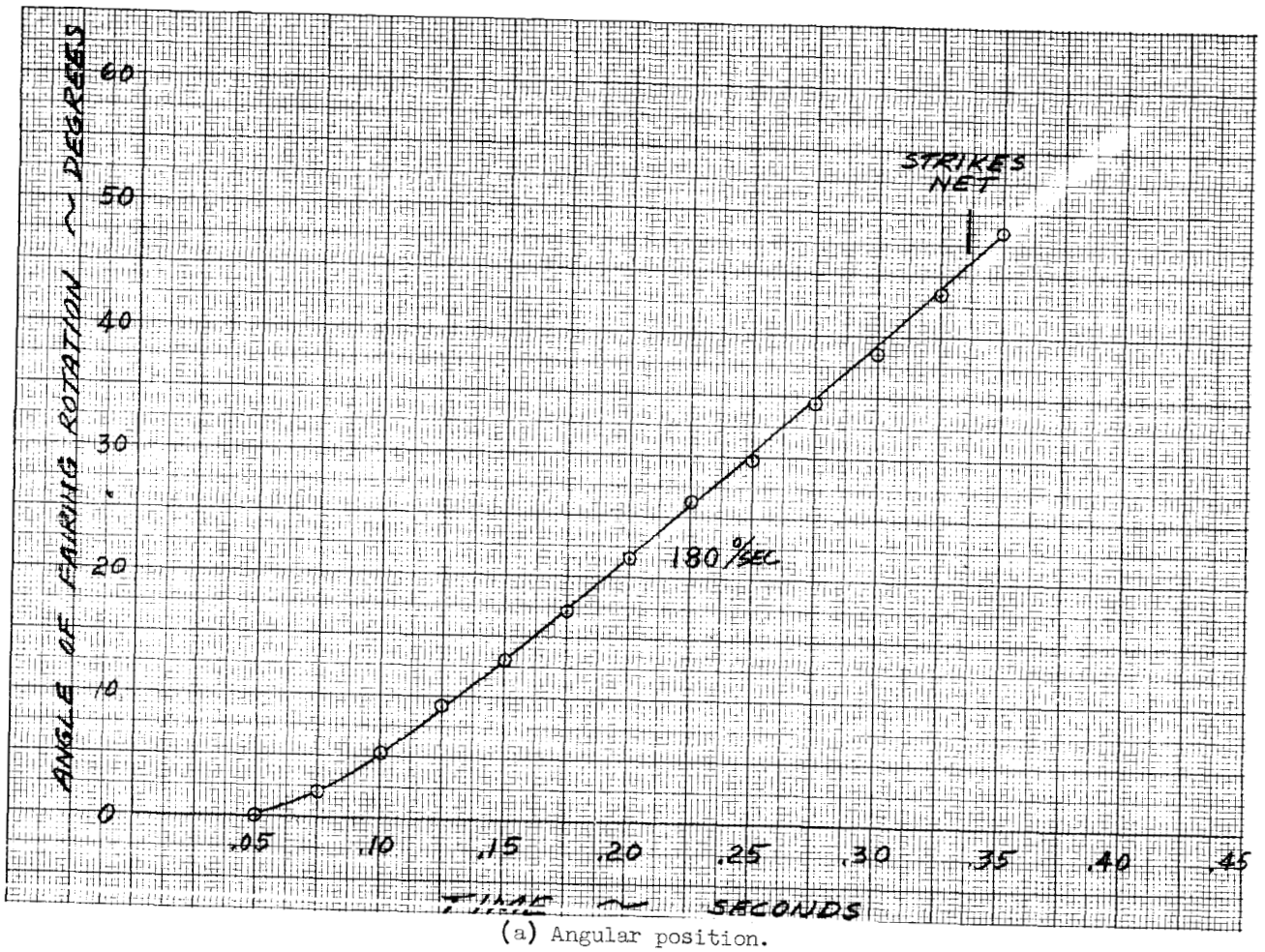

(a) Angular position.

Figure 34. - I-IV Centaur nose fairing half trajectory, Test 8.

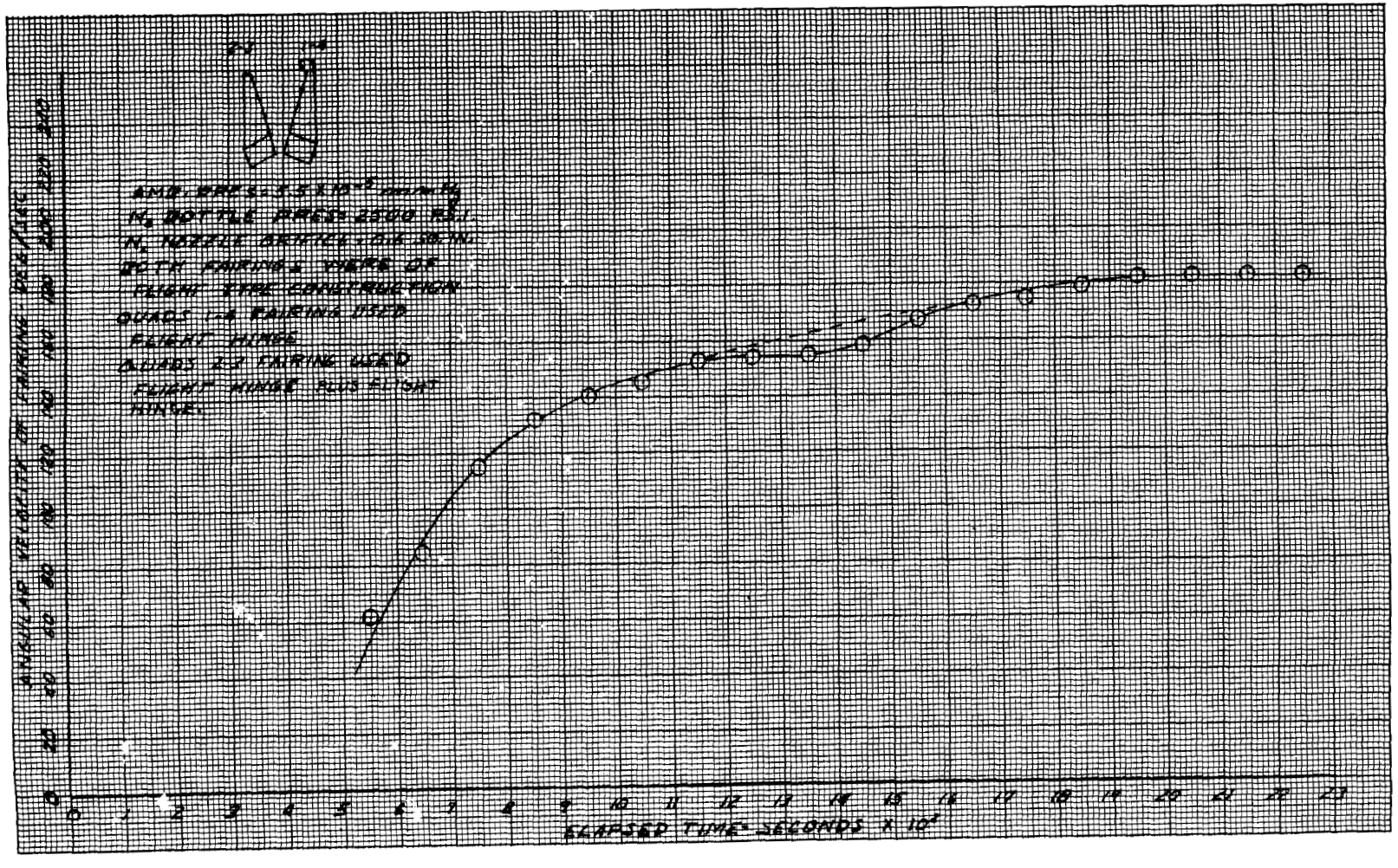

(b) Angular velocity.

Figure 34. - Continued.

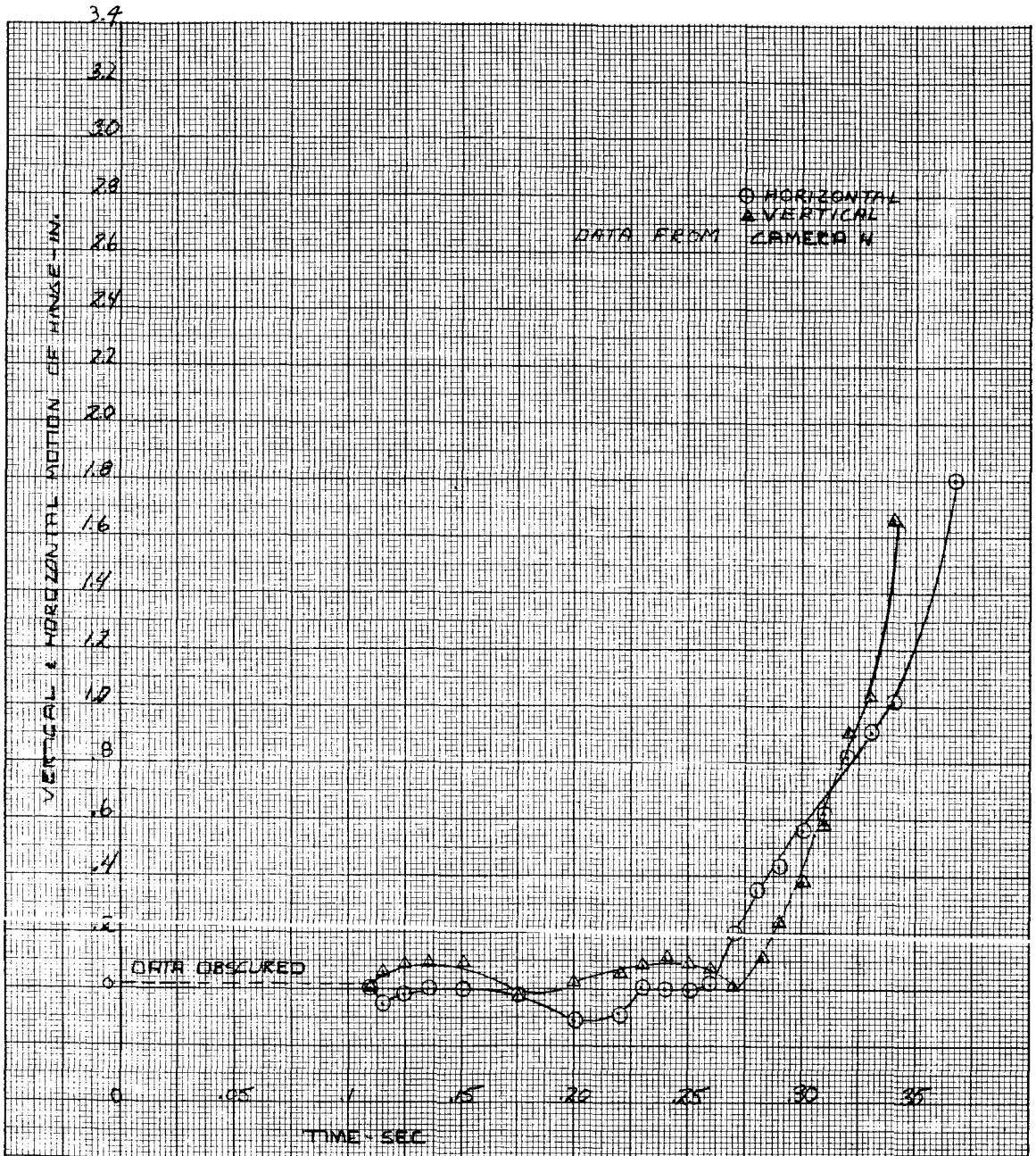

(c) Hinge motion.

Figure 34. - Concluded.

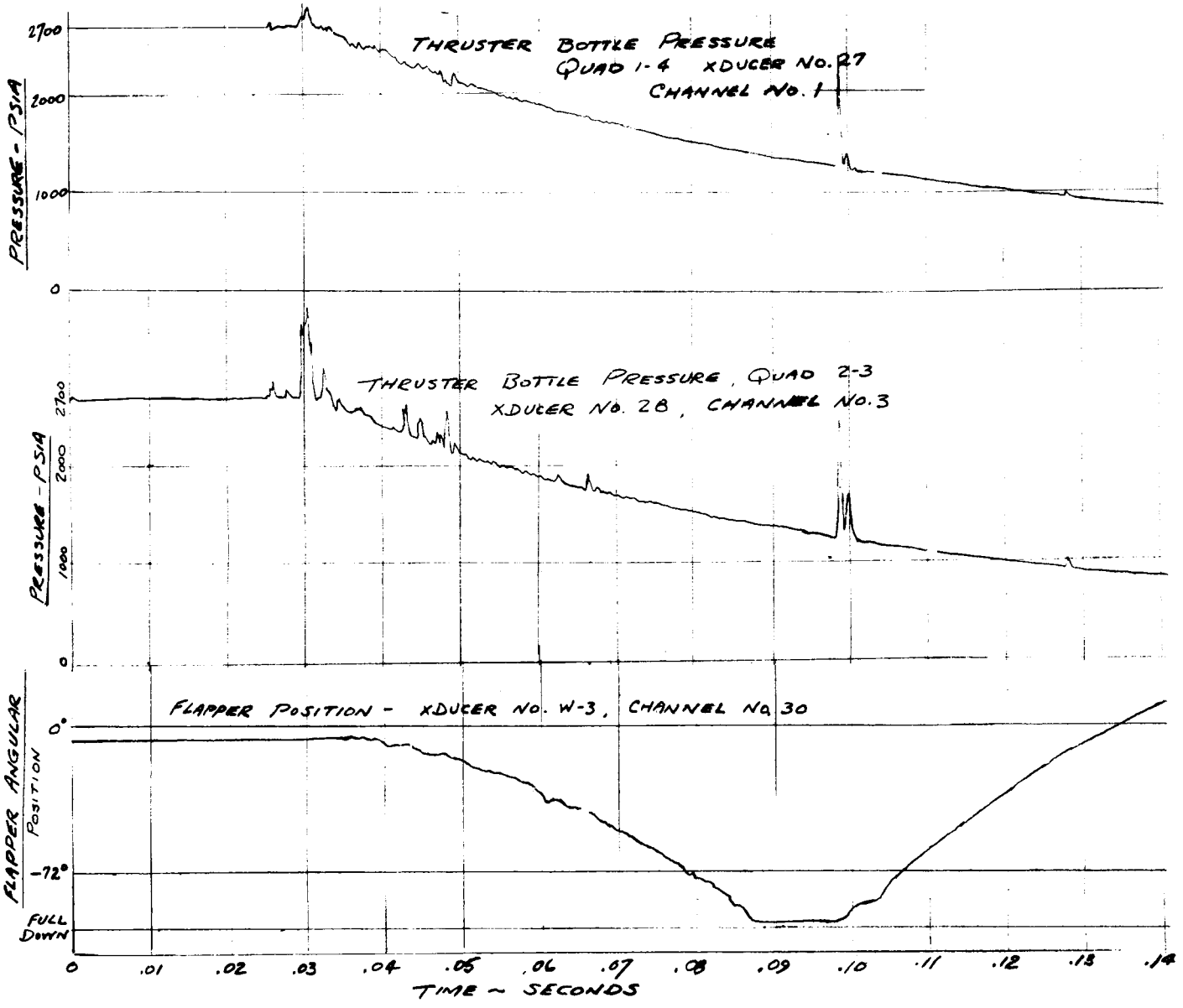

(a) Transducers 27, 28, and W3.

Figure 35. - Nose fairing separation data. Test 9.

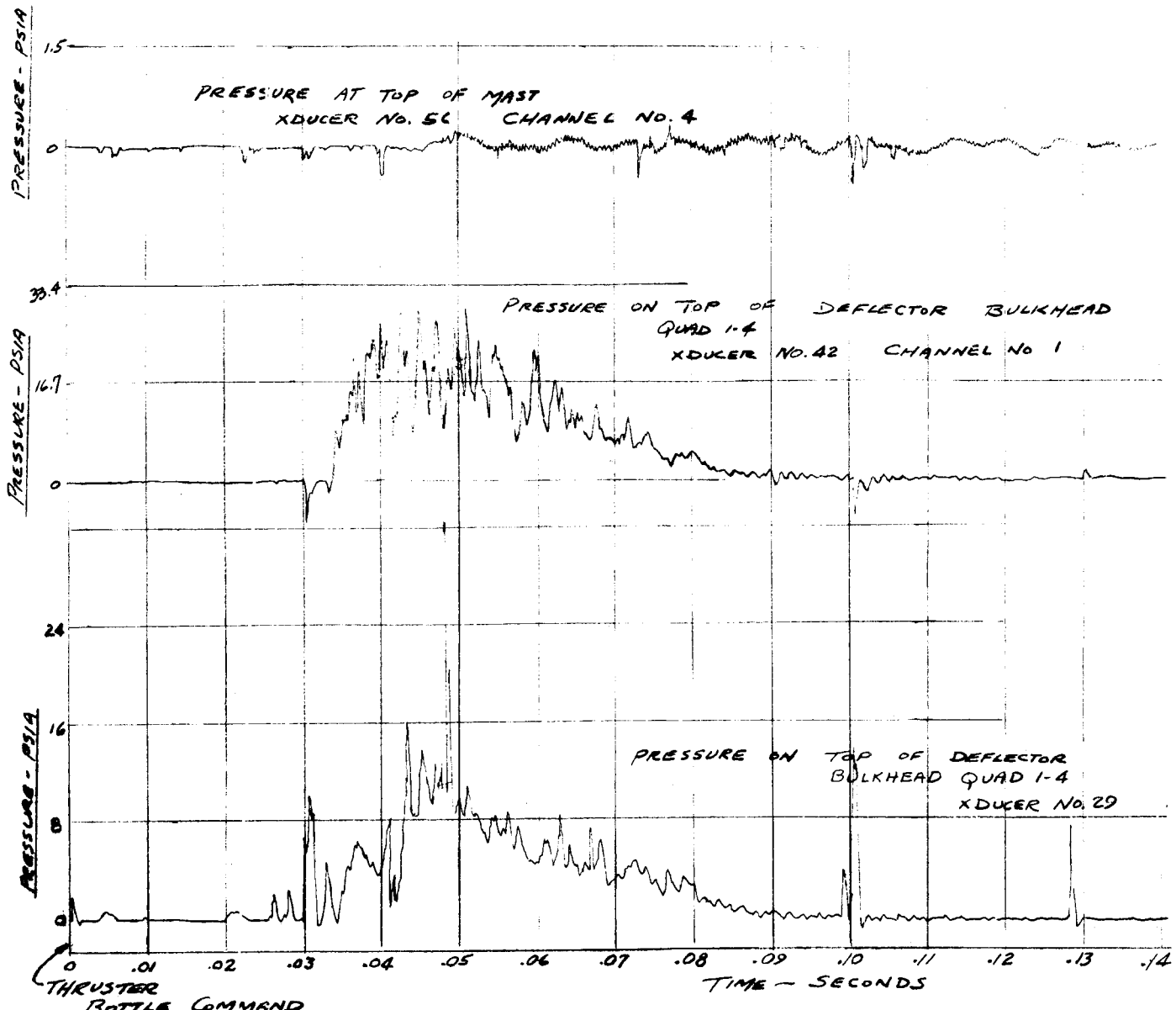

(b) Transducers 29, 42 and 56.

Figure 35. - Continued.

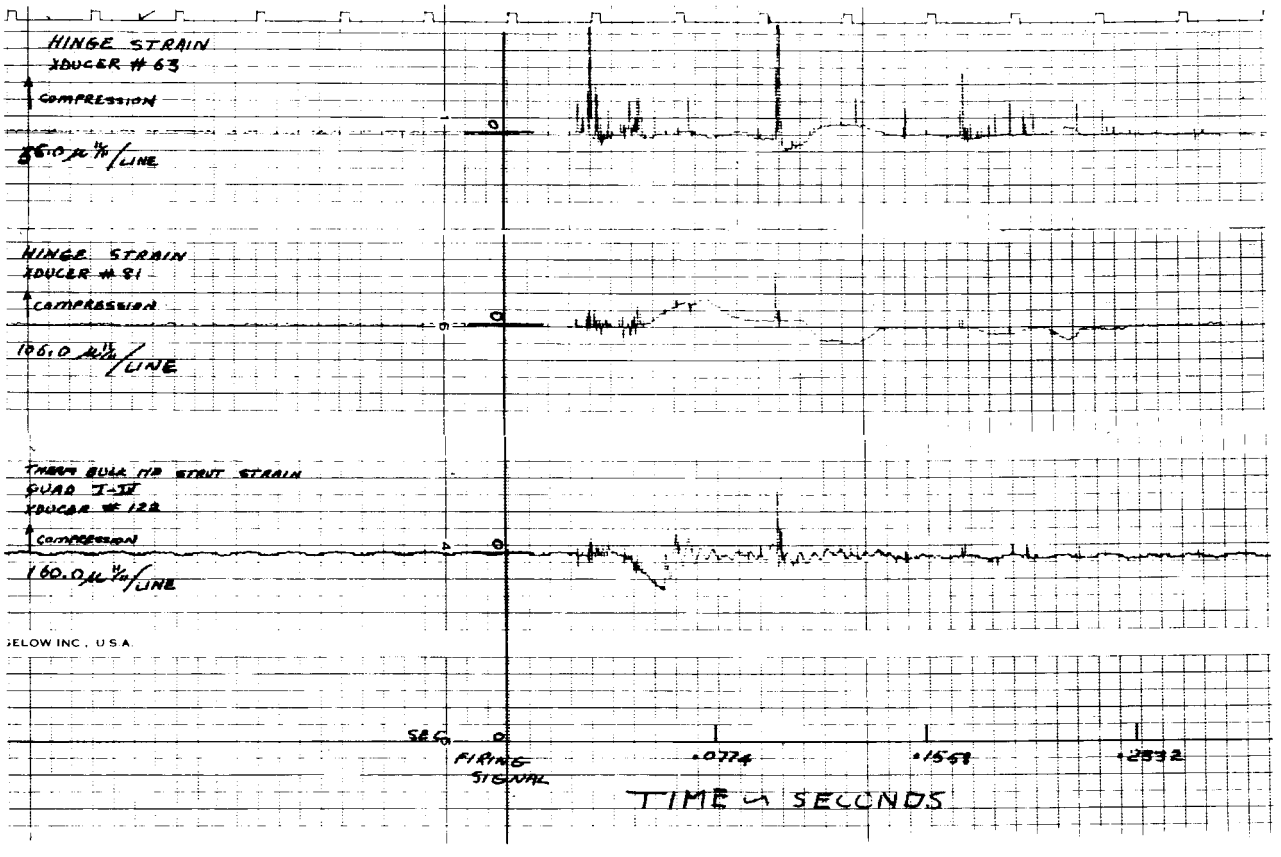

(c) Strain gages 63, 81, and 122.

Figure 35. - Continued.

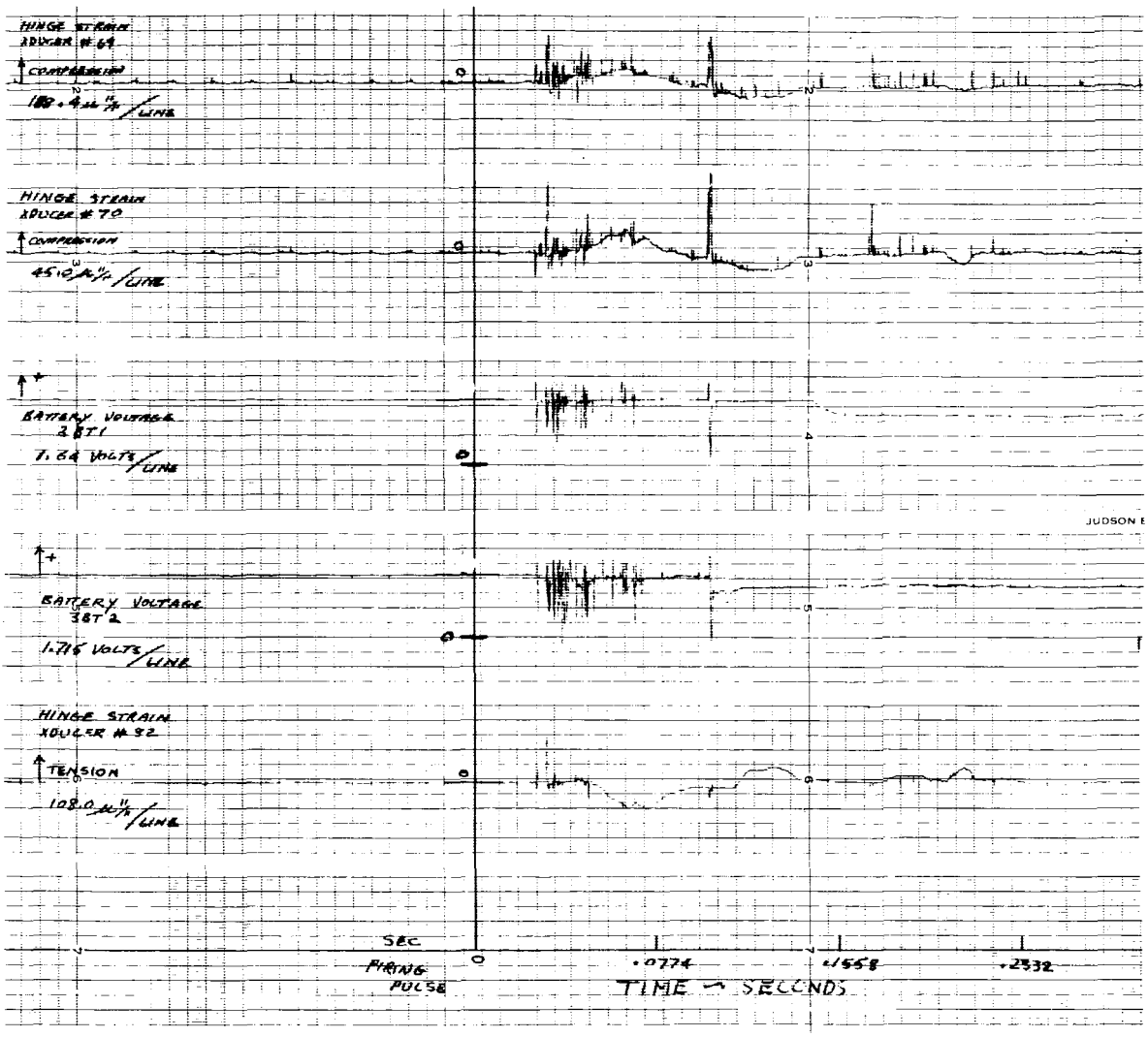

(d) Strain gages 69, 70, 82 and battery voltages.

Figure 35. - Concluded.

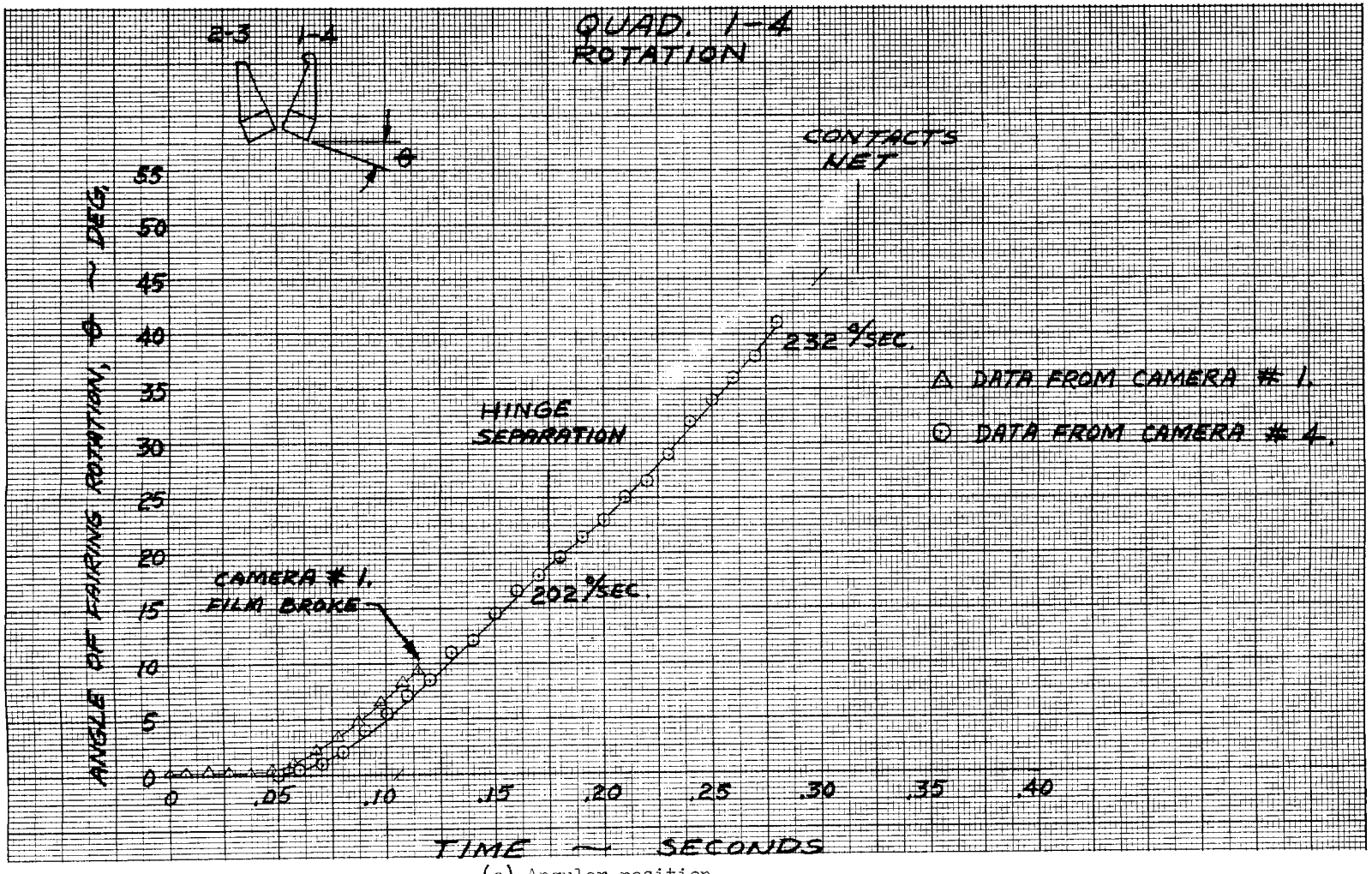

(a) Angular position.

Figure 36. - I-IV Centaur nose fairing half trajectory, Test 9.

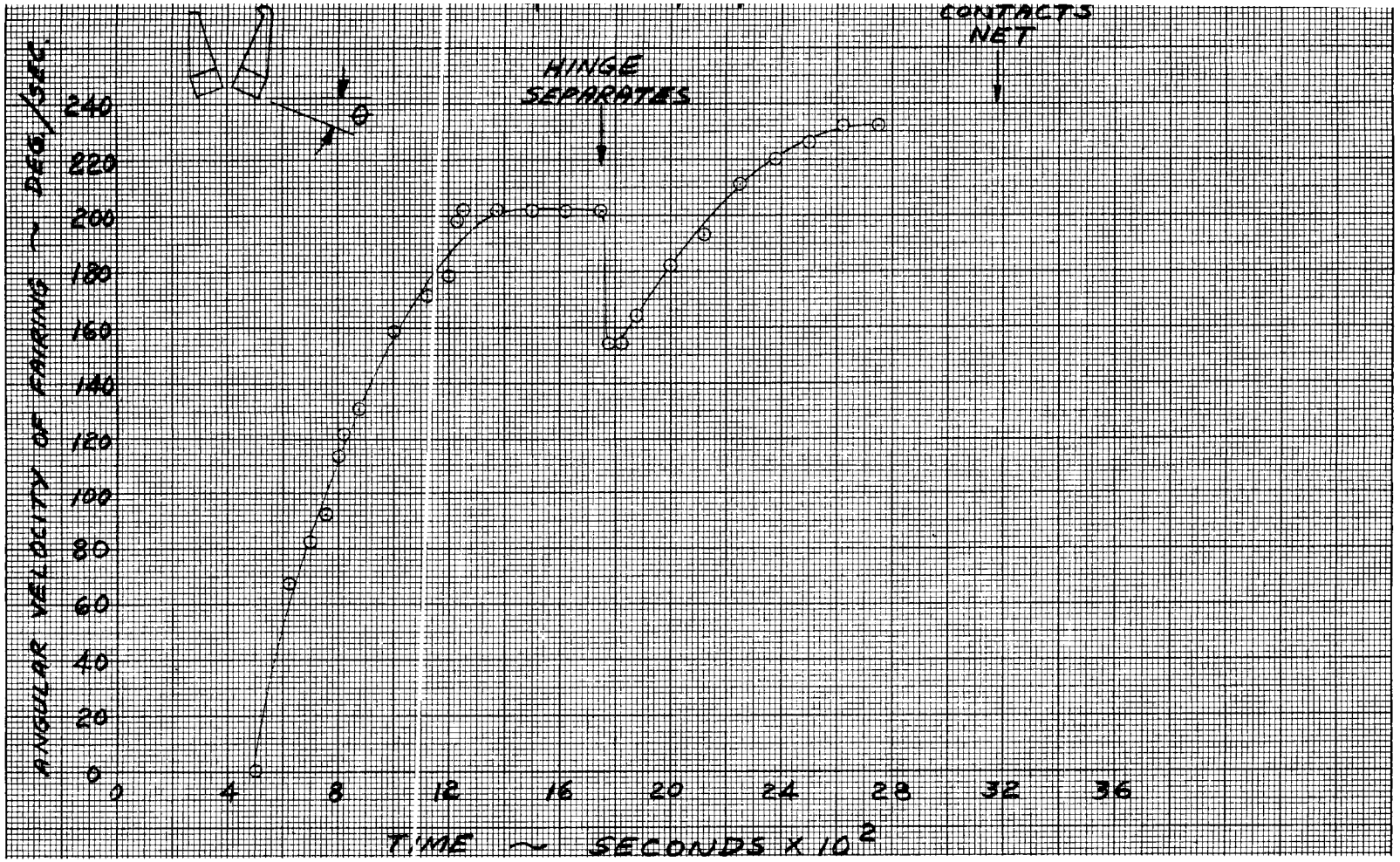

(b) Angular velocity.

Figure 36. - Continued.

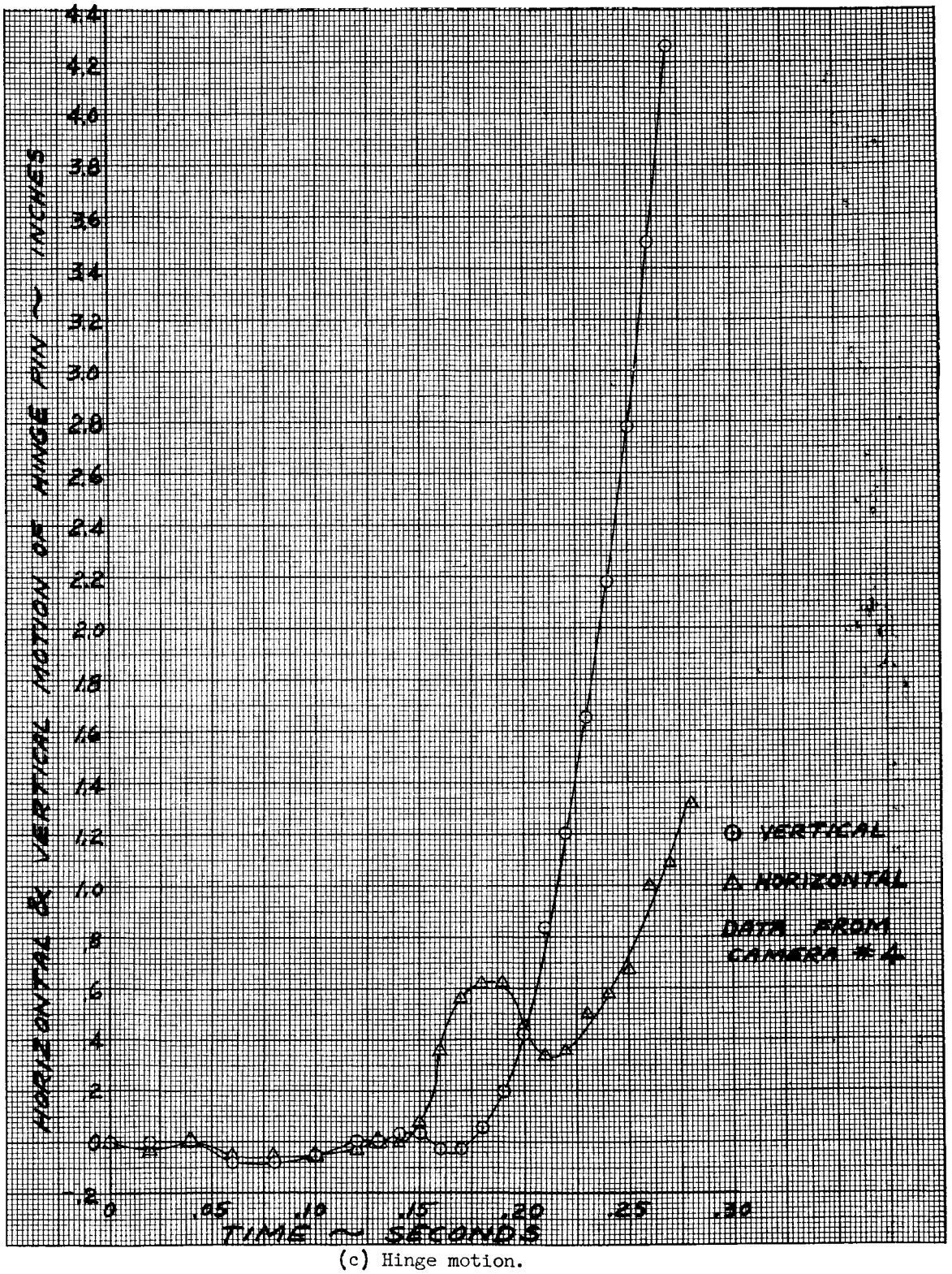

(c) Hinge motion.

Figure 36. - Concluded.

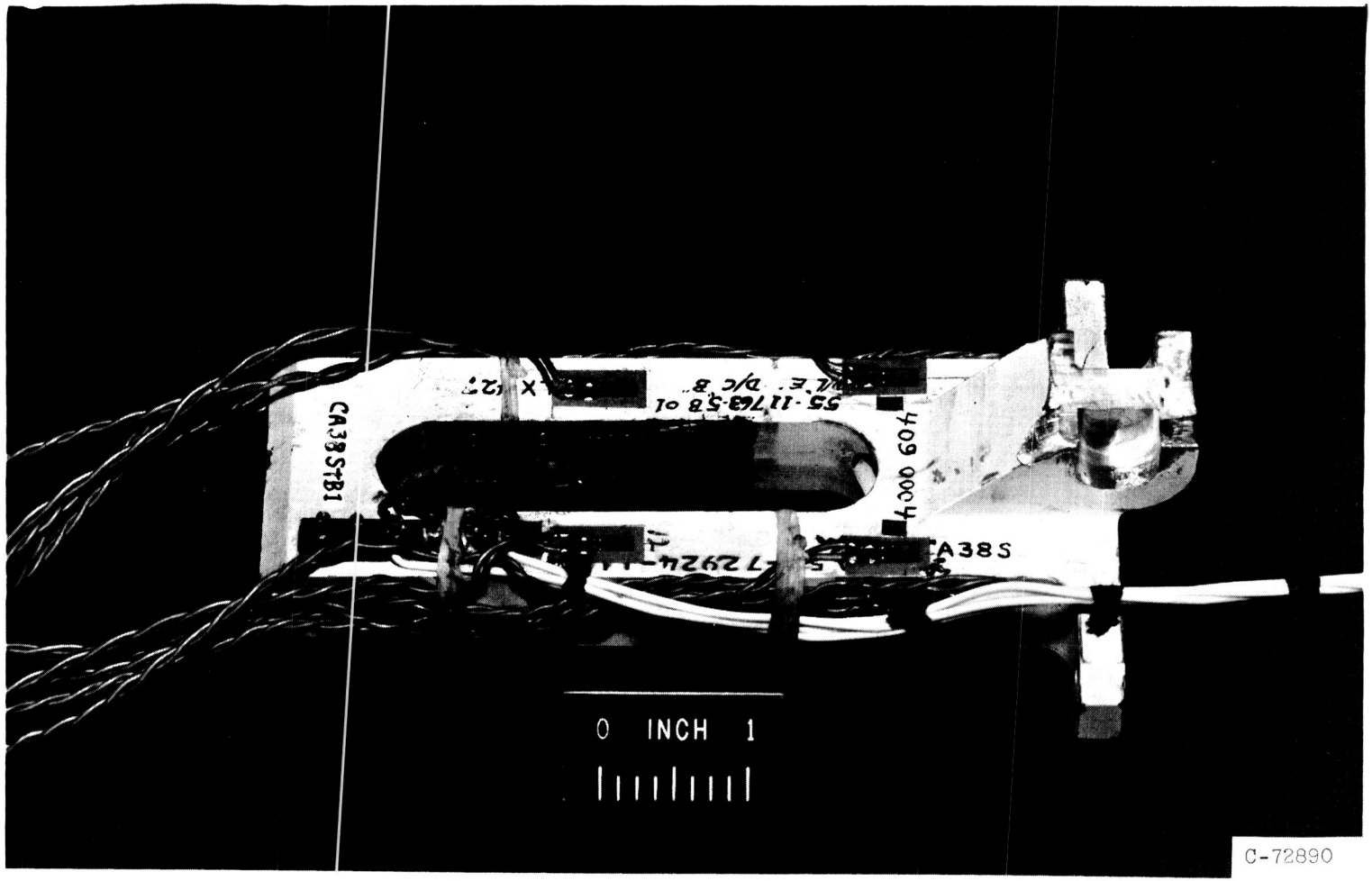

Figure 37. - Tank half of hinge instrumented by Lewis.

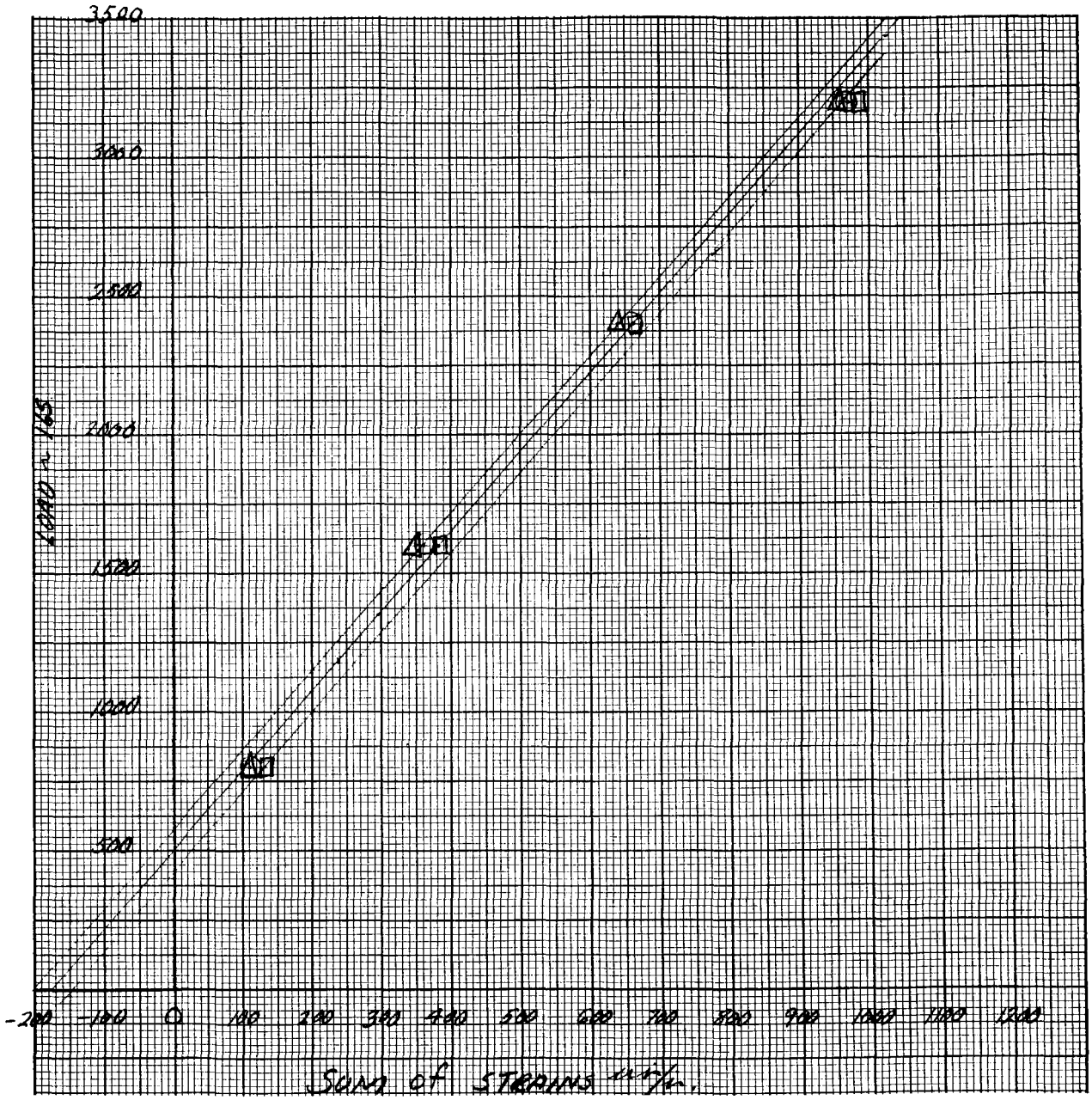

Figure 38. - Calibration of strain gages 47 and 48 in radial direction.

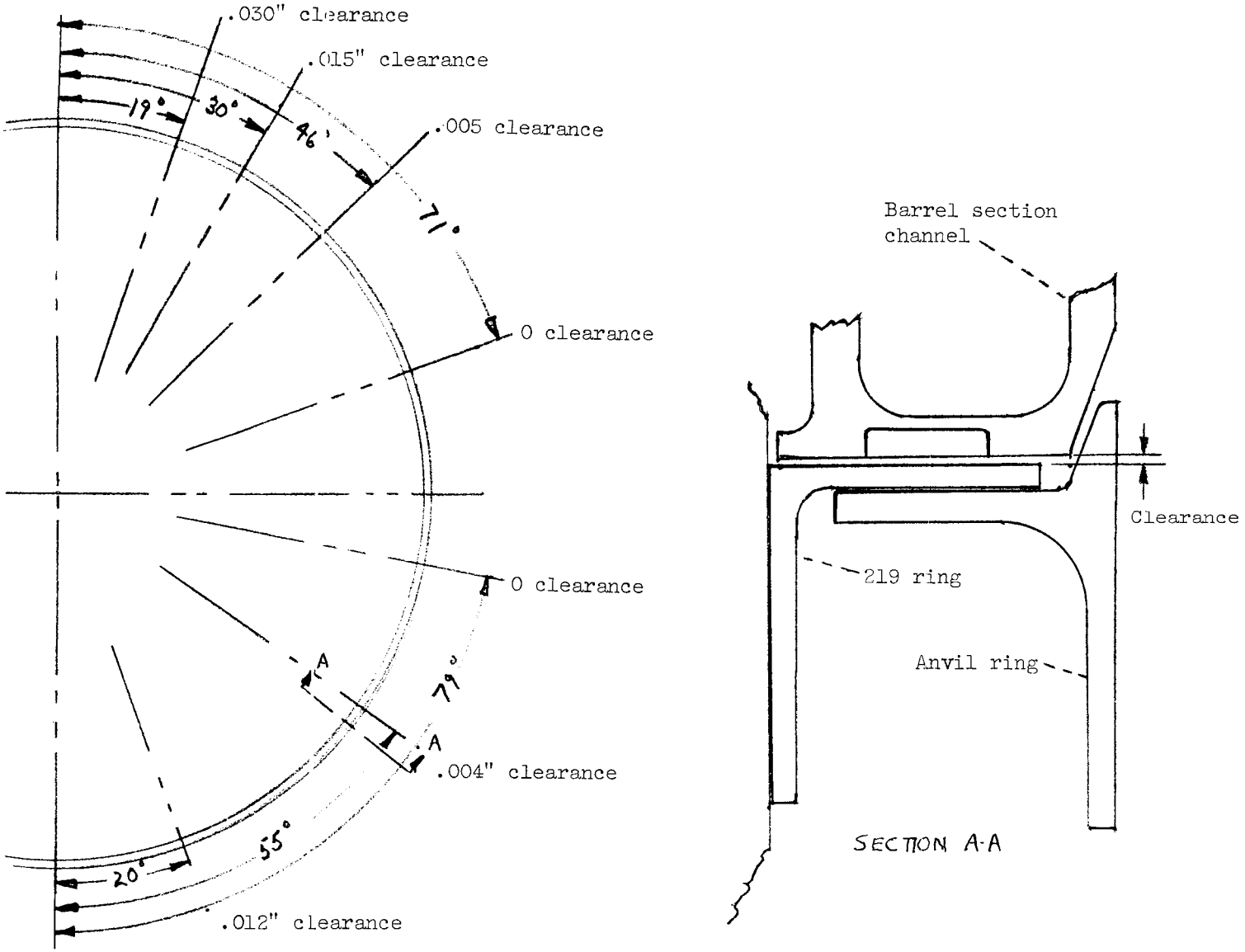

Figure 39. - Clearance between barrel section channel and 219 ring during Test 9.

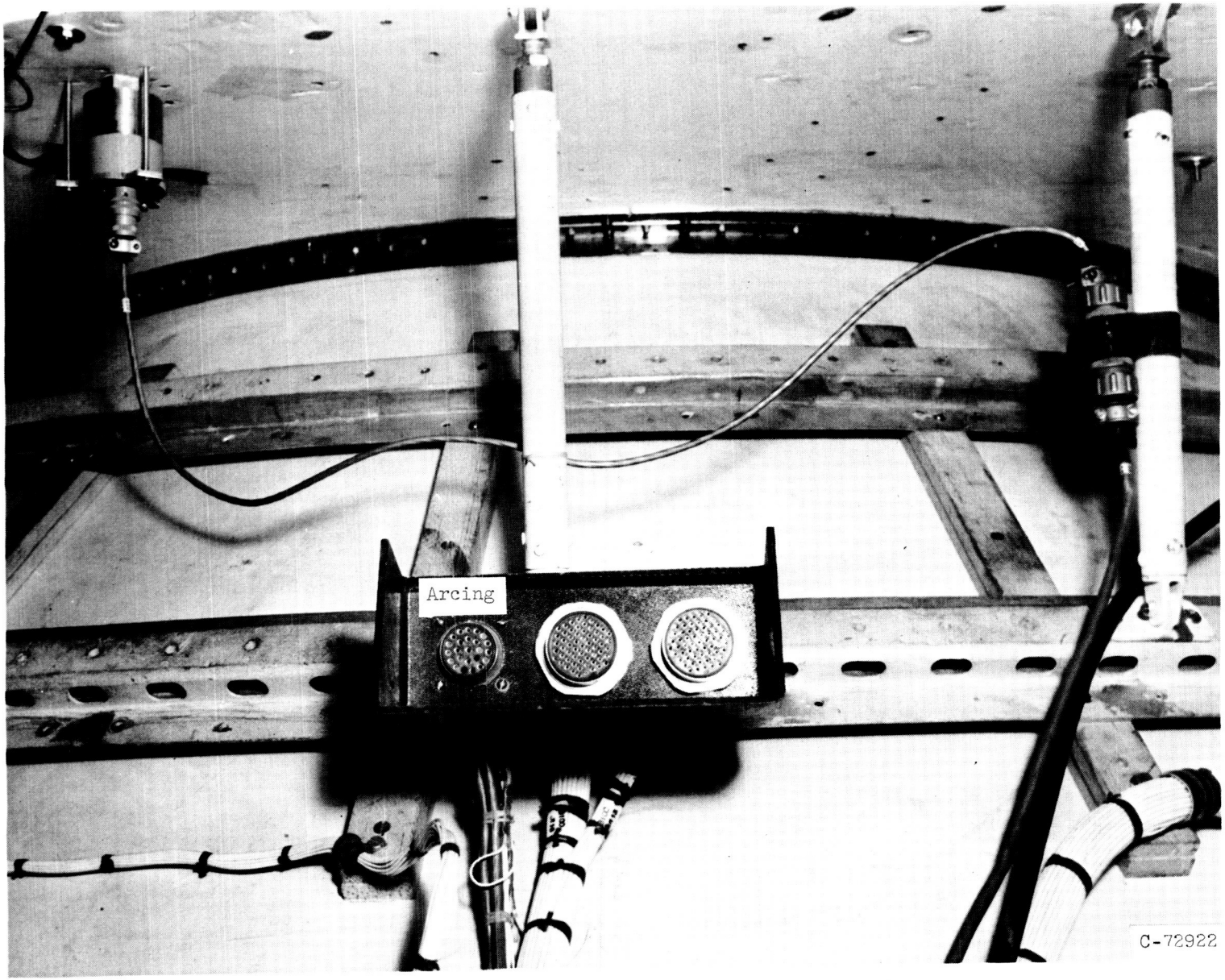

Figure 40. - Arcing on electrical disconnect fitting.

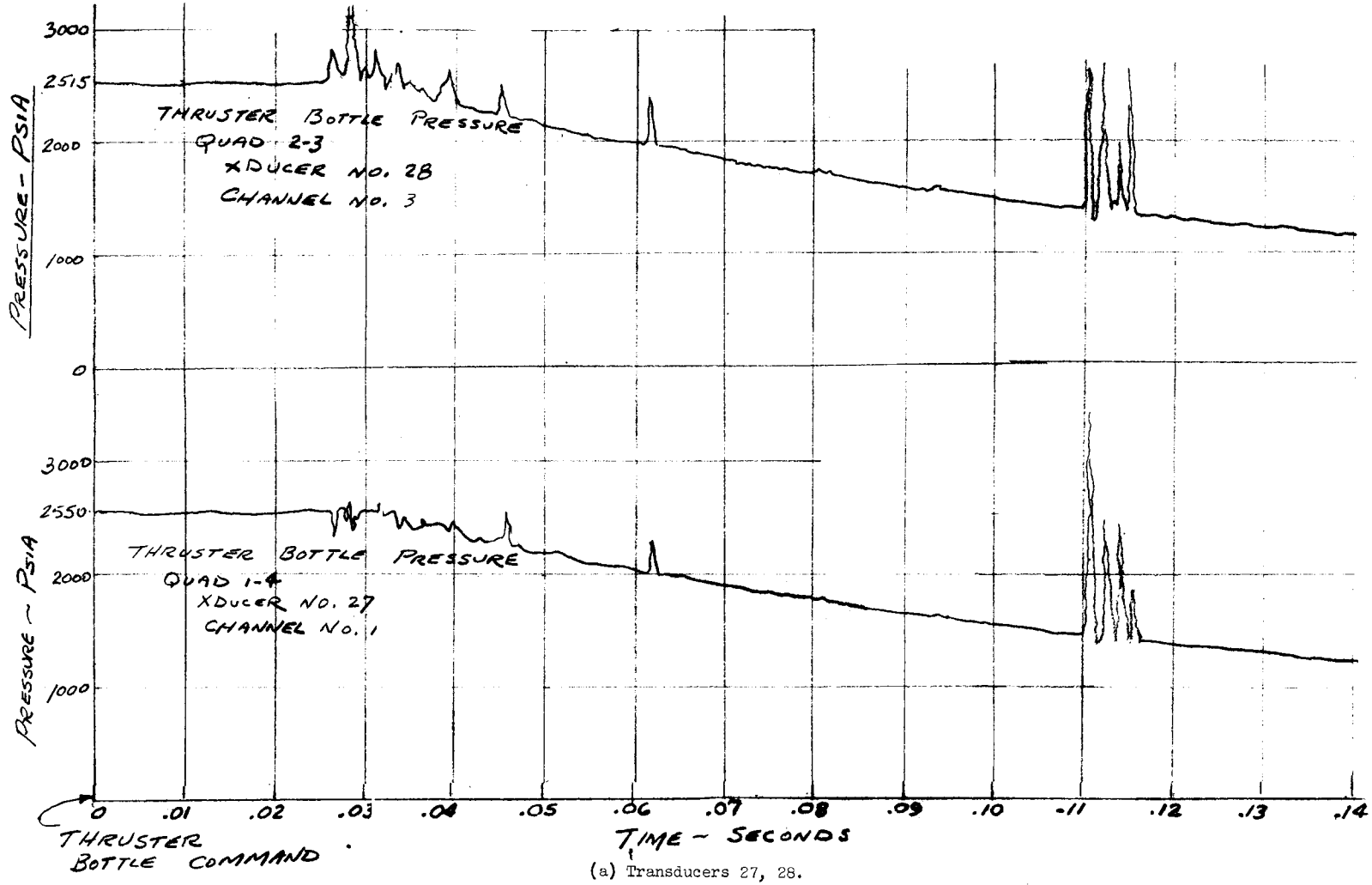

(a) Transducers 27, 28.

Figure 41. - Nose fairing separation data - test 1C.

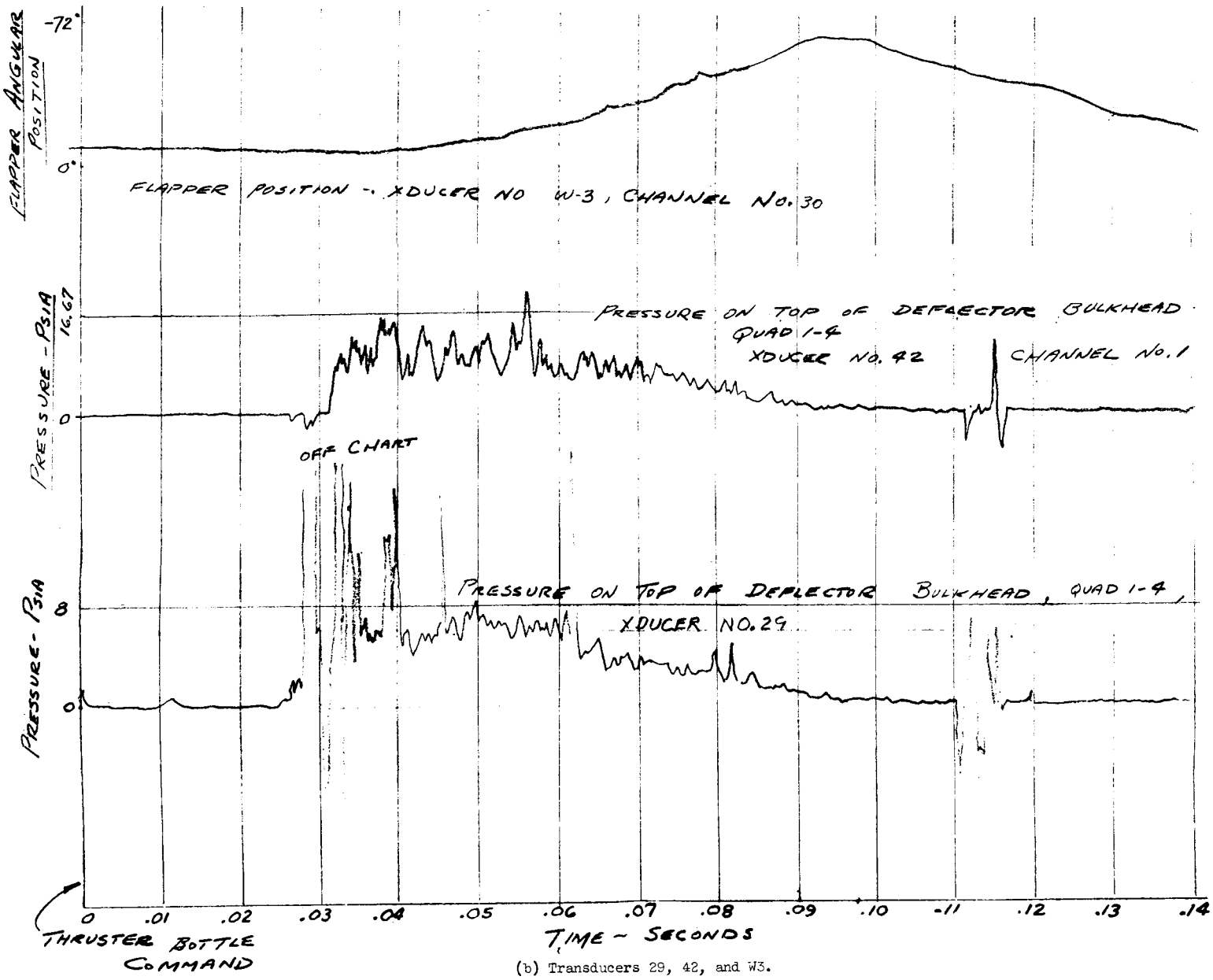

(b) Transducers 29, 42, and W3.

Figure 41. - Continued.

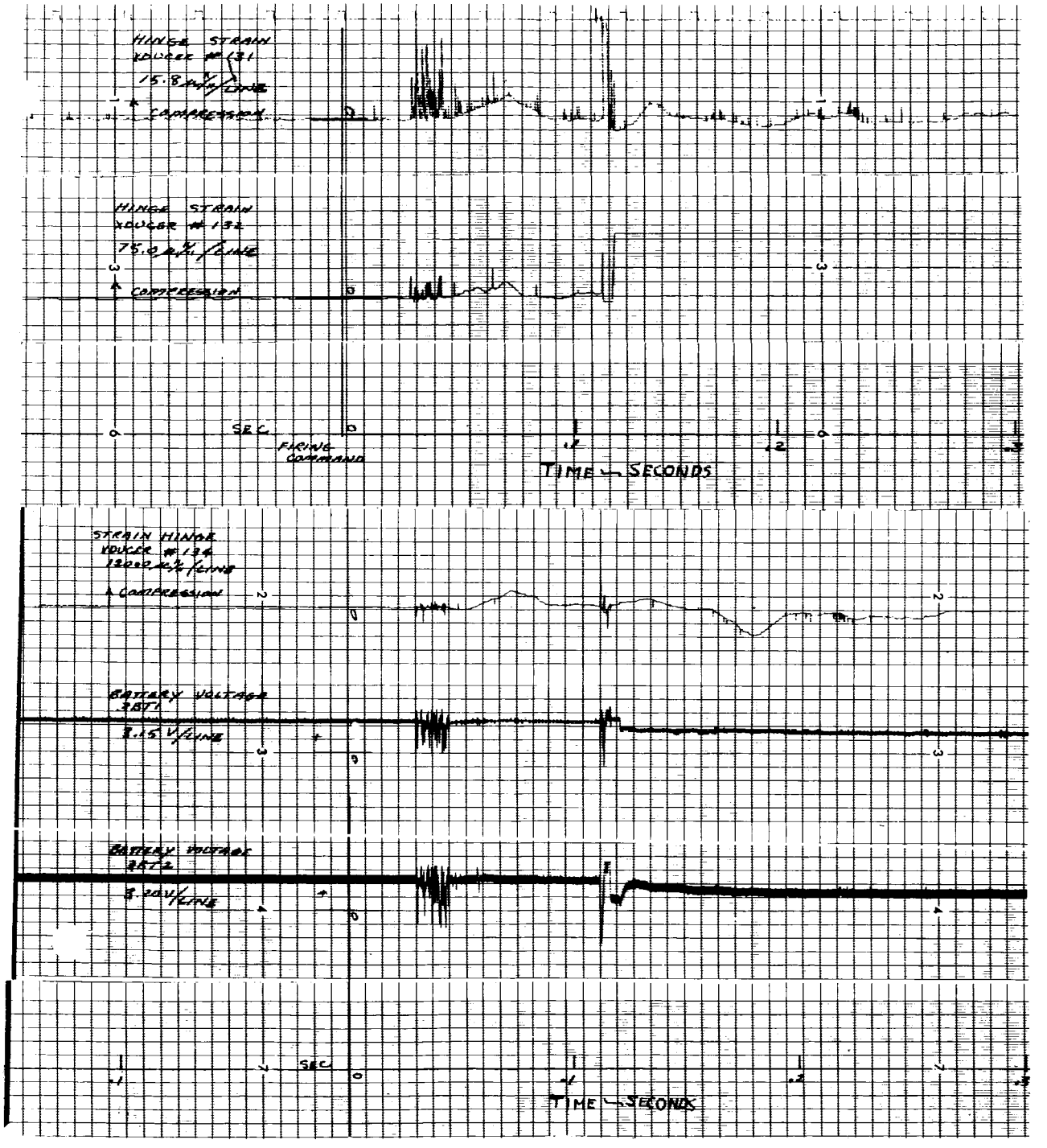

(c) Strain gages 131, 132, 134 and battery voltages.

Figure 41. - Continued.

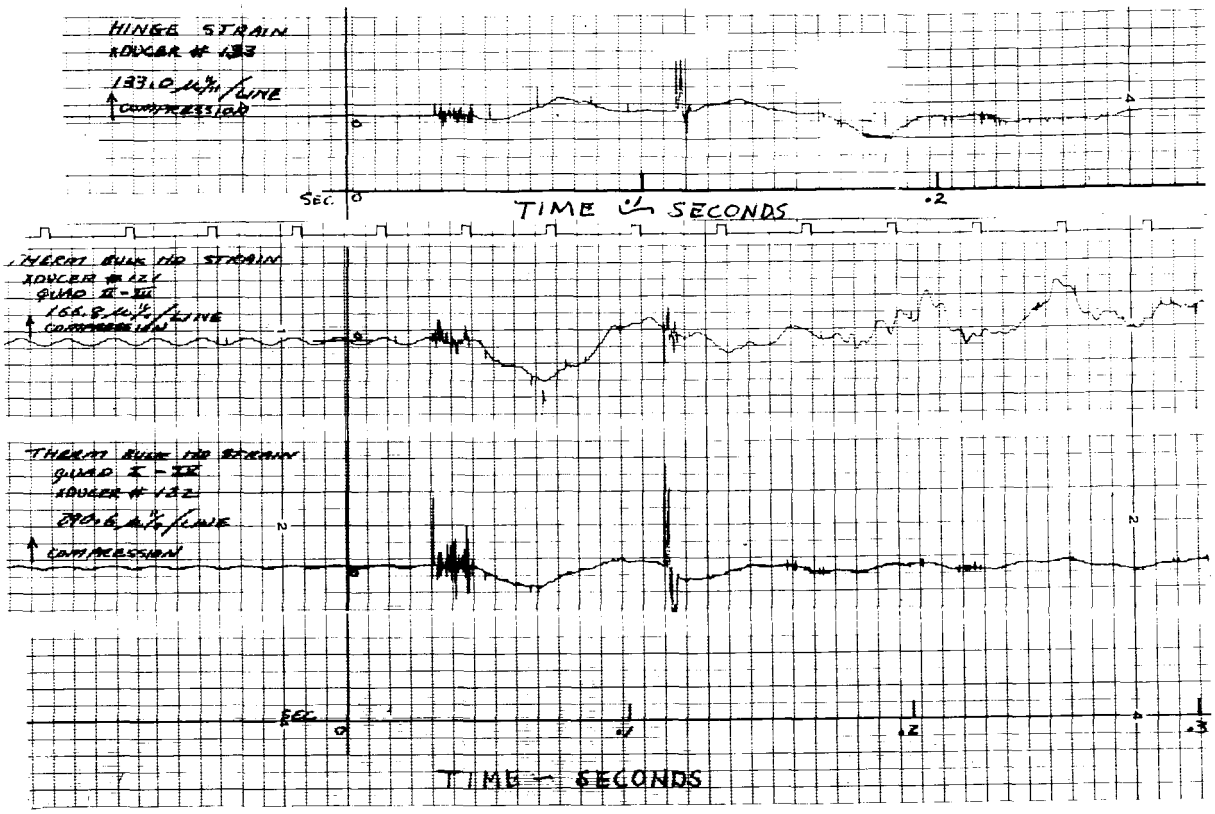

(d) Strain gages 121, 122 and 133.

Figure 41. - Continued.

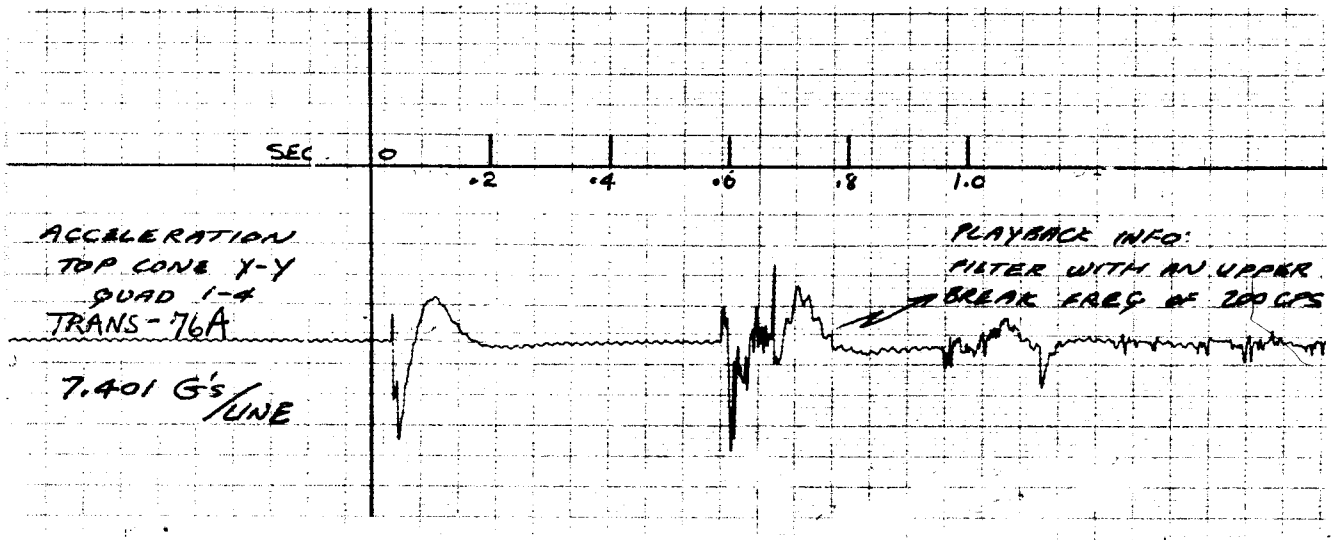

(e) Transducer 76A signal played through low pass 200 cps filter.

Figure 41. - Concluded.

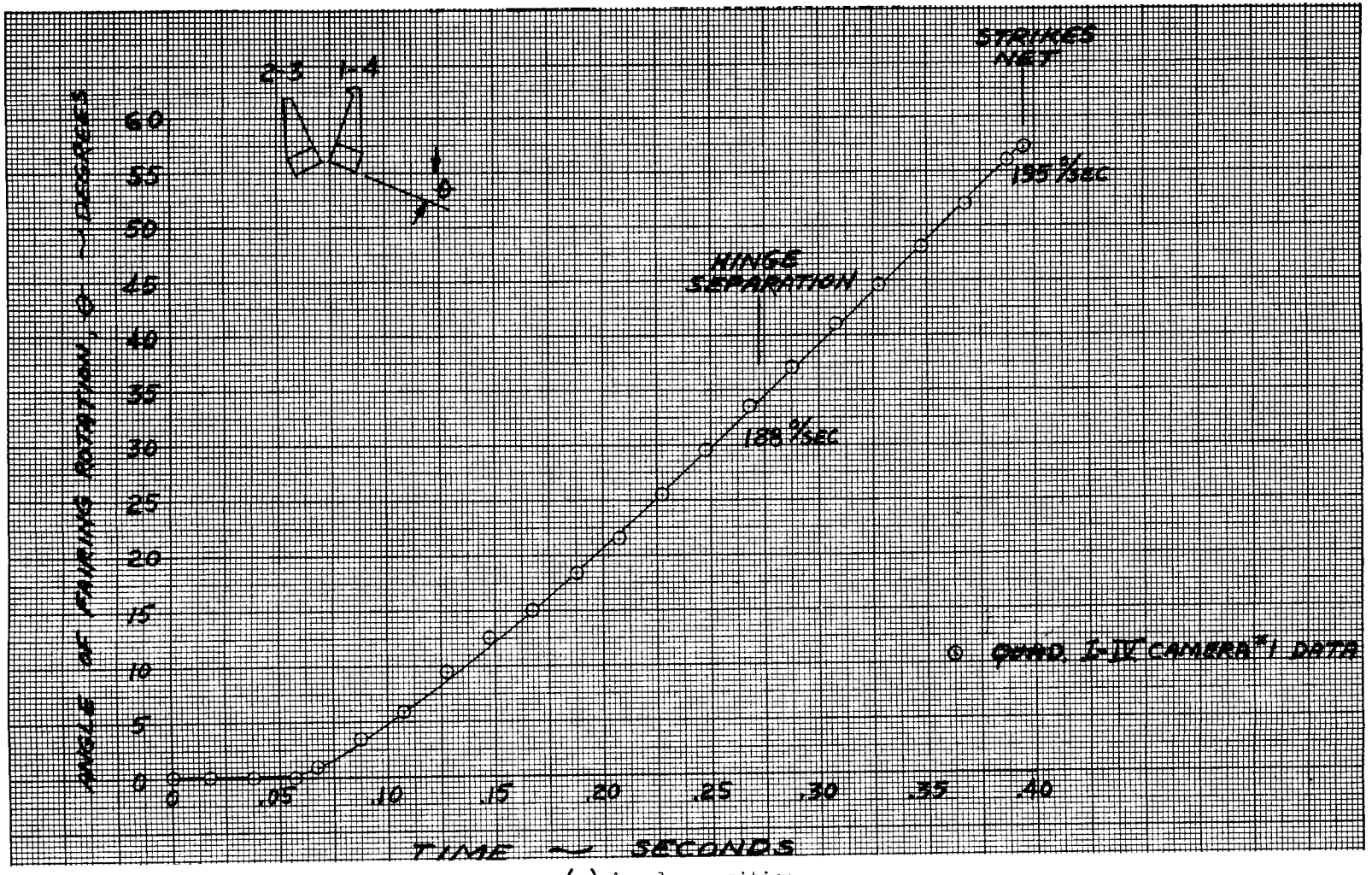

(a) Angular position.

Figure 42. - I-IV Centaur nose fairing half trajectory, Test 10.

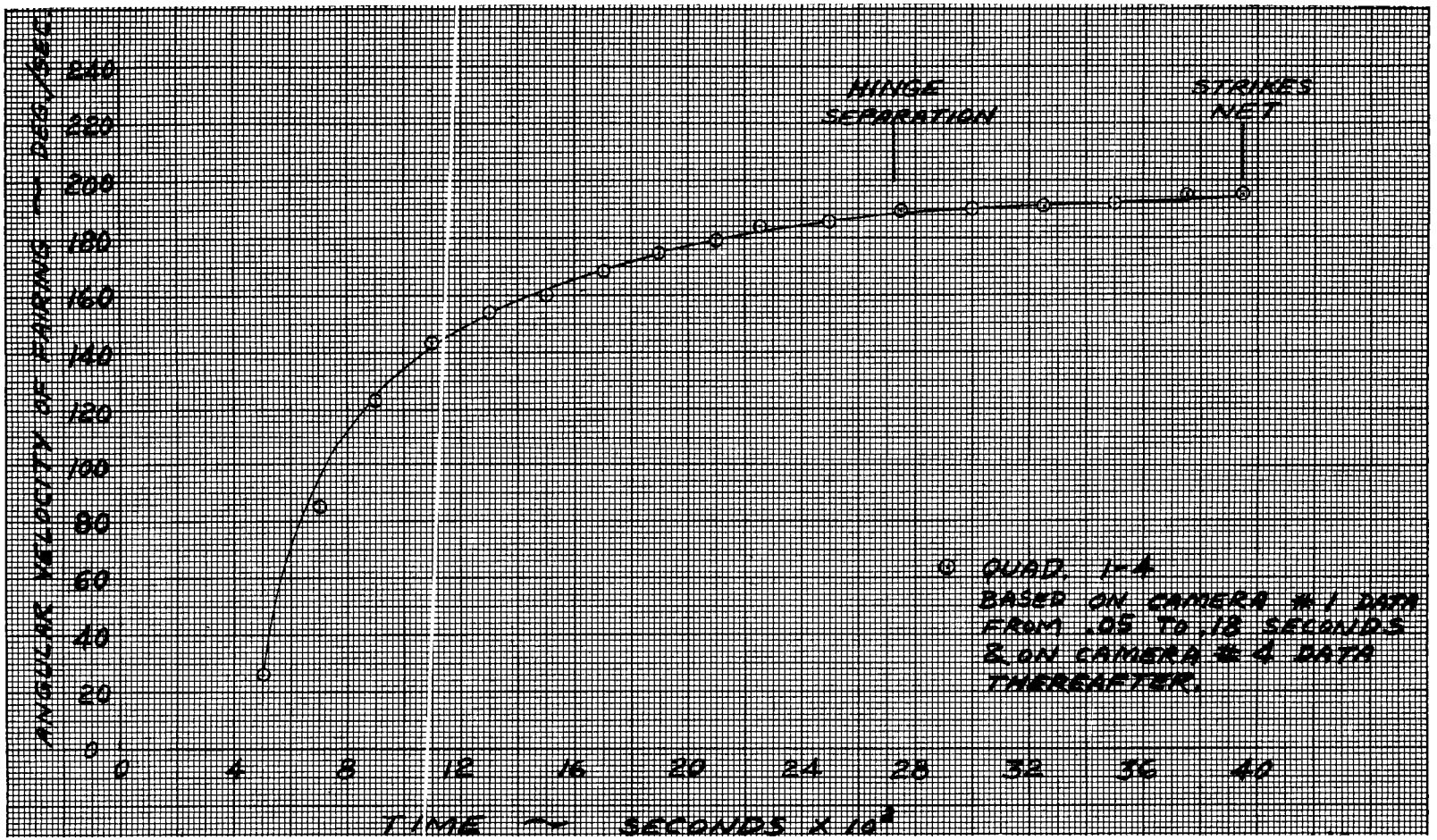

(b) Angular velocity.

Figure 42. - Continued.

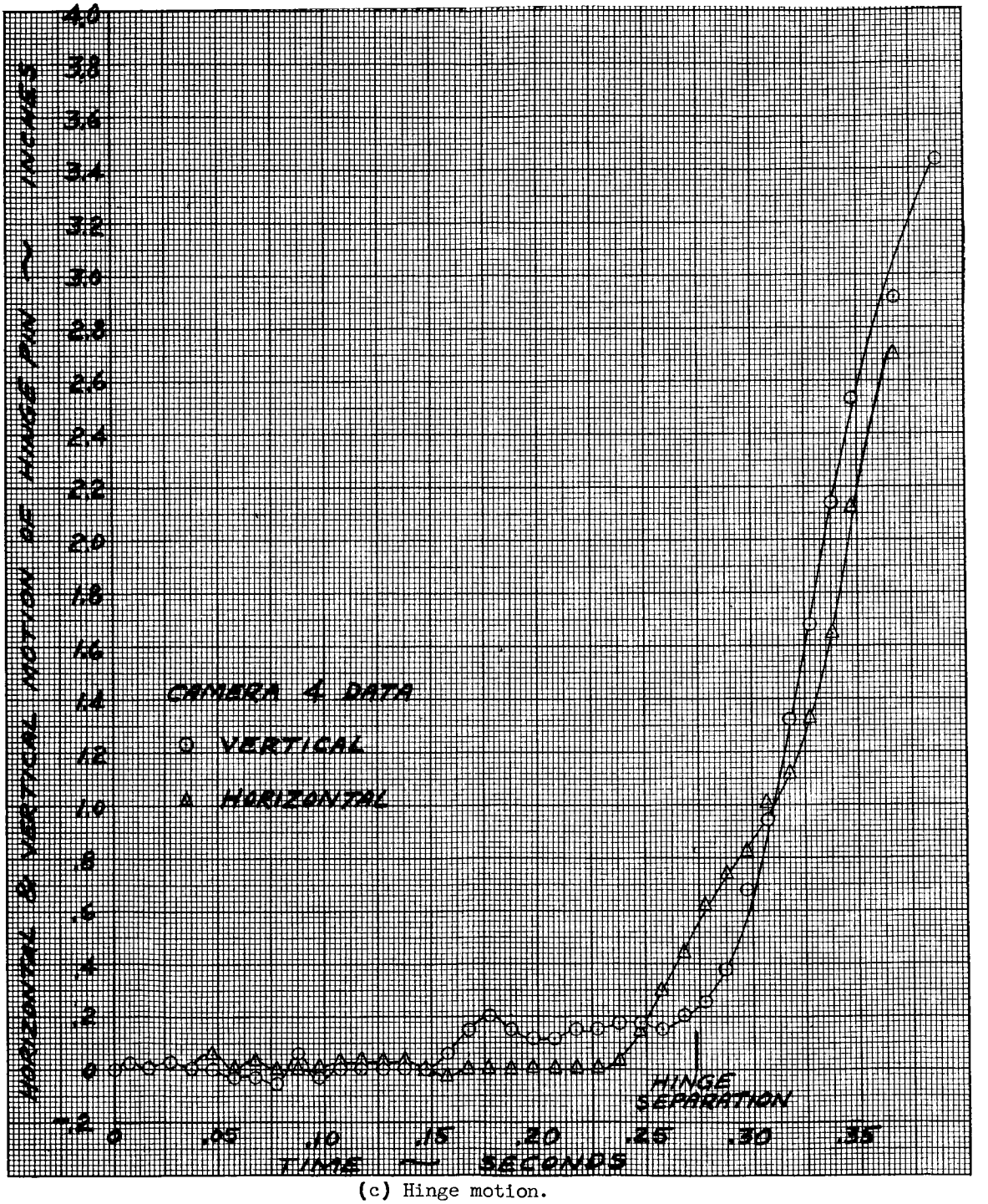

(c) Hinge motion.

Figure 42. - Concluded.

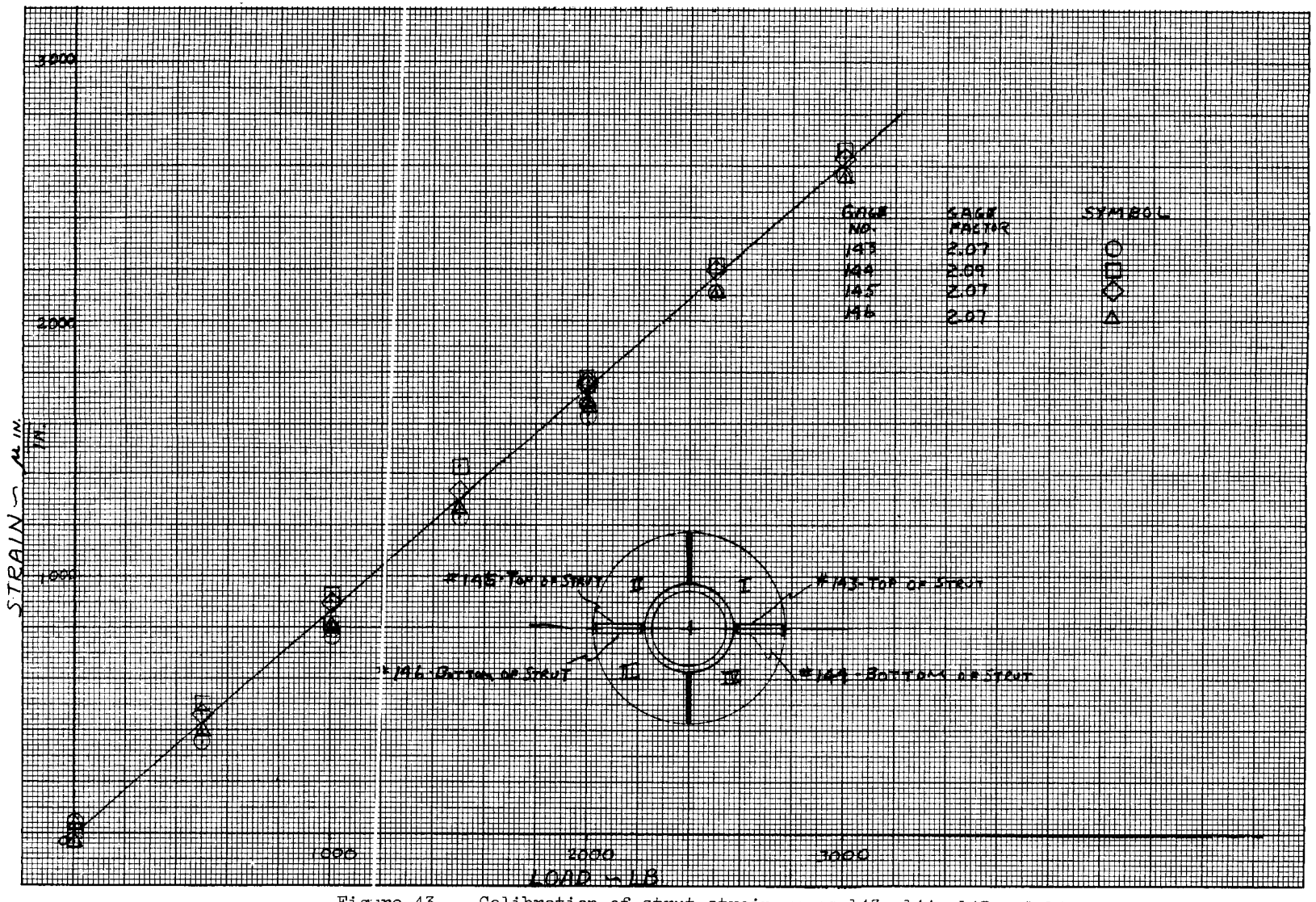

Figure 43. - Calibration of strut strain gages 143, 144, 145 and 146.

Figure 44. - Strut damage, Test 11.

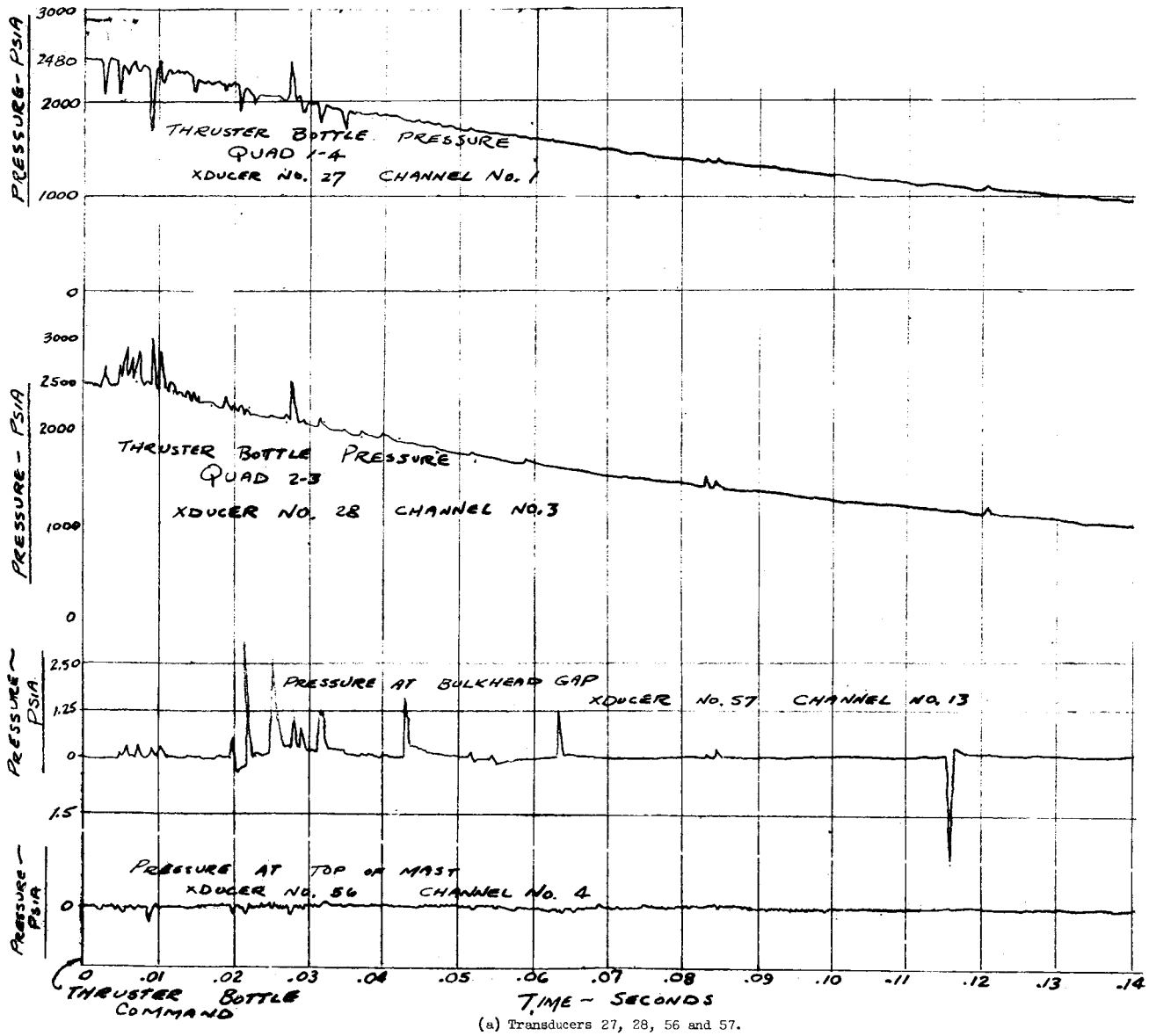

(a) Transducers 27, 28, 56 and 57.

Figure 45. - Nose fairing separation data. Test 11.

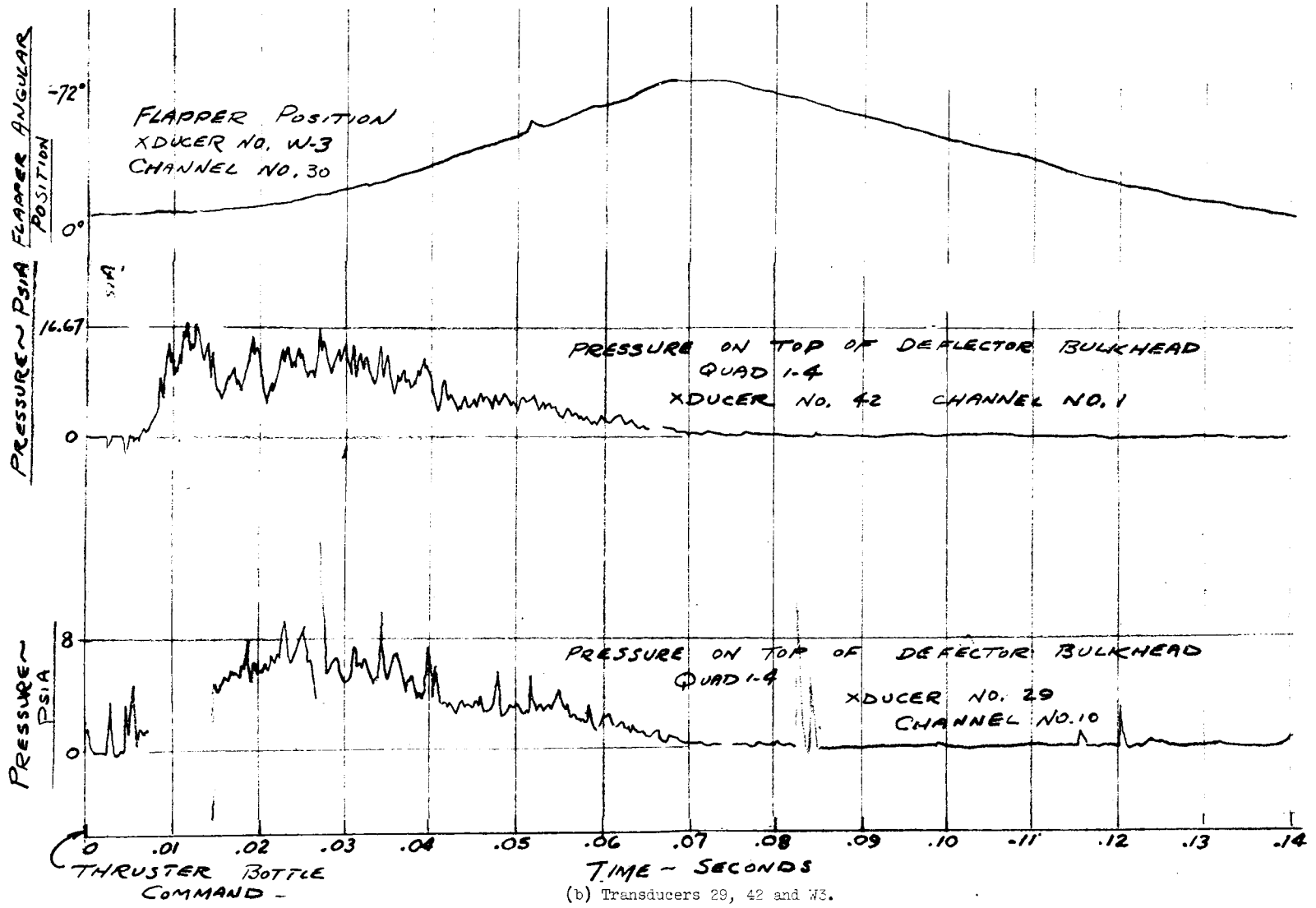

(b) Transducers 29, 42 and W3.

Figure 45. - Continued.

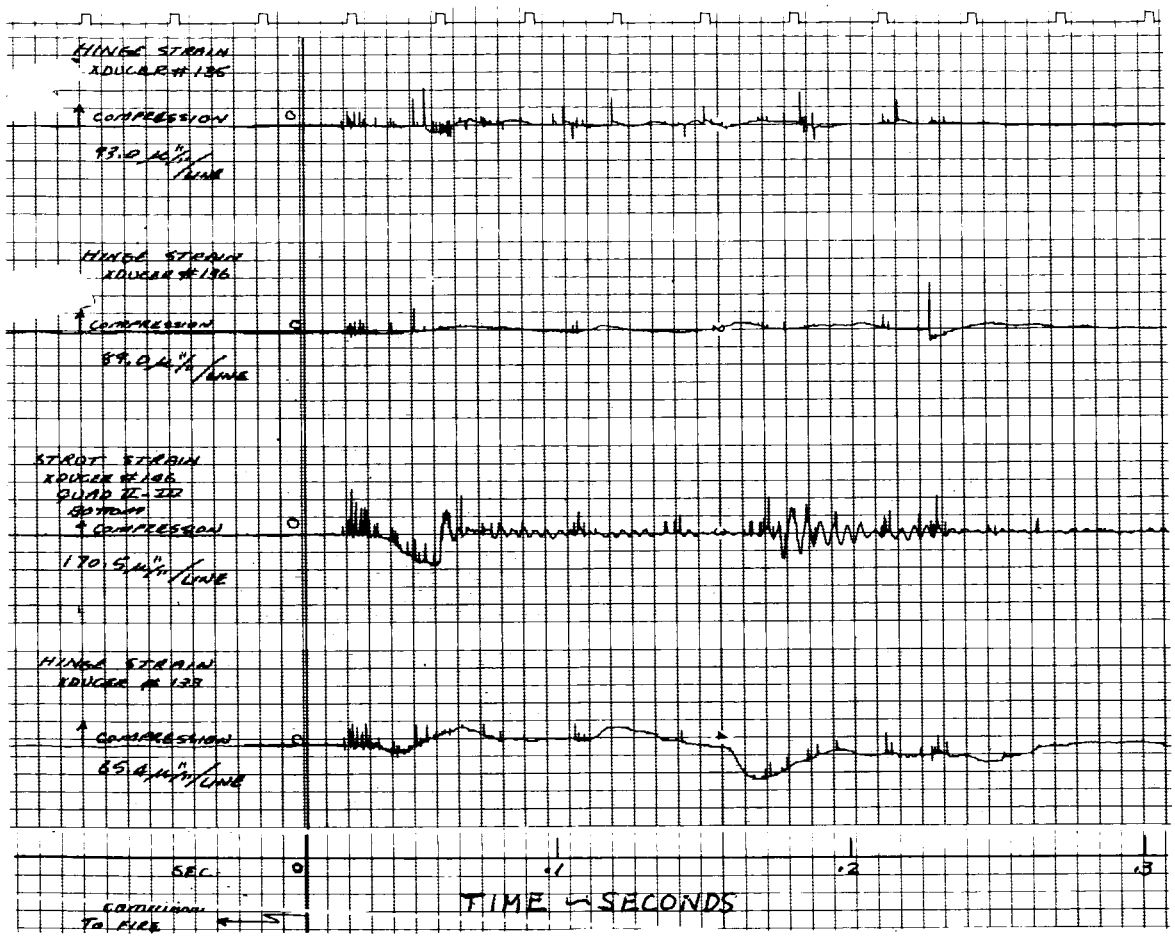

(c) Strain gages 133, 135, 136 and 146.

Figure 45. - Continued.

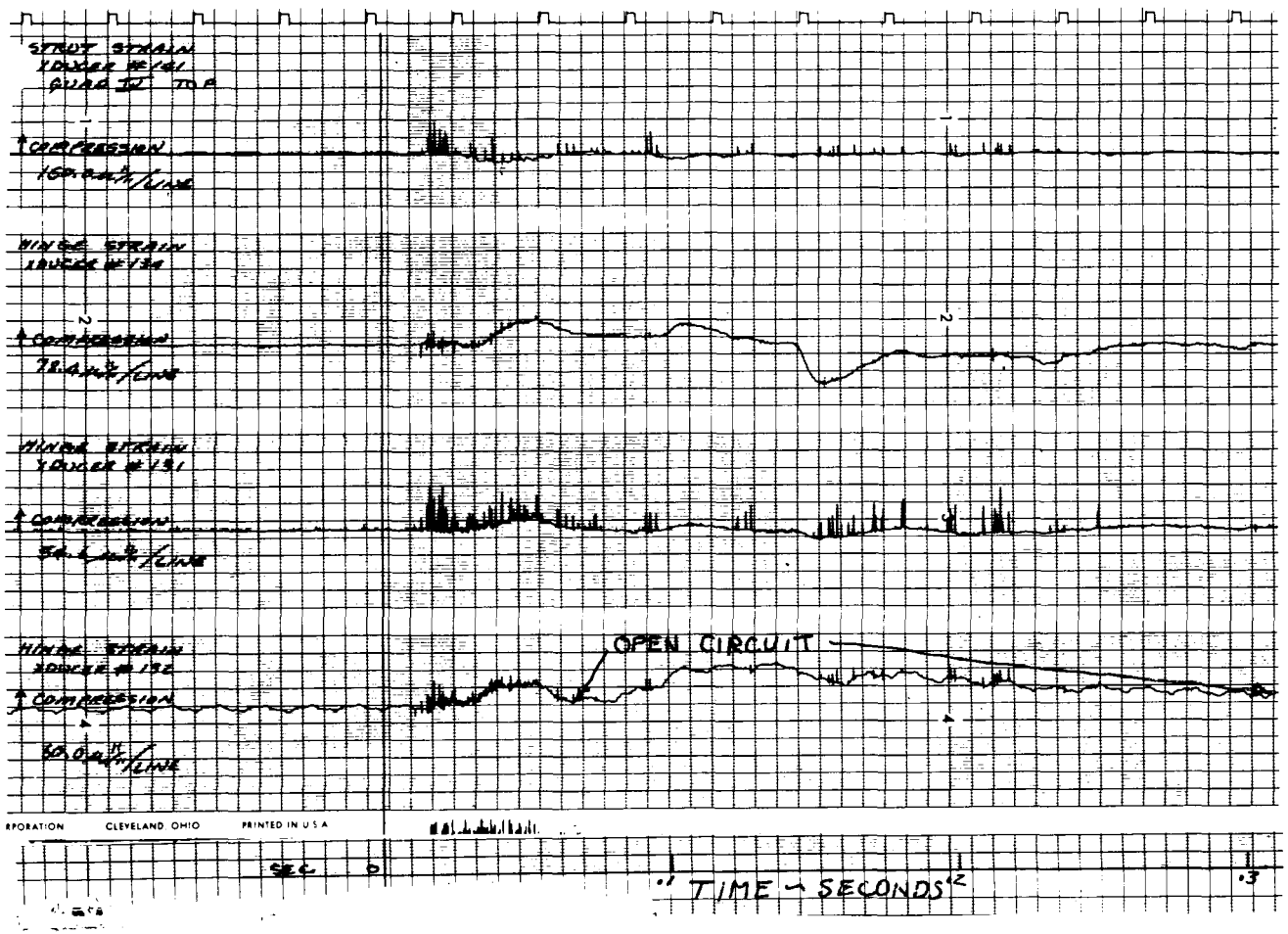

(d) Strain gages 131, 132, 134 and 141.

Figure 45. - Continued.

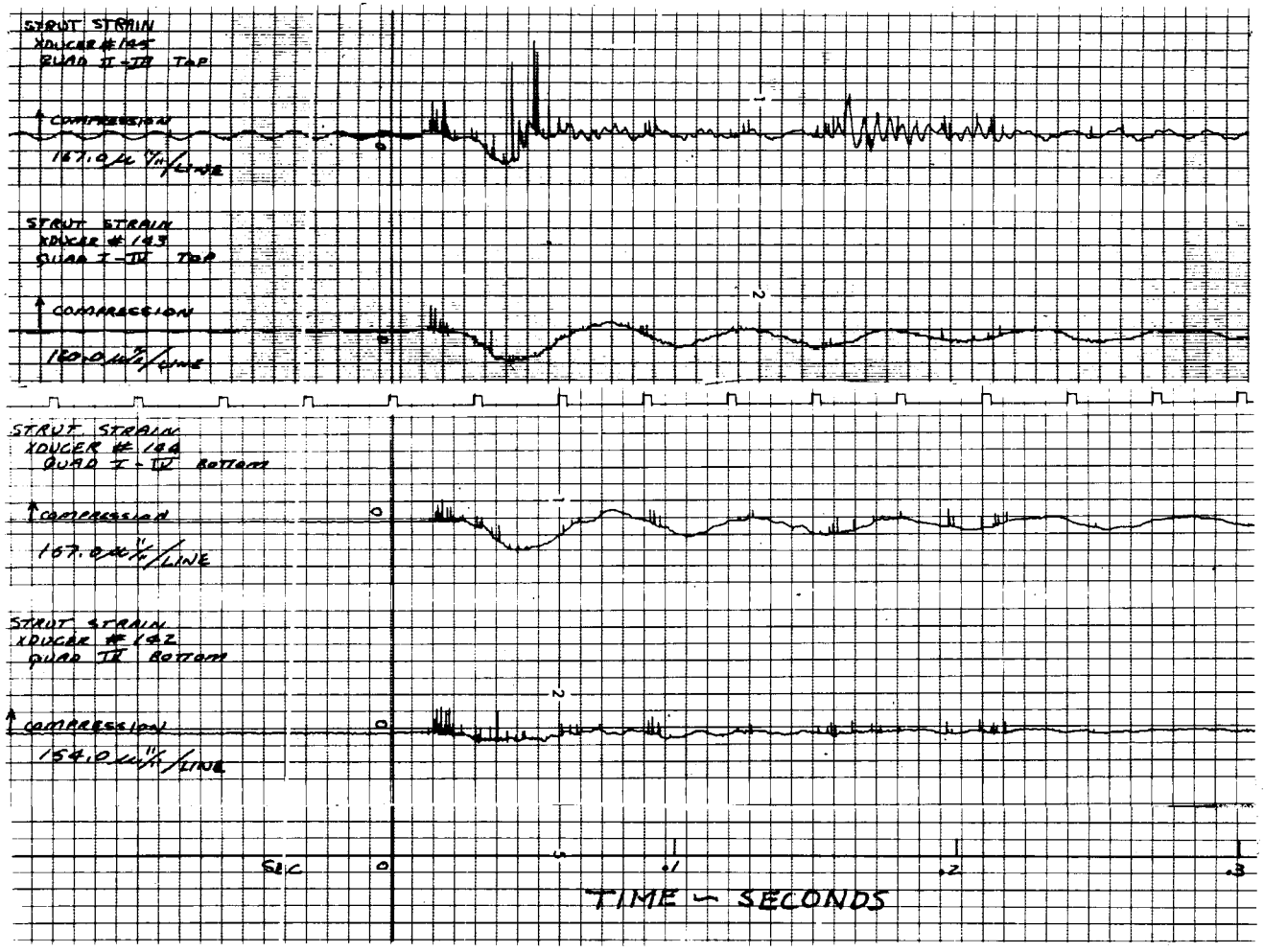

(e) Strain gages 142, 143, 144 and 145.

Figure 45. - Continued.

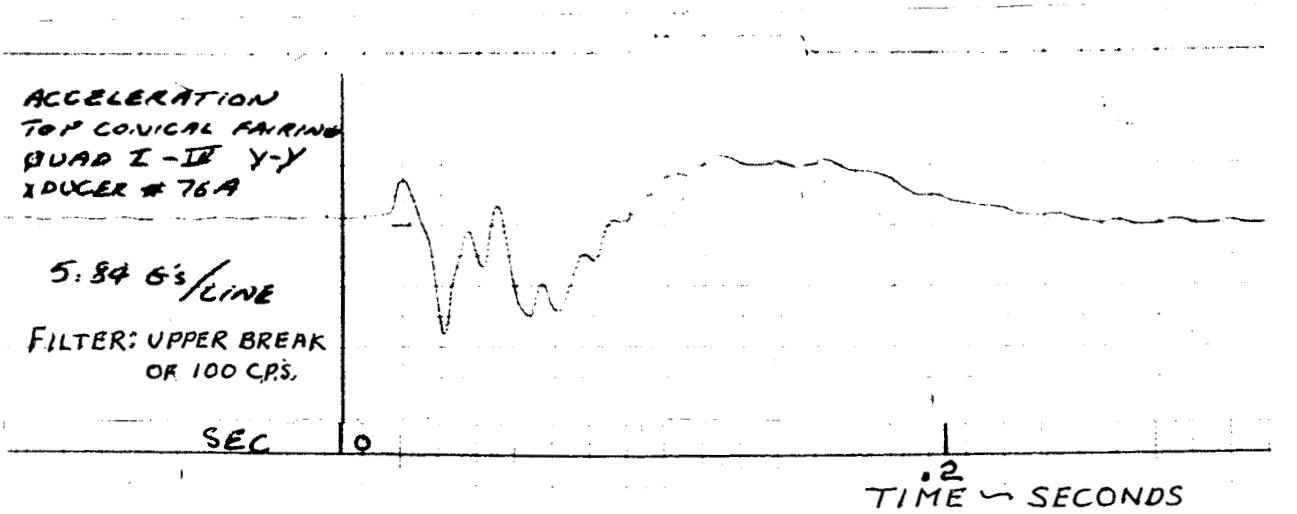

(f) Transducer 76A signal played through lo pass 200 cps filter.

Figure 45. - Concluded.

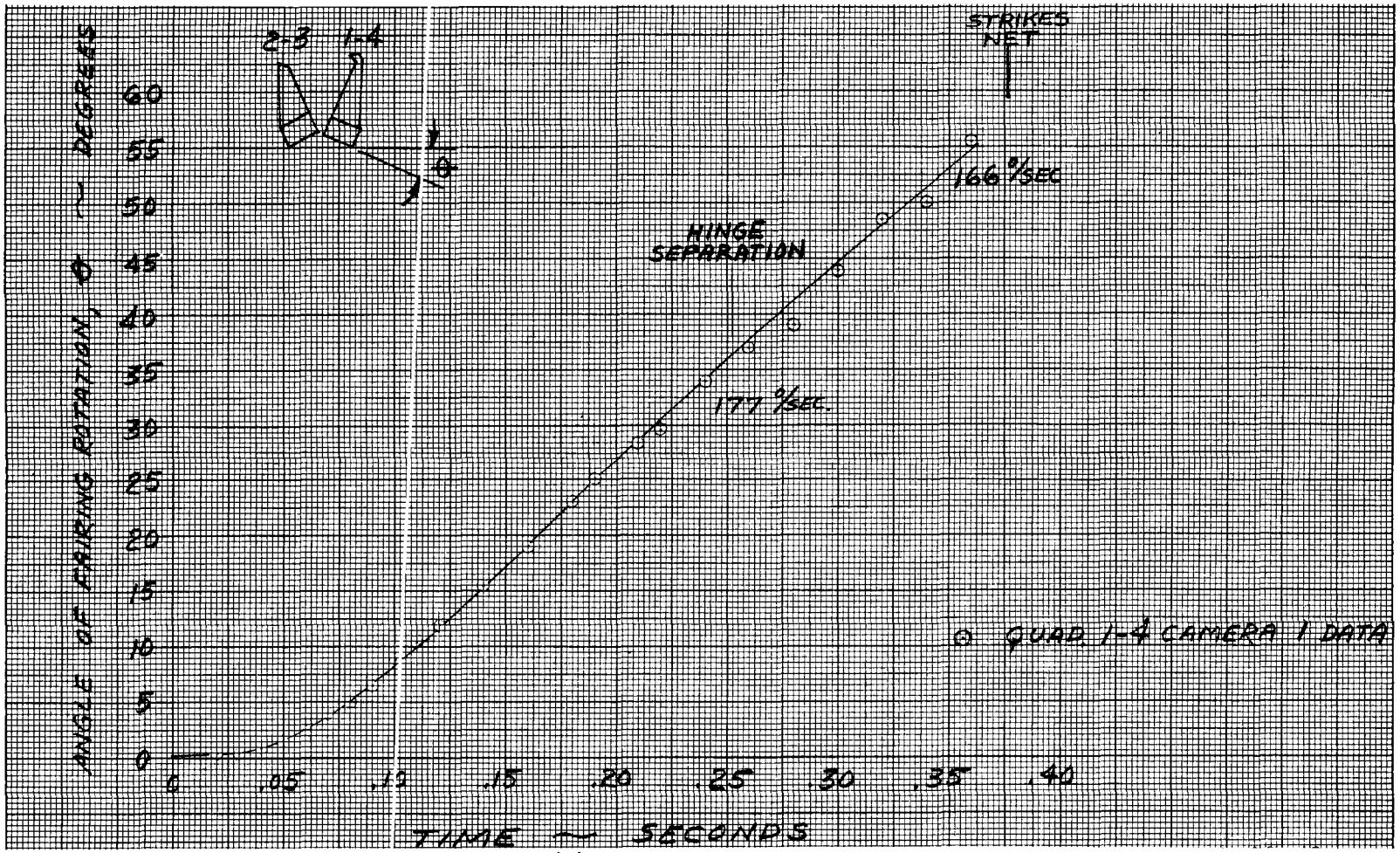

(a) Angular position.

Figure 46. - I-IV Centaur nose fairing half trajectory, Test 11.

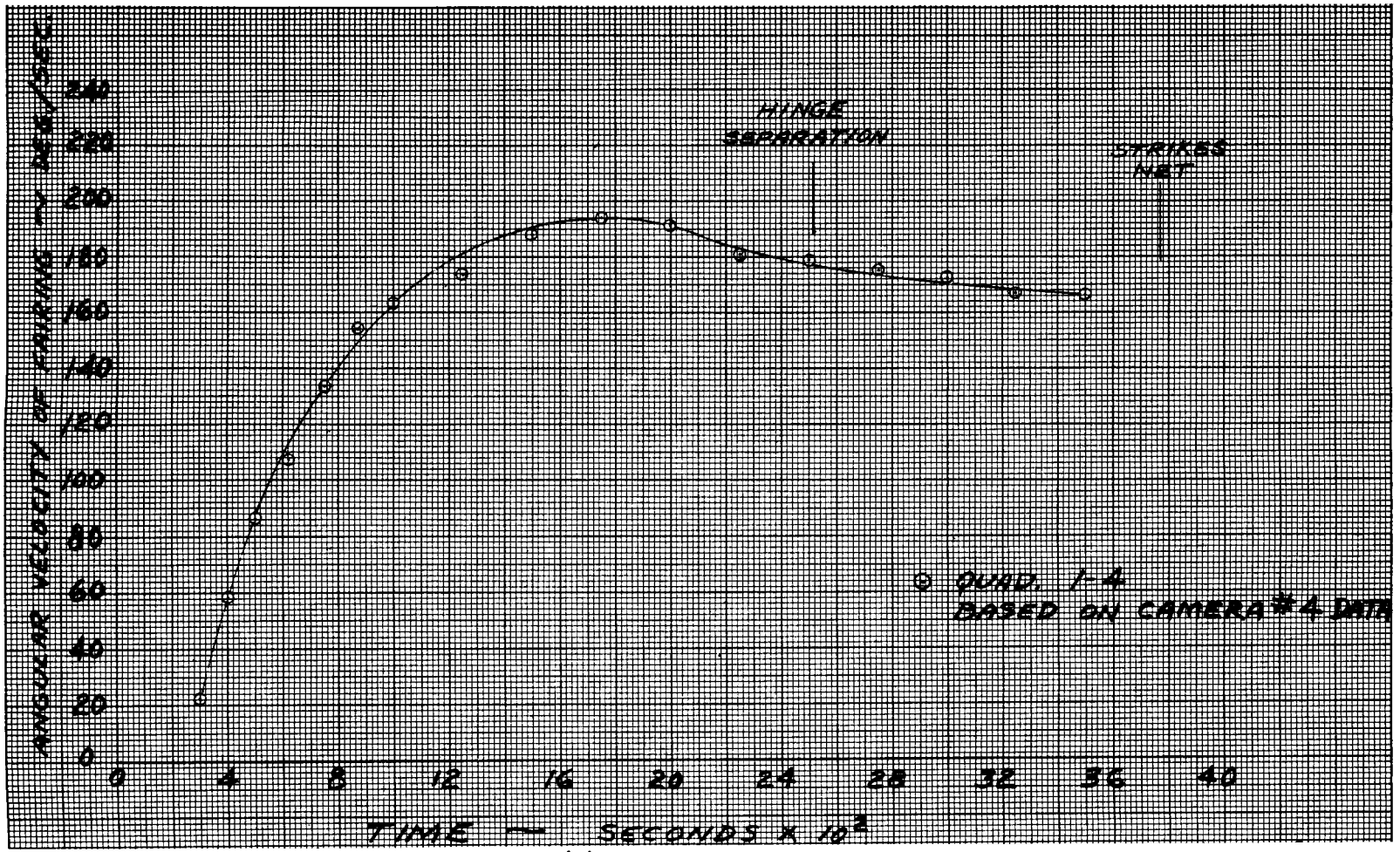

(b) Angular velocity.

Figure 46. - Continued.

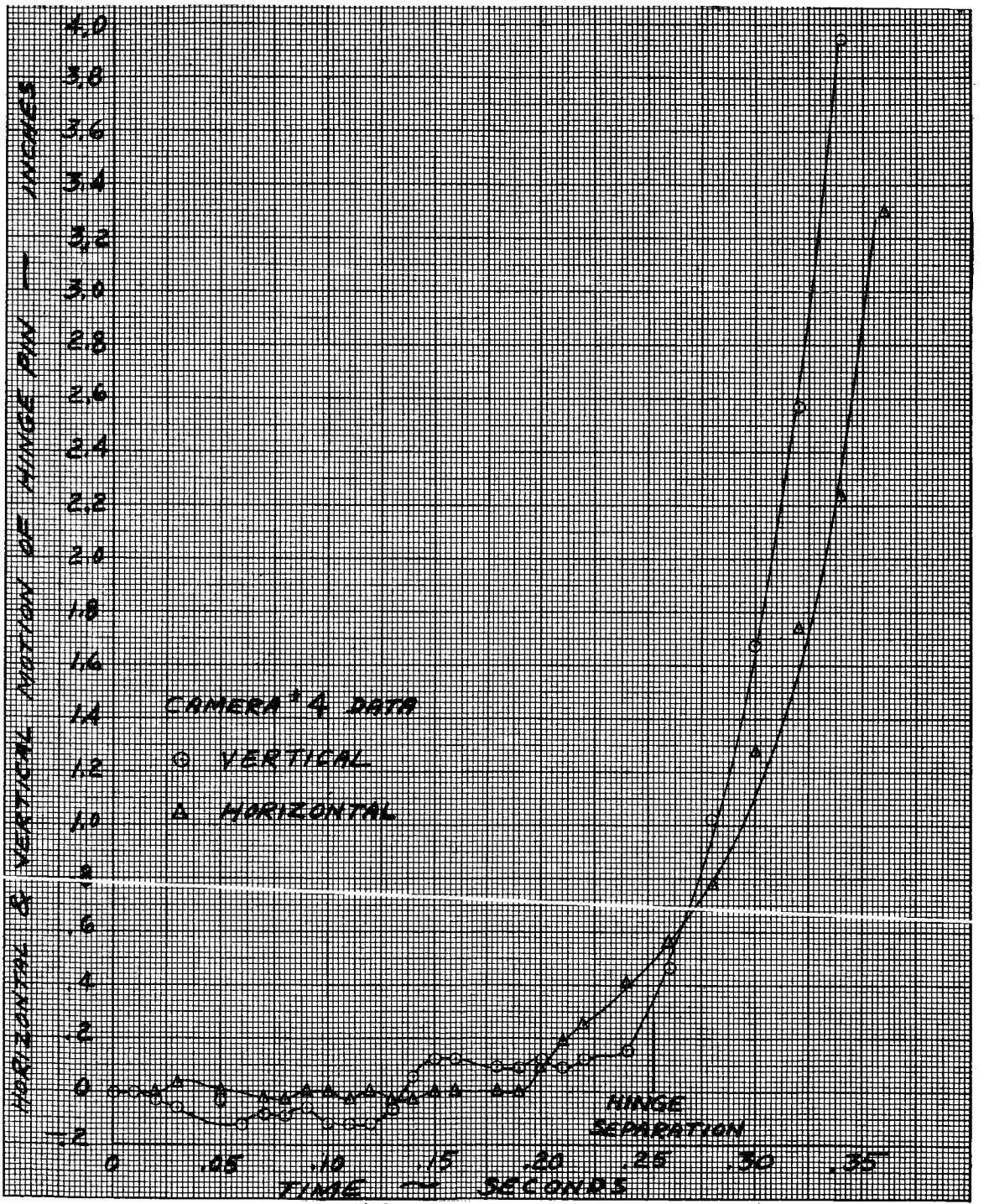

(c) Hinge motion.

Figure 46. - Concluded.

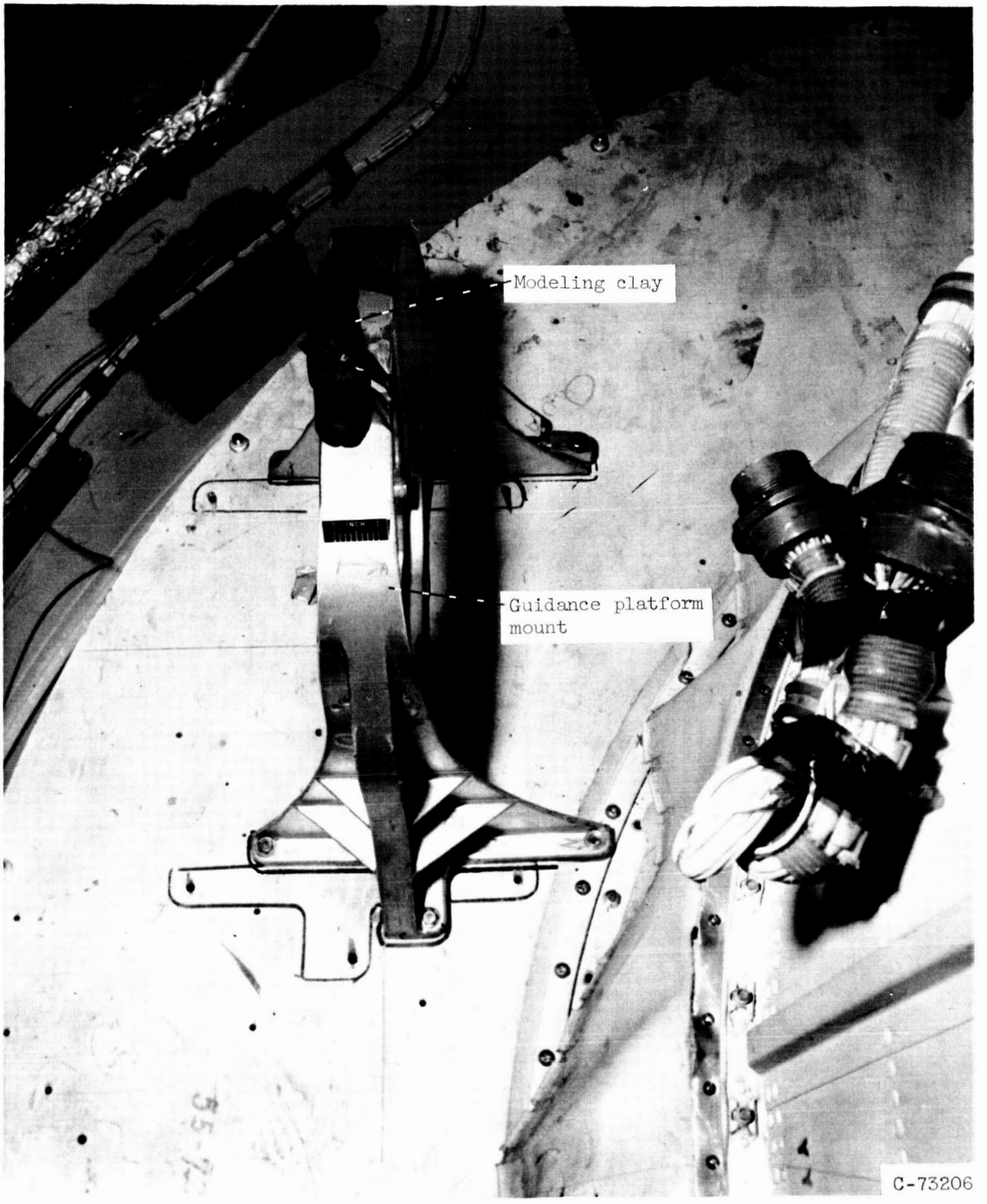

Figure 47. - Modeling clay on top guidance platform test 12.

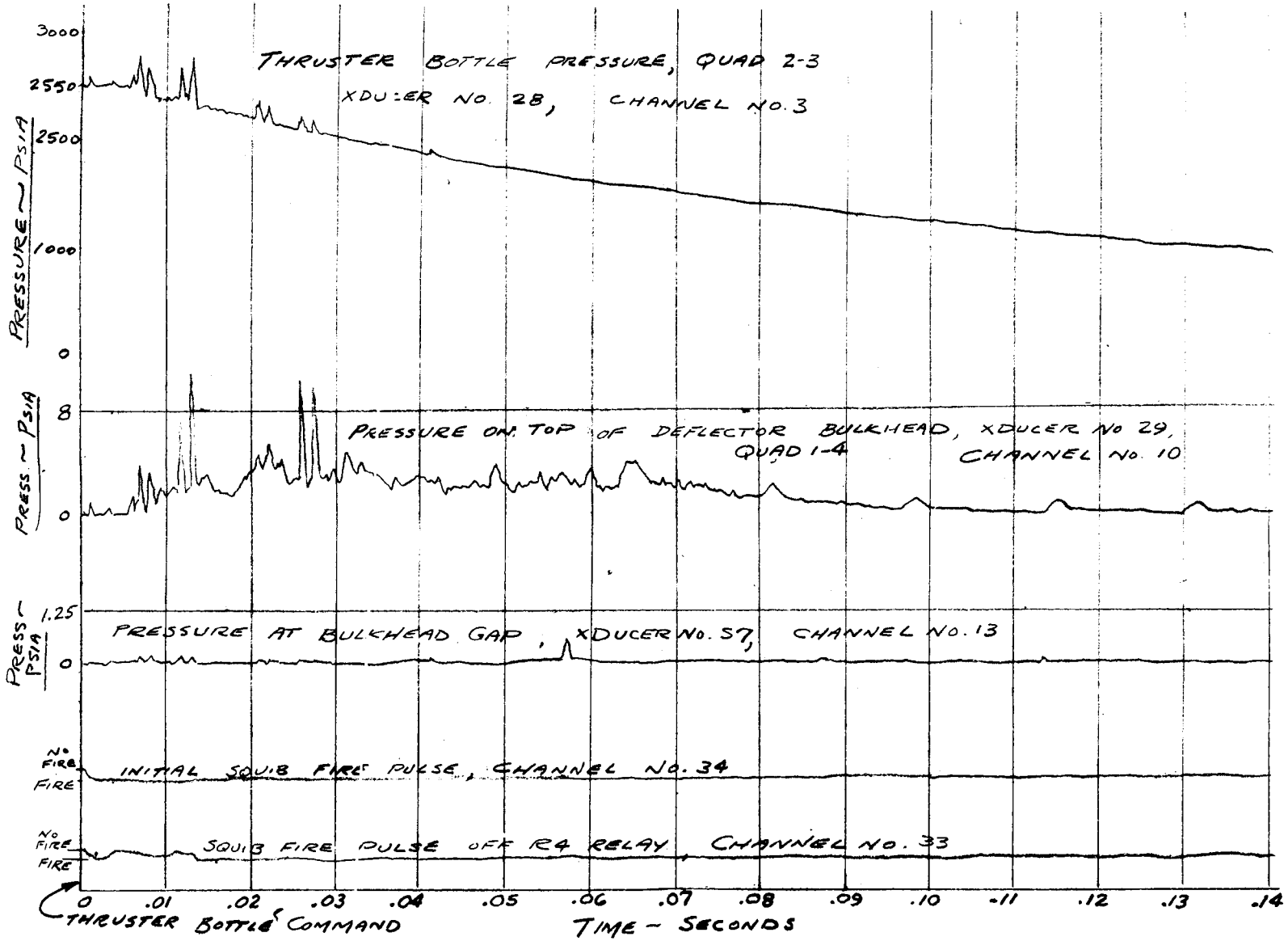

(a) Transducers 28, 29 and 57.

Figure 48. - Nose fairing separation data. Test 12.

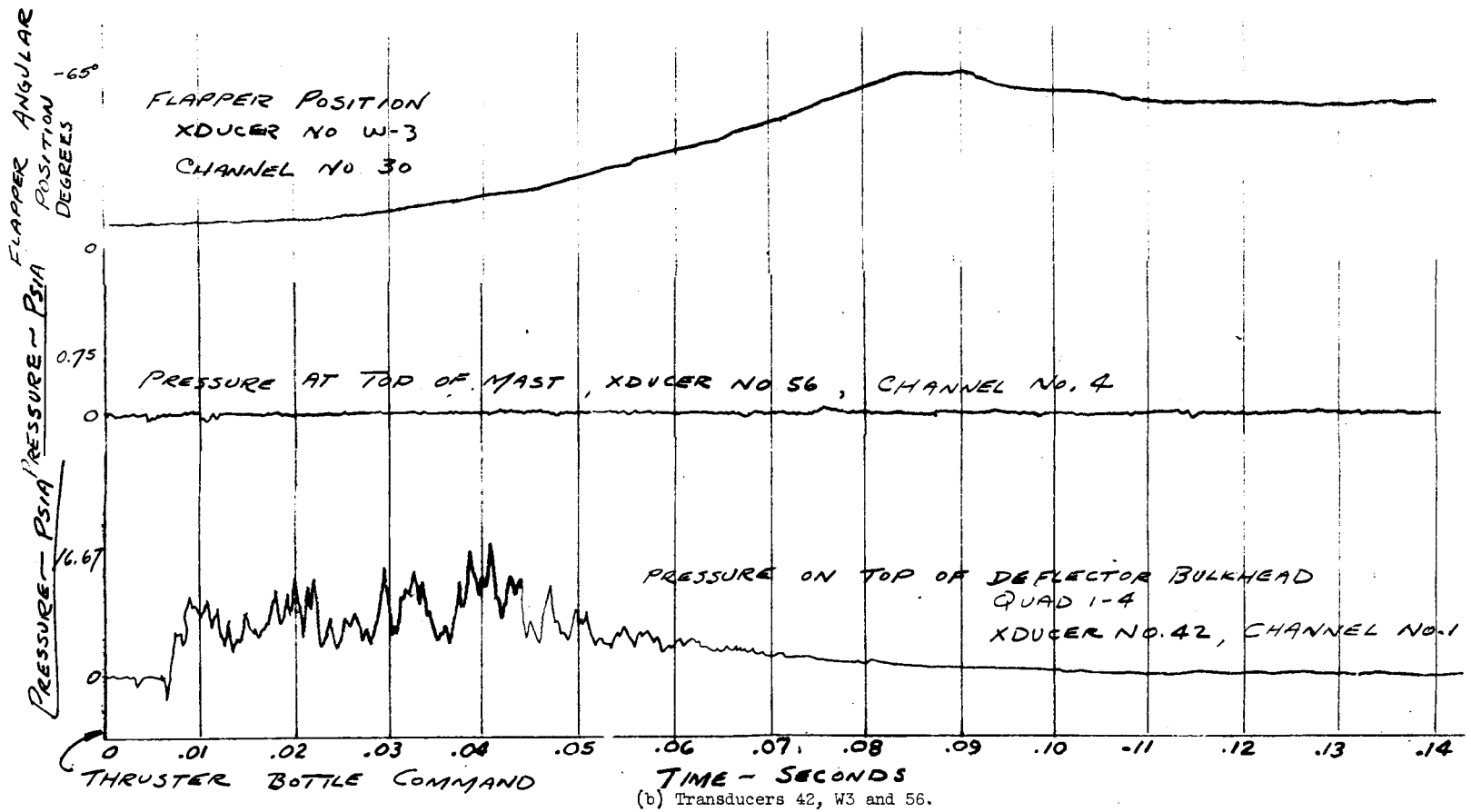

(b) Transducers 42, W3 and 56.

Figure 48. - Continued.

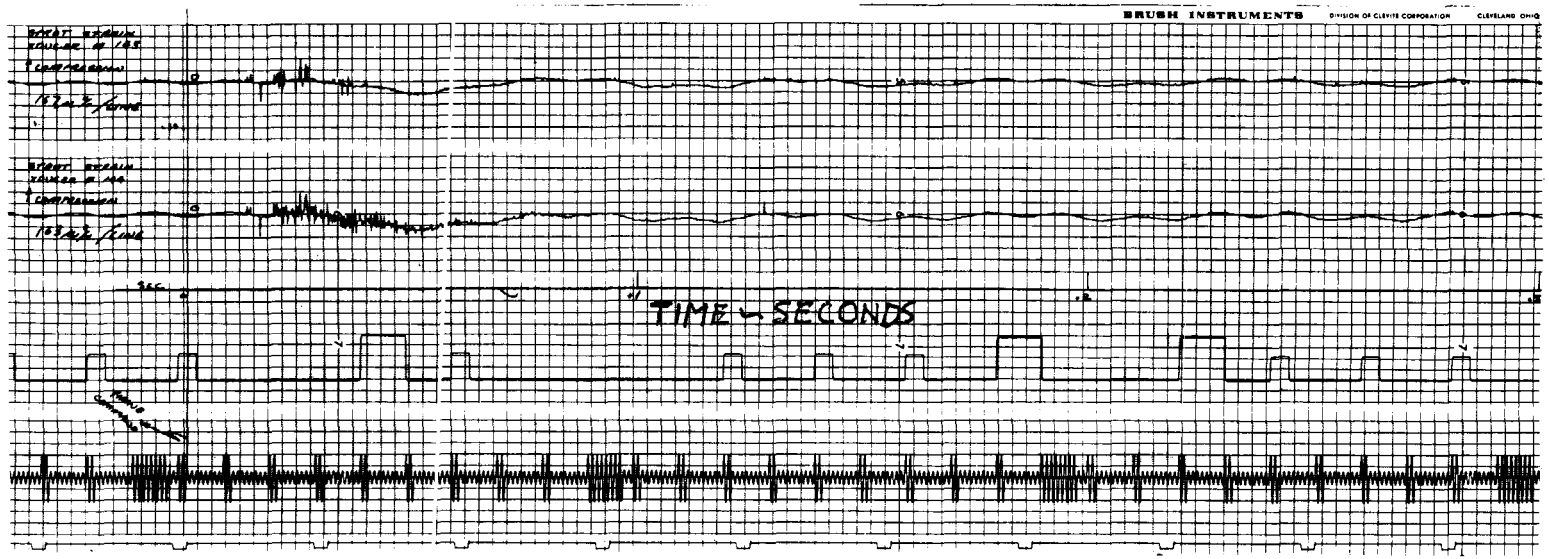

(c) Strain gages 143 and 144.

Figure 48. - Continued.

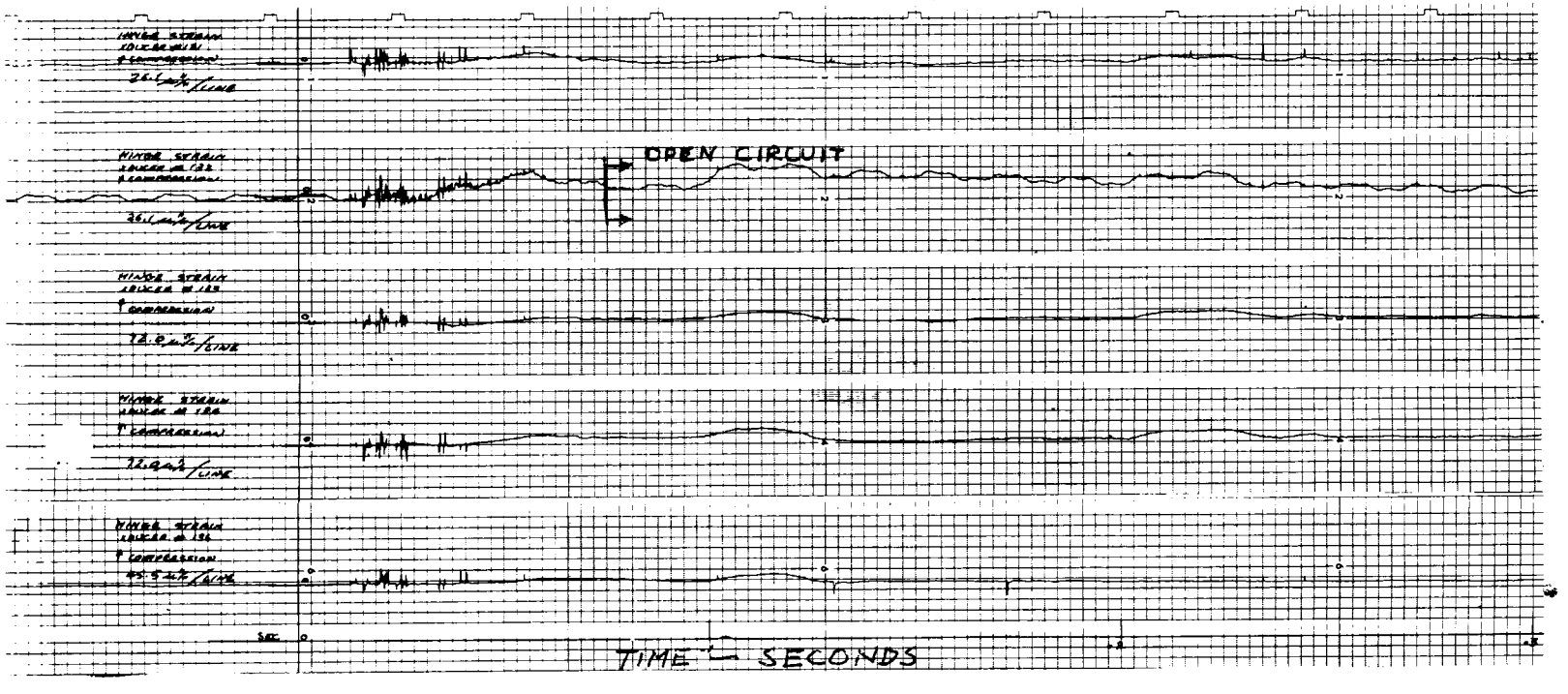

(d) Strain gages 131, 132, 133, 134 and 136.

Figure 48. - Continued.

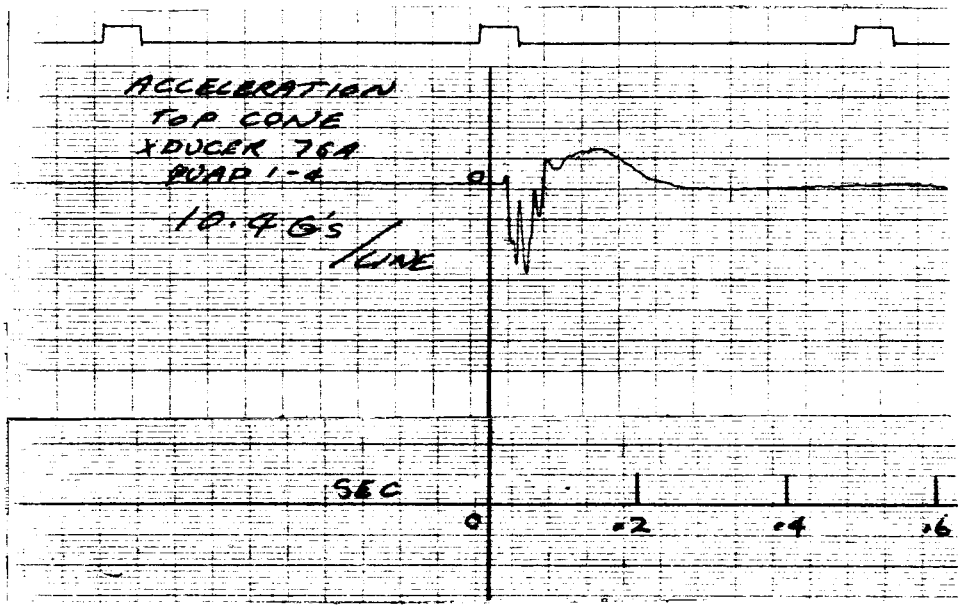

(e) Transducer 76A signal played through lo pass 100 cps filter.

Figure 48. - Concluded.

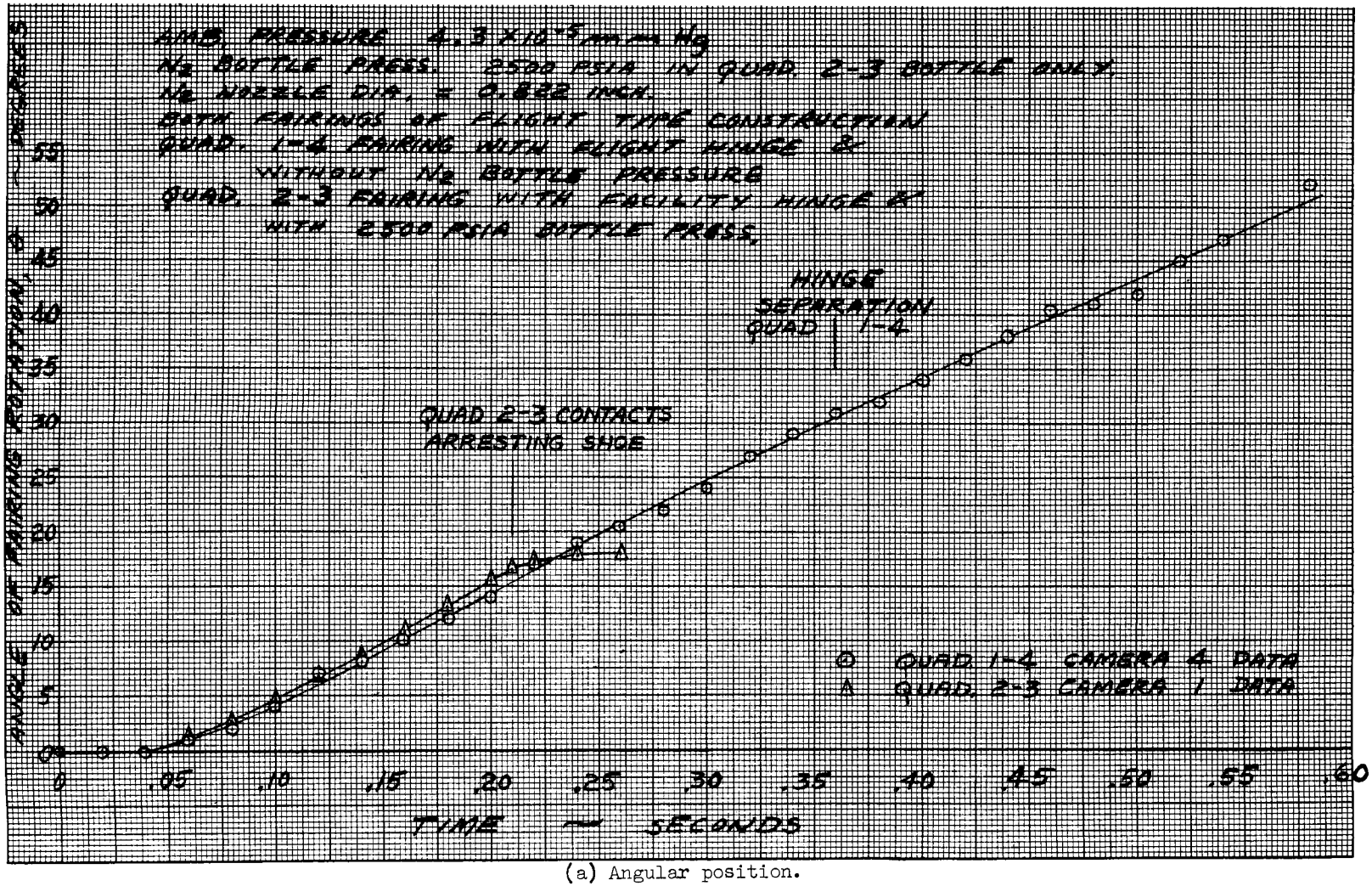

(a) Angular position.

Figure 49. - Centaur nose fairing half trajectory for both fairing halves, Test 12.

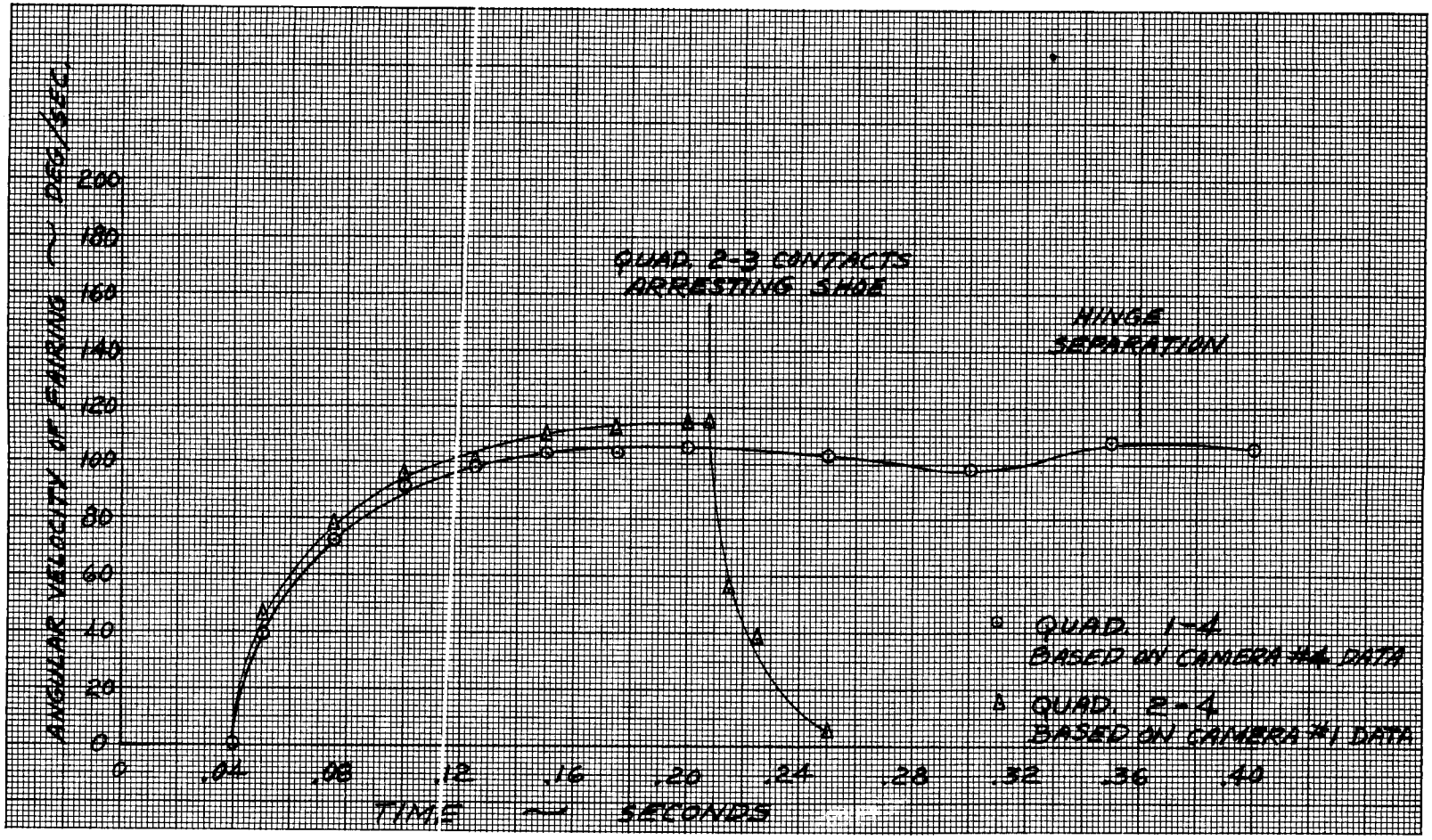

(b) Angular velocity.

Figure 49. - Continued.

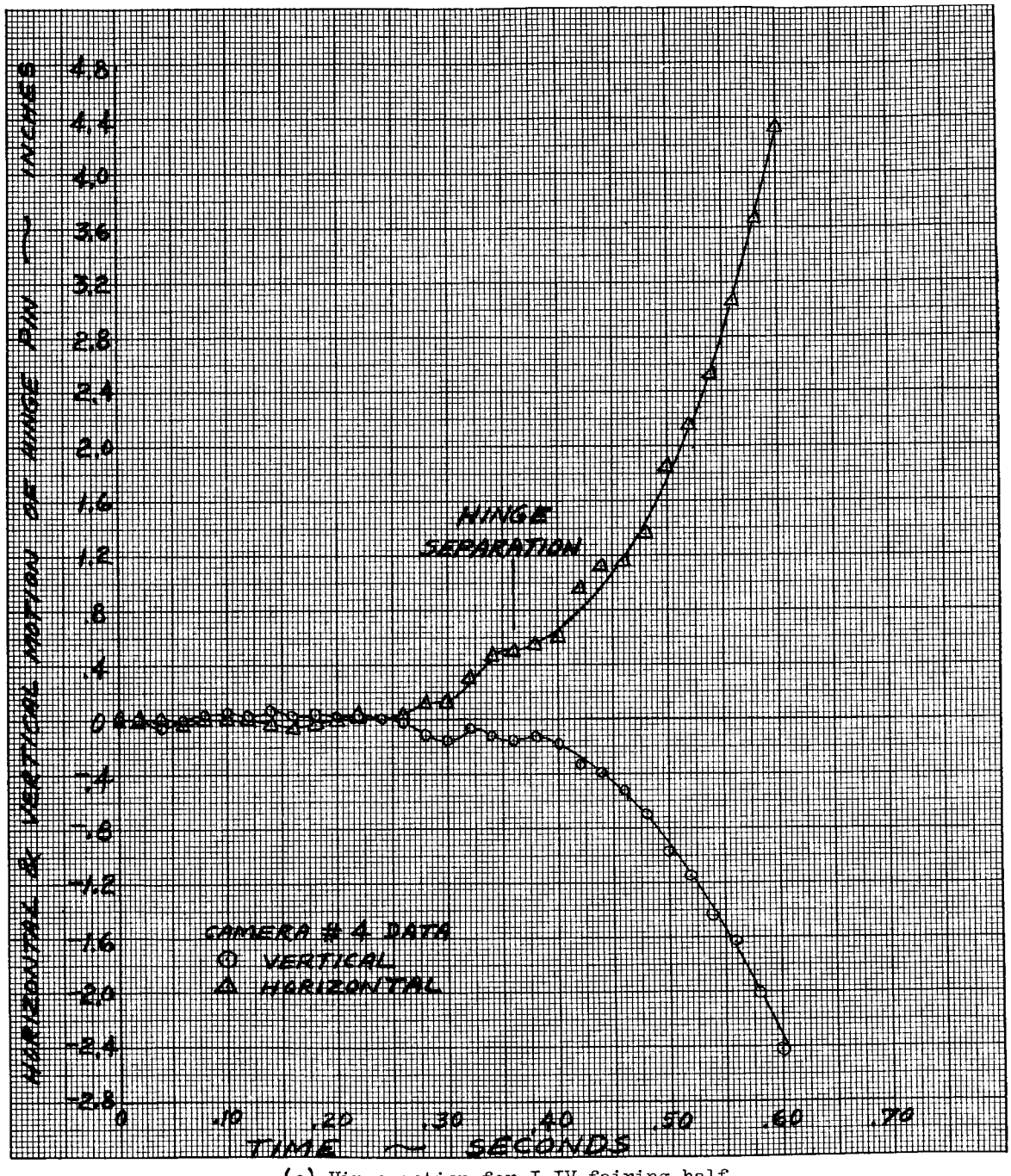

(c) Hinge motion for I-IV fairing half.

Figure 49. - Continued.

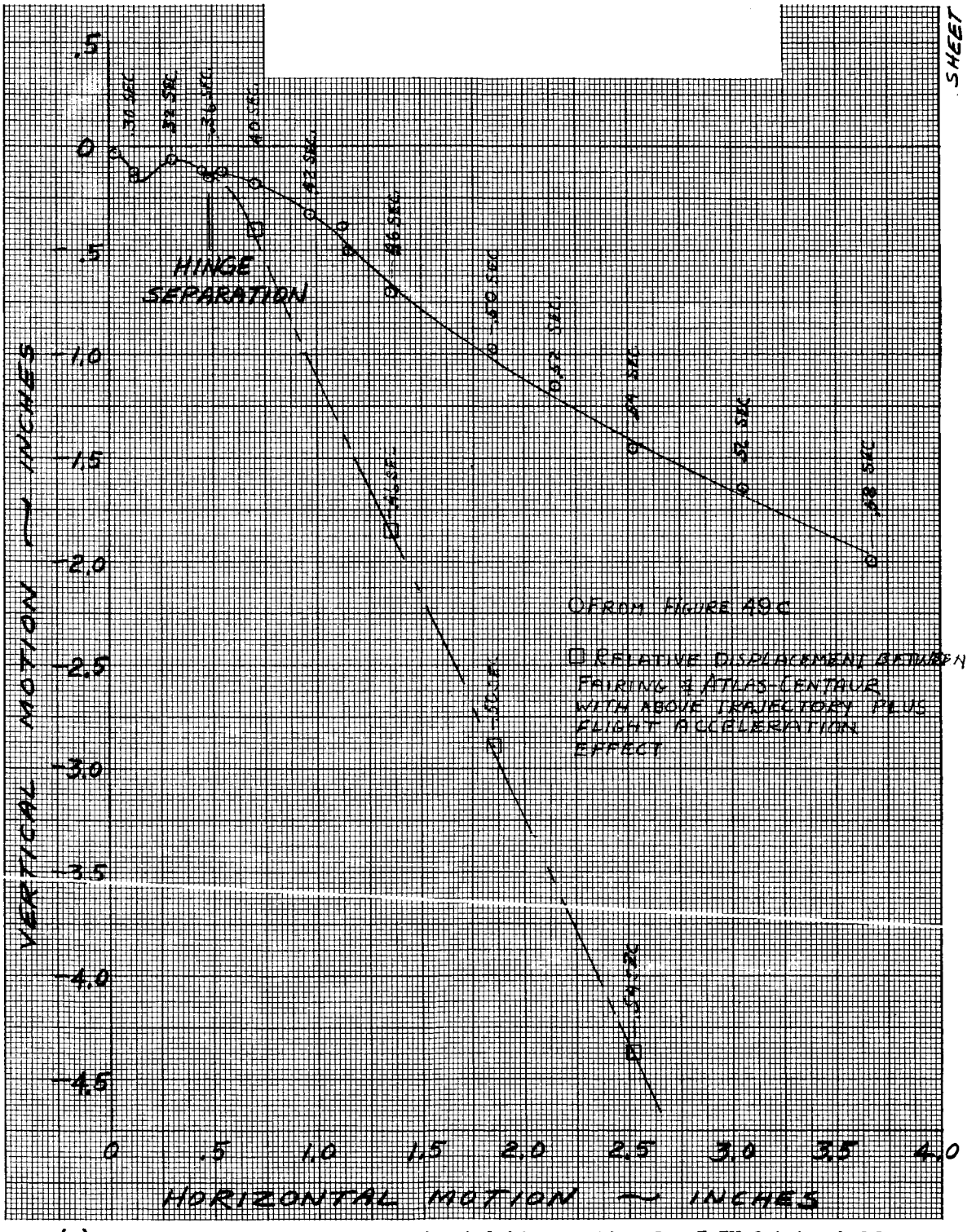

(d) Verticle hinge motion vs. horizontal hinge motion for I-IV fairing half.

Figure 49. - Concluded.

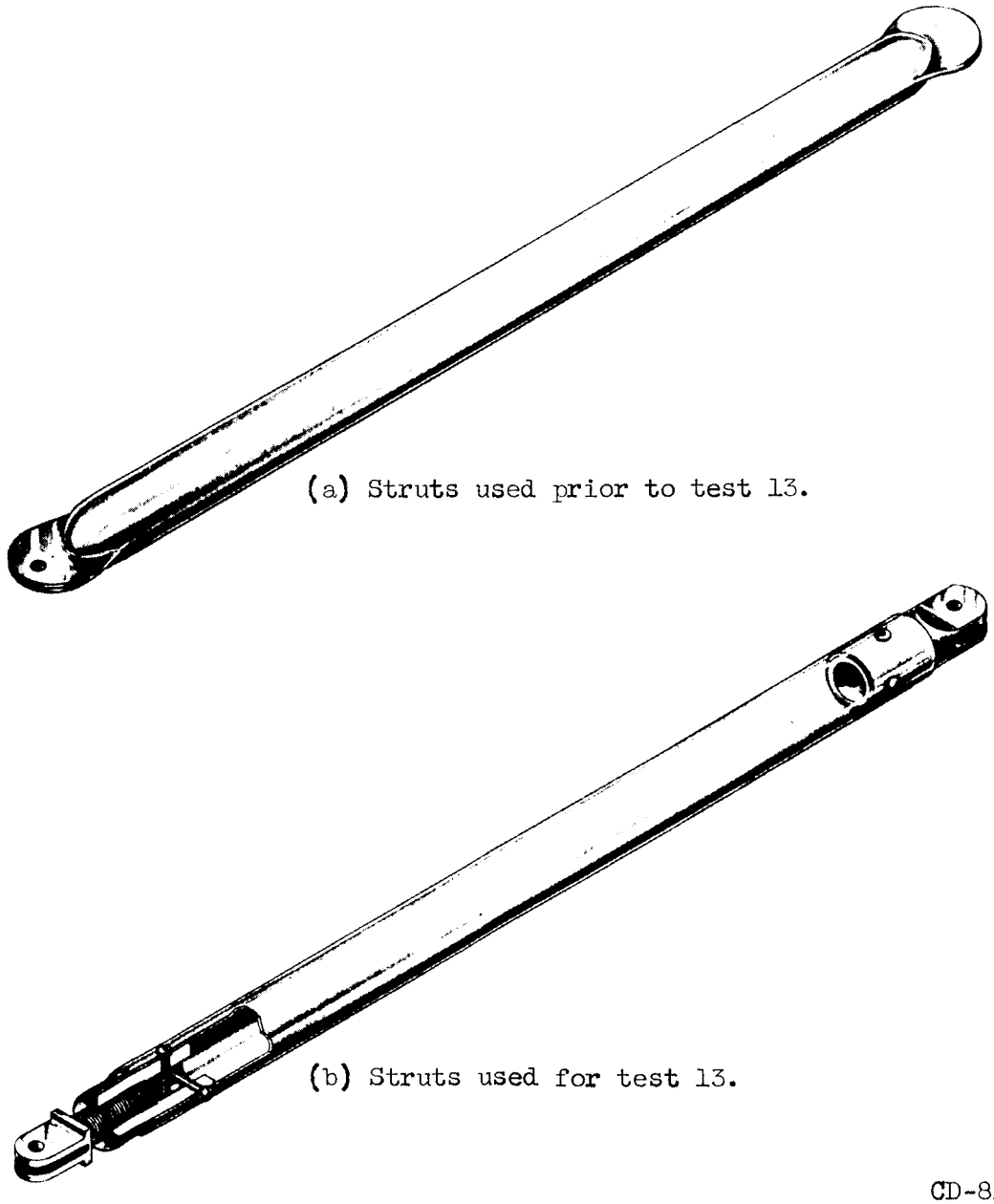

(a) Struts used prior to test 13.

(b) Struts used for test 13.

CD-8110

Figure 50. - Thermal bulkhead strut.

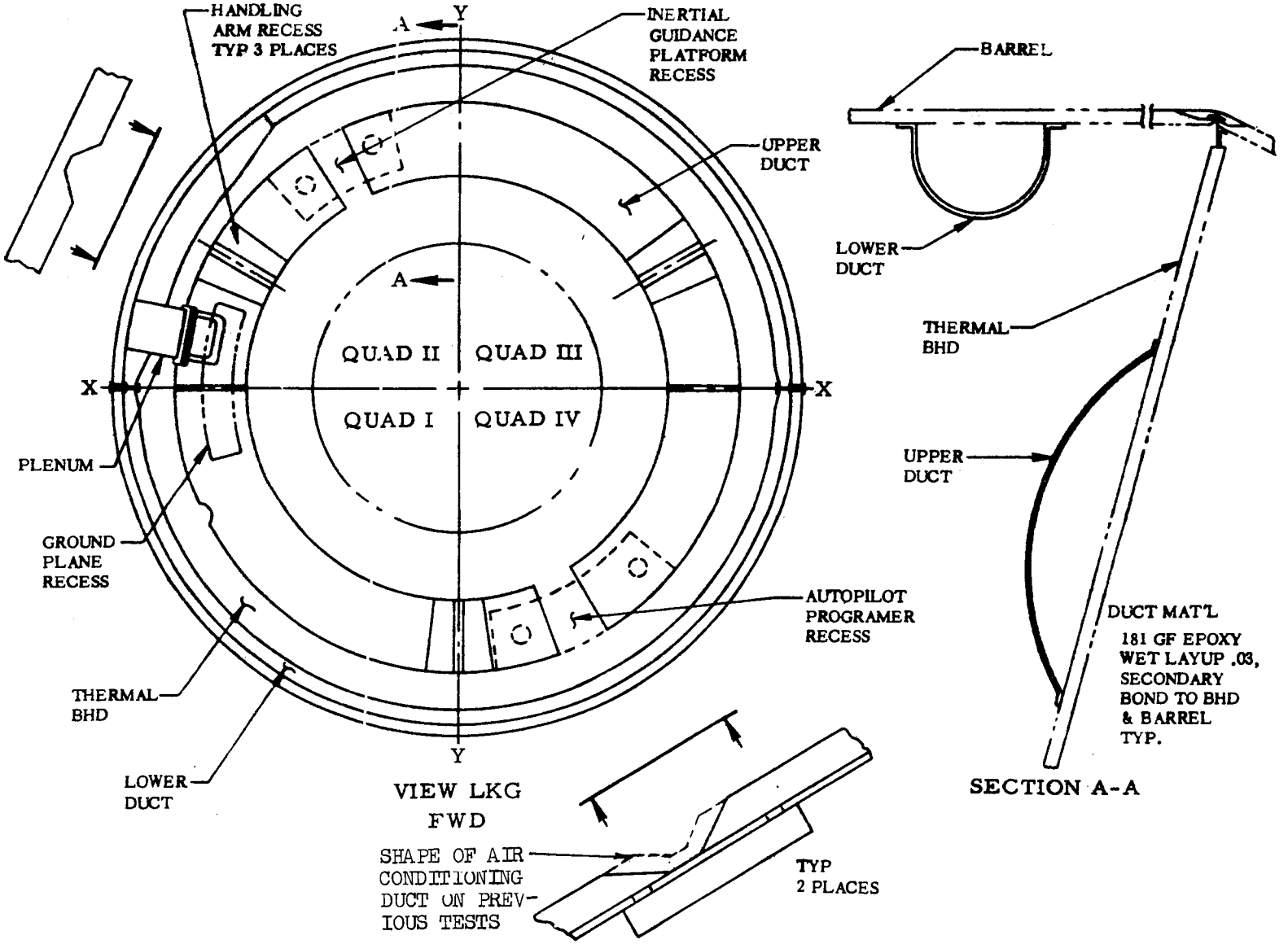

Figure 51. - Thermal bulkhead air conditioning duct.

10.6.25

Figure 52. - Top of redesigned thermal bulkhead above A/P Programmer.

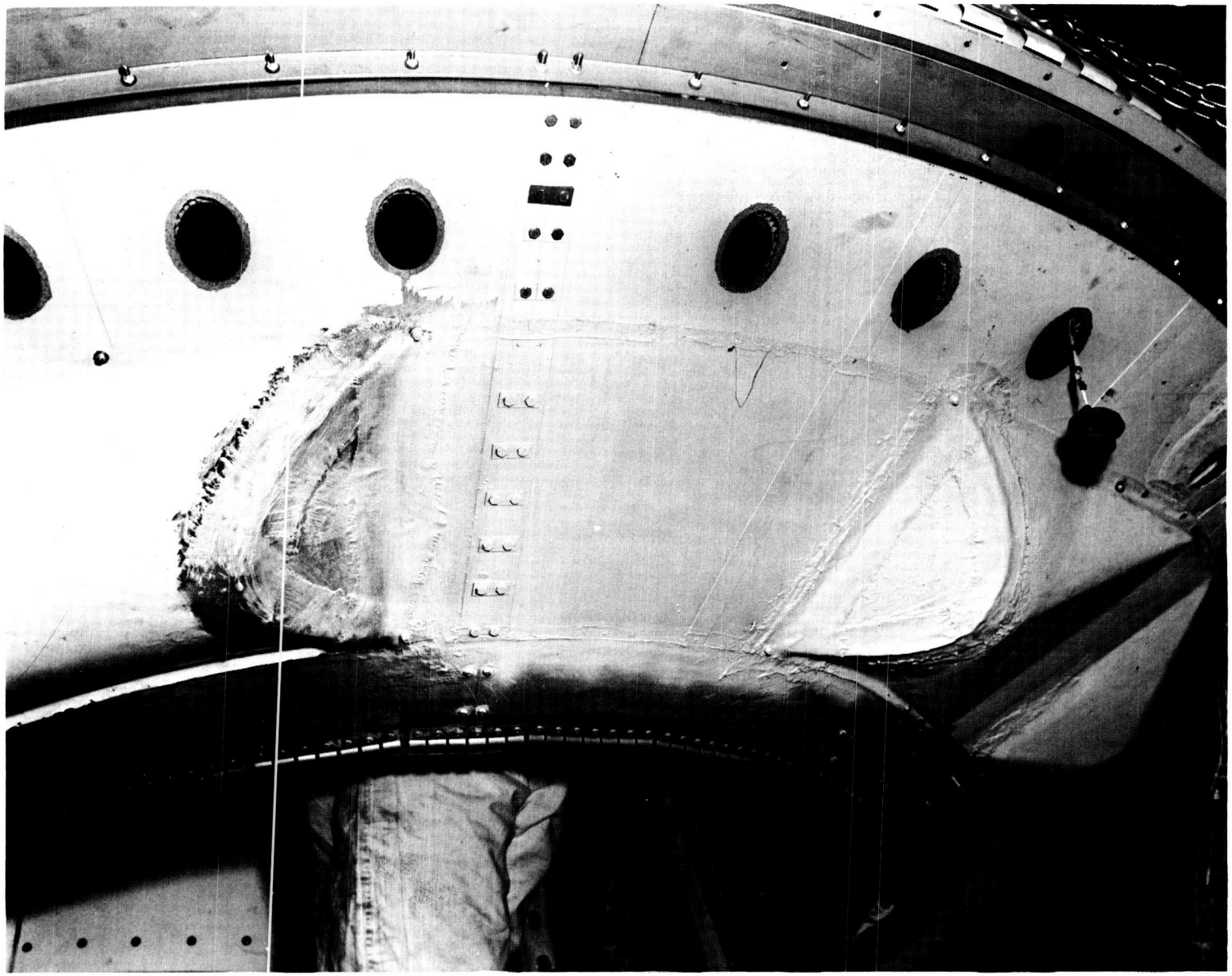

Figure 53. - Bottom of redesigned thermal bulkhead above A/P Programmer.

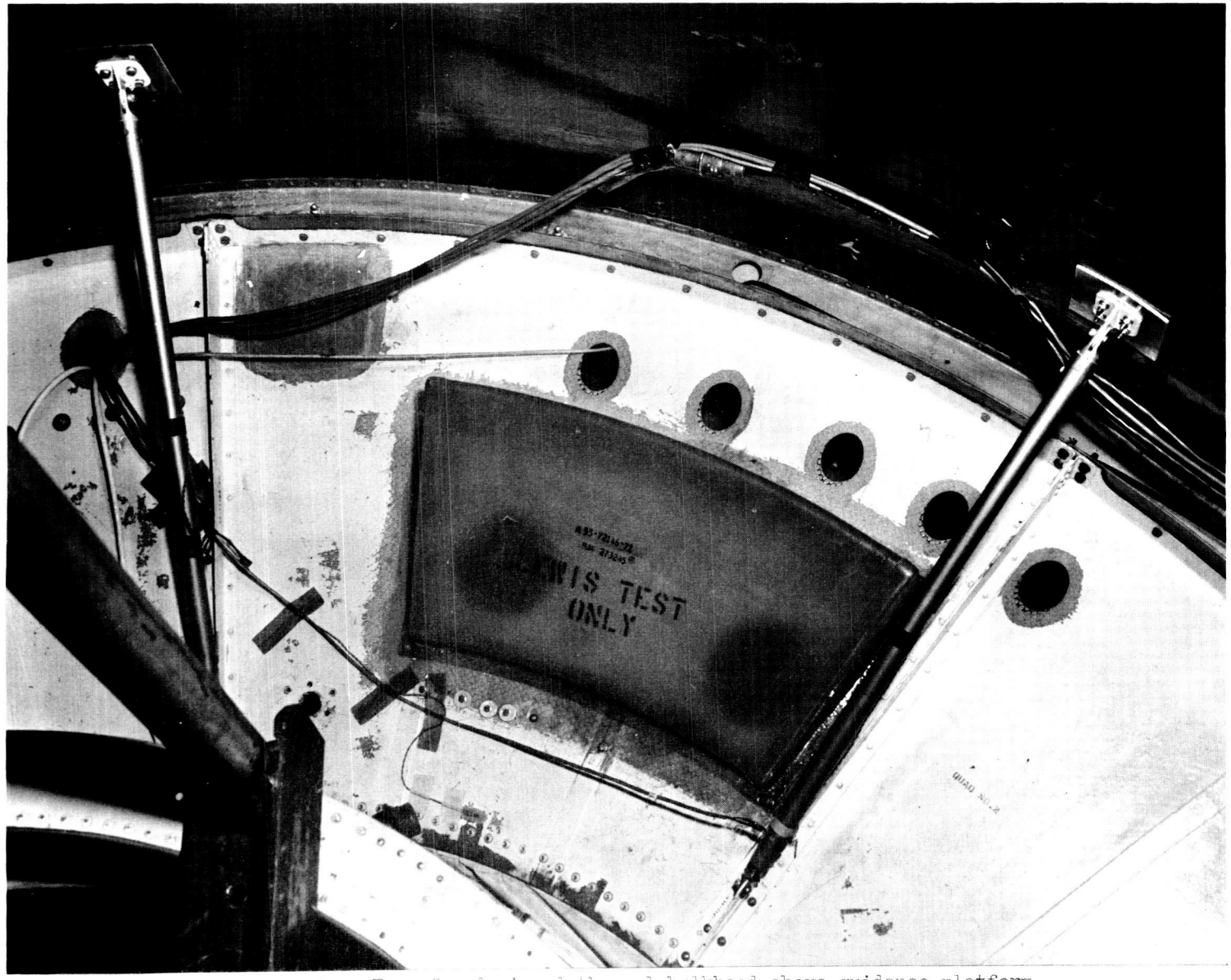

Figure 54. - Top of redesigned thermal bulkhead above guidance platform.

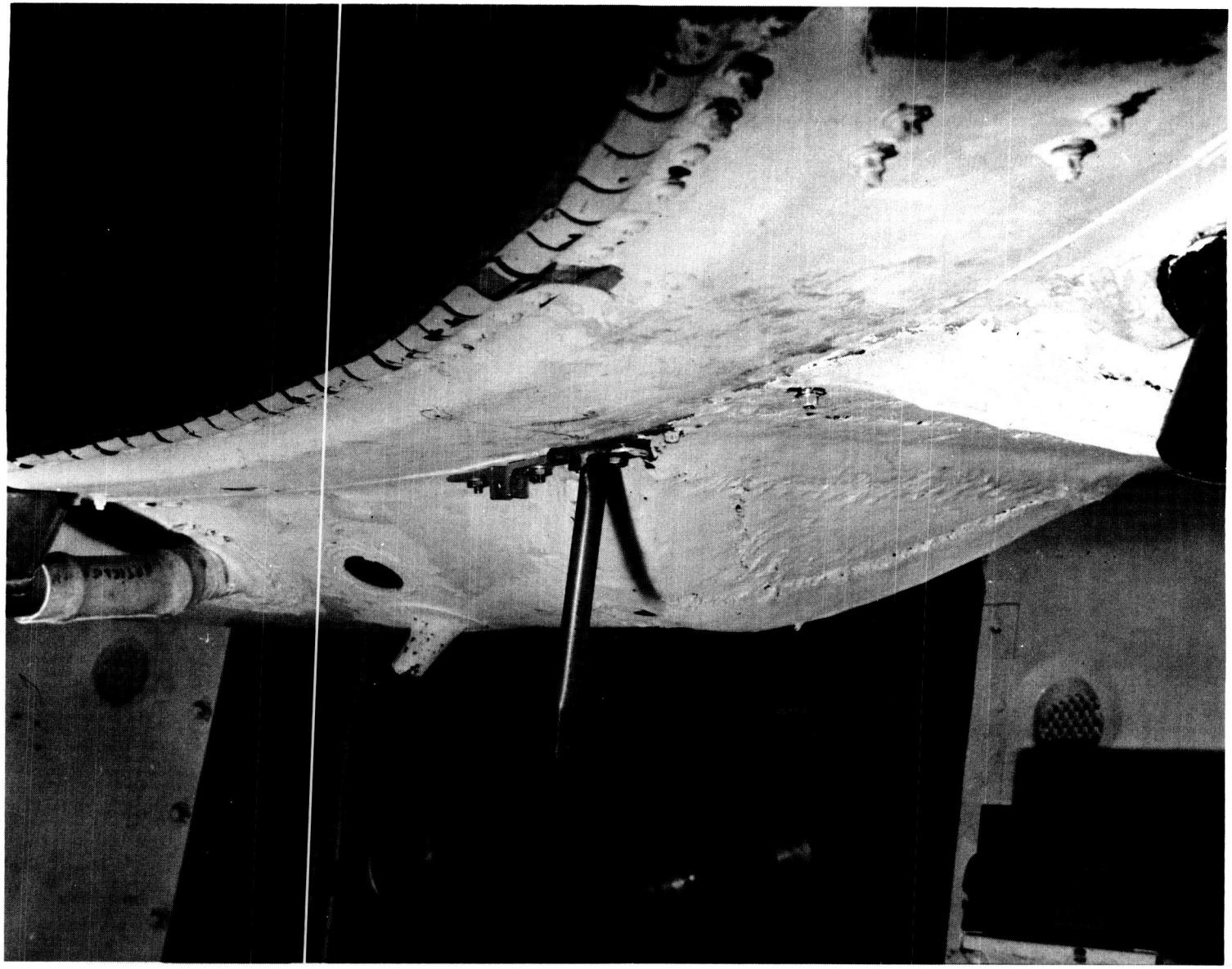

Figure 55. - Bottom of redesigned thermal bulkhead above guidance platform.

Figure 56. - Guidance platform mounted for test 13.

E-3265

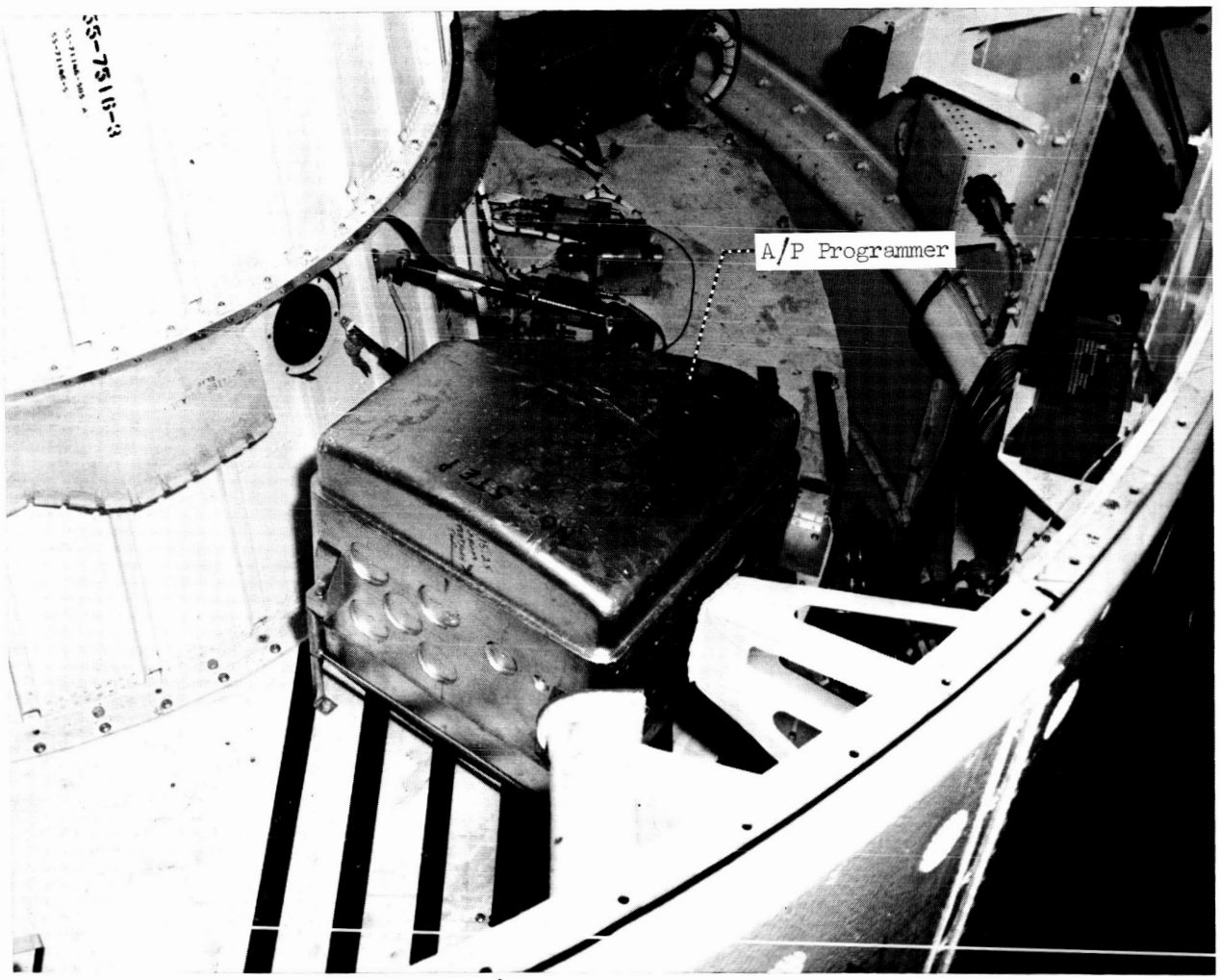

Figure 57. - A/P Programmer location, Test 13.

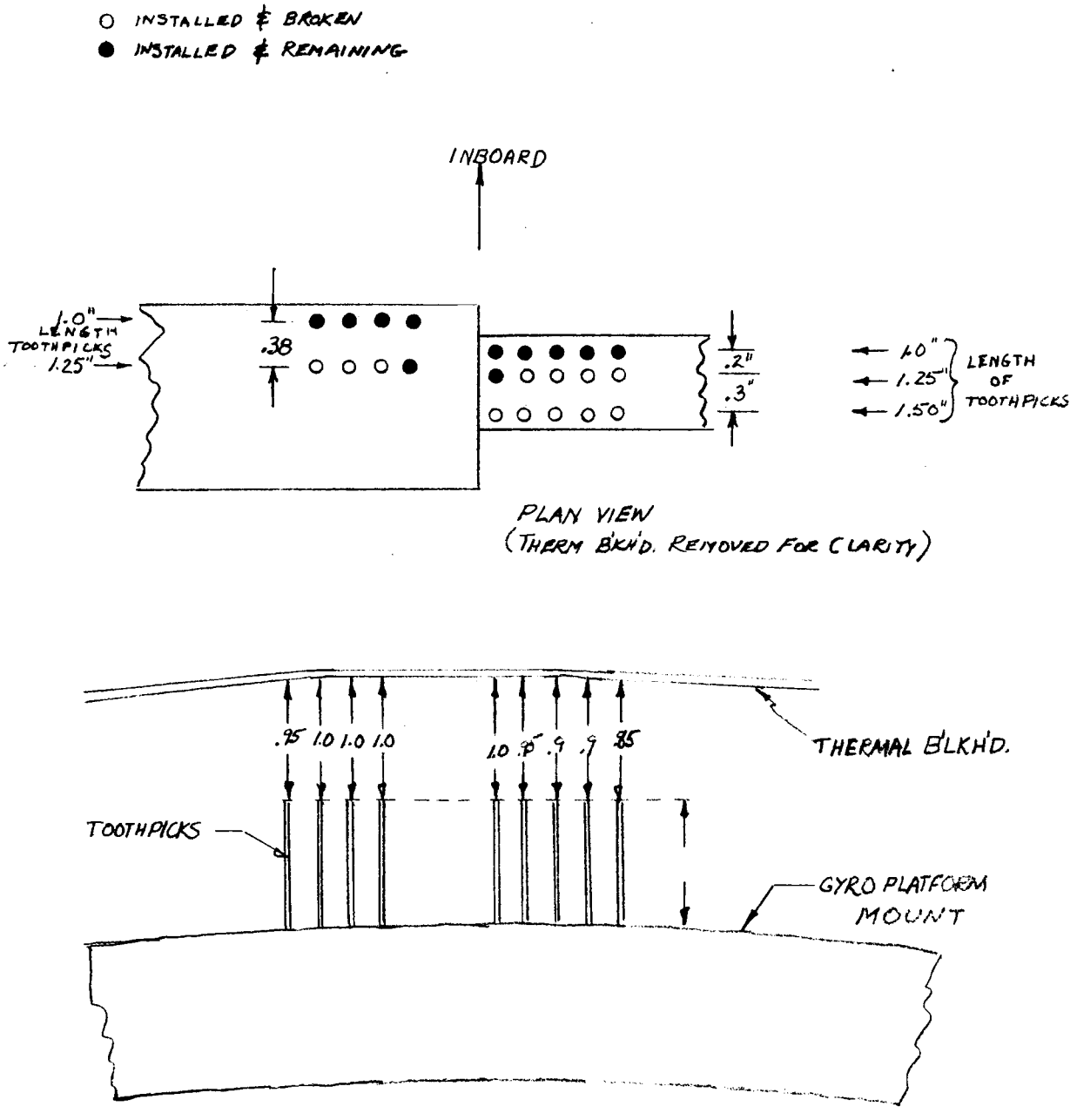

Figure 58. - Location of toothpicks on guidance platform.

E-3265

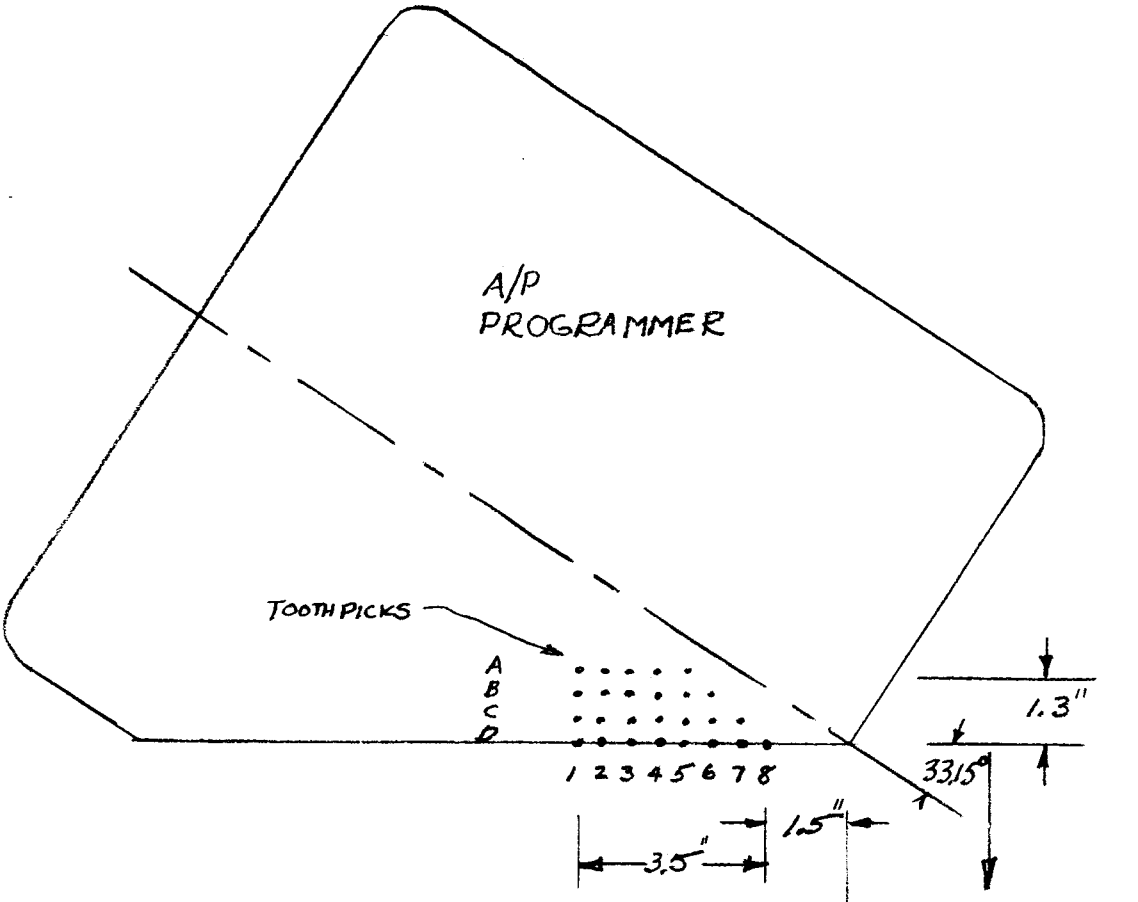

HEIGHT OF TOOTHPICKS (INCHES)

ROW								
A	1.35	1.15	.75	.65	.5			
B	1.55	1.3	1.0	.85	.7	.4		
C	1.75	1.5	1.25	1.10	.85	.5	.3	
D	1.9	1.7	1.5	1.25	1.00	.85	.6	.4
COLUMN	1	2	3	4	5	6	7	8

Figure 59. - Location of toothpicks on A/P Programmer.

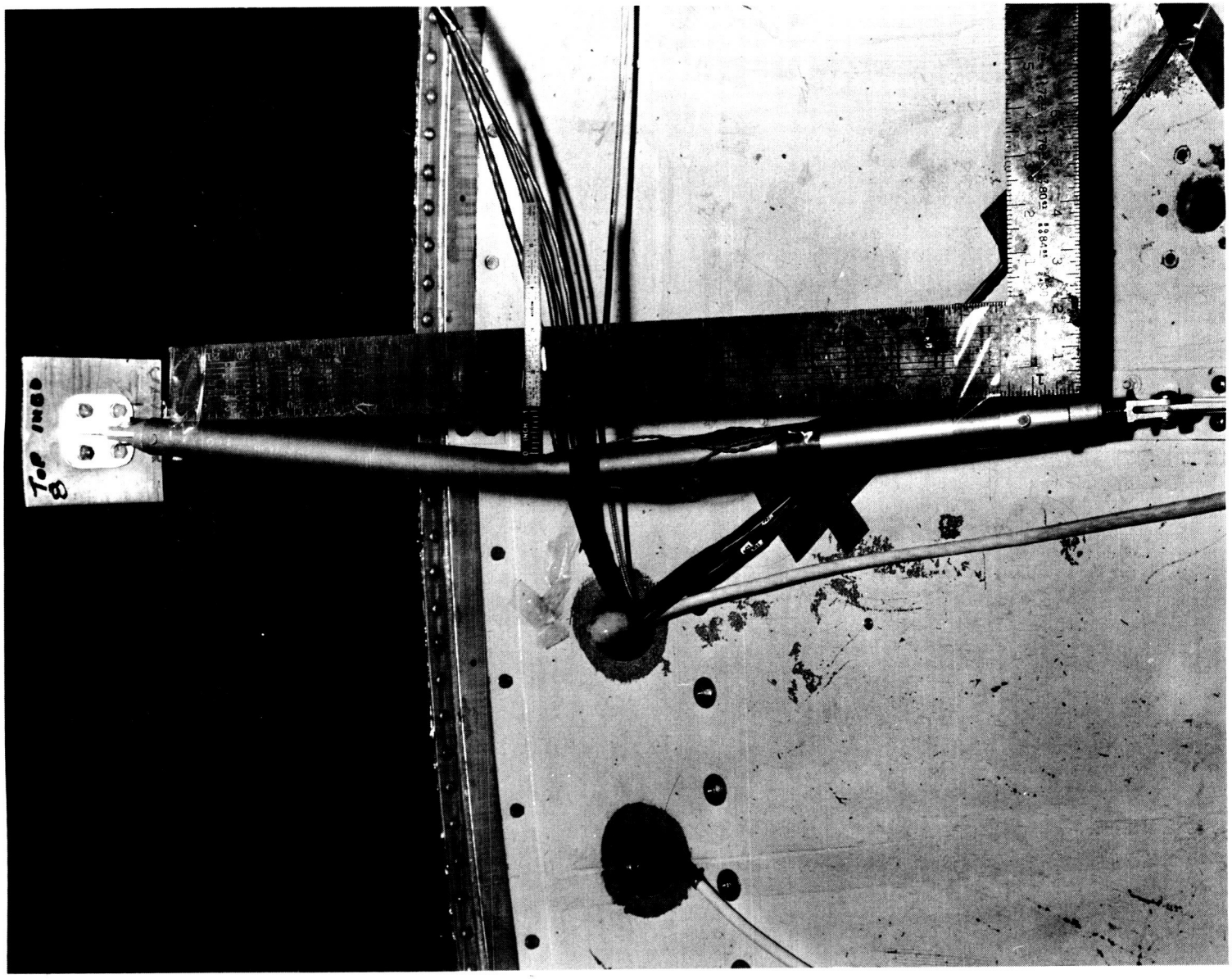

Figure 60. - Damaged strut Test 13.

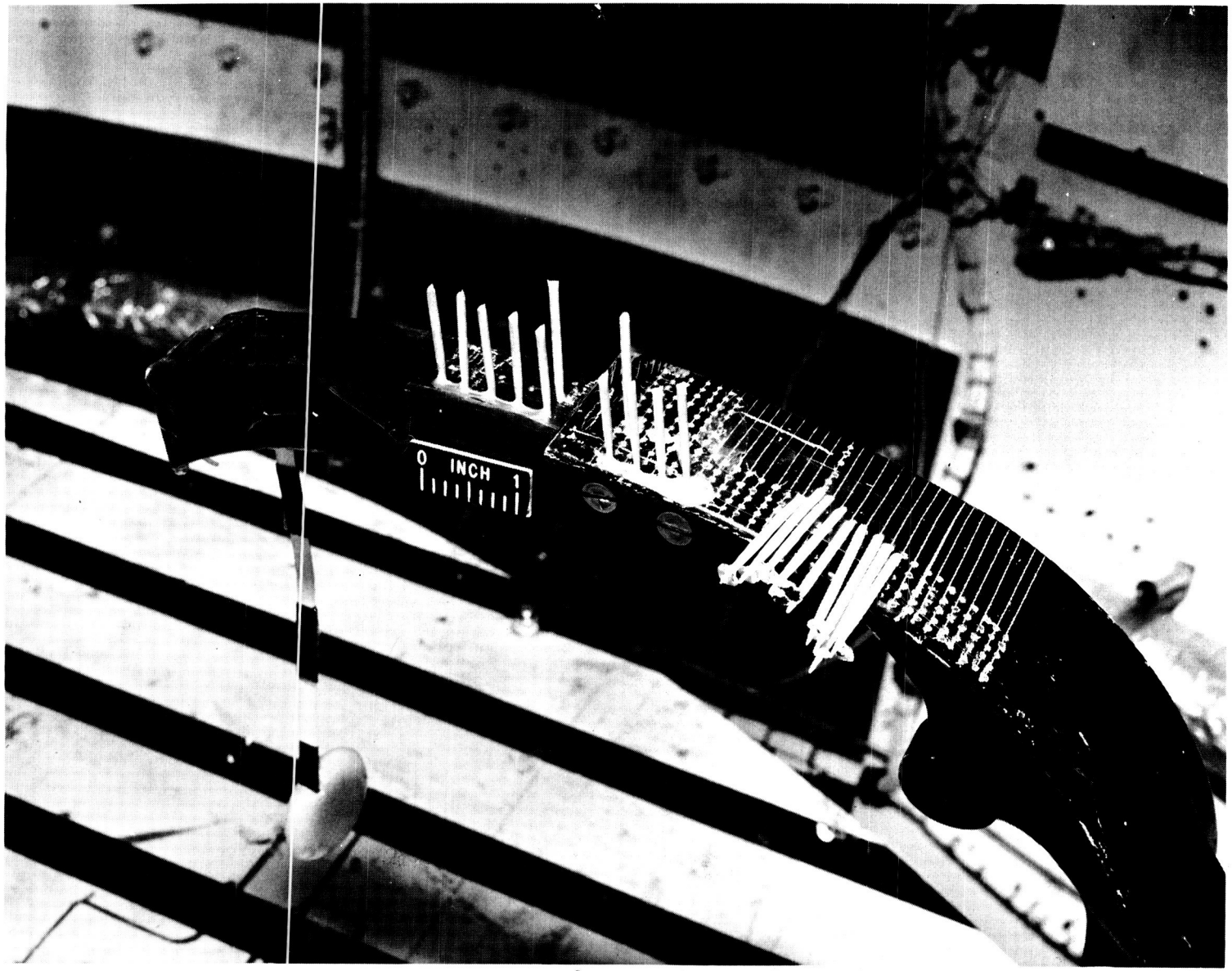

Figure 61. - Toothpicks on guidance platform after test 13.

Figure 62. - Toothpicks on A/P Programmer after test 13.

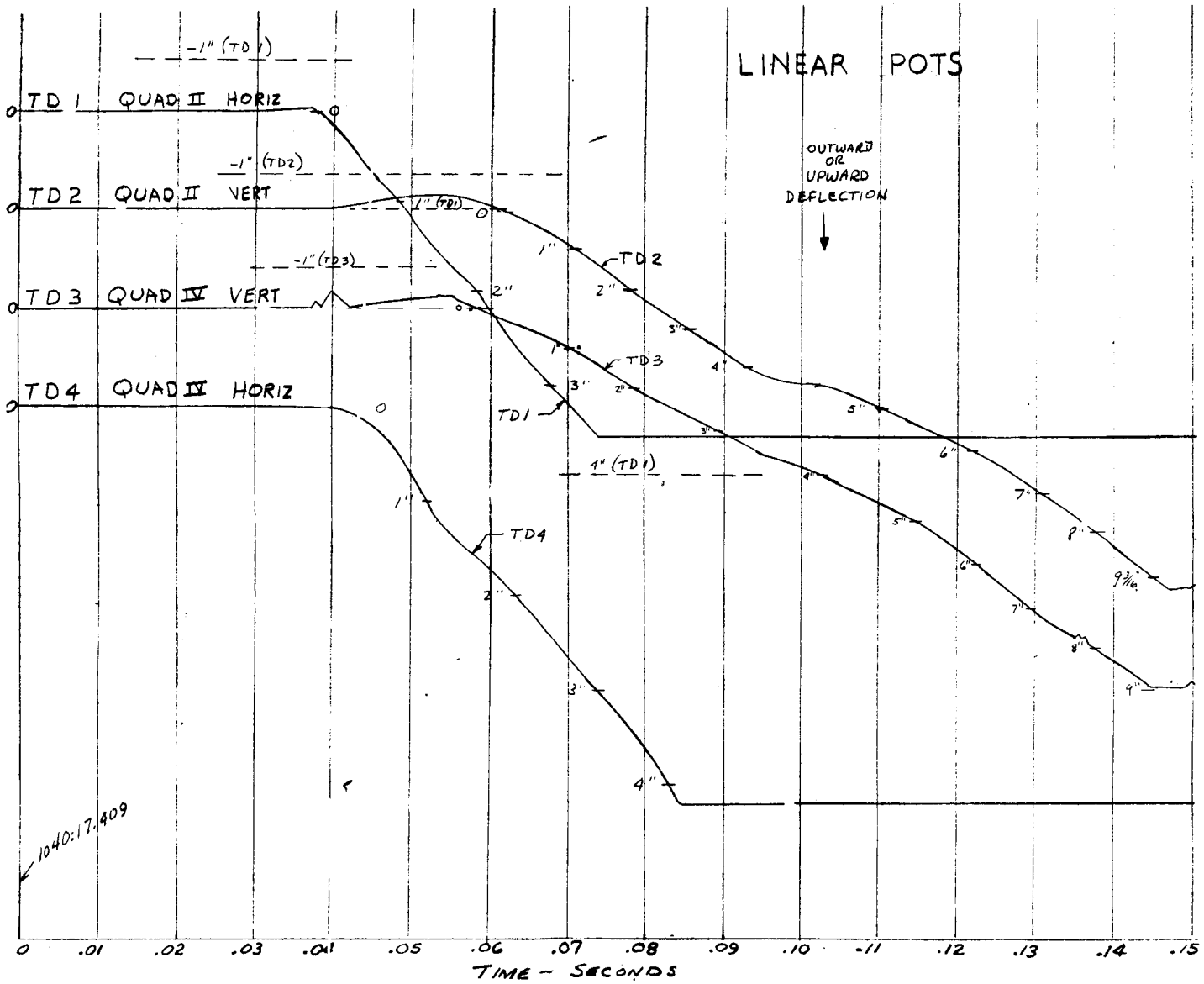

(a) Transducers TD1, TD2, TD3, and TD4.

Figure 63. - Nose fairing separation data. Test 13.

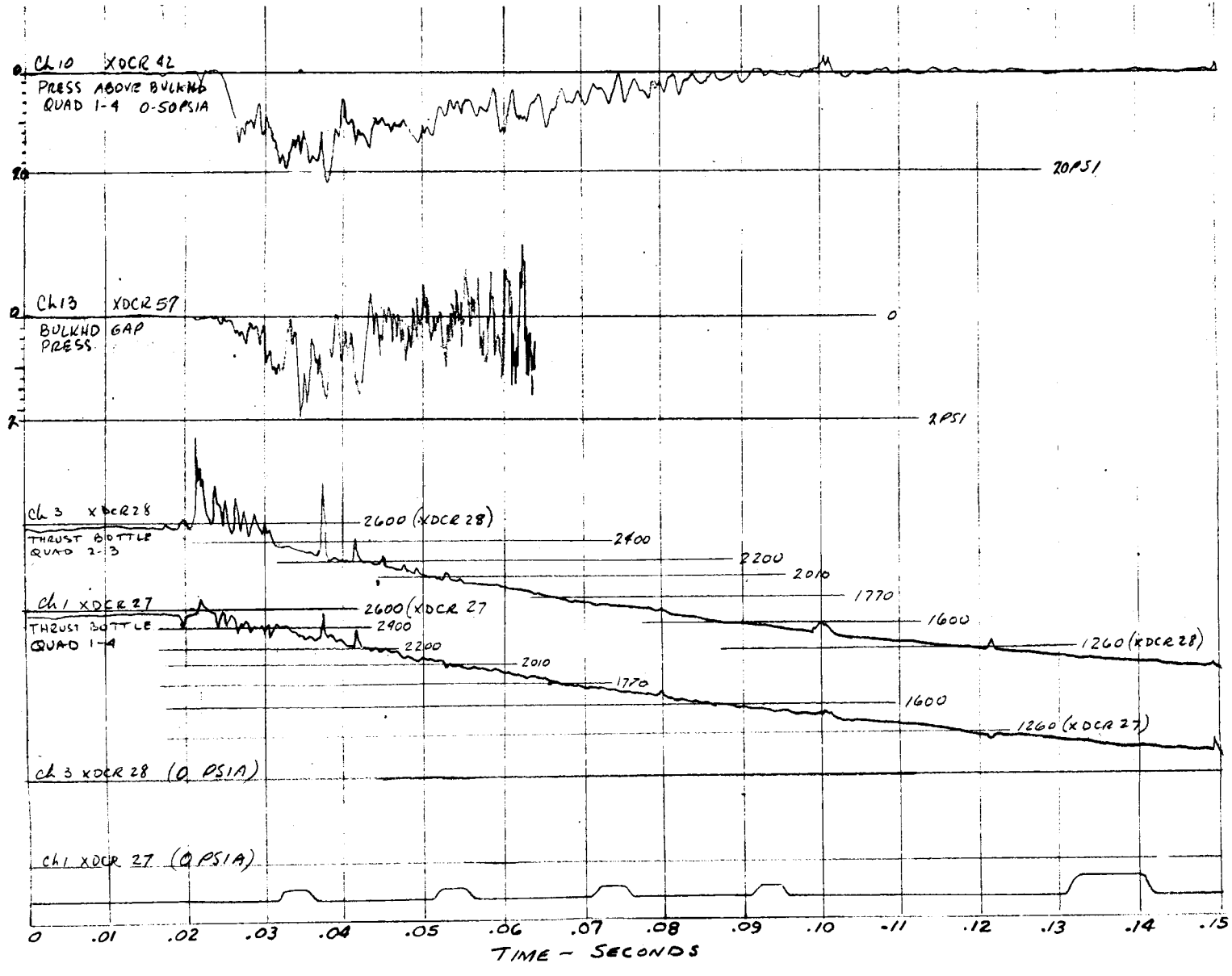

(b) Transducers 27, 28, 42 and 57.

Figure 63. - Continued.

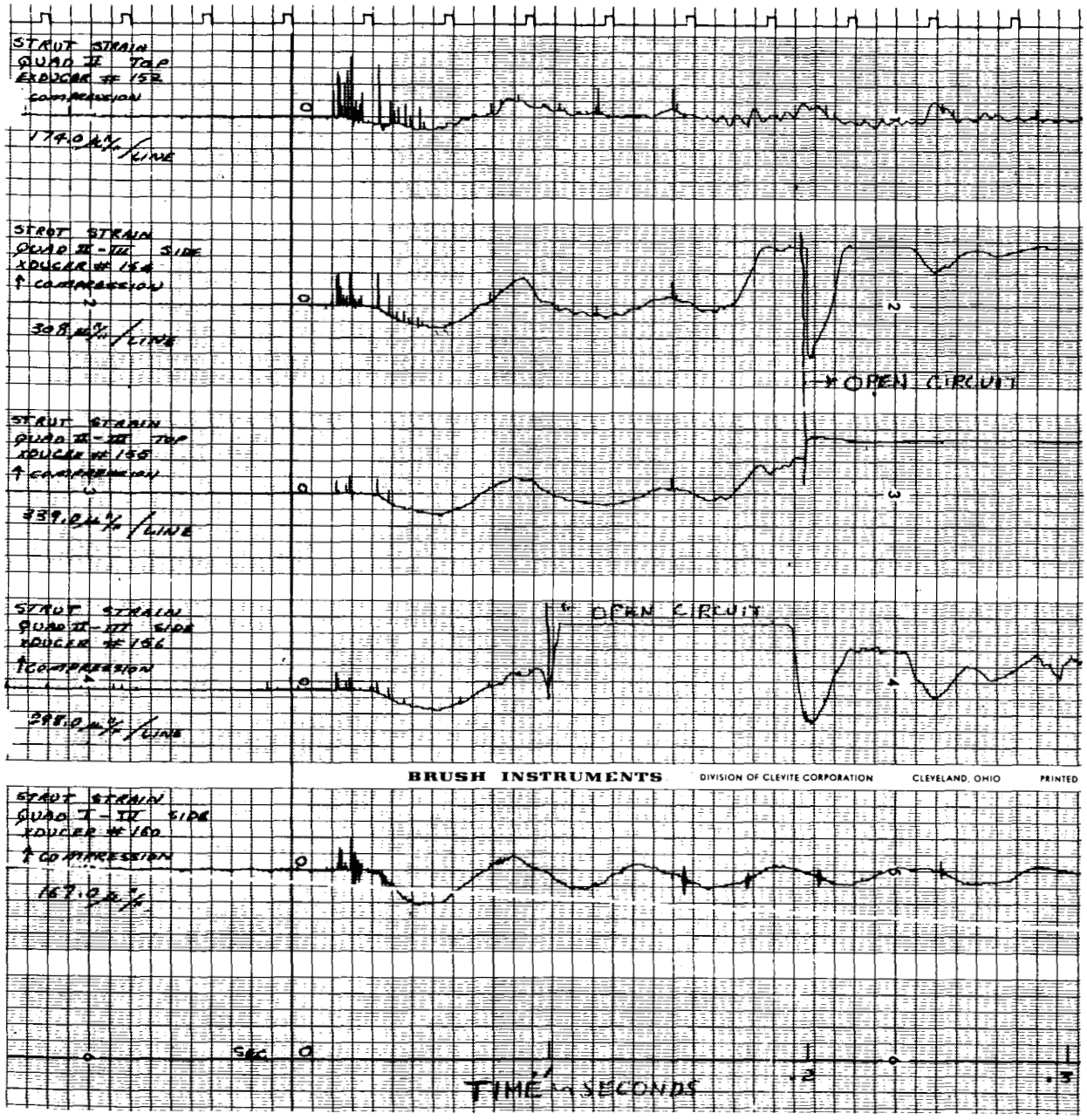

(c) Strain gages 152, 154, 155, 156 and 160.

Figure 63. - Continued.

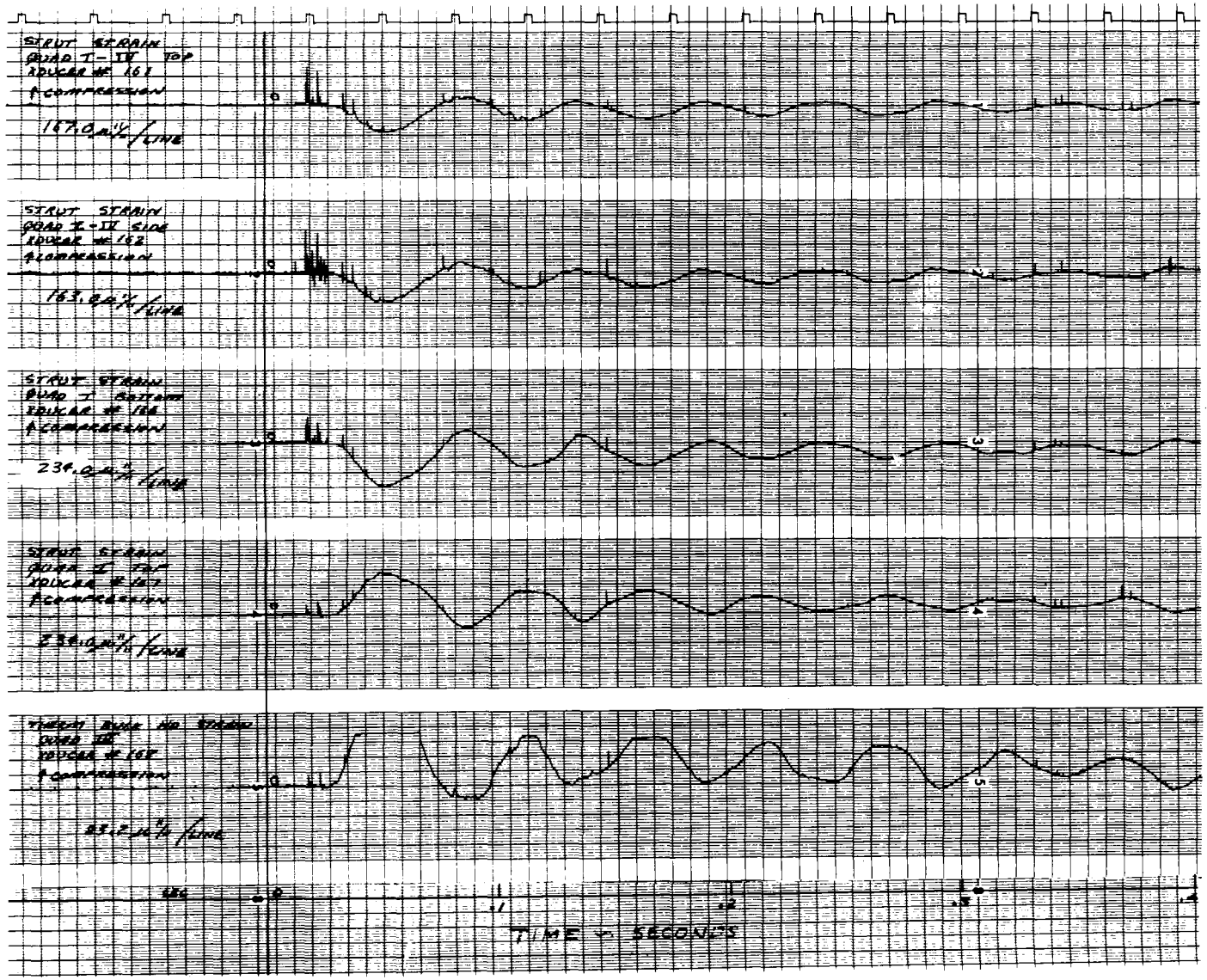

(d) Strain gages 161, 162, 166, 167 and 168.

Figure 63. - Continued.

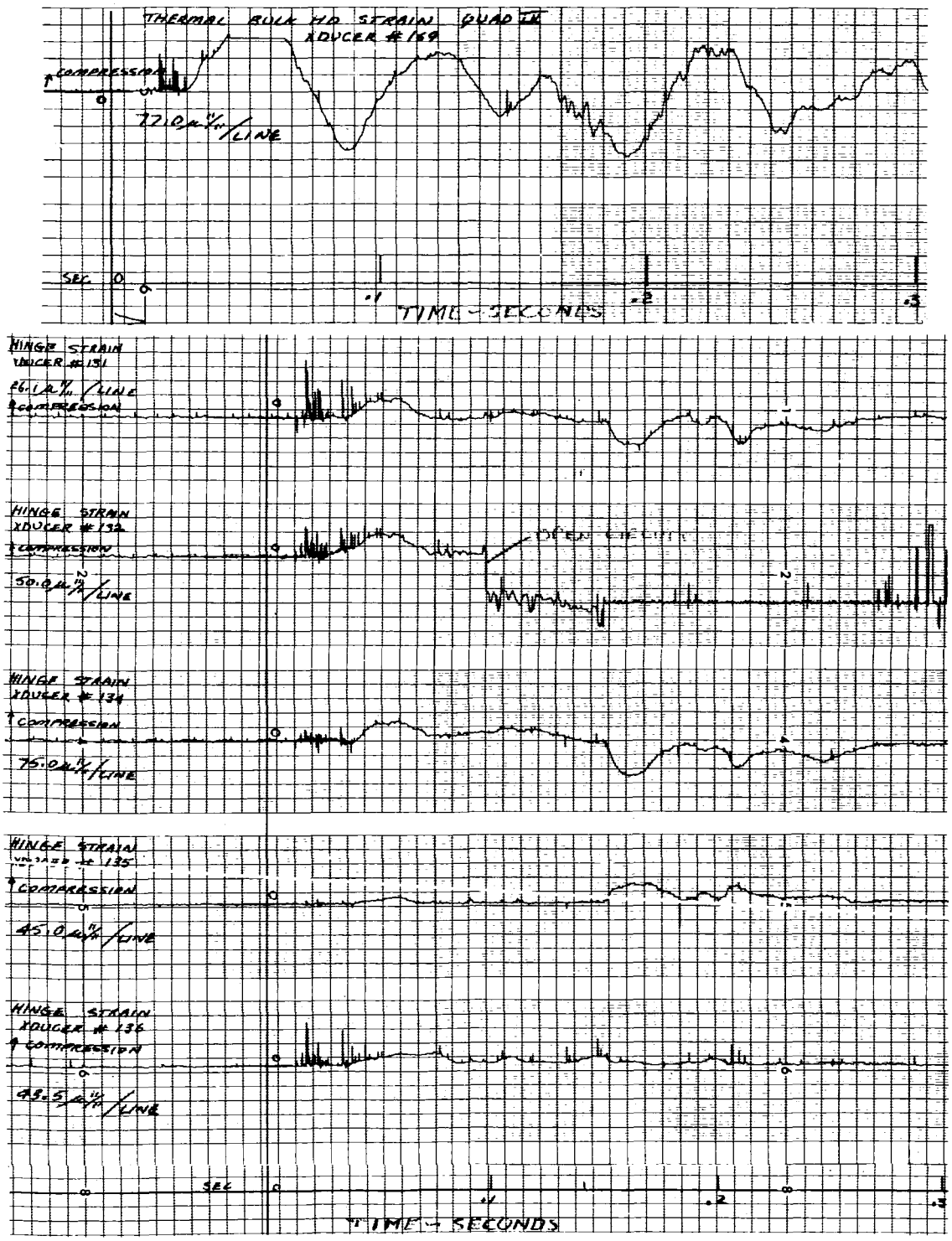

(e) Strain gages 131, 132, 134, 135, 136 and 169.

Figure 63. - Concluded.

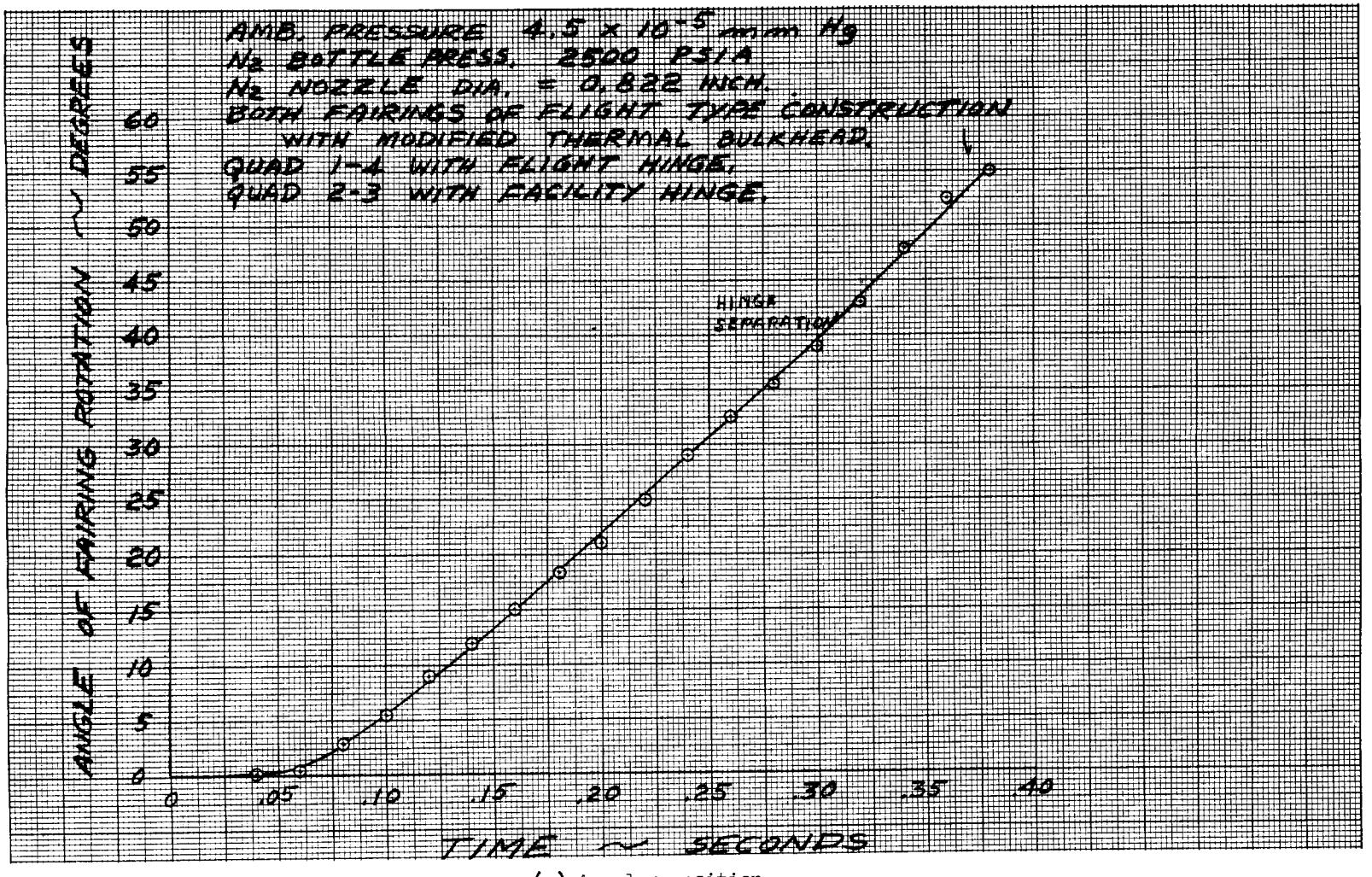

(a) Angular position.

Figure 64. - I-IV nose fairing half trajectory Test 13.

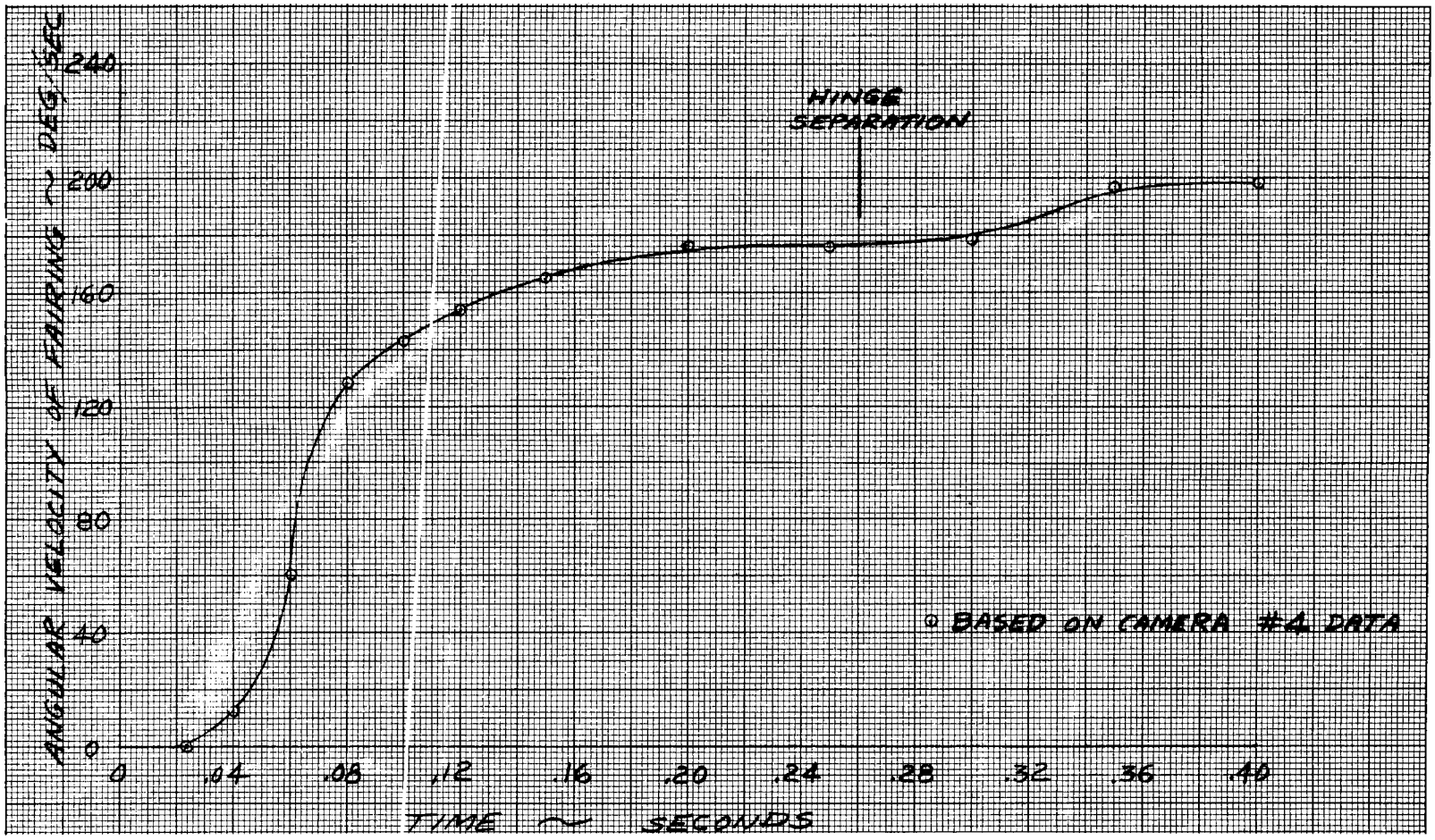

(b) Angular velocity.

Figure 64. - Continued.

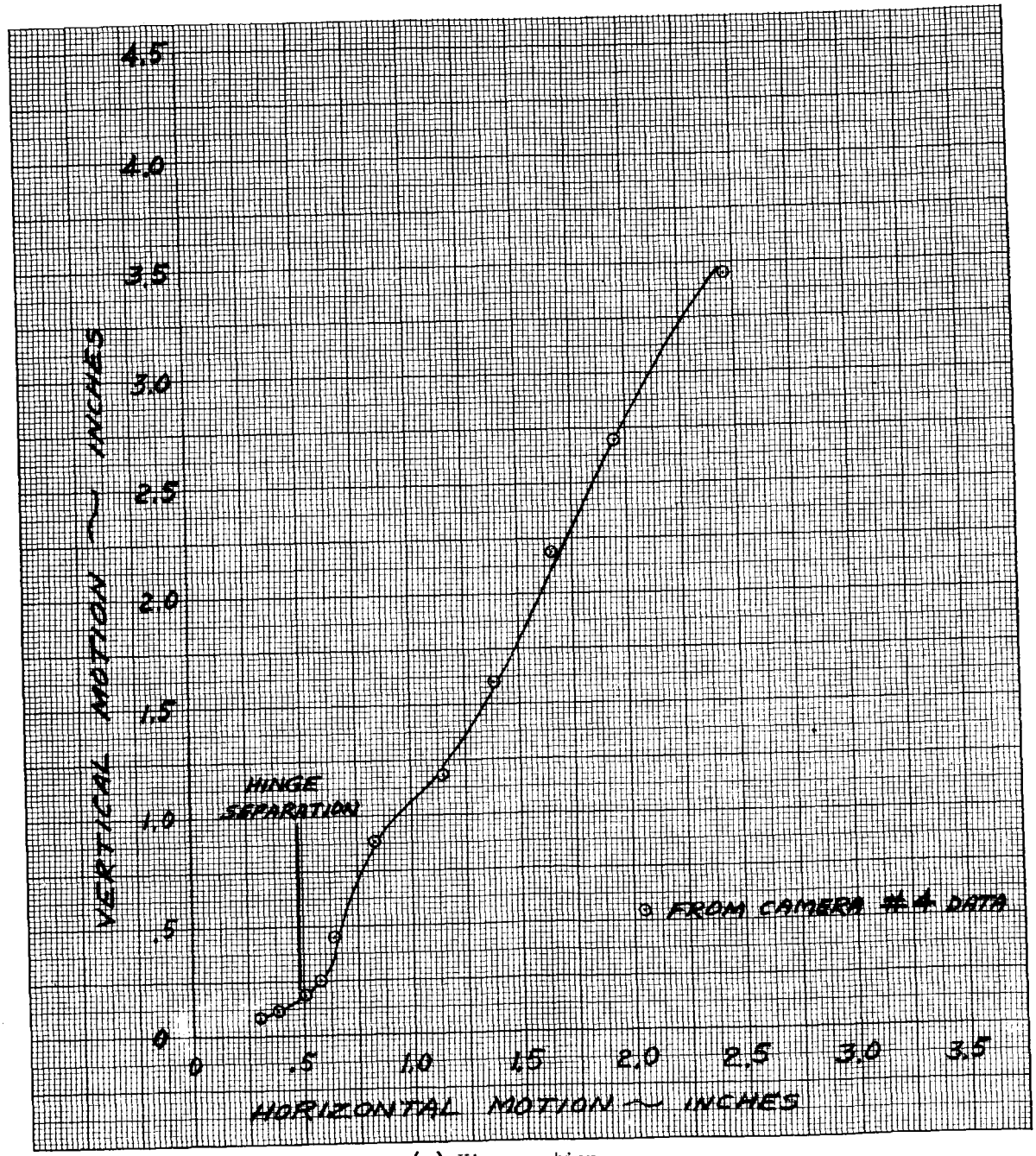

(c) Hinge motion.

Figure 64. - Concluded.

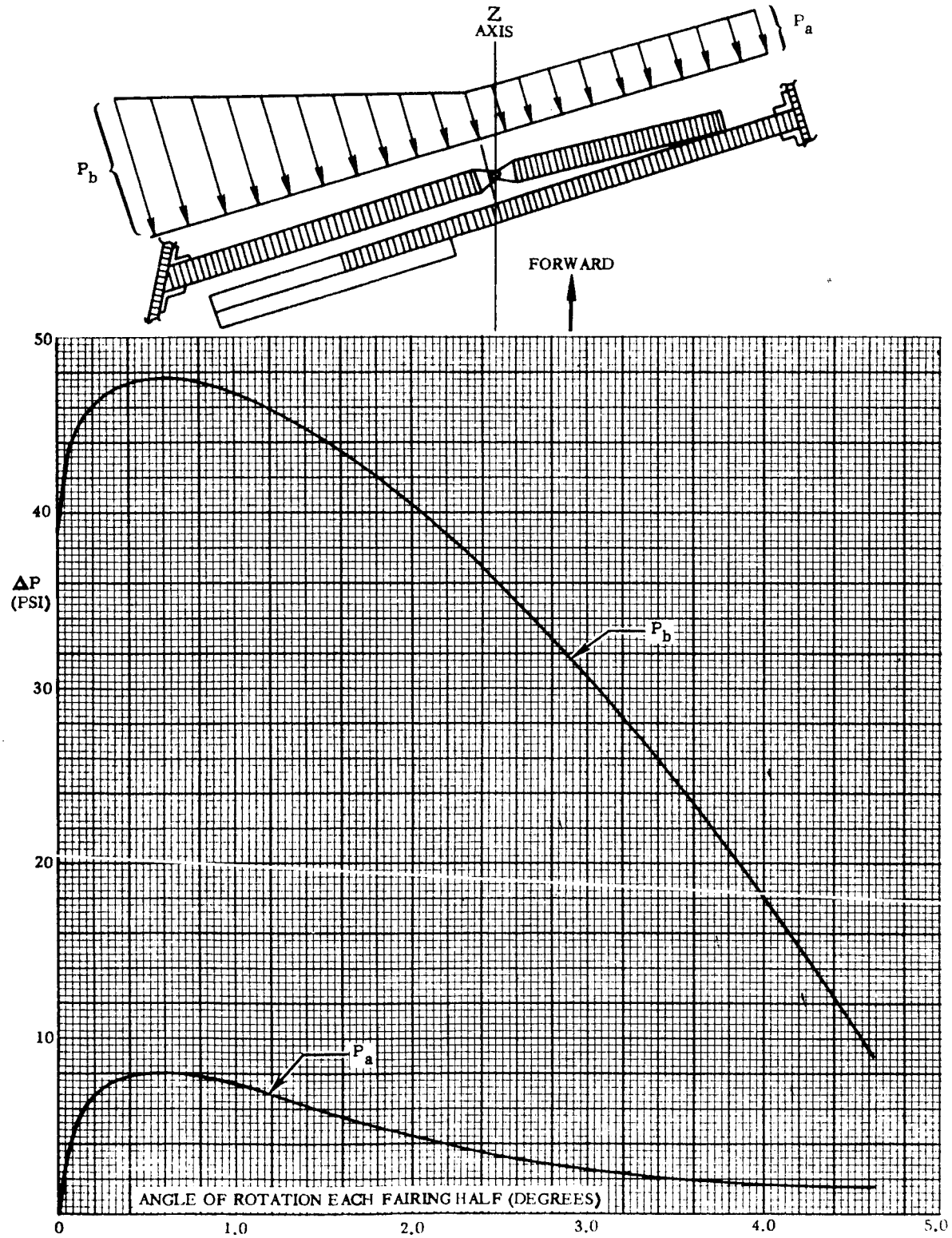

Figure 65. - Design pressures for AC-4 deflector bulkhead.

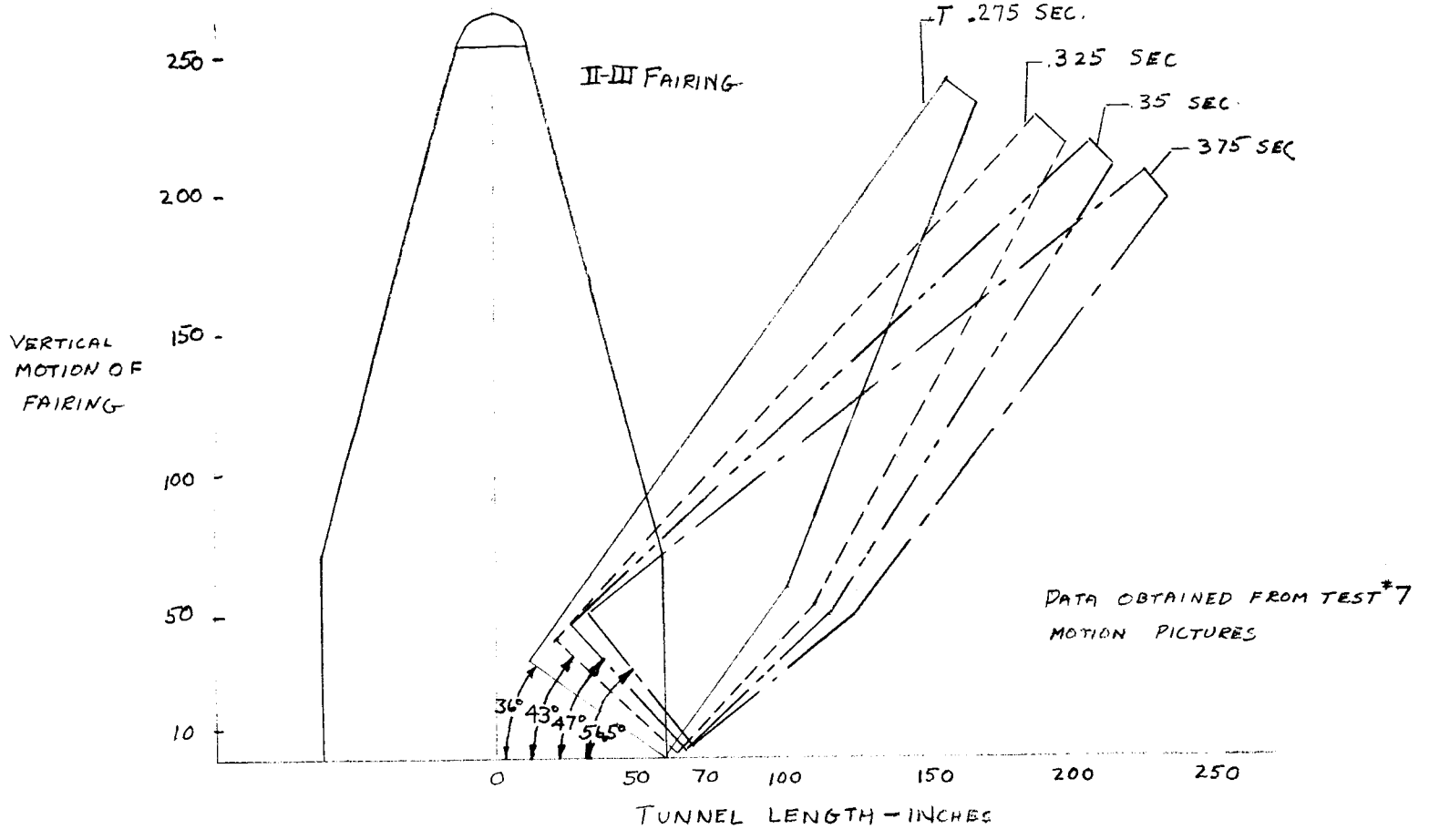

Figure 66. - Position of nose fairing with respect to time after thruster bottle firing.

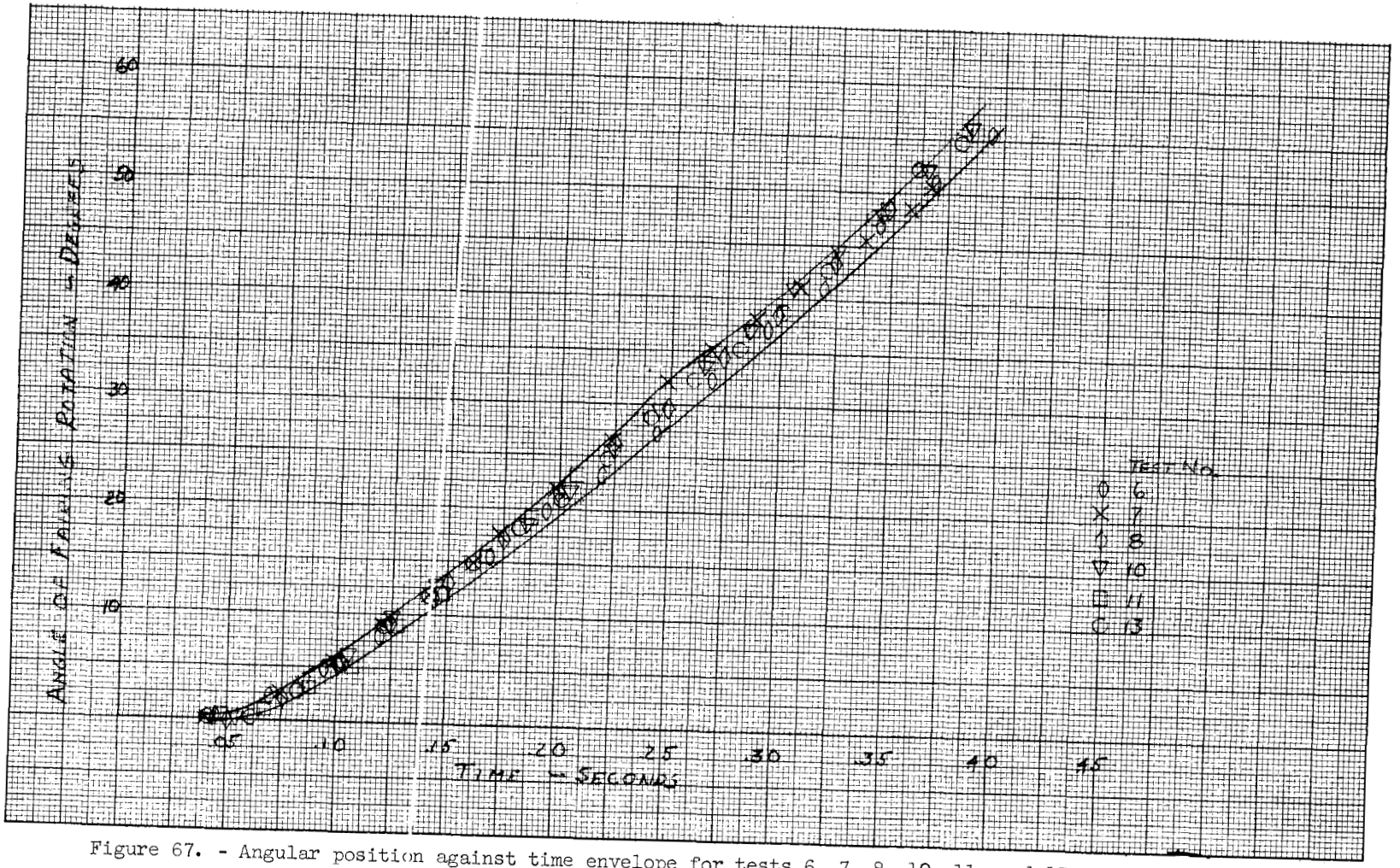

Figure 67. - Angular position against time envelope for tests 6, 7, 8, 10, 11, and 13.

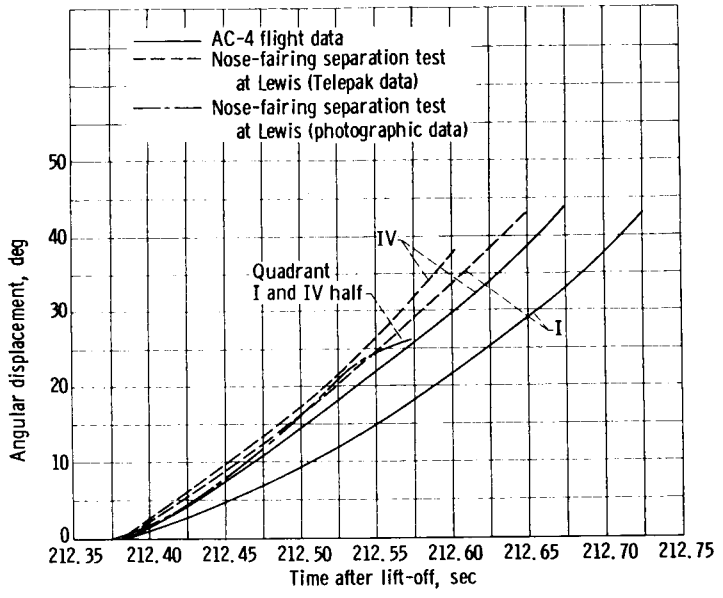

(a) I-IV fairing half.

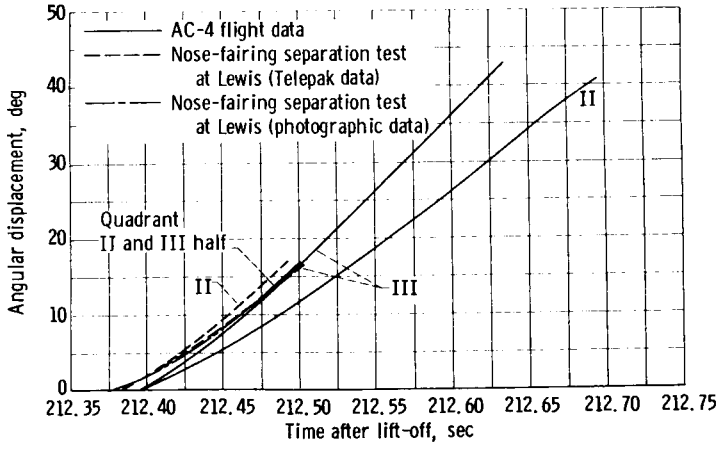

(b) II-III fairing half.

Figure 68. - Comparison of nose fairing angular position for AC-4 and LeRc test 11.